

The
University
Of
Sheffield.

**Developing novel biosensors for monitoring
antibody production in Chinese Hamster
Ovary (CHO) cells**

Jessica Anne Willmott

A thesis submitted for the degree of Doctor of Philosophy

Faculty of Science
School of Biosciences

May 2022

i. Abstract

Chinese Hamster Ovary (CHO) cells are the preferred expression system used by the biopharmaceutical industry to produce monoclonal antibodies (mAbs). mAbs are typically transfected into CHO cells and single cell cloned during Cell Line Development (CLD). The resulting clonal lines are then selected for based on their growth and titre capabilities to ensure the highest titres of product during mass-manufacture. Due to the low culture volumes used in CLD however, the product quality (PQ) of the mAb such as its propensity to fragment and aggregate is not measurable until further down the production pipeline. This results in progression of clones which are not suitable for mass-manufacture nor safe for patient usage, through CLD, before these undesirable qualities are identified.

The aim of this thesis was therefore to identify a phenotypic fingerprint for clones with desirable product titre and quality characteristics, and to use this to develop a novel genetic reporter which could be used alongside current CLD selection techniques. To achieve this, a panel of mAbs with inherent PQ issues were transfected into CHO cells, and digital droplet PCR used to quantify RNA transcripts of chaperones related to protein folding in the resulting clones, as guided by the literature. The results showed that high expressing clones typically had lower levels of protein folding chaperones and Endoplasmic Reticulum (ER) stress molecules, in contrast to previous literature. Based on this data, an exogenous fluorescent reporter construct was generated using Calreticulin. The reporter expression replicated the negative relationship with titre during CLD processes and showed an ER-localised fluorescent signal of Calreticulin on the Berkeley Lights Beacon. The titre relationship was also reproducible after progression from CLD into a fed-batch production study, during which the reporter showed a positive relationship with PQ factors such as fragmentation and charge variation.

Taken together, this thesis gives preliminary evidence to the importance of correct protein folding in CHO clones to produce high quantity *and* quality mAb, and suggests the use of a fluorescent Calreticulin reporter construct can be predictive of clones for a multitude of mAb quality and quantity phenotypes at the earliest stages of CLD.

ii. Acknowledgments

I would first like to thank my supervisors; Holly Corrigan, Andrew Peden and Robyn Emmins. Holly you have been an incredible mentor and teacher, and I can't thank you enough for all of encouragement, patience and support you have given me throughout the project. Andrew, thank you for being such a great teacher to me in the lab in Sheffield, and for the guidance and advice you continued to give me after moving to GlaxoSmithKline. Finally, Robyn, thank you for seeing so much potential in me and for all of the invaluable support, expertise and guidance you have given me along the way.

Thank you to my PhD advisors Mark Collins and Freek van Eeden, who have both been great mentors and have provided me with invaluable advice throughout my project. I would also like to thank the amazing friends I made in the lab at Sheffield; Amber Shun-Shion, Asral Wirda Ahmad Asnawi and Nabila Rahman. I couldn't have asked for a better lab group to start my PhD journey with and I will fondly remember the fun we had in the lab, as well as all of the afternoons complaining about experiments not working over cups of tea!

I would also like to thank and acknowledge so many people within GSK that helped me throughout my PhD project after moving from Sheffield. I would like to thank Robyn Coletta and Holly Corrigan for running my cell lines on the Beacon for me, and Carlos Rodrigues dos Reis and Claire Osborn for designing the 'poor quality' mAb panel for me to use in my thesis experiments. Further thanks goes to all of the many people that trained me on the various experimental techniques that I used throughout my PhD: Shawal Spencer for teaching me ddPCR, Emilie Bureau for training me on the Yokogawa microscope, Daniela Lega for training me in production studies, Sonya Godbert for expanding my knowledge in statistical analysis, Emily Burrows for training me in antibody purification and Alba Rodriguez for teaching me how to perform HPLC analysis. I would also like to thank the amazing Cell Line Development team, both past and present at GSK. Holly, Jo, Mike, Molly, Robyn C, Robyn E, Sally, Sharon and Shawal! Every single one of you have been so wonderful to me and I am so grateful for how you have all welcomed me into the group so warmly. I have learnt so much from everyone, and have enjoyed so many brilliant memories with you all both in and out of the lab.

A huge thank you finally goes to all of my family and friends from outside of the science world. I am so lucky to have every single one of you. I would like to dedicate this thesis to my partner Philip Colbourn, my parents Adam and Jeanette Willmott, and my sister Katie Willmott. Thank you for all of the love and support that you have given me throughout this PhD, and for never doubting me even when I doubted myself. I couldn't have done it without you.

iii. Author Declaration

I, the author, confirm that this thesis is my own work. I am aware of the University's Guidance on the Use of Unfair Means (www.sheffield.ac.uk/ssid/unfairimeans). This work has not been previously presented for an award at this, or any other, university.

iv. Abbreviations

ADCC	Antibody Dependent Cell Mediated Cytotoxicity
AIP1	ASK1-Interactive Protein 1
AMD	Age Related Macular Degeneration
ANOVA	Analysis of Variance
ATF4	Activating Transcription Factor 4
ATF6	Activating Transcription Factor 6
β2M	Beta-2 Microglobulin
BCL	B-cell Lymphoma Protein
BIP	Binding Immunoglobulin Protein
BIS-ANS	4,4'-Dianilino-1,1'-Binaphthyl-5,5'-Disulfonic Acid
BLI	Berkeley Lights
BLIMP1	B-Lymphocyte Induced Maturation Protein-1
CALR	Calreticulin
CANX	Calnexin
cATF6	Cleaved Activating Transcription Factor 6
CD20	Cluster of Differentiation 20
CDC	Complement Dependent Cytotoxicity
cDNA	Complementary Deoxyribonucleic Acid
CERS2	Ceramide Synthase 2
CEX	Cation Exchange Chromatography
CH (1-3)	Constant Heavy Chain (1-3) Region
CHO	Chinese Hamster Ovary
CHOP	CCAAT-Enhancer-Binding Protein Homologous Protein
CL	Constant Light Chain Region
CLD	Cell Line Development
CRISPR	Clustered Regularly Interspaced Palindromic Repeats
DAPI	4',6-Diamidino-2-Phenylindole
ddPCR	Digital Droplet Polymerase Chain Reaction
DHFR	Dihydrofolate Reductase

DLS	Dynamic Light Scattering
DMSO	Dimethyl Sulfoxide
DNA	Deoxyribose Nucleic Acid
EDEM(3)	Endoplasmic Reticulum Degradation Enhancing Alpha-Mannosidase-Like Protein
EIF2α	Eukaryotic Translation Initiation Factor 2A
ELISA	Enzyme-linked Immunosorbent Assay
ER	Endoplasmic Reticulum
ERAD	Endoplasmic Reticulum Associated Degradation
ERManI	Endoplasmic Reticulum Alpha-Mannosidase I
ERO1α	Endoplasmic Reticulum Oxidase 1 Alpha
ERSE	Endoplasmic Reticulum Stress Response Element
ERSI	Endoplasmic Reticulum Stress Index
Fab	Fragment of Antigen Binding
FACS	Fluorescence Activated Cell Sorting
Fc	Fragment Crystallisable Region
FDA	Food and Drug Administration
FISH	Fluorescence In Situ Hybridisation
FITC	Fluorescein Isothiocyanate
FRET	Förster Resonant Energy Transfer
FSC	Forward Scatter
GADD34	Growth Arrest and DNA-Damage-Inducible Protein
GAPDH	Glyceraldehyde 3-phosphate dehydrogenase
GFP	Green Fluorescent Protein
gMFI	Geometric Mean Fluorescence Intensity
GOI	Gene of Interest
GRP94	Glucose Regulated Protein 94
GS	Glutamine Synthetase
GSK	GlaxoSmithKline
HC	Heavy Chain
HEK293T	Human Embryonic Kidney 293T
HER2	Human Epidermal Growth Factor Receptor 2
HPLC	High Performance Liquid Chromatography
IgA	Immunoglobulin Alpha

IgD	Immunoglobulin Delta
IgE	Immunoglobulin Epsilon
IgG	Immunoglobulin Gamma
IgM	Immunoglobulin Mu
IRE1	Inositol-Requiring Enzyme 1
IVCD	Integral Viable Cell Density
JNK	c-Jun N-Terminal Kinase
LB	Liquid Broth
LC	Light Chain
LDH	Lactate Dehydrogenase
LN₂	Liquid Nitrogen
mAb	Monoclonal Antibody
MAC	Membrane Attack Complex
MAPK	Mitogen Activated Protein Kinase
mRNA	Messenger Ribonucleic Acid
MSX	Methionine Sulphoximine
MTX	Methotrexate
NRK	Normal Rat Kidney
OEP	Opto-Electropositioning
PBMC	Peripheral Blood Mononuclear Cells
PBS	Phosphate Buffered Saline
PD-1	Programmed Cell Death Protein 1
PDI	Protein Disulphide Isomerase
PDL-1	Programmed Cell Death Ligand 1
PERK	Protein Kinase RNA-Like Endoplasmic Reticulum Kinase
PI	Isoelectric Point
PK	Pharmacokinetics
PLS	Partial Least Squares
PTP	Protein Tyrosine Phosphatase
QP	Productivity
qPCR	Quantitative Polymerase Chain Reaction
RFP	Red Fluorescent Protein
RMCE	Recombinase Mediated Cassette Exchange

RNA	Ribonucleic Acid
SD	Standard Deviation
SEC	Size Exclusion Chromatography
SH	Sulphhydryl
SPR	Specific Productivity Rate
SRP14	Signal Recognition Peptide 14
SSC	Side Scatter
sXBP1	Spliced X-Box Binding Protein 1
TBE	Tris Borate EDTA
TNFα	Tumour Necrosis Factor Alpha
TOM20	Translocase Of Outer Mitochondrial Membrane 20 Protein
tPA	Tissue Plasminogen Activator
TRAF2	TNF-Receptor-Associated-Factor 2
UGGT	Uridine Diphosphate-Glucose:Glycoprotein-Glucosyltransferase
UPR	Unfolded Protein Response
uXBP1	Unspliced X-Box Binding Protein 1
VEGFA	Vascular Endothelial Growth Factor A
VH	Variable Heavy Chain Region
VL	Variable Light Chain Region

v. Contents

i. Abstract	ii
ii. Acknowledgments	iii
iii. Author Declaration	iv
iv. Abbreviations	v
v. Contents	ix
vi. List of Figures	xiv
vii. List of Tables	xvii
1. Introduction	1
1.1. Monoclonal antibodies in the biopharmaceutical industry.....	1
1.1.1. Monoclonal antibodies as a drug therapeutic	1
1.1.2. Expression systems for monoclonal antibody production.....	2
1.1.3. History of the CHO Cell Line	3
1.1.4. Cell Line Development	7
1.2. Antibody Structure, Function and Folding in CHO cells.....	11
1.2.1. Antibody Function.....	11
1.2.2. Antibody Structure.....	12
1.2.3. Antibody folding.....	15
1.2.4. Quality control of antibody folding.....	17
1.2.5. The effects of improper folding on mAb product	19
1.2.6. Complex monoclonal antibody formats.....	22
1.3. Monoclonal antibody production can lead to endoplasmic reticulum stress	25
1.3.1. Endoplasmic reticulum stress	25
1.3.2. The Unfolded Protein Response	25
1.3.2.1. The IRE1 Branch	26
1.3.2.2. The ATF6 Branch	27
1.3.2.3. The PERK Branch	27
1.3.3. The Unfolded Protein Response in mAb production	29
1.3.4. Manipulating the UPR to monitor mAb production	30
1.3.5. Engineering the UPR to enhance protein expression	31
1.3.6. Limitations to the literature.....	32
1.4. Project Aims and Objectives	34
2. Materials and Methods	35
2.1. Cell Culture.....	35
2.1.1. Sub-culture maintenance of CHO Cells.....	35

2.1.2. Cell Revival	35
2.1.3. Cell Freezing	36
2.1.4. Monitoring mAb Titre via the Octet HTX	36
2.1.5. mAb Naming Conventions	37
2.2. DNA Stock Production.....	38
2.2.1. Transformations.....	38
2.2.2. DNA Purification: Miniprep and Maxipreps.....	38
2.2.3. Restriction Digests	38
2.3. Infusion cloning of the reporter construct into GSK’s expression plasmid	39
2.3.1. Reporter String DNA and Plasmid Digest Preparation.....	39
2.3.2. Infusion Cloning	40
2.4. Mammalian Cell Transfections.....	41
2.4.1. Transient Cell Transfection	41
2.4.2. Stable Cell Transfection	42
2.4.3. Single Cell Cloning.....	43
2.4.4. Scale Up of Clonal Cell Lines	44
2.5. Digital Droplet PCR.....	45
2.5.1. RNA Isolation and cDNA Conversion.....	45
2.5.2. Digital Droplet PCR.....	45
2.5.3. Digital Droplet PCR Data Analysis	45
2.6. Western Blotting.....	48
2.6.1. Cell Lysis Sampling	48
2.6.2. SDS PAGE.....	48
2.6.3. Protein Transfer	49
2.6.4. Western Blotting.....	50
2.6.5. Coomassie Staining	50
2.7. Fluorescence Microscopy.....	51
2.7.1. Live Cell ER Tracker and DAPI Counter Staining.....	51
2.7.2. Fixed Cell Imaging	51
2.7.3. Imaging on the Yokogawa CV8000	52
2.7.4. Quantification of the fluorescence imaging.....	52
2.8. PrimeFlow RNA	53
2.8.1. PrimeFlow RNA: Day 1	53
2.8.2. PrimeFlow RNA: Day 2	54
2.9. Flow Cytometry using the iQue Screener	55
2.10. Production Study.....	56

2.10.1. Pre-Culture and Production Study Inoculation	56
2.10.2. Measuring GFP expression with the iQue flow cytometer	57
2.10.3. Production study sampling and feeding	57
2.10.4. Culture Harvest	57
2.11. mAb Product Quality Analysis.....	58
2.11.1. Sample Filtration and Purification	58
2.11.2. Measuring Sample Concentration and Normalisation.....	58
2.11.3. Running product quality analysis on the HPLC systems	59
2.11.4. Analysing the HPLC data sets	59
2.12. Statistical Analysis.....	59
3. Predicting mAb quality and quantity in CHO clones expressing a bispecific mAb using the Unfolded Protein Response (UPR).....	60
3.1. Introduction	60
3.1.1. Chapter Aims.....	63
3.2. Results.....	64
3.2.1. Designing a clonal cell line panel for testing techniques	64
3.2.2. Using a live ER Tracker Cell Stain to measure whole ER content.....	65
3.2.3. Human mAb staining showed distinct phenotypes in a high and low producer CHO clone when measured with immunofluorescence microscopy.....	67
3.2.4. Quantification of UPR targets with PrimeFlow RNA	70
3.2.5. Quantification of UPR RNA targets with Droplet Digital PCR	75
3.3. Discussion.....	78
3.3.1. Limitations of the study and future work	81
4. Monitoring the Unfolded Protein Response (UPR) in CHO clones expressing a panel of different mAb constructs	83
4.1. Introduction	83
4.1.1. Chapter Aims.....	85
4.2. Results.....	86
4.2.1. The mAb panel was successfully transfected into the CHO host, but showed varying recovery following MSX selection.....	86
4.2.2. Single cell clones were monitored for titre on the Beacon, and showed similar average titres to their pre-clonal pool titres	90
4.2.3. Clone productivity was affected by the static scale up stage.....	93
4.2.4. A negative correlation was seen between titre and the expression of pro-recovery UPR chaperones, but no correlation was seen with pro-apoptotic chaperones.	95
4.2.5. The non-producing CHO clones showed varying phenotypes of ER stress levels over 4 day sub-culture	98
4.2.6. The highly-stressed non-producing CHO clones had mAb present inside the cell	100

4.2.7. The highly stressed, non-producing mAb clones only express the mAb heavy chain	102
4.2.8. The heavy chain only producing clones still attempt to fold the heavy chain as evidenced by heavy chain homodimer presence in the cell lysate	104
4.3. Discussion.....	107
4.3.1. The negative relationship between UPR expression and titre was the opposite of that seen in the literature	108
4.3.2. Measuring mAb titre and mAb mRNA expression resulted in a different relationship with BIP	109
4.3.3. Non-producing clones often expressed individual mAb chains.....	111
5. Designing an ER resident fluorescent organelle reporter to monitor mAb production throughout Cell Line Development (CLD)	113
5.1. Introduction	113
5.1.1. Chapter Aims.....	116
5.2. Results.....	117
5.2.1. The fluorescently tagged reporter proteins are localised to the Endoplasmic Reticulum and Mitochondria following transfection into the CHO Host.....	117
5.2.2. Generation of clonal CALR-GFP, CALR-mOrange and TOM20-GFP expressing host lines	120
5.2.3. The expression of the reporters is retained during culture and does not impact the health of the CHO host.....	122
5.2.4. CALR-GFP reporter expression is retained, and can be seen during mitosis.....	125
5.2.5. Reporter host responds to chemically induced ER stress.....	127
5.2.6. CALR-GFP and TOM20-GFP reporter expression increases after transient transfection with plasmids expressing antibody	130
5.2.7. CALR-GFP and TOM20-GFP reporter localisation remains visible on the Beacon after mAb transfection.....	134
5.2.8. CALR-GFP reporter host expression negatively correlates to titre during static scale up	136
5.3. Discussion.....	140
5.3.1. Potential improvements to the reporter construct design.....	143
5.3.2. What are the most important predictive capabilities for CLD to be able to measure? ...	144
6. The CALR-GFP reporter host may be able to predict product titre and quality in a production study	146
6.1. Introduction	146
6.1.1. Production Studies.....	146
6.1.2. Product Quality Analysis: Product Size	148
6.1.3. Product Quality Analysis: Product Charge	149
6.1.4. Cell Lines Investigated In This Chapter	149
6.2. Results.....	150
6.2.1. Addition of the CALR-GFP reporter did not affect cell growth characteristics during the production study.....	150

6.2.2. Titre was higher on average in the CALR-GFP reporter host cell lines compared to the CHO host lines	153
6.2.3. Metabolite consumption was comparable across the hosts during fed-batch culture....	155
6.2.4. CALR-GFP reporter expression varied during fed-batch culture	158
6.2.5. Product size was not affected by the addition of the CALR-GFP reporter	162
6.2.6. Product charge was not affected by the addition of the CALR-GFP reporter.....	164
6.2.7. Product size was affected by the mAb expressed but not by the addition of the CALR-GFP reporter	166
6.2.8. Product charge was varied between the clones expressing different mAb types.....	169
6.2.9. CALR-GFP intensity showed predictive capabilities towards product quality at selected time points	172
6.2.10. Modelling of the CALR-GFP reporter expression cannot predict all product quality measurements at the current sample size	174
6.3. Discussion.....	175
6.3.1. The CALR-GFP reporter host as a tool to predict product quality	178
7. Discussion	181
7.1. Introduction	181
7.2. Using fluorescence imaging to monitor extracellular aggregates	182
7.3. The Beacon can successfully image the localised CALR-GFP reporter.....	183
7.4. The Unfolded Protein Response negatively correlated with mAb titre in the CHO model	184
7.5. Why do the levels of the CALR-GFP reporter change in response to titre and culture conditions?.....	187
7.6. Would an endogenously tagged gene marker be better at predicting mAb titre and quality than an exogenous marker?	189
7.7. Can the unfolded protein response be used to predict poor product quality?.....	190
7.8. Does the constant improvement of the CLD platform hinder the use of reporter cell lines?.	191
7.9. Limitations to the study	192
7.10. Future Studies	193
7.11. Concluding Remarks.....	193
8. Appendices.....	194
9. References.....	198

vi. List of Figures

Chapter 1 – Introduction.....	1
Figure 1.1. Evolution of the CHO Cell Line.....	6
Figure 1.2. Schematic of a typical Cell Line Development pipeline at GlaxoSmithKline.....	9
Figure 1.3. Typical antibody structure.....	14
Figure 1.4. Antibody folding from nascent polypeptides.....	16
Figure 1.5. The role of Calreticulin in protein folding within the endoplasmic reticulum.....	18
Figure 1.6. Examples of novel monoclonal antibody formats.....	24
Figure 1.7. Schematic of the Unfolded Protein Response.....	28
Chapter 3 – Results.....	60
Figure 3.1. The intensity of the ER Tracker staining was similar between the CHO clones.....	66
Figure 3.2. Large amounts of extracellular IgG was seen in clone A, a highly aggregated clone.....	69
Figure 3.3. PrimeFlow RNA was able to successfully detect IgG RNA transcripts although the biological reproducibility was very low.....	71
Figure 3.4. The levels of BIP RNA are positively correlated to fragment (%) when measured using PrimeFlow RNA in the clonal cell panel.....	73
Figure 3.5. The levels of PDI mRNA are negatively correlated to fragment (%) using PrimeFlow RNA in the clonal cell panel.....	74
Figure 3.6. RNA transcripts for markers of the UPR pathway were successfully quantified by ddPCR.....	77
Chapter 4 – Results.....	83
Figure 4.1. Recovered mAb pool titre and productivity were different dependent on the mAb type expressed.....	89
Figure 4.2. Titres of the clones varied dependent on the mAb type during single cell cloning on the Beacon, but still correlated to pre-clonal titres.....	92
Figure 4.3. Clone productivity fluctuated over each scale up time points, but remained relatively similar to the Beacon Au score.....	94
Figure 4.4. CALR, BIP and PDI mRNA transcript expression was negatively correlated to mAb titre in the 23 mAb expressing clones, but ATF4 mRNA transcript expression was not correlated.....	97
Figure 4.5. Variation in the expression of UPR component transcript quantities were seen over 4 days in the non-producing CHO clones.....	99
Figure 4.6. A strong positive correlation was seen between BIP and IgG fluorescence in the high producing clones, whilst some non-producing clones showed positive IgG expression.....	101
Figure 4.7. Multiple experimental methods confirm that only clones 3-D, 4-B and 4-F are expressing the heavy chain, whilst clone 2-B may express low copy numbers of the light chain.....	103

Figure 4.8. Western blots showed variation in expression of heavy chain and light chain across the 23 clonal cell lines.....	105
Figure 4.9. Summary of the expression of UPR transcripts in the non-producing clones measured by ddPCR.....	106
Chapter 5 – Results.....	113
Figure 5.1. Schematic of the fluorescent organelle reporter constructs prior to being cloned into a proprietary GSK plasmid.....	115
Figure 5.2. CALR-GFP, CALR-mOrange and TOM20-GFP all fluoresced in the CHO host, and localised to the ER and mitochondria respectively.....	118
Figure 5.3. Experimental plan for the development of host cell lines expressing the fluorescent reporters.....	119
Figure 5.4. The generation of clonal reporter host lines on the Beacon, and the subsequent scale up of the CALR-GFP and TOM20-GFP host cell lines.....	121
Figure 5.5. Removal of geneticin selection does not impact the expression of CALR-GFP or TOM20-GFP but improves the growth of the reporter cell lines.....	124
Figure 5.6. CALR-GFP reporter expression is retained in the host cell line during mitosis.....	126
Figure 5.7. Effects of Tunicamycin and Brefeldin A on the CALR-GFP and TOM20-GFP reporter host cell lines.....	129
Figure 5.8. Reporter expression was increased 24 hours post transient transfection with mAb constructs.....	132
Figure 5.9. Single cell cloning of the CALR-GFP reporter host transfected with a panel of mAb constructs.....	135
Figure 5.10. Monitoring GFP intensity in mAb expressing clonal lines during static scale up.....	138
Figure 5.11. GFP intensity negatively correlated to mAb titre during each stage of static scale up in mAb positive clones.....	139
Chapter 6 – Results.....	146
Figure 6.1. Cell growth and viability were not affected by the addition of the CALR-GFP reporter during the production study.....	151
Figure 6.2. Cell growth and viability were not affected by the type of mAb expressed during the production study.....	152
Figure 6.3. mAb titre and productivity were not affected by the addition of the CALR-GFP reporter during the production study.....	154
Figure 6.4. Glutamine, glutamate and glucose concentrations varied across the production study dependent on the mAb type expressed.....	156
Figure 6.5. Lactate, Lactate Dehydrogenase and Ammonia concentrations varied across the production study dependent on the mAb type expressed.....	157
Figure 6.6. CALR-GFP reporter host fluorescence intensity (gMFI) changes over time in a similar pattern across all of the reporter clones.....	160
Figure 6.7. CALR-GFP reporter fluorescence intensity correlated to titre (mg/L) during the production study.....	161

Figure 6.8. mAb product size was dependent on the mAb type expressed, and showed a largely monomeric population.....	163
Figure 6.9. mAb charge variants were diverse and peaks depended on the mAb type expressed.....	165
Figure 6.10. The CALR-GFP reporter did not affect the average product size in any of the mAbs when compared to the CHO host.....	168
Figure 6.11. CALR-GFP reporter addition increased product charge variants in some mAb types..	171
Figure 6.12. CALR-GFP intensity correlated to product quality phenotypes at different stages of the production study.....	173
Chapter 8 – Appendices.....	194
Figure 8.1. Heavy and light chain quantification via ddPCR positively correlated to mAb titre.....	194
Figure 8.2. Heavy and light chain RNA expression as measured by ddPCR, did not correlate with intracellular IgG quantification, as measured by imaging.....	195
Figure 8.3. BIP RNA expression as measured by ddPCR correlated with intracellular BIP staining. mAb titre and intracellular IgG staining did not correlate, however.....	196
Figure 8.4. Light chain and heavy chain staining was correlated when measured by microscopy and flow cytometry.....	197

vii. List of Tables

Chapter 2 – Materials and Methods.....	35
Table 2.1. Cell culture media and supplementation recipes.....	35
Table 2.2. mAb panel naming convention and rationale for use.....	37
Table 2.3. Sequences of primers used for infusion experiments.....	39
Table 2.4. ddPCR mastermix recipe.....	46
Table 2.5. Sequences of primers and internal probes used for ddPCR experiments.....	47
Table 2.6. Primary and secondary antibodies used for western blot experiments.....	50
Table 2.7. Primary and secondary antibodies used for fixed fluorescence imaging experiments.....	52
Table 2.8. PrimeFlow RNA target probe names and fluorophore information.....	54
Table 2.9. CEDEX metabolite settings used during production study experiments.....	56
Chapter 3 – Results.....	60
Table 3.1. Titre and quality characteristics of clones expressing a bispecific mAb construct.....	64
Chapter 4 – Results.....	83
Table 4.1. mAb panel naming convention and rationale for use.....	88
Chapter 6 – Results.....	146
Table 6.1. Size exclusion chromatography quantification.....	167
Table 6.2. Cation exchange chromatography quantification.....	170
Chapter 7 – Discussion.....	181
Table 7.1. Comparison of the experimental controls and techniques used in this thesis and the Kober et al., (2012) and the Prashad and Mehra (2015) studies.....	185

1. Introduction

1.1. Monoclonal antibodies in the biopharmaceutical industry

1.1.1. Monoclonal antibodies as a drug therapeutic

Monoclonal antibodies (mAbs) describe an antibody that has a monovalent affinity to a single epitope (Breedveld, 2000). This specificity has led to mAbs becoming an extremely popular drug therapeutic as they can target specific disease markers (Buss et al., 2012; Pento, 2017). The first mAb therapy approved for use in humans was muromonab, a mAb therapy used for the prevention of kidney transplant rejection in 1986 (Todd and Brogden, 1989). Since then mAbs have become an incredibly popular disease treatment with mAb based therapeutics comprising over 50 % of newly approved drugs from 2015-2018 globally, and they continue to be one of the most lucrative classes of biopharmaceutical products. For example, eight of the top ten biopharmaceutical products by sales in 2017 were mAb based; with total mAb sales reaching \$123 billion in that year alone (Walsh, 2018). This pattern appears to only be increasing, with 5 novel antibody therapies approved in the US and EU in 2019 alone, as well as 13 awaiting marketing approval and a further 79 undergoing late stage clinical study (Kaplon et al., 2020). Perhaps one of the most successful examples is Adalimumab (Humira), which topped the biggest-selling drug list in 2018 (Urquhart, 2019). Adalimumab binds to and inhibits the tumour necrosis factor alpha (TNF α). TNF α is dysregulated in a number of inflammatory and auto-immune conditions and has been trialled in many disease including rheumatoid arthritis, ankylosing spondylitis and psoriatic arthritis (Mease, 2007).

The costs involved in developing a regulatory approved mAb therapy are high, with the costs of taking one pharmaceutical to market approval estimated to be over \$2.5 billion in 2013 following a survey of 106 recently approved drugs (DiMasi et al., 2016). These costs are then further exacerbated when considering that only 16 % of biopharmaceutical drugs that entered phase I of clinical trials between 1993-2004 actually gained regulatory approval (DiMasi et al., 2010). Consideration needs to be taken into creating competitive pricing to compete with the biosimilars that emerge once the patent has expired (Ecker et al., 2015). Industry manufacturers therefore have to consider all of these factors when developing a cost-effective drug, and one important factor for this is the requirement to choose an expression system that can produce maximal mAb yields whilst remaining safe for usage in human patients.

1.1.2. Expression systems for monoclonal antibody production

A wide variety of expression systems are available for mAb expression and typically fall into three distinct categories: yeast, bacteria and mammalian (Verma et al., 1998). Bacteria such as *E. coli* are frequently used to express immunoglobulin fragments as they can produce large quantities of proteins and grow at a fast rate in comparison to other expression systems. However, *E. coli* are not able to glycosylate proteins, and thus whole antibody molecule expression is not possible (Verma et al., 1998). These problems can be resolved using yeast expression systems which are not only able to glycosylate proteins but can also form disulphide bonds and other post-translational modifications that are required for full format mAb expression. However, yeast have their own disadvantages; with evidence of hyperglycosylation and poor secretion efficiency found in some yeast systems (Bordes et al., 2007). Bacteria and yeast production systems therefore have their own merits, but as Walsh (2018) highlights in a review of current biopharmaceutical practices, the amount of mAbs expressed in mammalian cells is now greater than any other system. Before 1989, only 33 % of approved drugs were produced in mammalian cells, but between 2015-2018 this increased to 79 %. Walsh (2018) also showed that out of all mammalian expression systems the Chinese Hamster Ovary (CHO) system was the most popular choice, accounting for the expression system of over 80 % of all mammalian expressed mAbs. The popularity of the CHO cell line can be pin-pointed to its many beneficial characteristics for mAb production. Some of these factors are due to the inherent nature of CHO cells, whilst some are by-products of the improvement of the expression systems over time.

As a mammalian cell line one of the biggest benefits of using CHO cells for expressing mAb molecules designed for human usage is that the proteins expressed in CHO cells undergo similar post-translational modifications as human proteins (Kim et al., 2012). Many benefits can also be seen in the ways CHO cells can be cultured. For example, CHO cells can be grown in serum-free media. Serum contains hormones, growth factors and lipids which are necessary for cell growth. However, serum can be a source of bacterial and viral contamination that can be dangerous to humans, and present significant batch to batch variability meaning that these contaminations cannot be reliably and consistently prevented (Yao et al., 2017). Further to this, serum is an animal derived product that raises substantial regulatory issues and as such biopharmaceutical industries exclude them from their culture conditions (Cho et al., 2017; Kelley, 2009; Ritacco et al., 2018). CHO cells are also easily adaptable to suspension culture meaning that they can be grown in large bioreactors, ultimately allowing for higher cell densities and subsequent mAb yields to be achieved (Lai et al., 2013). These characteristics, paired with the CHO cell's natural ability to produce large amounts of protein means that concentrations of up to 13 g/L of mAb are now achievable during fed-batch culture (Kelley, 2009). The CHO cells genome has also been edited to take advantage of powerful gene amplification systems,

such as the dihydrofolate reductase (DHFR) system for the CHO-DG44 host or the glutamine synthetase (GS) system for the CHO-GS $-/-$ host (Fan et al., 2012; Dahodwala and Lee, 2019). These systems will be discussed further in Chapter 1.1.3.

Finally and perhaps most importantly, the CHO system has been used as an expression system for biotherapeutics since it was first used as the expression system for the recombinant protein tissue plasminogen activator (tPA), approved in 1986. As the CHO expression system already has prior approval by the FDA and over 30 years of safety data therefore it is not necessarily a cost-effective risk to move to a different expression system that would require new approval and safety testing (Kim et al., 2012; Kelley, 2009). Due to this, the CHO system has been subject to continual improvement over the past 30 years to improve the quantity and quality of mAb product produced.

1.1.3. History of the CHO Cell Line

Chinese hamsters (*Cricetulus griseus*) were first used in the laboratory in 1919, where they replaced mice as disease models for typing pneumococci (Jayapal et al., 2007). Their subsequent use led to an increased interest in the genetics of Chinese Hamsters where they were discovered to have a low chromosome number for mammals ($2n=22$), comprising of 10 autosomal chromosome pairs and two sex chromosomes. As a result of this the Chinese hamster was used for extensive mutagenic and genomic studies (Wurm, 2013; Corbascio et al., 1962). It was not until 1957 however, that the first Chinese Hamster Ovary (CHO) cell was isolated from the hamster by Tjio and Puck, who isolated them for genetic studies. There they noted the cells from the ovary had a highly variable karyotype, with 83.8 % of cells containing 22 chromosomes, but the remaining 16.2 % recording anywhere between 21 to > 44 chromosomes (Tjio and Puck, 1958). The study also showed that they were particularly suited to cell culture due to their fast generation time and resilience in culture plates. Following their isolation the CHO cells were kept in culture for more than 10 months, where they showed a 'particularly hardy and reliable' phenotype as their growth rate was sustained over this time whilst other cell types dropped in growth rate suggesting that cultures could be expanded indefinitely (Puck et al., 1958). Puck et al. (1964) noted the CHO cell had a generation time of ~12.4 hours. CHO cells thereafter became an incredibly popular cell line for research over the years, particularly in cell cycle and toxicology studies. CHO cells have been used as toxicology models to study many different chemicals over the years, from caffeine (Fernandez et al., 2003) to cancer treatments such as cis-platinum (Dritschilo et al., 1979).

As the use of the immortal CHO cells became more prevalent, further studies were performed confirming the instability of the CHO genome. Worton et al. (1977) compared the karyotype of a

fibroblast from the Chinese hamster with a CHO cell line. The results showed the CHO cell line to have a considerably altered karyotype from the original Chinese hamster cell with significant chromosomal rearrangements, however the majority of the rearrangement could still be identified.

It was this interest in the CHO cell line genome that led on to the generation of new CHO cell lines over the years in a complex family tree based on CHO cloning and mutagenesis that ultimately resulted in the CHO clones used in biopharmaceutical manufacture today. This family tree can be seen in Figure 1.1. Puck derived early clonal populations from the CHO cell line such as the CHO-K1 and CHO-Tobey lines (both named after those that worked on them) (Wurm, 2013). Gamma-ray induced mutagenesis studies were then performed by Dr. Chasin's team, who were interested in deleting the DHFR activity of the CHO cell, in attempts to be able to use the DHFR mutants in metabolic studies related to cancer chemotherapies (Urlaub and Chasin, 1980). The CHO-DXB11 cell line was therefore produced, carrying a deletion of one DHFR locus and a missense mutation on the other (Urlaub and Chasin, 1980; Wurm, 2013; Urlaub et al., 1983). It was soon realised that the cell line could be used for amplifying recombinant protein expression with the transgenesis of the DHFR gene (Wigler et al., 1980), and as such became the first CHO cell line used to generate an FDA approved drug – tissue plasminogen activator (Wurm, 2013; Zhu et al., 2017).

To this end, the mutagenesis and cloning of the CHO cell line resulted in a plethora of commercially available CHO clones that vary in features useful for drug manufacture, such as CHO-S clones that have been adapted to grow in suspension (Lewis et al., 2013), and the CHO K1- GS $-/-$ cell line designed by Lonza that amplifies signal in a similar mechanism to the DHFR $-/-$ mutant but with the knockout of Glutamine Synthetase instead (Fan et al., 2012). The DHFR enzyme catalyses the conversion of folate to tetrahydrofolate, which is crucial for the de-novo synthesis of purines and pyrimidines and subsequently, cell replication (Urlaub and Chasin, 1980). The CHO-DXB11 host contains the DHFR deletion, and thus cannot survive without the expression of the DHFR gene on the recombinant mAb DNA plasmid (Urlaub et al., 1986). Following transfection of the plasmid, the methotrexate (MTX) selection system is used to select for the CHO cells that have successfully expressed the plasmid. MTX binds to the DHFR enzyme, inhibiting cell replication, and thus only cells which has increased copies of the DHFR gene – and subsequently high copies of the recombinant mAb – will be selected for (Wurm, 2013; Urlaub and Chasin, 1980).

The GS system was the gene amplification system used in this thesis, and the principle is similar to that of the DHFR selection system. Glutamine is produced when GS catalyses ammonia and glutamate. The GS knockout CHO system therefore cannot survive without Glutamine supplementation in the culture media, or integration of the GS gene on a recombinant plasmid sequence. To amplify the cell's

need to retain integrated gene sequences, methionine sulphoximine (MSX), which is an analogue of glutamate, can be added as an additional selection pressure. MSX irreversibly inhibits GS by binding to the glutamate site of the enzyme. Thus in the presence of MSX, only the cells that have been transfected, and integrated, sufficient GS gene sequence can produce glutamine and survive. Consequently, when using the CHO-GS $-/-$ host system, mAb gene sequences are transfected on a plasmid also containing an exogenous GS sequence. This then relates to the amplification of the mAb as the GS construct is expressed on the same plasmid, conferring that the cells that survive due to a high GS expression also has a high mAb construct expression (Brown et al., 1992; Matasci et al., 2008).

The number of chromosomes in some CHO lineages, used in production capacities today, have changed unrecognisably to the first isolated CHO line (Vcelar et al., 2018). In a CHO DXB11 cell line for example, sequencing studies showed there to be high occurrences of haploidy compared to the original CHO genome (Kaas et al., 2015). The evolution of the CHO cell line into many commercially available options, can be seen in Figure 1.1. Whilst it was the plasticity of the CHO genome that helped it to become the expression system powerhouse of mAb production it is today, paired with the method of transfection by random integration into the genome, it became clear that there was highly heterogenous quantity and quality expression of mAb within individual cells of a CHO culture even after only a single transfection event (Ko et al., 2018). CHO heterogeneity has been shown experimentally whereby a single parental CHO cell expressing mAb was taken from a population and sub-cloned to generate 80 individual cell lines. Upon comparison, the sub clones showed a huge variation in proliferation and mAb titre, with mAb titre increasing up to 5x in comparison to the parental cell population (Davies et al., 2013).

In attempt to mitigate this, regulatory bodies brought in strict manufacturing guidelines for the biopharmaceutical industry, requiring all mAb product produced in CHO cells to be derived from a single progenitor CHO cell to ensure the production characteristics are uniform within the population. The World Health Organisation's Expert Committee summarise this requirement in their 61st report of Biological Standardisation, stating that:

'For proteins derived from transfection with recombinant plasmid DNA technology, a single fully documented round of cloning is sufficient, provided that product homogeneity and consistent characteristics are demonstrated throughout the production process and within a defined cell age beyond the production process.' (World Health Organisation, 2013, pg. 111).

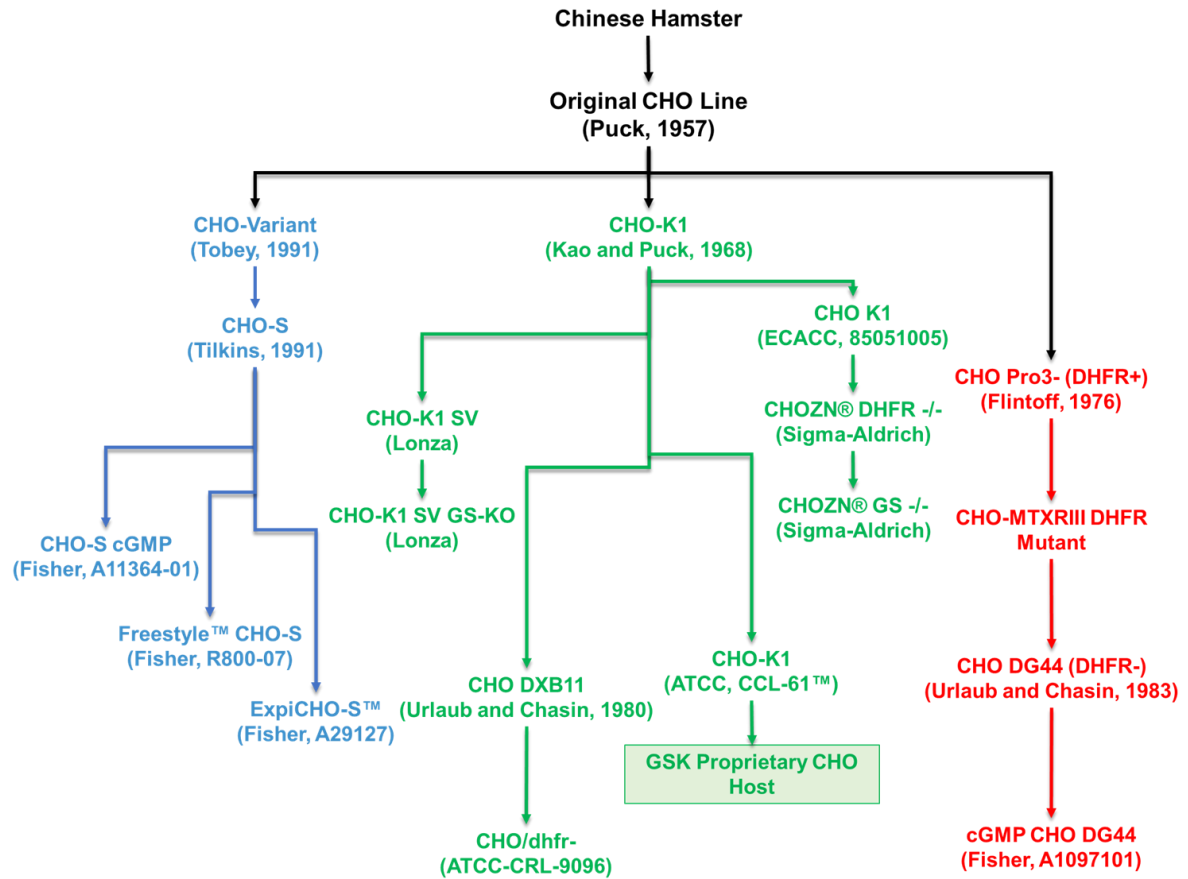


Figure 1.1. Evolution of the CHO Cell Line.

The CHO cell lines used in the biopharmaceutical industry today have been adapted since the first CHO cell line was generated in 1957. Many CHO lines exist, each with specific characteristics that make them desirable for biopharmaceutics. The majority of these CHO lines were derived from three CHO family lines: CHO-Variant, CHO-K1 and Cho Pro3-. Adapted from Lewis et al., 2013; Zhu et al., 2017; Xu et al., 2017b and Dempsey, 2020.

1.1.4. Cell Line Development

The requirement of generating single cell derived clones from a CHO population is typically performed at the Cell Line Development (CLD) stage of biopharmaceutical manufacture. The CLD stage typically starts from transfection of the mAb gene sequence into the host cell line. Following recovery from transfection, the heterogenous mAb expressing cell populations are then single-cell isolated and scaled up to obtain clonal populations (Figure 1.2.). From here, the CHO clones are selected based on their growth and titre characteristics to ensure that the highest concentrations of mAb product can be produced and manufactured when the cells are cultured in large-scale bioreactors. The CLD workflow varies between different companies depending on the host cell line in use and the technology available to the CLD group. These workflows are not readily published however an example protocol of the CLD platform at GSK can be found in methods Section 2.4.

Briefly, the first stage of CLD is the delivery of the gene of interest (GOI) into the CHO host. The mAb heavy and light chains are cloned into an expression plasmid that also contains a GS gene to allow for MSX selection, following the transfection of the expression plasmid into the CHO host by means of lipid transfection or electroporation. The transfected cells are then incubated with the MSX selection and left in static culture, in order to select for the clones with stable gene integration and with the highest amplification of the plasmid. A typical profile for this stage shows a rapid decline in cell viability as most of the cells in the culture are killed by the selection pressure. Normally, after ~3 weeks the culture viability recovers as the majority of cells are expressing the plasmids of interest and have become resistant to MSX. The resulting pre-clonal pools can then be scaled up and eventually transferred into shaking culture. During this process titre and viable cell count are used to triage any pools with poor characteristics. The resultant pre-clonal cell lines can then be single cell cloned.

Single cell cloning during cell line development can take many forms, with many technologies available on the market. Earliest methods included the limited dilution method, as well as fluorescence activated cell sorting (FACS) (Diep et al., 2021). Perhaps the most advanced cloning platform, and the method used in this thesis, is the Beacon microfluidics platform by Berkeley Lights. The Beacon System combines nanofluidic technology, opto-electropositioning (OEP) and fluorescence microscopy to monitor single CHO cells in culture (Le et al., 2020). Up to 1750 cells can be single cell cloned into nanopens within a microfluidic chip and then incubated within these pens for several days (Figure 1.2.B.). Following culture on the Beacon System (typically 5 days) the mAb titre of each clone can be measured using BL's proprietary on-chip Spotlight assay, a fluorescence based assay that binds to the expressed mAb within the pens. From here, the clonal populations can be selected for export from the Beacon based on their titre and growth characteristics. The Beacon System is a ground-breaking technique for clonality assurance as brightfield images are taken before and after cell load into the

nanopens to confirm clonality (Le et al., 2020; Berkeley Lights, 2022). This has resulted in improved clonality assurance values, with one study measuring clonality at 99.36 % for the Beacon compared to 98.52 % by FACS and 96.08 % by a standard limited dilution method (Le et al., 2020).

Following export the clonal cell lines undergo another round of scale-up, triaging at each stage for the best lines based on titre and viable cell count, again increasing in static culture until reaching shake flask cultures. This prevents the unnecessary cost and consumables of keeping poor producer cultures that will eventually be discarded further down the production pipeline. The final clonal populations with the best titres and growth characteristics are frozen and stored in cell banks for future use, as well as being passed onto the Upstream processing team for stability studies and product quality assessment.

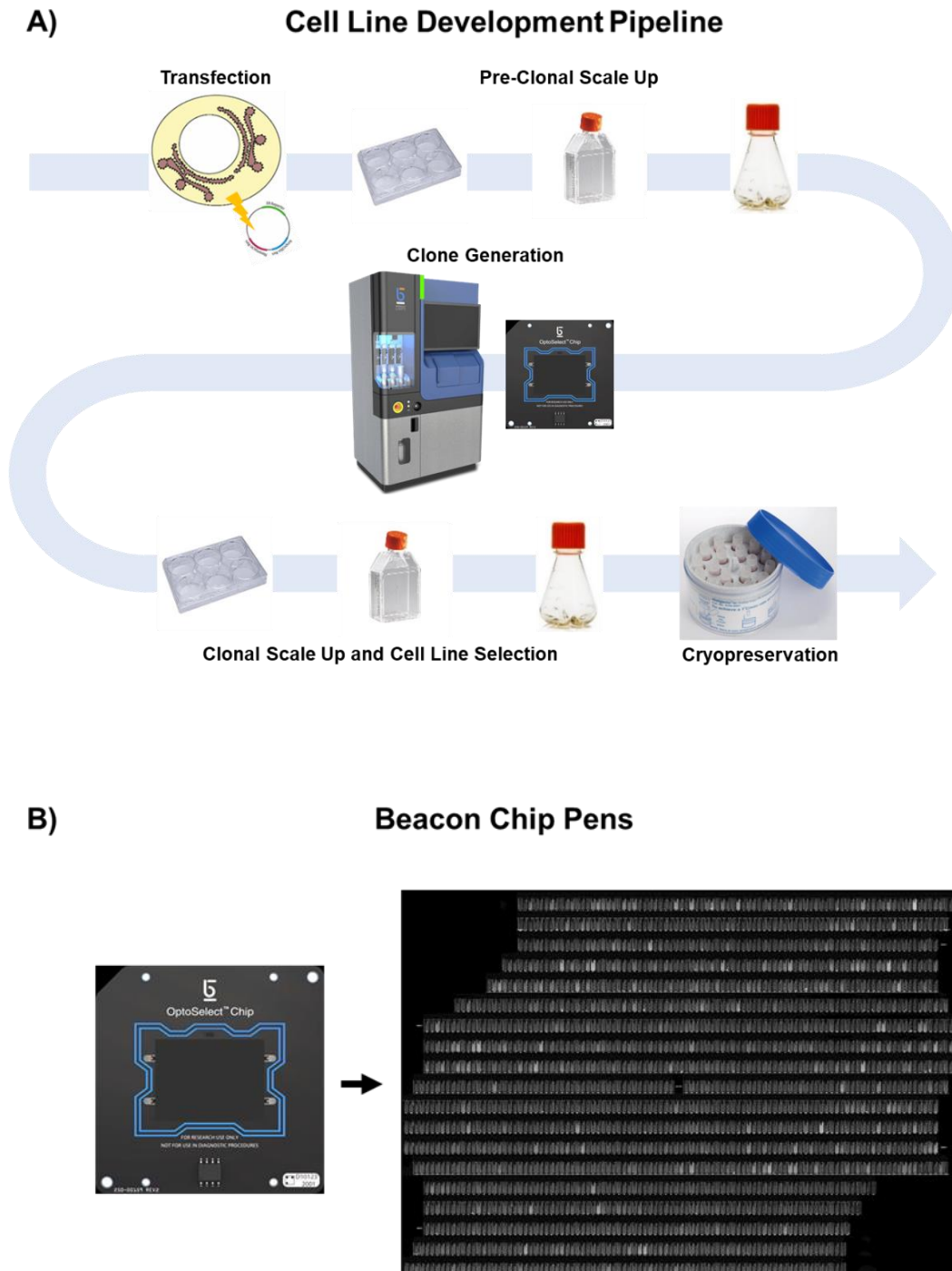


Figure 1.2. Schematic of a typical Cell Line Development pipeline at GlaxoSmithKline.

A) A CHO host cell line will be transfected with the mAb construct of interest, and an MSX selection pressure added to the culture media to ensure only mAb expressing clones survive. The resultant pre-clonal cell lines are scaled up into progressively larger culture vessels from static plate culture to shake flask culture. The pre-clonal pools are added to the Beacon System (BLI) to obtain single cell clones. Each cell is added to a separate nanopen and monitored for its growth and titre. Desired clones are exported into a 96 well plate, and the clonal cell lines are scaled up into progressively larger culture flasks. During this time the titre and growth of the clones are monitored, and undesirable clones are discarded. The final desirable clones are banked for storage (typically using Mr Frostys, Thermo Scientific), before being passed to the Upstream team for stability and product quality assessment. **B)** Image of the OptoSelect microfluidic chip used within the Beacon System (left) and an image of a representative chip following the performance of a Spotlight titre assay. Beacon chip image obtained from Berkeley Lights (2022).

The CLD process is an extremely effective method for selecting high producing CHO clones with good growth characteristics, however improvements in the process to further streamline selection of the highest producing CHO clones means that the CLD process is always evolving. Improvements in the plasmids used to express the gene of interest (GOI), transfection efficiency and selection attenuation are just a few examples of improvements seen to CLD in recent years (Lai et al., 2013).

Another area of interest for CLD is the ability to select CHO clones for their characteristics other than just mAb titre and growth, such as product quality, at earlier stages. Currently, these features cannot be measured during CLD due to the amount of time they take to analyse, or the volume of cells required for investigation. Consequently, the quality of the mAb produced cannot typically be measured until Upstream processing. Product quality, such as the mAbs propensity to aggregate or become charged can have dangerous effects for patient safety as it can illicit immunogenic responses and effect drug efficacy (Li et al., 2016), but typically are not measured until purification of the culture media of a 15 day production study. Specific product quality attributes for mAb therapies are discussed in Section 1.2.5.

The ability to predict these factors using cellular based assays and reporter genes during CLD is of key interest as it would help reduce the amount of undesirable cell lines that were progressed through CLD. To identify potentially relevant biological markers, the structure and folding of the mAb must be understood first.

1.2. Antibody Structure, Function and Folding in CHO cells

1.2.1. Antibody Function

Antibodies are produced by the immune system of all vertebrates and recognise foreign antigens on the surface of pathogens and trigger their destruction by immune cells. Antibodies are produced exclusively by B lymphocytes, with genetic diversity to bind to specific targets conferred by the individual B lymphocyte that produces it (Kemler and Schaffner, 1990). It was then discovered that antibodies with a monovalent affinity for a specific disease marker could be used to target specific cells for destruction by the patient's own immune system (Walsh, 2018). Trastuzumab for example revolutionised the treatment of a particularly aggressive form of breast cancer that overexpressed the Human Epidermal Growth Factor Receptor 2 (Her2) receptor (Carter et al., 1992). Trastuzumab was designed to bind to the Her2 receptor of the breast cancer cells, which ultimately marks them for destruction by natural killer cells of the immune system (Cooley et al., 1999) and prevents tumour cell growth by inhibiting the MAPK signalling pathway (Neve et al., 2001).

Antibodies can also use other mechanisms of action to destroy diseased cells. They can have an antagonistic effect on disease targets by binding to and inhibiting the receptors that would typically cause pathological downstream signalling (Hansel et al., 2010; Verhoeven et al., 2018). Infliximab works by this mechanism of action for example. Infliximab inhibits Tumour Necrosis Factor alpha (TNF- α), a pro-inflammatory cytokine, of which it's overexpression is seen in a number of inflammatory and auto-immune disorders (Winterfield and Menter, 2004). mAbs can also target diseases by attracting and binding to components of the immune system after binding to a diseased cell receptor. The Fc receptor of the mAb can mark the cells for death by phagocytosis, or to natural killer cells that destroy the diseased cells by antibody-dependent cell-mediated cytotoxicity (ADCC). Similarly to ADCC the binding of mAbs can cause complement-dependent cytotoxicity (CDC), whereby the presence of the mAb on the antigen triggers the binding of the C1q protein to the antibody which in turn activates the membrane attack complex (MAC) (Beum et al., 2008), that ultimately causes cell lysis of the diseased cell (Lutterotti and Martin, 2008). Rituximab, used as a blood cancer treatment, uses both ADCC and CDC to target B cells expressing the cell surface antigen CD20. Rituximab therefore actively marks all B cells for apoptosis by immune cells, whilst avoiding terminally differentiated plasma cells. The immune system can then replace the depleted B cell population with healthy B cells from lymphoid stem cells, and approximately 6 months after finishing Rituximab treatment the pool of B cells can be restored (De et al., 2017).

Finally, mAbs can block the inhibitory cell signalling interactions seen between T cells and diseased cells, that the diseased cells would typically use to mask their diseased state. An example of this signalling includes the programmed cell death protein 1 (PD-1) on T cells and programmed cell death ligand 1 (PD-L1) signalling reaction. T cells typically use the presence of PDL-1 receptors on somatic cells to recognise them as healthy cells by signalling with the PD-1 receptor present on the T cell surface. These PD-L1 receptors can also be present on diseased cells, and thus are masked from T cell mediated destruction. Antibodies designed to block either PD-1 or PD-L1 can therefore stop this evasion, and ensure that T cells can recognise the diseased cells. Multiple mAbs are now approved targeting PD-1 for example, including Nivolumab and Pembrolizumab. These mAbs have been approved for use in many diseases such as Hodgkin's lymphoma and non-small cell lung cancer (Prasad and Kaestner, 2017).

1.2.2. Antibody Structure

Generally, an antibody molecule consists of two identical heavy chains and two identical light chains. The chains form a 'Y-shaped' conformational structure, and are held together by intra and inter chain disulphide bonds (Feige et al., 2010; Huber, 1976; SinoBiological, 2022) (Figure 1.3.). Chiu et al. (2019) reviews the structure of the antibody. An antibody can be characterised by its two regions: the constant (C) region which is relatively conserved in amino acid structure between different mAbs, and the variable (V) region which is specific to each mAb and determines the type of antigen the mAb binds to. This specificity is determined specifically in the hypervariable regions, which is made up of stretches of diverse amino acids sequences (Feige et al., 2010).

The heavy and light chains can be further sub-divided into domains based on the folding of the mAb. A single heavy chain comprises four domains: CH1, CH2, CH3 and VH. A single light chain consists of only two domains: VL and CL (Amzel and Poljak, 1979). Each individual chain can be further divided into their effector function for the mAb. Each monomer has two antigen binding fragments (Fab), and are the regions where the mAb binds to the antigen and one fragment of crystallisation (Fc) fragment, which allows signalling to immune cells (Chiu et al., 2019).

The individual chains are classified dependent on the type of heavy and light polypeptide chain expressed. The heavy chain can be one of 5 different classes: Alpha (α or IgA), Delta (δ or IgD), Epsilon (ϵ or IgE), Gamma (γ or IgG) and Mu (μ or IgM). The heavy chain class determines the functional activity of the antibody molecule. IgG, IgA, IgE and IgD exist in humans in monomeric form as per Figure 1.3. IgA can also exist as a dimer in the human mucosa bound at the Fc region to prevent bacterial infection. IgM is always found in a pentamer formation as IgM is associated with the opsonising of

foreign antigens in the primary immune response thus the structure provides an efficient response (Schroeder Jr et al., 2010). The light chain can be either kappa (κ) or lambda (λ) in humans. Either type can bind to any of the heavy chain classes, however the pairs are always of the same type (Feige et al., 2010).

Despite the varieties of mAbs found in nature, all therapeutic mAbs currently approved are IgGs due to their well-characterised effector function and their prolonged half-life. IgGs can be further subdivided into IgGs 1-4 which have mutational differences in their γ heavy chain. The structural differences among these heavy chains include antibody flexibility, length of the hinge region, functional activity and the number and location of inter-chain disulphide bonds (Wang et al., 2007; Vidarsson et al., 2014). IgG1 and IgG4 have 2 disulphide bonds linking the two heavy chains together in the hinge region, whilst IgG2 and IgG3 have 4 and 11 respectively (Liu and May, 2012). All IgG subtypes are used in therapeutic mAb production, with the exception of IgG3 as it is rapidly cleared from the serum and has an extended hinge region that leaves the IgG3 prone to instability and aggregation. Of the remaining IgG subtypes, IgG1 is the most commonly used for mAb production. It has many benefits over the other subtypes including an increased stability and half-life, as well as its higher serum concentration (Muhammed, 2020). It also elicits a more potent effector mechanism than IgG2 and IgG4, as IgG1 can bind to all sub-classes of the Fc receptors on immune cells and the C1q component of the complement pathway with higher affinity than other IgG subtypes (Rayner et al., 2015).

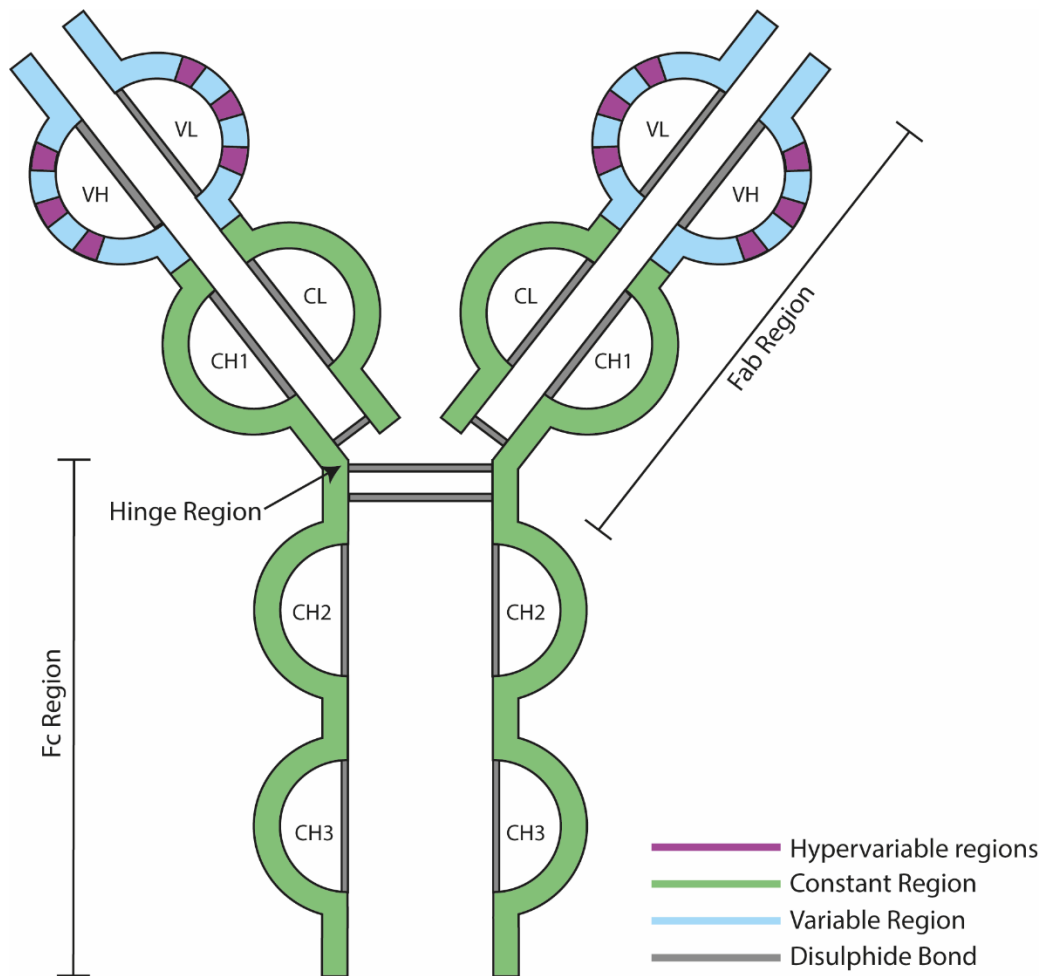


Figure 1.3. Typical antibody structure.

Antibody monomers are formed of two identical heavy and light chain peptide sequences, that form a 'Y' shaped confirmatory structure. The chains are held together via disulphide bonds. The antibody can be categorised by its two regions: the constant region (C) and the variable region (V). Each region is further split into domains, dictated by the way it is folded following translation. The constant region is made up of the CH1, CH2, CH3 and CL domains, whilst the variable domain is made up of the VH and VL domains. The variable domains contain the hypervariable regions, which gives the antibody its ability to bind to its specific antigen. The mAb structure can be further categorised by its two functional regions: The Fab region that binds to the target antigen (CL, VL and CH1, VH), and the Fc region that allows signalling to immune cells (CH2 and CH3). Adapted from SinoBiological (2022).

1.2.3. Antibody folding

Antibody heavy chains and light chains are co-translationally translocated into the endoplasmic reticulum (ER) and folding begins even before the polypeptide chains are completely translated. The folding process is complex, and IgGs typically assemble as heavy chain dimers before the binding of the light chains (Feige et al., 2010). The whole process of antibody folding can be seen in Figure 1.4. Initial folding occurs in a sequential manner for the individual chains, however the folding process itself is similar between the chains. This process has been described as the 'Ig Fold', whereby each domain in the independent light and heavy chains fold in the same manner. The Ig fold describes a distinctive fold in each antibody domain comprised of two anti-parallel β -sheets that oppose each other at an angle of 30° (Wang, 2013; Bork et al., 1994). One of the sheets is conserved in both heavy and light chain domains (sheets D, E, B and A), whilst the second sheet varies dependent on the domain type – three β -strands are found in the constant region (G, F and C) and five in the variable domain (G, F, C, C' and C'') (Williams and Barclay, 1988; Chatterjee et al., 2021). These two sheets are held together by a disulphide bond, perpendicular to the B and F strands of each sheet pair. The successful folding of the domain then allows the sequential folding of the next domain until the chains are ready for folding together (Wang, 2013).

Following the folding of each domain sequentially, further chains can be bound together to form the fully-folded mAb construct, and the order of this folding remains the same in all IgG mAbs. The molecular chaperone Binding Immunoglobulin Protein (BIP) binds to the nascent protein chains at the CH1 and VL regions of the chains to prevent them from passing out of the ER before being correctly folded. Heavy chain folding is then first achieved in the VH and CH2 domains, followed by the CH3 domain. After the folding of the CH3 domain is completed, the heavy chain can dimerise with another heavy chain, where they are held together by disulphide bonds. Protein Disulphide Isomerase (PDI) is an enzyme that catalyses the formation of these disulphide bonds between cysteine residues in the protein sequence. From here the folded light chain displaces the BIP which induces the folding of the CH1 domain. Following complete folding of the mAb in its 'Y shaped' tetramer, a disulphide bond bridge between the HC and LC is formed (Feige et al., 2010; Roth and Pierce, 1987).

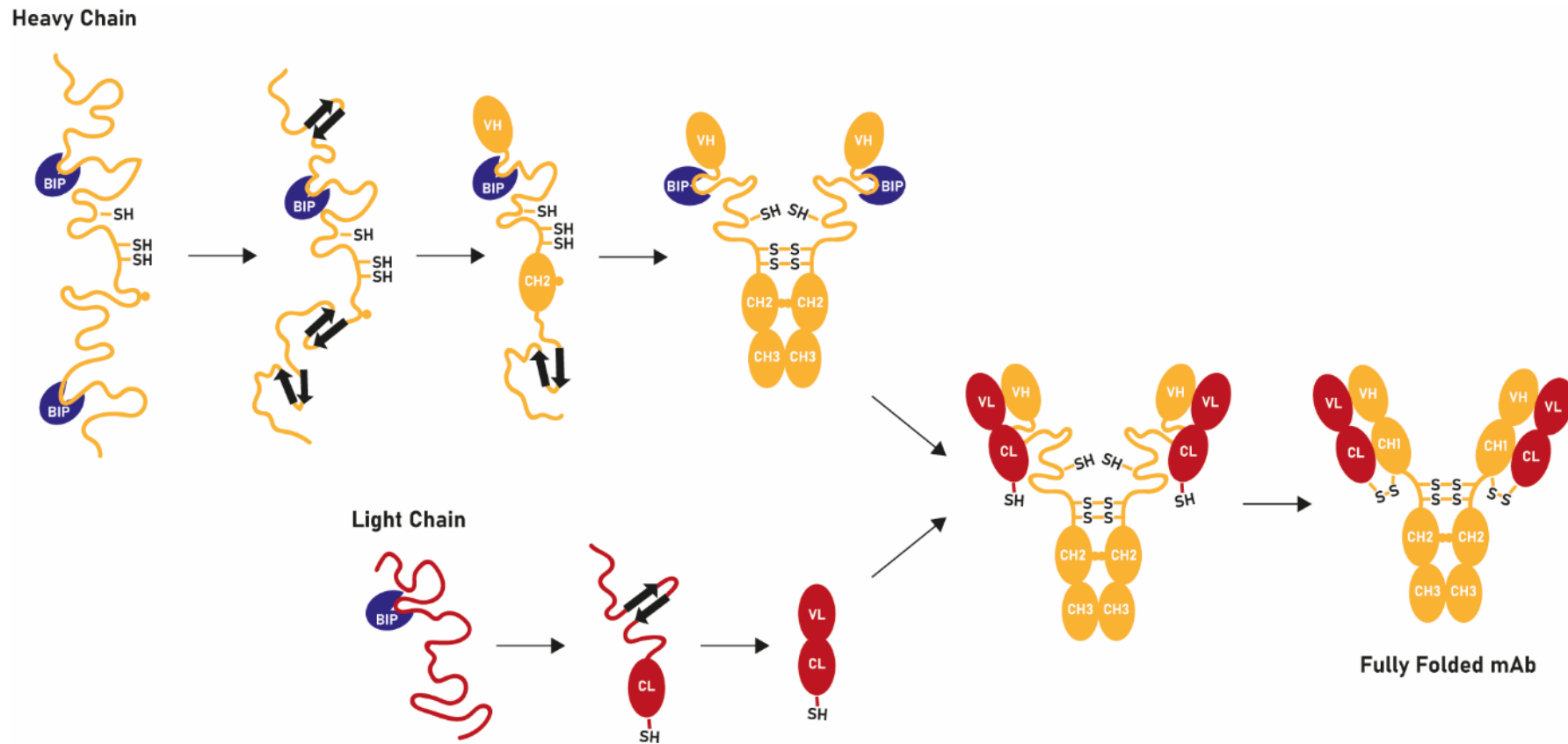


Figure 1.4. Antibody folding from nascent polypeptides.

The heavy chain and light chains are translated separately, and prevented from ER export by the association of BIP. Sulphydryl (SH) side chains are present on the nascent polypeptides, prior to disulphide bond formation. The nascent polypeptide chain folds into their respective domains sequentially, following the formation of the Ig fold (beta sheets, black arrows). In the light chain the constant light domain is first folded, followed by the variable light chain. In the heavy chain the CH2 and VH domains are folded first, followed by the CH3 domain. During this time the CH1 domain remains unfolded and associated with BIP. The folding of the CH3 domain allows for heavy chain dimerisation, held together by disulphide bonds at the hinge region. Disulphide bond formation is generated in an oxidation reaction between two SH chains and the chaperone Protein Disulphide Isomerase (PDI). The folded light chain can then associate to the heavy chain, and BIP dissociates from the CH1 region. The CH1 region can then fold, and a disulphide bond is formed between the CL and CH1 domains. The fully folded mAb is then ready for export from the ER. Adapted from Feige et al., (2010).

1.2.4. Quality control of antibody folding

The process of the mAb folding is closely maintained by quality control chaperones that ensure the proteins are folded into their functional state before translocation from the ER to the Golgi. Misfolding of antibodies can result in exposed hydrophobic regions, aggregation and/or un-paired cysteine residues (Chakrabarti et al., 2019), and have shown immunogenic reactions in humans, discussed in Section 1.2.5. Strict quality control checks are therefore present in the ER to ensure the production of correctly folded and functional mAb. Calreticulin, and its membrane bound homolog, Calnexin, is one molecular chaperone that modulates this (Ellgaard et al., 1999). The Calreticulin quality control pathway can be seen in Figure 1.5.

Following entry to the ER the nascent polypeptides are modified with the addition of an oligosaccharide asparagine chain, in ASN-X-SER/THR motifs. This chain is then sequentially modified by glucosidases I and II to form a mono-glucosylated intermediate that is recognised by the ER lectins Calreticulin (CALR) and Calnexin (CNX) (Hebert et al., 2005). CALR and CNX are homologs of each other, with only minor structural differences that results in CALR's presence in the ER lumen whilst CNX exists as a type I membrane protein (Ellgaard et al., 1999). The homologs bind to the mono-glucosylated proteins, preventing the export of the unfolded protein and protecting it from aggregation (Hebert et al., 1996). The two homologs also associate with PDI to promote disulphide bond formation in the proteins, as mentioned above. The mAb structures are released from CALR and CNX following further glucose cleavage by glucosidase II. From here the proteins can fold into their final state. Uridine diphosphate-glucose:glycoprotein-glucosyltransferase (UGGT) performs a final regulatory step on the folded protein, after which it can be transported to the Golgi if correctly folded (Määttä et al., 2010; Jiang et al., 2014). Incorrectly folded proteins are cycled back for more refolding attempts by adding a glucose moiety to the protein. Continuously unsuccessful recycling of misfolded protein is prevented by ER α -mannosidase I (ERManI) and ER degradation enhancing α -mannosidase-like protein (EDEM) which cleave mannose moieties from the glycan that would be reglucosylated by UGGT for recycling (Eriksson et al., 2004; Jiang et al., 2014). From here, the incorrectly folded protein can be removed by the ER-associated degradation (ERAD) pathway, where it is ubiquitylated and degraded by proteosomes (Travers et al., 2000).

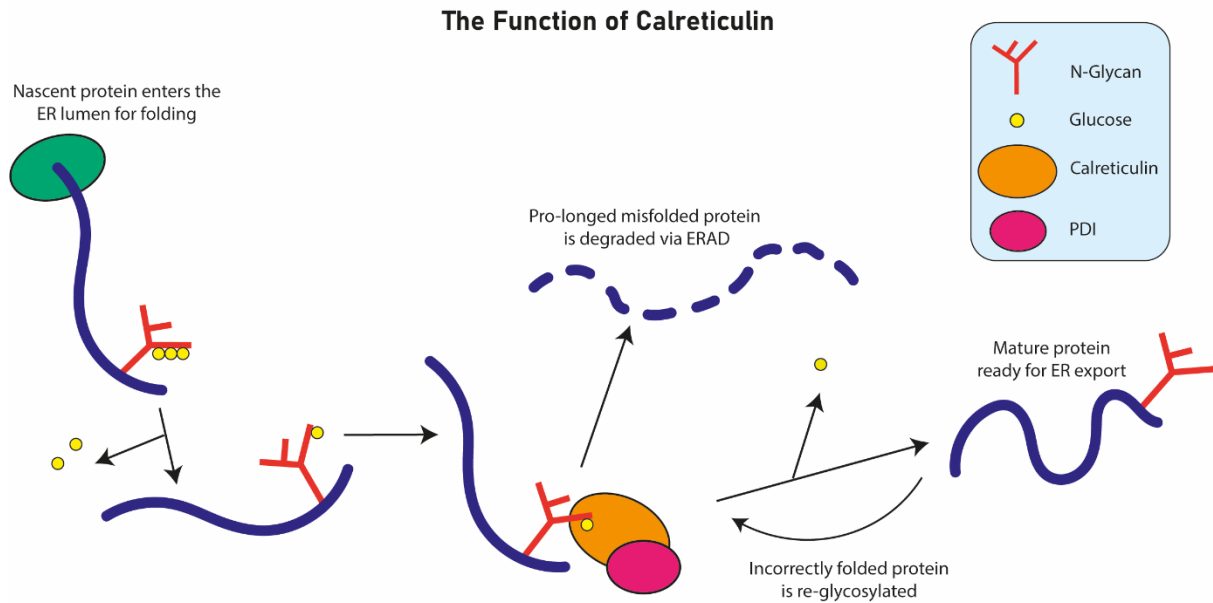


Figure 1.5. The role of Calreticulin in protein folding within the endoplasmic reticulum.

Nascent polypeptides enters the ER lumen from the ribosome for protein folding. The peptide is modified with the addition of an oligosaccharide asparagine chain. Two glucose residues are sequentially removed to allow Calreticulin chaperone recognition of the protein. Calreticulin holds the peptide to prevent it from ER export and associates with PDI to catalyze disulphide bond formation. The final glucose residue can then be removed from the protein, and the mature, folded protein is ready for ER export. If the mature protein is incorrectly folded however, the polypeptide will be re-glucosylated to mark it for Calreticulin binding and re-folding. If this process of re-folding is repeated many times then the protein can instead be marked for degradation via ER-associated degradation (ERAD). Adapted from Jiang et al., (2014).

1.2.5. The effects of improper folding on mAb product

When the protein folding pathway is not able to cope with the demand of folding, improper folding can occur and exposed regions on the mAbs can then result in product quality issues such as the aggregation of the mAb product. Aggregates are clusters of denatured antibodies, and are of increasing concern to regulators as they expose normally hidden epitopes that increases the risk of inadvertent immunogenicity (Li et al., 2016; Xu et al., 2017a). It is crucial therefore to ensure that aggregated mAb product is not present in the final drug formulation, as this could have extremely dangerous effects on patients especially if the product has to be administered over a long-term basis (Singh, 2011).

Aggregated products can present in small soluble aggregates or as insoluble, macroscopic aggregates (Kijanka et al., 2018). Aggregates can be reversible or irreversible, with the reversible aggregates typically being smaller in size. The irreversible aggregates on the other hand are not readily dissociable unless extreme temperature or chemical pressure are placed on them (Roberts, 2014). These aggregates have typically lost their folded structure and as a result are able to create very strong hydrophobic interactions with each other (Bajaj et al., 2006). The effect of aggregate size on immunogenicity has been greatly debated, and much contradictory evidence has been shown. Rosenberg (2006) highlighted that low molecular weight aggregates (e.g. 2-3 monomers) were inefficient at inducing an immune response, whilst larger multimers were much more efficient, as shown in murine models (Fradkin et al., 2009). Telikepalli et al. (2015) also showed that when peripheral blood mononuclear cells (PBMCs) were incubated with a sample of aggregated mAbs of either micron-sized particles or nanometre-sized particles, the strongest release of cytokines was seen in the larger, micron sized particles. Conversely to this, Kijanka et al. (2018) showed that submicron sized particles were more immunogenic than soluble or micron-sized particles in mouse models administered with a murine mAb. Thus the presence of aggregates at any size should be considered immunogenic and problematic for mAb quality, in fact special consideration may be required for smaller aggregates as these cannot be as easily detected via purification processes unless using high performance liquid chromatography (HPLC) techniques like Size Exclusion Chromatography (SEC) that can detect particles in the sub-visible 10-25 nm range (Narhi et al., 2012; Bansal et al., 2019).

The identification of what causes aggregation is difficult, as aggregation can be caused by incorrect protein folding by the CHO protein synthesis machinery or by external culture factors such as extremes of pH, temperature and ionic strength (Li et al., 2016). In addition, downstream processing procedures following harvest such as freeze-thaw cycles can also have an impact on aggregation (Cromwell et al., 2006, Hassell *et al.*, 1991). Joshi et al. (2014) showed that increasing the ionic strength of the buffer

the mAb was incubated in during size exclusion chromatography (SEC) resulted in an increase in percentage of product that was aggregated and was exacerbated even further when the temperature was increased from 4 °C to 30 °C. The speed of product thawing can also affect aggregate formation. For example, when a molecule is slowly thawed there can be up to 3 times more aggregate compared to a sample which was thawed quickly (Desai et al., 2017). The external factors can be mitigated for with strict controls on culture, thawing and storage conditions, however the cellular causes of aggregation from the CHO clones inherent capacity to fold proteins correctly cannot be controlled as easily and means its removal is required during downstream processing. Biological based aggregation can be caused by the mAb structure itself as well as environmental factors of cell culture such as temperature, pH and media components (Gomez et al., 2020; Jing et al., 2012; Masuda et al., 2021). Other biological factors that can affect aggregates include the location in the genome that the plasmids integrates into, which can affect translation and result in truncated proteins (Cooper et al., 1998). A high concentration of UPR chaperones such as Protein Disulphide Isomerase (PDI) and Binding Immunoglobulin Protein (BIP) that assist in protein folding have also shown to correlate with aggregation (Ishii et al., 2014). One attempt to control cellular based aggregates has focused on manipulation of the CHO host. Le Fourn et al. (2014) for example, overexpressed the signal retention peptide 14 (SRP14) in a CHO host cell line. Upon mAb expression, the SRP14 overexpressing CHO host abolished all aggregated light chain that had been seen in the wildtype CHO host. These aggregated proteins however had only been seen in a low mAb producing wildtype CHO host, and were not seen in a high producer equivalent suggesting that the issue of aggregation was not relevant to the high producing clones that would be typically chosen. Instead, it highlights how much of a clonal variation there is in mAb expressing clones and how overexpression of proteins such as SRP14 may not be necessary.

Aggregation is not the only product quality issue that has to be considered for effective mAb production. Fragmentation is another well-described disruptive process to antibody production and describes the mAb product that is smaller than its fully-folded state (Wang et al., 2018). Similarly to aggregation the cause of fragmentation can be caused by external environmental factors such as pH and temperature, as well as cellular factors. Fragmentation can occur during protein production and in the purification process, or later during storage. There has even been a link seen between aggregation and fragmentation, as the build-up of fragmented protein with exposed hydrophobic regions can result in the formation of aggregation (Vlasak and Ionescu, 2011). mAb product storage is one environmental factor shown to impact fragmentation, as increasing mAb product storage temperatures was directly proportional to increasing amounts of fragmented product at the hinge region (Cordoba et al., 2005). Vlasak and Ionescu (2011) reviewed the many potential effects of

fragmentation on the mAb as a drug target at different regions of the construct, with an emphasis on non-enzymatic causes such as pH and temperature. Firstly, fragmentation in the hinge region of the mAb could affect its function due to the loss of the Fc-mediated effector function, whilst the potency of the Fab binding may be reduced due to the loss of the second Fab arm. Similarly, fragmentation at the constant region could reduce Fc-mediated effector function and the mAb circulation half-time.

The cause of fragmentation is complex however, and appears to be heavily intertwined with cellular, environmental and recombinant protein expression factors. One cellular cause of fragmentation has been documented by the secretion of host cell proteins such as Cathepsin's, that are purified alongside the mAb product following purification (Dovgan et al., 2021; Luo et al., 2019). Dovgan et al. (2021) showed that the knock-down of Cathepsin D in CHO pools expressing two different mAb constructs reduced fragmentation levels significantly (from ~ 20 % to less than 5 % total product in one mAb expressing cell line) suggesting that Cathepsin D causes fragmentation. However, when Cathepsin D was knocked out and fragmentation measured in clones generated from these pools, variable results were observed - some clones had limited fragmentation (< 5%) whilst others had levels similar of the wildtype host (> 20%). The authors hypothesised that this fragmentation was caused by the upregulation of other host cell proteases in response to the knockout of Cathepsin D, making the prevention of fragmentation extremely difficult. Another protease which could also be causing fragmentation is Cathepsin L, which Luo et al. (2019) showed to be a cause of fragmentation. However, host cell proteases are unlikely to be the sole cause of fragmentation, as shown by the Cordoba et al. (2005) temperature study discussed above. The study showed that none of the fragmentation was caused by cell proteases, including Cathepsin D and L, as the addition of protease inhibitors Pepstatin A and E64 did not reduce fragmentation which are the families of proteinases for Cathepsin D and L respectively. This highlights that fragmentation may be highly dependent on the mAb type expressed, or the CHO clone themselves. Fragmentation has also been shown to be caused by frameshift mutations that result in premature termination of the protein expression, with Lian et al. (2016) showing that a fragmented peak that was present in a high producing mAb expressing CHO clone was actually caused by a frameshift mutation in the heavy chain constant region of the mAb.

The variation in mAb product charge is another crucial product quality that has to be addressed when designing drugs for patient usage. The charge on the mAb product is determined by the isoelectric point (pI) of the molecule which is where the mAb has no electrical charge and is determined by the presence of charged amino acids within the mAb. Variations in the charge from the main isoform is caused by a shift in pI. Charge variants with a lower pI are referred to as acidic variants, whilst those with a higher pI are basic variants (Miao et al., 2017). The variation of charge, and thus the shift in pI

into the production of the acidic and basic isoforms depends greatly on the specific modifications and their locations (Du et al., 2012). Acidic charges have been shown to form from many different modifications, such as the presence of sialic acid, deamidation and glycation (Khawli et al., 2010; Vlasak et al., 2009; Quan et al., 2008). Basic isoforms on the other hand have been shown to form as a result of amidation, fragmentation and the incomplete formation of disulphide bonds, among others (Johnson et al., 2007; Zhang et al., 2011; Ouellette et al., 2010). The variation of charge may substantially affect the antibodies effectiveness as a drug target; with target binding, tissue distribution and tissue penetration all being potentially affected by variation from the main isoform.

Regardless of the product quality attribute, it could be proposed that any future research on product quality should focus on the uncontrollable CHO clonal variation, compared to the more controllable environmental factors. Common CHO clonal factors impacting fragmentation for example include the expression of protein folding chaperones such as Protein Disulphide Isomerase (PDI) that folds the mAb structure. One study showed that clones with lower PDI mRNA expression resulted in higher fragmented product (Ishii et al., 2014). As PDI is crucial to the disulphide bond formation that holds the mAb structure together this is not surprising. Taken together these studies highlight substantial evidence for the effects of improper folding on the mAb product quality.

1.2.6. Complex monoclonal antibody formats

The importance of correct mAb folding becomes even more significant when considering novel mAbs, which are becoming increasingly complex and diverse in format (Figure 1.6. Upper). Many novel formats of mAb constructs are now being considered for their potentially beneficial features. Smaller mAb formats such as Fab fragments, and monovalent IgGs that contain only one heavy and light chain half-body, have the benefit of being able to reach antigens in hard to reach areas. Ranibizumab for example, is a Fab fragment that inhibits angiogenesis by inhibiting vascular endothelial growth factor A (VEGFA) and is approved for use in age-related macular degeneration (AMD) among other diseases. The loss of vision from AMD is characterised by the creation of new bloody vessels in the choroid layer of the eye, that is stimulated by excessive expression of VEGF. The Fab format of Ranibizumab is therefore particularly beneficial for diseases, such as AMD, as the small molecule can penetrate deeply into the retinal pigment epithelial cells (Zou et al., 2011).

Fc fusion proteins, that contain a therapeutic protein bound to a mAb Fc sequence, can pair the immune effector function of the Fc region of the mAb with the effector function of the attached drug (Linderholm and Chamow, 2014; Nelson, 2010; Absolute Antibodies, 2022). Bispecific mAbs are one

of the most popular classes of antibodies currently in development. Bispecific mAbs contain the same Y-shaped mAb molecule but express two different heavy and light chains, with the aim to target multiple antigen targets on a single molecule (Kontermann, 2011). The antibody can be directed to different epitopes on the same antigen to increase mAb response, or they can target different antigens to have two effector actions on the disease target. Bispecifics with two targets can be used to target a diseased cell on one arm, and recruit immune cells on the other arm for example, inducing an immune effector response (Kontermann, 2011). Blinatumomab is an approved bispecific mAb fragment that uses this effector function, by binding to the CD19 receptor on cancerous B cell targets on one arm, whilst binding to the CD3 receptor of cytotoxic T cells on the other, ultimately engaging them for T cell mediated cell death (Przepiorka et al., 2015; Topp et al., 2008).

Bispecifics present a unique challenge for production in the CHO expression system as the folding of the chains can result in up to 9 different heavy and light chain combinations (Figure 1.6. Lower), which can drastically reduce the percentage of heterodimer in the final product (Carter, 2001). Efforts have been made to address this concern with techniques such as the 'knob in hole' technology, whereby complementary mutations between the two heavy chains in the CH3 domain are made which non-covalently bind to each other (Shatz et al., 2013; Merchant et al., 1998). Although, this does not address the issue of light chain pairing to the correct heavy chain. Whilst these technologies have improved bispecific productivity, problems still exist. For example, Gong et al. (2021) performed a study to try and engineer the heavy chain to increase the amount of desired bispecific product produced. 32 combinations of mutations were made and tested. However, only about half of the molecules tested contained at least 50 % desired bispecific mAb.

Most literature suggests that the capacity of the protein folding pathway is crucial for producing fully folded and functional product, and this will only be exacerbated by the expression of the more complex formats that are now coming into the forefront of biopharmaceutical production. To consider the effect of poor protein folding capacity in CHO cells, there must also be consideration to the recovery mechanisms they have in response. When the requirements for protein folding are higher than that of the cells protein folding capacity (pg/cell/day), the Endoplasmic Reticulum (ER) enter a state of stress and the cell attempts to initiate pathways to recover the folding capacity (Lee et al., 1999). Thus, there has been significant interest in recent years in the antibody production community to either monitor ER stress or use it to enhance antibody production (Prashad and Mehra, 2015; Kober et al., 2012; Chandrawanshi et al., 2020; Roy et al., 2017). More recently, the effect of ER stress has also been measured in bispecific expressing cell lines (Guo *et al.*, 2021).

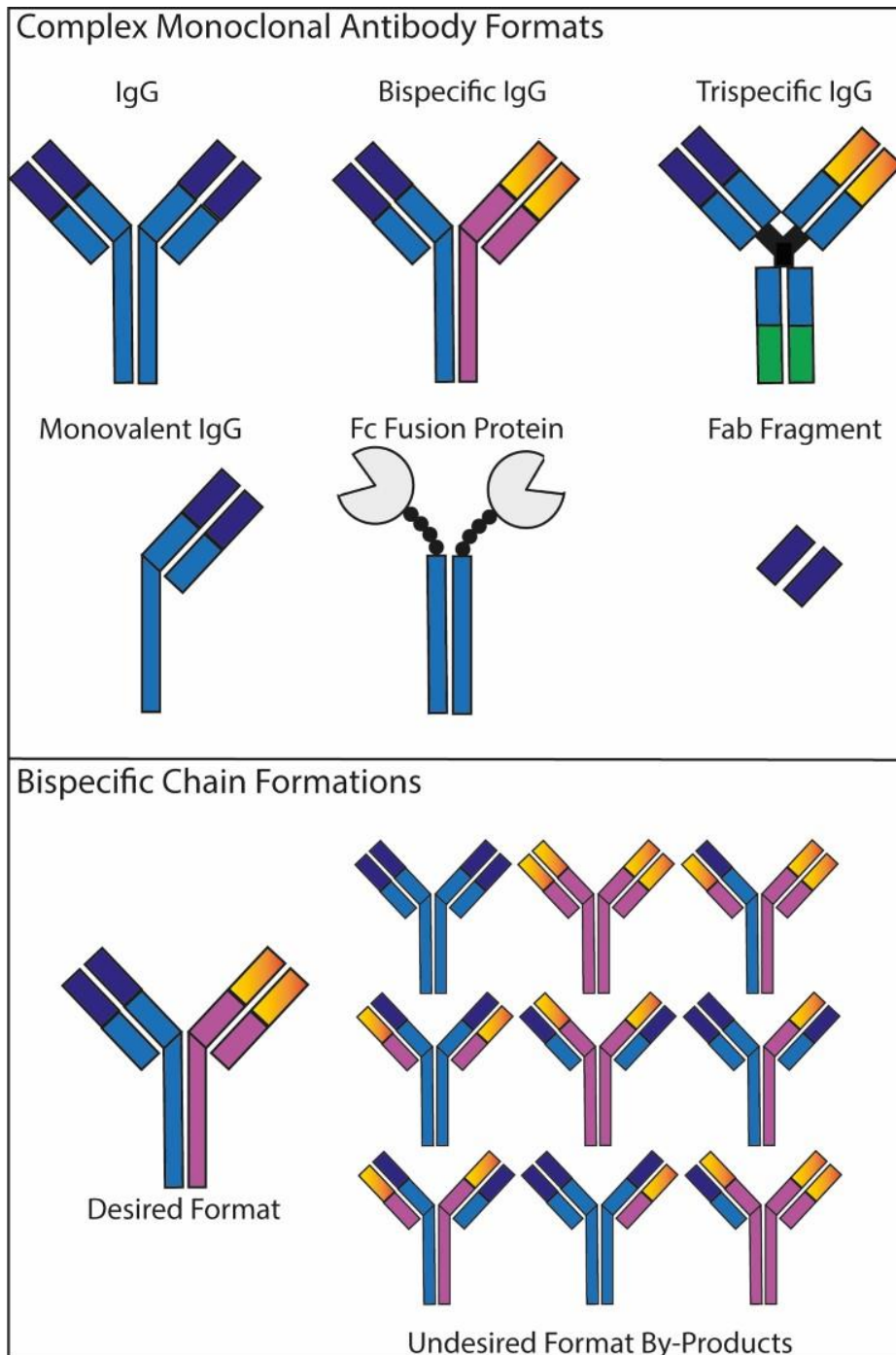


Figure 1.6. Examples of novel monoclonal antibody formats.

Monoclonal antibody formats are becoming increasingly complex and sophisticated in their design but lead to production issues. **A)** Examples of complex mAb formats. Bi-specific mAbs contain two different heavy and light chains to bind two different antigens. Similarly, trispecific molecules can target three different antigens. Smaller versions of standard mAb formats also exist such as monovalent IgGs, that contains only one heavy and light chain and even smaller, Fab fragments can then target the smallest of epitope sites. Finally, Fc fusion proteins contain a therapeutic protein bound to an Fc sequence, allowing the protein drug to also interact with the immune system. Adapted from Absolute Antibodies (2022). **B)** Bispecific chain combinations that can arise from expressing two different heavy and light chains. The desired format is followed with 9 unwanted to combinations including homodimers in the heavy chain and light chain. Adapted from Carter (2001).

1.3. Monoclonal antibody production can lead to endoplasmic reticulum stress

1.3.1. Endoplasmic reticulum stress

Whether the mAb is a simple or complex format, its expression causes an intense pressure on the CHO cells host machinery. Kallehauge et al. (2017) found that ~ 15% of all ribosomes in a mAb expressing CHO cell line were actively translating mRNAs related to the expression plasmid, reducing the cell's capacity to synthesise its own endogenous proteins. This increased translation has a knock on effect for the Endoplasmic Reticulum (ER) as it has an increased amount of exogenous protein to correctly fold as well as maintaining host protein expression. This increase in folding requirement can result in a state of ER stress, whereby the number of proteins being folded overwhelms the folding capacity of the ER and results in a build-up of misfolded protein in the ER lumen (Prashad and Mehra, 2015; Walter and Ron, 2011).

1.3.2. The Unfolded Protein Response

Upon ER stress cells initiate the unfolded protein response (UPR), a pathway that aims to remove the misfolded or unfolded protein that have accumulated in the ER lumen and return the organelle to a state of protein-folding homeostasis. To alleviate the build-up of misfolded protein, the UPR will trigger the upregulation of protein folding chaperones in an attempt to re-fold the misfolded proteins, as well as temporarily attenuating further protein translation to prevent more build up. In some cases, it becomes impossible to save the ER and apoptosis will be initiated. This transition between correcting ER stress and initiating apoptosis has to be finely controlled, and is achieved by initiation of the three different branches of the UPR pathway, each activated by a separate effector molecule (Figure 1.7.) (Chakrabarti et al., 2011; Du et al., 2013). These three effector sensor molecules are: activating transcription factor 6 (ATF6), Inositol-requiring enzyme 1 (IRE1) and protein kinase RNA-like endoplasmic reticulum kinase (PERK) (Cao and Kaufman, 2012). Whilst each of these pathways perform their own distinct effector pathway, they can produce responses that either restore the ER or initiate apoptosis, and a significant amount of cross-talk between the three pathways have been identified (Walter and Ron, 2011).

The first description of the UPR was shown by Cox et al. (1993), using yeast to identify the role of IRE1 in the activation of protein folding following ER stress conditions. Further development of the UPR pathway resulted in the emergence of the PERK and ATF6 pathways, described by Bertolotti et al. (2000) and Haze et al. (1999) respectively. During homeostatic conditions, these sensors are inhibited by Binding Immunoglobulin (BIP), preventing their downstream affects. Upon build-up of

mis/unfolded proteins, BIP dissociates from these UPR initiators and binds to the problematic nascent polypeptide sequences, preventing them from being exported from the ER (Cao and Kaufman, 2012). As BIP also plays a key role in preventing pre-folded nascent polypeptide from leaving the cell in homeostatic conditions (Section 1.2.3.), it is important to note that BIP is always present in the ER regardless of whether the UPR has been activated or not. In fact, many of the enzymes used in nascent polypeptide folding such as PDI are up-regulated in a UPR response (Yu et al., 2020). Therefore, the difference between BIP expression in homeostatic ER conditions and stressed conditions would be its substantial up-regulation, rather than just its presence.

1.3.2.1. The IRE1 Branch

The IRE1 branch is the most conserved branch of the UPR pathway. IRE1 is an endoribonuclease that uses nonconventional mRNA splicing to bring about a UPR response (Walter and Ron, 2011). Oligomerisation of IRE1 results in conformational changes of the IRE1 sensor, which in turn activates its endoribonuclease function (Korenykh et al., 2009). IRE1 splices a 26 bp intron from X-box binding protein 1 (XBP1) using this function in the cytoplasm, which in turn generates spliced XBP1 (sXBP1) (Yoshida et al., 2001). The sXBP1 transcription factor translocates to the nucleus, where it can control the transcription of protein folding chaperones such as BIP, ERDJ4, PDI, EDEM and HEDJ (Lee et al., 2003). sXBP1 has also been shown to upregulate Protein 58 (P58), an inhibitor of PERK, another key pathway sensor of the UPR (van Huizen et al., 2003).

The IRE1 pathway can also initiate apoptosis by the c-Jun N-terminal kinase (JNK) pathway. The recruitment of TNF-receptor-associated-factor 2 (TRAF2) to IRE1 can activate stress signals to JNK (Urano et al., 2000). JNK then can phosphorylate the family of B-cell lymphoma (BCL2) proteins. In unstressed conditions, BCL2 proteins keep the pro-apoptotic Bax and Bak factors inactive in the ER and mitochondrial membranes (Brunelle and Letai, 2009). Thus, the phosphorylation of BCL2 proteins by JNK allows the activation of the apoptotic Bax and Bak factors to occur. The activity of the active IRE1 protein has been shown to be regulated by a number of proteins such as tyrosine phosphatase 1B (PTP-1B) and ASK1-interactive protein 1 (AIP1) (Luo et al., 2008; Gu et al., 2004).

1.3.2.2. The ATF6 Branch

The ATF6 sensor contains a large ER-luminal domain allowing its residence as an ER transmembrane protein. Upon the build-up of misfolded protein ATF6 translocates to the Golgi apparatus via transport vesicle where its luminal domain and transmembrane sequence are removed by site-1 and site-2 proteases (Ye et al., 2000; Chen et al., 2002). The cleaved, cytosolic N-terminal of ATF6 (cATF6) can then move to the nucleus where it activates target UPR genes. cATF6 targets genes with an ER stress response element (ERSE). Examples include Calreticulin, ER resident folding chaperones such as the previously described BIP and PDI, as well as glucose-regulated protein 94 (GRP94) (Yoshida et al., 1998) which has multiple functions in the ER including as a protein folding chaperone and as a calcium-binding protein (Michalak et al., 2002; Argon and Simen, 1999).

The ATF6 branch is thought to be inactivated by the unspliced variant of XBP1 (uXBP1) upon resolving the build-up of ER stress. Yoshida et al. (2006) showed there to be a high level of uXBP1 in cells in the recovery phase of ER stress, and subsequently showed that uXBP1 can bind to sXBP1, as well as cleaved ATF6 (Yoshida et al., 2009), which subsequently promoted degradation of the complexes.

1.3.2.3. The PERK Branch

Finally, the PERK branch of the pathway responds to stress by temporarily attenuating protein translation. This reduces the amount of nascent protein that requires folding and consequently alleviates stress in the ER. This is achieved by the phosphorylation of eukaryotic translation initiation factor 2A (EIF2 α) (Harding et al., 1999). There are some mRNA's however that translate favourably when eIF2 is limiting such as activating transcription factor 4 (ATF4), which in turn targets CCAAAT-enhancer-binding protein homologous protein (CHOP) that itself induces the expression of other pro-apoptotic proteins (Walter and Ron, 2011). This pro-apoptotic response is only activated during chronic ER stress, and proposed mechanisms for its initiation include the build-up of calcium release from the ER following CHOP induced activation of ER oxidase 1 α (ERO1 α), that affects the opening of the mitochondrial permeability transition pore (PTP)- triggering apoptosis (Urrea et al., 2013; Tsujimoto et al., 2006).

The attenuation of translation activated by the PERK pathway can however be stopped if the build-up of misfolded protein in the ER is resolved, negating the need for apoptosis. This is mediated by growth arrest and DNA damage-inducible gene 34 (GADD34), which encodes a PERK-inducible regulatory subunit of the protein phosphatase PP1C which dephosphorylates EIF2 α , counteracting the effects of PERK (Novoa et al., 2001).

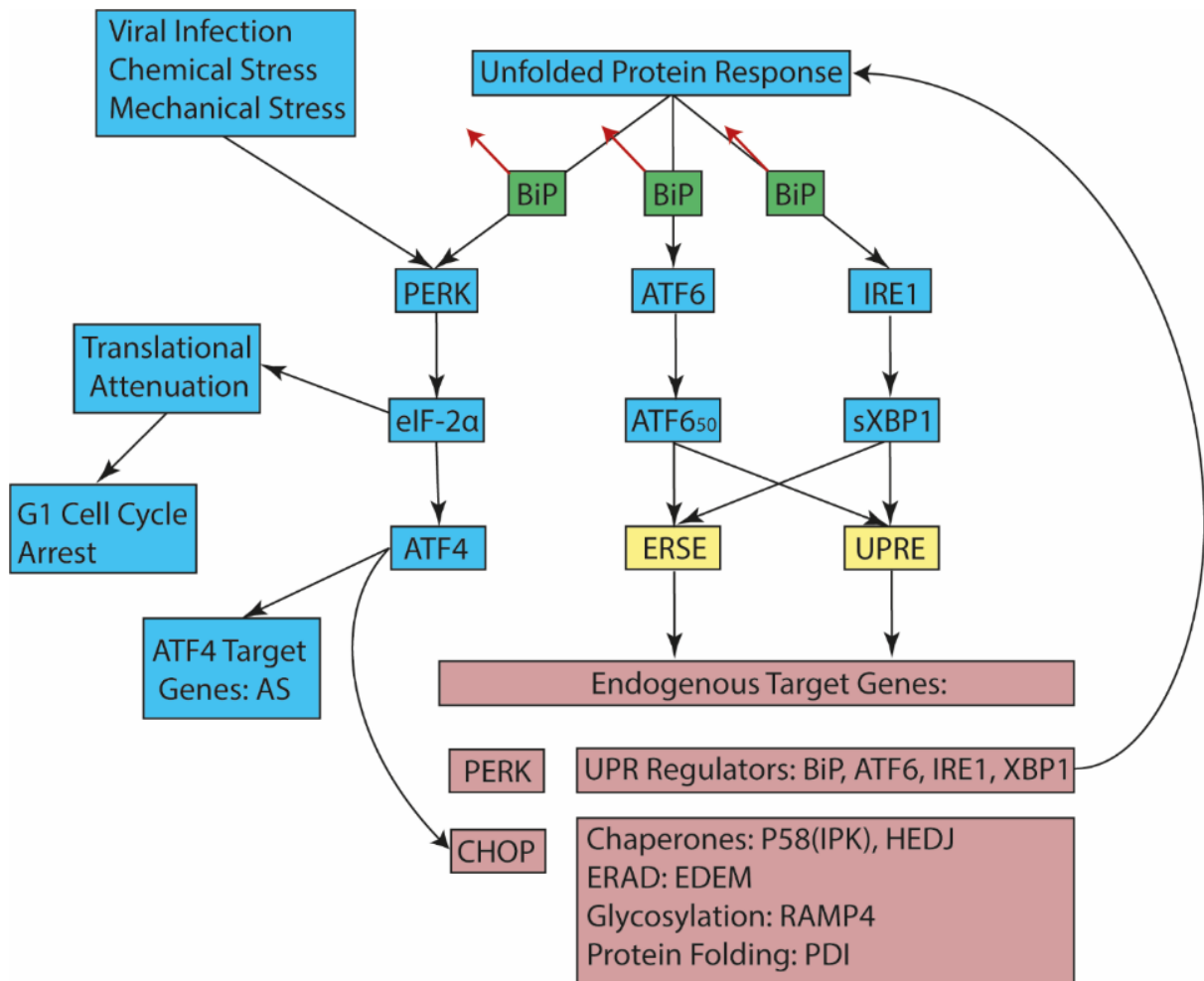


Figure 1.7. Schematic of the Unfolded Protein Response.

The Unfolded Protein Response is initiated during periods of ER stress in cells, caused by a build-up of mis/unfolded protein. The UPR is made up of three response pathways, all of which are inhibited during homeostasis by the molecular chaperone BIP. In the presence of mis-folded protein, BIP dissociates from the pathway sensors: PERK, ATF6 and IRE1, to bind to the protein and prevent it from ER export. Here, the UPR pathway sensors activate downstream signalling pathways that results in the expression of protein folding chaperones that help to return the ER to homeostasis by refolding the protein. The PERK pathway can also attenuate translation, and initiate apoptosis in irreparable conditions. Adapted from Du et al., (2013).

1.3.3. The Unfolded Protein Response in mAb production

The presence of ER stress and thus the activation of the UPR and its resulting expression of key folding chaperones has been extensively linked to the expression of mAbs in CHO cells. Multiple studies have shown that higher producing CHO clones have a higher concentration of endogenous UPR components. Prashad and Mehra (2015) highlighted this when monitoring the mRNA transcript concentrations of markers across the whole of the UPR in a high producing CHO clone and a low producing CHO clone. They found many UPR markers including BIP, ATF4, CHOP, GADD34 and XBP1 were all more highly expressed in the high producing clone. This was replicated in a similar study by Kober et al. (2012) that investigated UPR mRNA transcripts in a panel of CHO DG44 clones expressing the same mAb construct. Correlations were seen between BIP ($R^2= 0.78$), GRP94 ($R^2= 0.75$) and sXBP1 ($R^2= 0.81$) against mAb product. Further evidence that up-regulation of UPR stress markers results in increased titre has been shown during batch and fed-batch culture of erythropoietin expressing CHO cells kept at 32 and 37 °C culture temperatures (Torres et al., 2020). The study showed that the same CHO line expressed relatively similar titres regardless of the temperatures used, but the relative mRNA expression of the erythropoietin construct cultures kept at 32 °C were significantly higher than the 37 °C cultures. The specific cell growth rate showed the exact opposite, with the 32 °C cultures being significantly lower than the 37 °C. Whilst these effects of temperature appeared to balance themselves out in regard to titre, the shift of the populations energy from cell growth to protein production is important. The study went further to show that key UPR transcription factors such as sXBP1, BIP and CHOP were significantly up-regulated in the 32 °C cultures compared to the 37 °C, further suggesting that there is a link between the activation of the UPR and efficient protein production. Interestingly, the signal transducers of the UPR: IRE1, ATF6 and PERK, as well as the pro-apoptotic factor ATF4, did not show any significant difference in expression between the cultures at different temperatures, thought to be due to their activity at the post-translational level. Genes involved in Endoplasmic Reticulum associated degradation (ERAD) such as EDEM3, a pathway that removes in-correctly folded proteins were significantly decreased however, this appears to be due to the lower temperatures shift to protein synthesis homeostasis and a lowered requirement for protein degradation.

This link between specific UPR markers such as BIP, sXBP1 and CHOP with titre suggests that an increased UPR may be beneficial and perhaps predictive of high titres. However, it does not appear to be a global increase in UPR activation markers rather specific branches of the UPR. It is important therefore to consider which transcription factors are not only the best at predicting good antibody production and protein quality but also those that produce a CHO phenotype that is beneficial for industrial manufacture of monoclonal antibodies as, for example, the effector function of pro-

apoptotic transcription factors such as CHOP or ATF4 may be more predictive of CHO clones with a propensity for cell death rather than recovery.

1.3.4. Manipulating the UPR to monitor mAb production

Manipulation of the UPR to monitor antibody production in CHO cells has been seen within the literature for the monitoring of antibody titre. In the same study that showed correlations of BIP, GRP94 and sXBP1 with antibody titre (Kober et al., 2012), the study went on to demonstrate that a truncated BIP promoter construct (trunc GRP78) in the CHO host using recombinase mediated cassette exchange (RMCE), showed a moderate positive correlation with antibody titre (mg/L) and specific productivity (pg/cell/day) ($R^2= 0.63$ for both).

In another study, Roy et al. (2017) generated a dual synthetic reporter system whereby an RFP was placed at the N-terminus of an XBP-1 sequence and a GFP tag at the C-terminus. The IRE1 mediated splicing of the XBP-1 sequence resulted in a frameshift, which placed GFP in frame with RFP and resulted in dual fluorescence expression during UPR activation. The study then calculated the change in fluorescence from RFP to GFP and dubbed the result as an 'ER Stress Index (ERSI)' value. Importantly, the study confirmed that the reporter was monitoring ER stress using Tunicamycin, and Thapsigargin (chemical ER stressors) as a time-dependent relationship between ERSI and incubation time was seen. The study went on to transiently transfect the reporter into mAb expressing CHO cells and determined low, medium and high ERSI pools. When the mAb clones were measured for their titre during fed-batch study the high ERSI clones had a statistically significant higher titre than the medium ERSI and low ERSI pool clones. Using 1 g/L as a benchmark for high producers, 42 % of the clones derived from the high ERSI pool were high producers whilst only 15 % from the medium and low groups were high producers, suggesting that the reporter could at least remove the lowest producers from selection. However, when only the 5 highest producing clones from each of the high and low ERSI stress pools were compared to each other for titre during shake flask culture there was no significant difference between the titres of the high and low ERSI expressors. This suggested that whilst a higher ERSI index may be beneficial for improving the number of high titre clones during CLD, plenty of clones with low ERSI values are also able to produce high titres. This may be due to the study attempting to measure only one specific UPR gene, that covers only one branch of the UPR. As the three UPR branches each elicit different responses (such as apoptosis, translation attenuation and increased chaperone activity), using just one marker on one branch of the UPR may not be sufficient for titre predictability. Instead, designing a reporter that can target multiple branches of the UPR or the over-arching sensor of the UPR, BIP, that regulates all three pathways may be more advantageous.

1.3.5. Engineering the UPR to enhance protein expression

Aside from monitoring the endogenous folding machinery, studies upregulating certain components of the protein folding pathway have shown to have a positive effect on antibody production. Pybus et al. (2014) overexpressed the UPR transcription factors sXBP1 and cleaved ATF6 in a panel of four 'difficult to express' mAbs. The productivity of the clones were significantly increased in 3 of the 4 mAbs for both transcription factors. The increase in the productivity (Qp) appeared to be mostly due to an increased trend in mAb titre and a decrease in integral viable cell density (IVCD). Interestingly, the up-regulation of the inactive form of ATF6 and XBP1 did not significantly affect Qp. This suggests that even following engineering of the CHO host to increase the UPR if there is not also an increase in the pre-cursor transcription factors to activate ATF6 and splice XBP1 then there will be no benefit of the engineering, and is important to consider in future engineering designs.

Another interesting approach to engineering the CHO host line is to increase proteins related to protein secretion as well as folding. The combined overexpression of sXBP1 and B lymphocyte-induced maturation protein-1 (BLIMP1) in the CHO host was undertaken in one study (Torres and Dickson, 2021). BLIMP1 is a driver of differentiation of B cells into plasma cells, the professional mAb secretion cell line. Thus, a favourable characteristic for mAb production in CHO cells. The results of the study showed there to be an increase in mAb titre when sXBP1 and BLIMP1 were up-regulated separately following a 12 day batch culture, in comparison to the control. An even stronger, phenotype was observed (3.8 fold increase in mAb titre) when both sXBP1 and BLIMP1 were co-expressed in the CHO line compared to the control cells. A significant reduction in viable cell density was also seen in the cell line compared to the control suggesting that the up-regulation turns the CHO cell closer to a production phenotype rather than a growth phenotype. These data suggests that factors external to the UPR may also be another area for investigation, but the bolstering of the UPR is still very important as seen by the increase in titre when sXBP1 was increased alongside BLIMP1.

1.3.6. Limitations to the literature

The antibody production field has been successful at identifying transcription factors and chaperones related to the UPR that may be predictive of mAb titre in CHO clones and has started to investigate whether components of these pathways can be used to generate synthetic reporters which can be used to monitor mAb production. However, at the time of writing this thesis there is very little evidence to show that these markers are predicting high titre clones that also have good product quality characteristics. Even less evidence is present to show that mAb product quality can be predicted in clones. Perhaps one of the reasons for this is due to 'product quality' encompassing so many factors – such as the size or charge of the mAb product. It is also difficult to pin-point whether the poor quality phenotypes are caused by both environmental and/or biological factors. Despite these challenges product quality would be an extremely important characteristic to be able to monitor, as quality cannot typically be monitored until a much later stage than CLD. This is problematic when clones that appear to have high titres are actually producing poor quality mAbs that are not suitable for human use, and results in the removal of the clone from final cell line selection. The literature does suggest that the UPR may have some effects on some areas of product quality such as the Ishii et al. (2014) study that showed low PDI mRNA expression resulted in higher fragmented product, and thus investigating this further through the use of a UPR based reporter for CLD would be an extremely useful tool for removing poor titre and quality mAbs at the same time.

Further to this, the mAb titre produced in CHO clones is already easily predicted. Over the past few years a multitude of industry 'gold-standard' methods have been developed to monitor antibody titre without the need to introduce an exogenous reporter construct into the CHO genome that may have a negative impact on mAb production. For example, the Octet HTX (ForteBio) which utilises Protein A binding (Tejwani et al., 2021; Huhn et al., 2021), the CEDEX (Roche) that uses detection antibodies (Roche, 2019), or more recently the Spotlight assay used on the Beacon (BLI) (Le et al., 2018), all reliably measures titre whilst performing single cell cloning and thus another method of measuring this is unnecessary. This is where product quality becomes an important aspect to consider for the future advancement of CLD, as these aspects cannot be currently measured and thus a reporter or assay that could measure these would be invaluable for the CLD pipeline.

A second limitation to the current literature field to consider pertains to the number of CHO clones and mAb types used in the experiments monitoring the UPR. The majority of studies have only followed one type of antibody in their study and used limited numbers of clones to monitor and manipulate the UPR (Kober et al., 2012; Prashad and Mehra, 2015; Roy et al., 2017). Whether the mAb type affects the tools designed in these studies is unknown therefore, and this would limit the adoption of the tool into CLD until its universal effectiveness is proven. Thus, it is crucial for any future reporter assay or tool that could monitor product titre and quality in CHO clones to be reproducible regardless of the mAb type.

This thesis therefore aims to answer whether a UPR based reporter construct can be designed to monitor both antibody production *and* antibody quality across a broad panel of cell lines and antibody formats during cell line development.

1.4. Project Aims and Objectives

The first aim of this thesis project was to identify a phenotypic fingerprint for CHO clones that produce both desirable quantity and quality mAb product. The characteristics explored within this thesis focuses on the role of protein folding of the mAbs, and in particular the role of ER stress and its response mechanism the Unfolded Protein Response, as guided by the literature. In order to do this a selection of CHO clones expressing mAbs with a variety of different product quality issues were investigated, and their relationship between these product quality characteristics were compared to the quantities of key protein folding chaperones.

The second aim was to use the data obtained to identify a single protein folding marker that appeared to have a predictive capacity for product quantity and quality across the CHO clones, and design a reporter construct to monitor its expression throughout CHO culture. The expression of the reporter in the CHO host would then be monitorable during CLD at almost any stage. To do this the CHO host containing the reporter construct was run through a typical CLD platform using a panel of mAbs with different product quality issues inherent in their design. The clones were then taken through production studies to generate sufficient product for product quality study. The product quality and titre of the clones could then be correlated to the reporter expression retrospectively during CLD to test its effectiveness.

To achieve these aims the following specific objectives were set for the project:

- Establish a range of reproducible assays for monitoring the UPR and use them to identify differentially expressed genes, which correlate with antibody titre and product quality.
- Create a panel of antibody producing cell lines with well-defined antibody titre and product quality characteristics, which can be used to study the host response to antibody production.
- Generate a UPR reporter cell line using the Beacon and establish whether it responds to ER stress using a range of pharmacological stressors.
- Determine whether the reporter CHO cell line can be used as an expression host, following transfection with the panel of the mAb constructs. Collect product quality and titre data from these clonal cell lines expressing the mAb to determine whether the reporter could predict quality retrospectively.

2. Materials and Methods

2.1. Cell Culture

2.1.1. Sub-culture maintenance of CHO Cells

All Chinese hamster ovary (CHO) cell cultures were maintained on a 3-4 day passage routine, typically to a total culture volume of 30 ml in 125 ml shake flasks (Corning), in a Multitron shaking incubator (Infors HT) set to 140 RPM, 37 °C and 5% CO₂. To count the cells, 500 µl of culture was incubated with 500 µl of TrypleE (Gibco) for 5 minutes at 37 °C in a ViCell sample cup (Beckman Coulter). The cultures were counted on a ViCell XR (Beckman Coulter) under the CHO cell type, using Trypan Blue exclusion staining to monitor viability (Beckman Coulter).

Cells were passaged to a density of 0.3x10⁶ viable cells/ml, unless otherwise stated, in GSK's proprietary CHO media and appropriate supplements. Table 2.1. highlights which supplements and selection markers were required for each cell type.

Cell Line	Media Addition 1	Media Addition 2
CHO Host	8 mM L-Glutamine	N/A
Null Host	400 µg/ml Geneticin	N/A
Bispecific mAb Line	25 µM MSX	400 µg/ml Geneticin
mAb Panel molecule 1-8	25 µM MSX	N/A
CALR and TOM20 Fluorescent Reporter Hosts	8mM L-Glutamine	400 µg/ml Geneticin

Table 2.1. Concentration of supplements and selection markers required for cell lines in culture. L-Glutamine (Gibco) was used as a CHO host supplementation, whilst MSX (Merck Millipore) and Geneticin (Gibco) were used as selection markers.

2.1.2. Cell Revival

Cryovials (Thermofisher) containing the desired cells were removed from LN₂ storage and thawed in a water bath of 37 °C PBS (Gibco). The vial contents were added dropwise to 18 ml of pre-warmed culture media in a 50 ml falcon tube, and centrifuged at 180 xg for 5 minutes in a Legend HT centrifuge (Sorvall) with no brake. The supernatant was removed and the pellet resuspended in 20 ml fresh culture media. Cells were counted on the ViCell XR as described above, and further media added to

give a final cell concentration of 0.5×10^6 viable cells/ml in a 125 ml shake flask. The shake flasks were incubated, and passaged three days post revival as per Section 2.1.1.

2.1.3. Cell Freezing

Cell lines were frozen on day 3, during their mid log growth phase, at a concentration of 1.5×10^7 viable cells per cryovial. Cell lines were counted (Section 2.1.1.) and the desired volume of cells were centrifuged at 180 xg with no brake, and the supernatant discarded. The pellet was resuspended in 1 ml of freezing media (7.5% v/v DMSO, JT Baker, in the respective culture media specified in table 2.1.), and aliquoted into each vial. The cryovials were placed in a Mr. Frosty freezing container (Nalgene) filled with isopropanol (Sigma Aldrich). Mr. Frostys were placed in a -80 °C freezer overnight and the following day the cryovials were moved to LN₂ for long term storage.

2.1.4. Monitoring mAb Titre via the Octet HTX

The Octet HTX (ForteBio) was used to monitor mAb titre in cell cultures on the day of passage. 500 µl of cell culture was centrifuged at 15,000 xg in a microcentrifuge (Eppendorf) for 4 minutes to pellet the cells. 80 µl of the supernatant was added to a 384 well Octet plate (ForteBio), alongside 80 µl of media reference control, and the required regeneration (10 mM Glycine at pH 1.5) and neutralisation solutions (culture media). An Octet Protein A Biosensor tray (ForteBio) was re-hydrated in a 96 well plate containing 100 µl of culture media for 10 minutes prior to use, and both were loaded onto the Octet HTX alongside the 384 well sample plate. Samples were analysed in triplicate under a 'basic quantification with regeneration' template on the Data Acquisition software (ForteBio) with pre and post conditioned sensors.

Analysis of the samples was performed using the Octet's Data Analysis software (ForteBio). Samples were compared to a previously generated standard curve specific to the mAb being expressed under the 'Dose response – 5PL (unweighted)' setting, and the binding rate equation calculated by the 'initial slope'. The resulting titres were exported into excel, and an average mAb concentration automatically generated for the samples. The standard curves used to quantify mAb titre in the clonal mAb panel 1-8 were obtained by performing a serial dilution of known concentration purified material (kindly provided by GSK) in HEK cells from a range of 1 - 500 µg/ml. The bispecific mAb line had a standard curve pre-made by GSK using the same technique.

2.1.5. mAb Naming Conventions

All the constructs used in this thesis were obtained from GlaxoSmithKline, and as such have been anonymised for this thesis. The mAb panel used in Chapters 4, 5 and 6 were named mAbs 1-8. Subsequent clones expressing each mAb construct were named alphabetically e.g. mAb 1-A, mAb 1-B. Each of the mAbs were designed to target different antigens,. Each of the mAbs were chosen based on a 'poor quality' attribute that was seen during their development at GlaxoSmithKline. The rationale behind the mAbs chosen can be seen in Table 2.2.

mAb Construct	Problematic Quality Rationale
mAb 1	Prone to aggregation
mAb 2	High molecular weight species present in Acetate and Phosphate
mAb 3	Poor developability
mAb 4	Control mAb used during final structure selection of project molecules
mAb 5	Poor expressor
mAb 6	Engineered variant of mAb 5, aiming to increase expression titres
mAb 7	Engineered variant of mAb 5, aiming to increase expression titres
mAb 8	Prone to dimerising and aggregation

Table 2.2. Anonymised mAb panel naming convention, and the rationale as to why they were chosen as poor quality mAbs.

2.2. DNA Stock Production

2.2.1. Transformations

Transformations were performed using Stellar Competent Cells (Clontech). Competent cells were thawed on ice and mixed via pipetting. 5 ng of DNA was added to 50 µl of competent cells per transformation, alongside a negative control where no DNA was added, and left on ice for 30 minutes. The cells were heat shocked at 42 °C for 45 seconds and returned to ice for 2 minutes. 500 µl of liquid broth (LB) media (in house) were added to the transformations to aid recovery and incubated by shaking on a Climo-Shake- ISF-X plate (Kuhner) at 37 °C for 1 hour at 200 RPM. 50 µl of the transformation mix was spread onto an agar LB plate containing 100 µg/ml ampicillin (in house) using a sterile plastic spreader. The plates were incubated at 37 °C overnight, before moving to 4 °C for short term storage after colony growth.

2.2.2. DNA Purification: Miniprep and Maxipreps

A single colony was selected from LB agar plates using a sterile loop (COPAN), and added to 5 ml of LB media containing 100 µg/ml ampicillin in a 15 ml Falcon tube and incubated overnight at 37 °C in a shaking incubator set to 200 RPM.

DNA purification was performed using a QIAprep Spin Miniprep kit (Qiagen), as per the manufacturer's instructions. To create larger DNA stocks, 1ml of the overnight starter cultures was added to 200 ml of fresh LB media containing ampicillin in a 1 L vented shake flask (Corning) and incubated overnight under the same conditions. The DNA was extracted from the larger culture the following day using an EndoFree Plasmid Maxi Kit (Qiagen), as per the manufacturer's instructions. All DNA stocks were measured for their concentration and 260/280 quality value on a QIAxpert (Qiagen).

2.2.3. Restriction Digests

Restriction digests were performed at 50 µL volumes using restriction enzymes and buffers from New England BioLabs (NEB), as per the manufacturer's instructions. 1 µg of DNA was added to 1 µl of the enzyme(s) of interest, alongside 5 µl of the enzyme's respective buffer. The samples were then topped up to 50 µl with sterile water. Digests were incubated at 37 °C for 3 hours in a T100 thermal cycler (BioRad). The digests were run on a 0.8 % Agarose TBE gel containing a 1:10,000 dilution of SYBR Safe dye (all Invitrogen), and imaged on the blue tray of a Gel Doc™ EZ System (BioRad).

2.3. Infusion cloning of the reporter construct into GSK's expression plasmid

2.3.1. Reporter String DNA and Plasmid Digest Preparation

The reporter GFP sequences were synthesised by Thermofisher's DNA Gene Strings service and were amplified by polymerase chain reaction (PCR) to increase concentration. 12.5 µl of ClonAmpHiFi PCR premix (Takara) was added to 0.75 µl of forward and reverse primers (10 µM), 10 µl of sterile water (Sigma) and 50 ng of template DNA. Table 2.3. shows the primer sequences. Initial denaturation was run at 94 °C for 5 minutes. 30 cycles of 94 °C for 30 seconds for denaturation, 60 °C for 30 seconds for primer annealing and 72 °C for 1 minute for extension were repeated. A final 10 minute extension at 72 °C was performed before a 4 °C hold.

One of GSK's proprietary expression plasmids was obtained, transformed and maxiprepped as per Section 2.2.2. An aliquot of the resulting maxiprep was linearised using a HindIII restriction enzyme (NEB). 2 µg of plasmid DNA was mixed with 1.5 µl of HindIII, 8 µl of CutSmart buffer (NEB) and 68.5 µl of sterile water, and incubated in a Thermocycler for 3 hours at 37 °C.

To confirm amplification of the PCR products, 5 µl of the PCR products were mixed with 1 µl of loading buffer (NEB), and ran on a 0.8% agarose TBE gel, containing a 1:10,000 dilution of SYBR Safe stain (all Invitrogen). Linearisation of the plasmid was also confirmed on the same gel, with 5 µl of the vector digest mixed with 1 µl of loading buffer. Uncut controls were also analysed. The gel was run at 80 V for 1.5 hours and imaged on the BioRad Gel Doc EZ Imager using the blue tray that is used for all nucleic acid applications. The successful resulting bands of the digested plasmid and amplified inserts were extracted from the gel and purified into a 30 µl product using a QIAquick PCR Purification Kit (Qiagen), as per the manufacturer's instructions.

Primer	Sequence (5' to 3')
CALR-GFP Forward	GAAACTACCAGCTTAATGCTGCTGAGCGTGCC
CALR-GFP Reverse	CGACTGCAGCAAGCTCCTTACTTGTACAGCTCGTCCATGC
CALR-mOrange Forward	GAAACTACCAGCTTAATGCTGCTGAGCGTGCC
CALR-mOrange Reverse	CGACTGCAGCAAGCTCGCCTTACTTGTACAGTTCGTCC
TOM20-GFP Forward	GAAACTACCAGCTTCTCAATGGTGGGCAGGAACAG
TOM20-GFP Reverse	CGACTGCAGCAAGCTCCTTACTTGTACAGCTCGTCC

Table 2.3. Primers used during infusion cloning to isolate the reporter constructs.

2.3.2. Infusion Cloning

The Clontech Infusion Kit (Takara) was used to insert the reporter inserts into the linearised plasmid, as per manufacturer's instructions. 50 ng of linearised vector (1.2 µl) and 50 ng of PCR product (1-1.2 µl) were added to 2 µl of infusion enzyme and topped up to a total volume of 10 µl with sterile water. The samples were incubated in a 50 °C water bath for 15 minutes before placing on ice. Infused plasmids were then transformed into Stellar Competent cells (Takara) as per Section 2.2.1.

6 colonies from each reporter were minipreped (as per Section 2.2.2.) and digested to confirm successful cloning. 1 µl of extracted plasmid DNA from each miniprep was incubated with 1µl of restriction enzymes HindIII and NheI-HF (NEB), 2.5 µl of CutSmart Buffer and topped up with sterile water to a total volume of 25 µl. Digests were performed at 37 °C for 3 hours, followed by a 20 minute 60 °C enzyme inactivation step. The plasmid was designed to remove the HindIII restriction site upon successful infusion of the gene insert. Successful infusion was therefore confirmed when only a linearised band was seen on the gel, created by the NheI-HF enzyme.

2.4. Mammalian Cell Transfections

2.4.1. Transient Cell Transfection

All transient transfection experiments were performed using Lonza's SF Cell Line 4D-Nucleofector X L kit, on the 4D Nucleofector System (Lonza). One day prior to transfection, cells were passaged to a density of 0.8×10^6 viable cells/ml. On the day of transfection cells were counted on the ViCell XR, and 5×10^6 viable cells per transfection were pelleted at 180 xg for 5 minutes. The supernatant was removed, the pellet washed in 10 ml PBS (Gibco) and centrifuged again under the same conditions. The PBS was decanted and the cells resuspended in 100 μ l of Amaxa 4D Cell Line Nucleofection Buffer, per transfection. A nucleocuvette was filled with 10 μ g of plasmid (or 15 μ l of PBS for the negative control) and 100 μ l of cells. The cells were electroporated using the CHOK1 (DT-133) program and then transferred to a 6 well-suspension plate (Corning) containing 4 ml of pre-warmed non-selective culture media, using a sterile Pasteur pipette (provided in electroporation kit)

2.4.2. Stable Cell Transfection

All stable transfections were performed using FreeStyle MAX (Gibco) lipid transfection. 24 hours prior to transfection, cells were passaged to a density of 1×10^6 viable cells/ml in cell culture media (~10 ml of cells were required per transfection). On the day of transfection the cells were counted on the ViCell XR and 1.5×10^7 viable cells per transfection were pelleted at 180 xg for 10 minutes. The pellets were resuspended into 15 ml of OptiPRO SFM (Gibco) containing 8 mM L-Glutamine and added to 125 ml shake flasks before incubating in a shaking incubator at 37 °C, 75 RPM and 5% CO₂.

Two aliquots of 600 µl of OptiPro SFM containing 8mM L-Glutamine were pipetted into 1.5 ml sterile tubes (Eppendorf). 25 µl of FreeStyle MAX reagent was added to one tube and 18 µg of plasmid DNA to the other. The contents of the FreeStyle MAX mixture was immediately added to the plasmid DNA solution tube and mixed 3 times by pipetting. The solution was incubated for 15 minutes at room temperature to allow for lipid complexes to form. The DNA-lipid solution was added dropwise into the 125 ml shake flasks before returning to the incubator.

24 hours post transfection the cells were counted on the ViCell XR and the cells centrifuged at 180 xg for 10 minutes before resuspending in 15 ml of GSK's proprietary culture media without L-Glutamine. 3ml of cell culture was pipetted into 5 wells of a 6 well plate and incubated into a static HeraCell incubator (Heraeus) at 37 °C and 5% CO₂. 48 hours post transfection, 3 ml of selection media was added to each well (see Table 2.1. for selection supplements).

The viability and counts of the cells (see Section 2.1.1.) were monitored approximately every 5 days until the cells had fully recovered from selection. The cells were fed fresh culture media on the days they were counted. 2 ml of media was removed, without disturbing the cells, and exchanged with 2ml of fresh selective media. Once the cells had recovered, the cultures were scaled up into a T25 flask (Greiner) to a total volume of 10 ml and moved to shaking incubation. 3 days post scale up the culture was counted again and the entire volume of the T25 culture scaled up into a 125 ml shake flask to a total volume of 30 ml. Once counting showed complete recovery (>95% viability in 125 ml shake flask culture) the pre-clonal pools were frozen into cell banks (see Section 2.1.3), before single cell cloning on the Berkeley Lights Beacon.

2.4.3. Single Cell Cloning

Single cell cloning was performed on the Beacon Lights System (Berkeley Lights) by members of the Cell Line Development group at GlaxoSmithKline, under a proprietary technique. The cells were prepared prior to Beacon load by filtering a 5 ml sample of cell culture through a 40 µM cell strainer (Fisherbrand) into a 50 ml tube (Falcon) and counted on the ViCell XR. An aliquot of 5×10^6 cells was taken and centrifuged, before resuspending in 500 µl of proprietary media. 200 µl of the culture was sampled into a round bottom 96 well plate (Corning) and placed into the Beacon. Load parameters were set to ensure each cell type was loaded into designated fields of view on the chip.

Productivity of the cell lines was assessed after 4-5 days in culture using a Spotlight HuFc assay (Berkeley Lights). Upon completion the results were assessed on the Assay Analyser software, where cell line selection could be performed – see relevant chapters for selection criteria. The selected cells were exported into flat-bottom 96 well plates (Corning) containing 200 µl of fresh media and incubated in a HeraCell static incubator (Heraeus) prior to scale up.

2.4.4. Scale Up of Clonal Cell Lines

96 well plates were imaged 0, 7 and 14 days post export on the CellMetric (Solentim) to monitor outgrowth. During static plate culture, the cultures were kept in a HeraCell (Heraeus) incubator at 37 °C and 5% CO₂. After two weeks in culture the contents of the 96 wells were transferred to 24 well plates containing 1 ml of culture media. After 5 days the 24 well plates were screened for their titre via the Octet HTX (see Section 2.1.4.), as well as cell count and viability on a FACS Array (BD Biosciences). Briefly, the cells were resuspended by pipetting and 100 µl of cell culture transferred to a 96 well plate containing 100 µl of TrypleE. The plate was incubated for 20 minutes at 37 °C and 1150 RPM in an iEMS Incubator/Shaker (Thermo LabSystems). 10 µl of Flow-Count Fluorospheres (Beckman Coulter) and 5 µl of Propidium Iodide (BD Biosciences) were added to each well before running on a pre-determined FACS Array template. Fluorospheres were used to enable equal gating between samples with different cell counts in, and to ensure fluorescence was accurately being monitored. Briefly, the FACS Array was set to record 1000 bead events per well with a forward scatter (FSC) voltage of 80 and a side scatter (SSC) voltage of 306. The PI stain was measured on the Yellow filter set at a voltage of 363 (logged). The mixed fluorescence spheres were measured on the Far Red (70 voltage, logged), NIR (80 voltage, logged) and Red (584, logged) filters.

The contents of the 24 well plates were scaled up to 12 well plates containing 1 ml fresh culture media the following day. A further two days later the contents of the 12 well plates were scaled up to a 6 well plate containing 3 ml fresh culture media. Five days after scale up to 6 well plates, the cultures were screened for titre and cell growth as described above and selection made for which cell lines to progress (selection criteria can be found in respective chapter methods Sections), to T25 shake flasks. The contents of the 6 well plates were added to T25 flasks containing 6 ml of culture media and moved into a Multitron shaking incubator (Infors HT) set to 140 RPM, 37 °C and 5% CO₂.

Two days post T25 scale up a further screen was performed for mAb titre on the Octet HTX, and cell growth on the ViCell XR at a 4.0 dilution in TrypleE. Further selection was performed if required. Cultures were scaled up to 125 ml shake flasks, by adding the contents of the T25 to 25 ml culture media. Following successful scale up, shake flask cultures were frozen down to create cell banks (see Section 2.1.3).

2.5. Digital Droplet PCR

2.5.1. RNA Isolation and cDNA Conversion

Total RNA was isolated from 5×10^6 viable cells/ml using a RNeasy Mini Kit and QiaShredder (both Qiagen), as per the manufacturer's instructions. RNA concentrations were measured on a QIAxpert (Qiagen). A High Capacity RNA-to-cDNA kit (Applied Biosystems) was used to convert the isolated RNA to cDNA, as per the manufacturer's instructions and quantified on a QIAxpert. The cDNA samples were diluted in distilled water to a final concentration of 1.75 ng/ μ l.

2.5.2. Digital Droplet PCR

A mastermix of primer, probe and reaction buffer (ddPCR supermix) was created for the plate as per Table 2.4. Primer and probe sequences can be found in Table 2.5. 17 μ l of the mastermix was added to each well of a 96 well PCR plate, alongside 5 μ l of the diluted cDNA sample. Distilled water was used as a negative control. The plate was sealed with a foil cover using a PX1 PCR Plate Sealer (BioRad). The plate was then vortexed and centrifuged at 250 xg for 5 minutes.

Droplets were generated on the Automated Droplet Generator (BioRad). The necessary BioRad consumables were loaded into the droplet generator- pipette tips, oil cartridges, sample plate and collection plate. Oil droplet generation was then performed and the resulting sample plate was sealed with a foil lid as per above.

PCR was performed on the resulting droplet plate on a C1000 Thermocycler (BioRad). The sample volume was set to 35 μ l, with a heated lid set to 105 °C. For the PCR run, an initial enzyme activation step of 94 °C was set for 10 minutes. 40 cycles at 94 °C for 30 seconds, as well as the annealing step of 60 °C for 1 minute (at a ramp of 2 °C per minutes) were then completed. A final enzyme deactivation step of 98 °C for 10 minutes was then added, with a ramp of 2 °C per minute was performed before holding at 4 °C. The plate was read on a QX200 Droplet Reader (BioRad), measuring for FAM and HEX dyes. The data was analysed on the QuantaSoft Analysis Pro software.

2.5.3. Digital Droplet PCR Data Analysis

Once the samples are run on the ddPCR plate reader the raw data can be exported into an excel file, where the copies/ μ l of the target and the Beta-2 Microglobulin (β 2M) or β -Actin reference gene for each sample is stored. All of the samples are run in technical triplicate to prevent any experimental or machine error. A plate control is also included for the experiments, as each target explored require 3 full 96 well plates of samples. The standard deviation of the three plate replicates were calculated,

and if any of the individual plate values resided outside of the standard deviation error bars of the sample, then plate variation is presumed and the experiment run again.

- The number of target gene copies in each sample are first normalised to the number of reference gene copies (e.g. CALR copies / β 2M copies).
- If any of the technical replicates failed, noted by a 'No Call' reading for either the target or reference measurement then the replicate was removed from analysis. (Note: The heavy and light chain analysis excluded this rule, as it was expected that some cell lines would not have any expression of the targets. In this case, the lack of expression was confirmed when all three technical triplicates gave a 'No Call' reading).
- The technical triplicates of the normalised samples are then averaged in excel, giving a final value for each cell line for one biological replicate.
- The same process is then repeated for the two other biological replicates.
- The values for each sample from all three biological replicates are then averaged in excel to give the final, normalised target concentration. The standard deviation is also calculated in excel from the biological triplicates using the 'STDEV.P' function. The +- 1 SD value is then used for the error bars in graphical analysis.

Mastermix Component	Volume (μ l per well)
Target Gene Forward Primer (100 μ M Stock)	1
Target Gene Reverse Primer (100 μ M Stock)	1
Target Gene Probe (100 μ M Stock)	1
Reference Gene Forward Primer (100 μ M Stock)	1
Reference Gene Reverse Primer (100 μ M Stock)	1
Reference Gene Probe (100 μ M Stock)	1
ddPCR Supermix (No dUTP)(BioRad)	12

Table 2.4. Mastermix for ddPCR reaction.

Target	Forward (5' to 3')	Reverse (5' to 3')	Internal Probe (5' to 3')	Ensembl Reference
ATF4	GGTTCTCCAGCGACAAGGC	ACATCCAGTCTGTCCCGGAG	GGGCTCCTCCGAATGGCTGGCTGT	ENSCGRT00001023390.1
ATF6	ACACTACCAGCCCTTATGCCA	GCAAGAACTGGTTGAGCAGAAGG	ACAGCCTGCACCCACCAAAGGTCAG	ENSCGRT00001006542.1
β -Actin	GCCGTCTCCCATCCATCGT	TGGGGTACTTCAGGGTCAGAA	GGGCGTGATGGTGGGCATGGGC	ENSCGRT00001019312.1
β -2M	AGTGGTCTGCTTGATGCCA	GGACAGATCTGACAGCTCGACT	CCAGCGTCCCCACAAGTGCAAGT	ENSCGRT00015030570.1
BIP	TGCCGGCTTACTTCAATGATGC	AGGATGTTCTTCTCGCCCTCT	GCAGCTGCTATTGCGTATGGCCTGGA	ENSCGRT00000004547.1
CALR	GACATCTGTGGTCCTGGCAC	CCTGGCTGTTGTCAATTTTCACC	CTGATTGTGCGGCCAGACAACACCT	ENSCGRT00001025534.1
CERS2	TCCTTCTACTGGTCCCTGCTCT	GCCATGATGAGAGTCCCTGCT	ACGTGGCCACCATCATTCTCCTCAGCT	ENSCGRT00001016940.1
PDI	TGCTATTCTGCCCAAGAGTGT	CTTCAGGCCAAAGAACTCAAGGA	CGACAGCGACCACACTGACAACCAGCG	ENSCGRT00015040709.1
XBP1	CGCTTGGAATGGATGTGCT	CTGGGGAGGTGACAACCTGGG	GGCCGGGTCTGCTGAGTCCGCA	ENSCGRT00000013049.1

Table 2.5. Primer and internal probes sequences for ddPCR, and the Ensembl reference they were designed from. Primers were obtained from Sigma Aldrich, and internal probes from Integrated DNA Technologies (IDT). β -Actin and β -2M internal probes were tagged with the HEX dye as reference genes, the remaining target genes were tagged with FAM dye.

2.6. Western Blotting

2.6.1. Cell Lysis Sampling

Cell cultures were counted on the ViCell XR (Section 2.1.1.), and 5×10^6 viable cells per culture sample were aliquoted into 1.5 ml tubes (Eppendorf) for cell lysis. The samples were lysed with RIPA lysis buffer containing Halt Protease Inhibitor Cocktail (both Thermofisher), as per manufacturer's instructions. Briefly, the cells were spun at 2500 g for 5 minutes and the pellet washed with ice cold PBS twice. 1 ml of RIPA lysis buffer was added to each cell pellet, resuspending by pipetting. The mixture was kept on ice for 15 minutes with gentle agitation, before centrifugation at 10,000 g for 15 minutes.

2.6.2. SDS PAGE

Samples were prepared for SDS-PAGE to a total volume of 15 μ l, under both reduced and non-reduced conditions. 0.1 μ g (4 μ l) of sample was added to 3.8 μ l of NuPAGE LDS Sample Buffer (Invitrogen), and 1.5 μ l of NuPAGE Reducing Agent (Invitrogen) if run under reducing conditions. The volume was made up to 15 μ l with deionised water. The samples were vortexed to mix and heated to 70 °C for 10 minutes on a heat block.

10 μ l of the samples were loaded into pre-cast NuPAGE 4-12% Bis-Tris, 1 mm mini gels (Invitrogen) in an X-Cell SureLock gel tank (Invitrogen), containing an SDS running buffer made of NuPAGE MES Running Buffer (Invitrogen), diluted as per the manufacturer's instructions. 5 μ l of Thermofisher's BenchMark™ Fluorescent Protein Standard was used as a protein standard, and the gel resolved at 200 V for 35 minutes.

2.6.3. Protein Transfer

Protein transfer was performed using an iBlot2 Dry Blotting System with iBlot2 transfer stack kits containing the PVDF membrane (both Invitrogen), as per the manufacturer's instructions. Briefly, the SDS PAGE gel was sandwiched between the transfer stacks, PVDF membrane and water soaked filter paper, using a roller on the filter paper surface to remove any air bubbles. Two electrode covers were placed onto the PVDF membrane and filter membrane sides. The completed transfer stack was placed into the iBlot2 system and transfer performed at 20 V for 7 minutes.

After transfer the PVDF membrane was retrieved for immunostaining. Successful staining was confirmed by the visibility of the blue bands of the protein ladder on the membrane. The membrane was agitated in deionised water on a shaker plate, in the dark for 5 minutes at room temperature. The gels were retained if Coomassie blue staining was required.

2.6.4. Western Blotting

The blots were blocked in 20 ml of SuperBlock buffer (ThermoScientific) for 2 hours at room temperature. Unless otherwise stated all wash and incubation steps were performed in the dark, with gentle agitation on a Model R100 Rotatest shaker (Luckham). All antibodies used and their dilutions can be found in Table 2.6. The primary antibodies were diluted in SuperBlock buffer to a volume of 20 ml and incubated with the blots at 4 °C overnight. The blots were washed 3 x with 0.05 % v/v PBS-Tween (in house) for 5 minutes. The secondary antibodies were then diluted in SuperBlock buffer and 20 ml of the diluted antibodies were added to each blot and incubated for 1 hour at room temperature. The blots were washed for three times with 0.05 % PBS-Tween and imaged on a Typhoon FLA9500 (GE Healthcare) under the LPR ch.2 and LPB filters, with a pixel size of 10 µm.

The images were made in ImageQuantTL software (Cytiva) and quantification performed on ImageJ (National Institutes of Health). To quantify the target bands, the first sample band was outlined using the rectangle tool and selected as the first well under the Analyze > Gels > Select First Lane command. Subsequent bands were identified using the 'Select Next Lane' command and the intensity plotted as a curve using the 'Plot Lanes' command. The area under the peak from each sample was calculated with the wand tool and the quantification produced by it transferred to excel for full analysis. This process was repeated with the GAPDH reference bands and used to normalise the results.

Primary Antibodies	Manufacturer	Cat No.	Dilution
Goat Anti-Human FcY IgG	Jackson ImmunoResearch	109-005-008	1:5000
Goat Anti-Human Kappa Light Chain	BioRad	STAR127	1:5000
Mouse Anti-GAPDH	ProteinTech	60004-1-Ig	1:5000

Secondary Antibodies	Manufacturer	Cat No.	Dilution
Rabbit Anti Mouse, AlexaFluor488	Invitrogen	A-11059	1:5000
Donkey Anti Goat, AlexaFluor647	Invitrogen	A-21447	1:5000

Table 2.6. Primary and secondary antibodies used during western blot staining.

2.6.5. Coomassie Staining

To confirm that blot transfer was completed, the gel was washed with 20 ml of deionised water for 5 minutes with gentle agitation. 20 ml of SimplyBlue SafeStain (Invitrogen) was incubated with the gel for 1 hour at room temperature, with gentle agitation. The stain was removed and replaced with 20 ml of deionised water and incubated for a further hour under the same conditions. The gel was removed from the water and imaged on a EZ Gel Doc Imager (BioRad) under the white tray filter.

2.7. Fluorescence Microscopy

2.7.1. Live Cell ER Tracker and DAPI Counter Staining

Live cell imaging of the Endoplasmic Reticulum was performed using ER-Tracker™ Green (BODIPY™ FL Glibenclamide) (Invitrogen). Imaging was performed on 1×10^6 viable cells/ml, one day post passage. Cells were centrifuged at 180 xg for 4 minutes and the supernatant discarded. 1 ml of ER Tracker diluted to 1 μ M in culture media was added to the cells and incubated for 30 minutes at 37 °C. The cells were washed using 1 ml of pre-warmed culture media. Cells were pelleted and resuspended in 1ml pre-warmed media to wash, before repeating the wash step. Pelleted cells were resuspended in 1ml of culture media and 100 μ l of the sample was plated into a 96 well Poly-Lysine coated plate (Greiner). The plate was centrifuged at 180 xg for 4 minutes to ensure the cells lay flat for imaging. The plate was read on the Yokogawa CV8000 as per Section 2.7.3.

2.7.2. Fixed Cell Imaging

The antibodies used for immunostaining have been summarised in Table 2.7. To fix the cells for immunolabelling they were counted on the ViCell XR and 50,000 cells aliquoted into a Poly-Lysine coated 96 well plate (Greiner). The plate was centrifuged at 720 xg for 4 minutes to ensure the cells had adhered to the bottom of the dish. The supernatant was removed from the wells and replaced with 200 μ l of ice cold methanol (Merck). Cells were incubated for 20 minutes in a – 20 °C freezer. The plate was centrifuged and the wells were washed twice in 200 μ l of PBS (Gibco) with a centrifugation step between washes. Primary antibodies were diluted to their desired concentration in PBS and 100 μ l added to culture wells, vortexed to mix and incubated in the dark for 1 hour at room temperature. After incubation the wells were washed twice in 200 μ l of PBS, with a centrifugation step between washes. Secondary antibodies were diluted to their desired concentration in PBS and 100 μ l added to the wells, vortexed to mix and incubated in the dark for 1 hour at room temperature. Wells were washed twice in 200 μ l of PBS, with a centrifugation step between washes. 100 μ l of DAPI counterstain (Thermofisher, stock conc 10 mg/ml) diluted 1:500 was added to the wells and incubated in the dark for 15 minutes at room temperature. The wells were washed twice in 200 μ l of PBS, with a centrifugation step between washes. 100 μ l of PBS was added to each well and the plate spun down ready for imaging on the Yokogawa CV8000.

Antibody/Stain	Antibody Type	Manufacturer	Cat No.	Dilution
Rabbit Anti-BIP IgG	Primary	Abcam	ab21685	1:1000
Goat Anti-Human IgG (H+L Chain), AlexaFluor488	Conjugated Primary	Thermofisher	A-11013	1:1000
Goat Anti-Human IgG, FcY Fragment Specific	Primary	Jackson ImmunoResearch	109-005-008	1:1000
Goat Anti-Human Kappa Light Chain IgG	Primary	BioRad	STAR127	1:1000
Donkey Anti-Goat IgG, AlexaFluor647	Secondary	Thermofisher	A-21447	1:1000

Table 2.7. Primary and secondary antibodies used for fixed fluorescence imaging experiments.

2.7.3. Imaging on the Yokogawa CV8000

Plates were imaged on the Yokogawa CV8000 at 1 Z slice in confocal fluorescence mode, using the 60x water objective. Imaging parameters and wavelength settings for individual experiments will be discussed in the relevant chapters.

2.7.4. Quantification of the fluorescence imaging

Quantification of the images produced from fluorescence microscopy were analysed in Columbus software (version 2.9.1.). The images were imported into the software and a bespoke quantification script run on them. Briefly, the size and location of the ER and nucleus were identified via their positive staining for BIP and DAPI respectively. From here quantification of a variety of cell characteristics of the whole cell, cytoplasm and nucleus were possible. These factors included the staining intensity of each fluorescence filter and morphology features e.g. diameter, length and area. Once the script had been designed it was then run over all of the images obtained by the microscope, and the geometric mean for each cell characteristic was calculated by the Columbus software using the cells in each well. The geometric mean was achieved by measuring the product of the cellular characteristic values and was then divided by the number of cells identified in the sample. The geometric mean was used in attempts to reduce skewing of the average by any cells present in the sample that were not representative of the population e.g. cells undergoing late stage of mitosis or in the process of apoptosis. The values were then saved in a csv file for further analysis.

2.8. PrimeFlow RNA

PrimeFlow RNA (Invitrogen) uses fluorescence in situ hybridisation (FISH) to quantify specific RNA targets inside fixed cells. Briefly, a target specific probe set is incubated with the fixed cells, and these target specific probes then have their signal amplified by a set of branched DNA structures that are ultimately attached to fluorescent labels. The fluorescence signal can then be detected by flow cytometry (Invitrogen, 2017). A full explanation and schematic of the protocol can be found in Chapter 3. PrimeFlow RNA was performed over two days, using the PrimeFlow RNA kit as per the manufacturer's instructions (Thermofisher). Cells were seeded to a density of 0.4×10^6 viable cells/ml to a volume of 30 ml 1 day prior to experiment start. Unless otherwise stated all buffers were taken from the PrimeFlow RNA kit and all centrifugation steps performed at 400 xg for 5 minutes followed by supernatant aspiration.

2.8.1. PrimeFlow RNA: Day 1

5×10^6 viable cells were centrifuged, and resuspended in 100 μ l of FACS Staining Buffer (1% BSA, Sigma Aldrich, in PBS). The cells were pelleted and the supernatant removed. Fixation buffer 1 was made up of equal parts fixation buffer 1A and 1B, and 1 ml was added to each of the cell samples. The cells were vortexed to mix and incubated for 30 minutes at 2-8 °C. The cells were pelleted and resuspended in 1 ml of 1x Permeabilisation Buffer containing RNase Inhibitors. Samples were mixed, centrifuged and the addition of permeabilisation buffer, spinning and supernatant decanting repeated. 100 μ l AlexaFluor488 conjugated Goat Anti-human IgG H+L Chain (Thermofisher, A11013), diluted to 10 μ g/ml in FACS buffer, was added to the samples and incubated for 30 minutes in the dark at 2-8 °C. A further 1 ml of 1x Permeabilisation Buffer was added, inverted to mix and centrifuged. Meanwhile Fixation Buffer 2 was diluted 1 in 8 in PrimeFlow RNA Wash Buffer, and 1 ml added to the cell pellet after removal of the supernatant and incubated for 60 minutes in the dark at room temperature after inverting to mix.

The samples were pelleted and resuspended in the residual volume by vortexing. 1 ml of PrimeFlow RNA Wash Buffer was added, inverted to mix and centrifuged. The wash step was repeated. The target probe diluent was pre-warmed to 40 °C in an Innova 4000 shaking incubator (New Brunswick Scientific), set to 90 RPM. The target probes were diluted 1/20 in the pre-warmed Target Probe Diluent to a total volume of 100 μ l per sample, and thoroughly mixed by pipetting. Target probes used can be seen in Table 2.8. 100 μ l of diluted target probes were added to the samples and vortexed to mix, before incubating for 2 hours at 40 °C with an inversion mix after 1 hour. 1 ml of Wash Buffer was

added, inverted to mix and centrifuged. All but ~100 μ l of supernatant was removed, and cells resuspended in 1 ml of Wash Buffer containing RNase Inhibitors (diluted 1 in 100 in wash buffer). The samples were inverted to mix, centrifuged and all but ~100 μ l of supernatant removed. Samples were vortexed and stored overnight in the dark at 2-8 °C.

2.8.2. PrimeFlow RNA: Day 2

The PreAmp mix, Amp mix and Label Probes that were used to amplify the signal were pre-warmed to 40 °C in an Innova 4000 shaking incubator (New Brunswick Scientific) set to 90 RPM. After warming, 100 μ l of PreAmp mix was added to the samples, vortexed to mix and incubated for 1.5 hours at 40 °C in a shaking incubator. 1 ml of wash buffer was added to each sample, inverted to mix and centrifuged. All but ~100 μ l of supernatant was removed and the wash step repeated twice. The pelleted cells were resuspended in 100 μ l of Amp mix, vortexed to mix and incubated at 40 °C for 1.5 hours in a shaking incubator. The three wash buffer steps were repeated after incubation.

Label probes were diluted (100x) in Label Probe Diluent, and 100 μ l added to each pelleted cell sample, before incubating for 1 hour at 40 °C in a shaking incubator, covered in tin foil. Three wash buffer steps were performed, keeping the samples in the dark where possible. 1 ml of FACS buffer was added to each pelleted sample, inverted to mix and centrifuged. The cell pellets were resuspended in 100 μ l of FACS buffer and passed through a FACS tube containing a 70 μ m cell strainer (Falcon).

20 μ l of the filtered sample was added to a 384 well plate in triplicate. The iQue flow cytometer (Intellicyt) was cleaned and quality control checked as per Section 2.9. The plate was run with a sample sip time of 5 seconds and an additional up time of 0.5 seconds.

Target	Cat No.	Fluorophore
IgG	VPKA3A9 (Custom Made)	AlexaFluor750
PDI	VF1-4105104	AlexaFluor647
BIP	VF1-4104984	AlexaFluor647
XBP1	VF10-4104855	AlexaFluor647

Table 2.8. PrimeFlow RNA target constructs, catalogue numbers (Thermofisher Scientific) and bound fluorophores.

2.9. Flow Cytometry using the iQue Screener

All flow cytometry experiments were performed on the iQue Screener Plus (Intellicyt), with the exception of cell counting during static scale up (described in Section 2.4.4.). The parameters and settings for individual experiments using the iQue will be discussed in the relevant chapters. A 20 minute clean was performed upon start-up of the iQue, followed by a quality control test. Two drops of Intellicyt iQue Validation Beads (Intellicyt) were diluted in 300 μ l of PBS (Gibco) before reading on the iQue under the preinstalled quality control template. After completion of the experiment a post-plate clean (30 seconds flush, 30 seconds clean and 60 seconds water) was performed, followed by a 20 minute shutdown clean.

2.10. Production Study

2.10.1. Pre-Culture and Production Study Inoculation

Fed-batch production studies were run in 250 ml shake flasks (Thomson) using a GSK proprietary feeding protocol. Production studies were performed on cultures after approximately 5 passages from revival. 4 days prior to inoculation the cultures were passaged to 0.3×10^6 viable cells/ml to a total volume of 60 ml.

On the day of inoculation, 1 ml of the culture was sampled and 500 μ l counted on the ViCell XR (as per Section 2.1.1.) at a 2.0 dilution in TrypleE. The remaining 500 μ l was transferred to a CEDEX tube (Roche) and centrifuged at 15,000 xg in a microcentrifuge (Eppendorf) for 2 minutes to pellet the cells. The tubes were transferred to the CEDEX Bio HT Analyser (Roche) to measure metabolite concentration and mAb titre so that metabolite and mAb carryover after inoculation could be calculated. The CEDEX measured the following metabolites and mAb titre highlighted in Table 2.9, using the CEDEX BioAnalyser software (Roche).

CEDEX Setting	Metabolite Measured
GLC3B	Glucose
GLN2B	Glutamine
GLU2B	Glutamate
IGGHB	IgG (80-1600 mg/L)
IGGLB	IgG (10-80 mg/L)
LAC2B	Lactate
LDH2B	Lactate Dehydrogenase
NH3B	Ammonia

Table 2.9. Metabolite settings used on the CEDEX Bio HT Analyser, and the metabolites they measure for. Human IgG was first measured on the lower range setting (IGGLB) until day 6, where increasing titre required the higher range setting (IGGHB).

1×10^6 viable cells/ml were inoculated into 100 ml of production media (GSK proprietary media + 25 μ m MSX), alongside 1 ml of proprietary feed. The cultures were then sampled again for ViCell counting and the CEDEX to obtain a baseline reading of the titre and metabolites. A further 200 μ l of sample was aliquoted into a 1.5 ml tube (Eppendorf) from the CALR-GFP reporter host lines to quantify the GFP reporter expression. Cultures were kept in a Multitron shaking incubator (Infors HT) at 35 °C, 140 RPM and 5 % CO₂ for the 15 day production study.

2.10.2. Measuring GFP expression with the iQue flow cytometer

The cells were spun down at 720 xg for 4 minutes, the supernatant discarded and 200 µl FACS buffer (0.5% BSA, Sigma Aldrich in PBS) was added. 50 µl of the resuspended cells were added to a flat bottom 96 well plate (Corning), and topped up with a further 50 µl of FACS buffer. The plate was run on the iQue using the BL1-H filter to measure GFP. A pre-plate shake was run for 15 seconds at 1000 RPM and the samples agitated after every 4th sample to stop the cells sedimenting. Each sample was read with a sip time of 45 seconds and an additional up time of 0.5 seconds. The resulting FSC and SSC plots were gated for single cells, and the geometric mean for the FSC, SSC and BL1-H filter calculated.

2.10.3. Production study sampling and feeding

Culture sampling and feeding was performed on days 3, 6, 8, 10, 13 and 15 post inoculation. Cell counts were measured on the ViCell XR as per day 0, until day 8 whereafter a 4.0 dilution with TrypleE was used as cell concentrations increased. The CEDEX was used to measure metabolites as per day 0, and the GFP expression also monitored using the same technique until day 8, where samples were resuspended in 1 ml of FACS buffer as samples were more concentrated.

A pre-determined volume of feed was added to the samples at each time point. Glucose was also added to the cultures where needed, adding sufficient volume to bring the glucose to the required concentration (7-9 g/L dependent on the feed date), using the calculated measurement on the CEDEX.

2.10.4. Culture Harvest

Culture media was harvested at day 15 of the production study so that product quality analysis could be performed on the mAb product. 30 ml of the culture was decanted into a 50 ml tube (Falcon) and centrifuged at 2800 xg for 20 minutes to pellet the cells and debris. 10 ml of the resulting supernatant was carefully poured into a 15 ml tube (Falcon), and the samples immediately frozen at – 80 °C for storage.

2.11. mAb Product Quality Analysis

Product quality analysis was performed on the samples using an automated High Performance Liquid Chromatography (HPLC) system and script by ChemStation (Agilent). Size Exclusion Chromatography (SEC) was used to measure product size, whilst Cation Exchange Chromatography (CEX) measured product charge. Product filtration and purification was required before performing any HPLC studies.

2.11.1. Sample Filtration and Purification

Frozen media were thawed and spun at 2800 xg for 20 minutes with no brake before filtering to ensure any remaining cell debris was separated from the product. A Freedom EVO 200 liquid handler (Tecan) was used to filter the samples, using a proprietary script. Briefly, the samples were passed through a Unifilter 96 well plate (Whatman), and into a 48 deep well plate to a total volume of 4 ml. At the beginning and end of each script a maintenance clean was performed to ensure the Tecan tips were clean.

The filtered samples were also purified on the Freedom EVO 200, using a MabSelect PrismaA column (Cytiva). The filtered samples were passed through the column, and eluates of the samples were collected in a plastic UV-STAR 96 well plate (Greiner). The samples were eluted into individual rows of a plate which moved across during elution, resulting in a full row of one eluates from one sample.

2.11.2. Measuring Sample Concentration and Normalisation

After the elution was complete the plates were measured for product concentration using a Magellan plate reader (Tecan) on the A280 filter. As the eluates varied in concentration, only wells with a value above 1 in the same row were pooled into a fresh 96 deep well plate, to ensure a concentrated, purified sample. The process was repeated for each sample row. The pooled eluates were then measured on a Lunatic spectrometer (Unchained Labs) under the 'protein turbidity (A280)' setting using the pre-determined mAb extinction coefficient. 3 µl of each sample was added to individual wells of a 'high lunatic plate', alongside a water blank. The resulting concentrations were noted and used to calculate the dilution required to normalise the samples for HPLC analysis.

Sample normalisation was also performed on the Freedom EVO 200. The samples were normalised for SEC analysis to 2 mg/ml in sterile water on the Tecan into a V bottomed 96 well HPLC plate (Greiner). The process was then repeated for CEX analysis, at a concentration of 1 mg/ml in mobile phase buffer 'CX-1 pH Gradient Buffer A (Thermo Scientific). The sample concentrations were confirmed using the Lunatic plate reader, and were then ready for HPLC analysis.

2.11.3. Running product quality analysis on the HPLC systems

The SEC and CEX sample plates were sealed with a Zone Free Sealing Film (Excel Scientific) and loaded into their respective HPLC systems using ChemStation software (Agilent). Samples were run on the HPLC systems using a proprietary protocol.

A 25 μ l injection volume was used for CEX analysis, eluted over an acidic to basic gradient change in mobile phase, using the CX-1 pH Gradient Buffer A and CX-1 pH Gradient Buffer B (both Thermo Scientific). An 18 μ l injection volume was used for SEC analysis, eluted over a gradient change in mobile phase using 100 mM Sodium Phosphate, 400mM Sodium Chloride at pH 6.8 and sterile water (both in house).

2.11.4. Analysing the HPLC data sets

Both CEX and SEC samples were analysed using the same technique on ChemStation software (Agilent). Peaks were manually identified on one representative chromatogram for each mAb type expressed, and copied into all other chromatograms containing the same mAb. Each individual chromatogram was then checked to ensure the correct peaks had been identified. The quantitative values obtained from the peaks were exported into an excel file. Chromatograms were visualised on Chromview software (ChemStation).

2.12. Statistical Analysis

All graph design and statistical analysis was performed in GraphPad Prism (version 9.2.0.), unless otherwise stated. Statistical analysis was performed using the most appropriate test for the data concerned and repeated in biological triplicate unless otherwise stated. Variation was deemed statistically significant when $p < 0.05$. Details regarding the specific tests used for each experiment can be found in their corresponding chapter.

3. Predicting mAb quality and quantity in CHO clones expressing a bispecific mAb using the Unfolded Protein Response (UPR)

3.1. Introduction

Chinese Hamster Ovary (CHO) cells are one of the most commonly used expression systems to produce biopharmaceutical products, being used as an expression system in 35% of all approved biopharmaceutical products between 1982-2014 (Walsh, 2018). CHO cells become even more common when focusing solely on monoclonal antibody (mAb) production, being 60% of the mAb market's expression system of choice between 2012-2017 (Grilo and Mantalaris, 2019).

The CHO expression systems high market share can be accredited to multiple factors. Their approval in 1987 means that CHO cells have over 30 years of demonstrated safety as an expression system, making marketing approval by regulatory bodies an easier step than in a less tested expression system. CHO cells can also perform complex post-translational modifications that are required in the correct folding of human proteins (Kim et al., 2012; Durocher and Butler, 2009; Walsh and Jefferis, 2006). Further to this, their ability to be easily grown in suspension culture paired with their ability to produce high quantities of exogenous protein, means CHO cells are also readily scalable into mass-manufacture bio-reactors to culture volumes up to 20,000 L (Jayapal et al., 2007; Merten, 2006).

Despite these advantageous qualities, the plasticity of the CHO genome paired with the random integration of the mAb into the CHO genome during transfection results in CHO clones producing mAbs of varying quality and quantity. The CHO genome has been shown to be genetically unstable, with the literature showing that the number of chromosomes in CHO lineages, as well as the presence of chromosomal rearrangements have changed since the first isolation of the CHO line (Vcelar et al., 2018). This plasticity has allowed for the development of modern day CHO lineages used in biopharmaceuticals by chemical mutagenesis, but it does mean that the variation across single cells in a population is apparent even after only one transfection event (Urlaub and Chasin, 1980; Reinhart et al., 2019). To mitigate the potential variation of mAb expression in CHO cells, regulatory bodies require all mAb product to be produced from a single progenitor CHO cell to ensure the mAb characteristics are uniform within the population (Frye et al., 2016). This is achieved by single cell cloning a population of CHO cells transfected with the mAb construct and scaling up the individual cells into a population that has been derived from one progenitor cell.

The subsequent screening of the single cell clones initially focuses on selecting clones with the highest mAb titre and best growth characteristics. This early stage is referred to as Cell Line Development (CLD) in biopharmaceutical production (see Section 1.1.5.) (Lai et al., 2013; Tejwani et al., 2021; Nakamura et al., 2015). This approach has been shown to be reliable throughout the industry, with Porter *et al.*, (2010) showing that selection during scale up is reliable when following cultures through to bioreactor study, whereby 29 cell lines that had been measured and selected for based on titre during shake flask culture of clonal scale up were compared to their titre expression during 10 L bioreactor culture. A statistically significant positive correlation was seen between the two titre measurements ($R^2 = 0.669$), suggesting that the titre obtained during scale up is relevant to subsequent bioreactor study.

Whilst this approach works effectively to select for high producing CHO clones, there are many other crucial factors that cannot be measured during the CLD culture stage, such as the quality of the mAb and whether the titre expression is stable over a long period of time in culture (Nakamura et al., 2015). These are tested much later in the production process and often results in the removal of cell lines that were deemed acceptable during CLD, but then appear to be problematic for these other reasons, causing a huge burden on time and resources. This thesis therefore aims to define a phenotypic fingerprint of clones expressing mAbs with favourable product titre and quality characteristics that can be used to select clones during early cell line development. Ultimately this would reduce the number of poor quality clones that would be removed after CLD, and allow a greater pool of potentially manufacturable clones to be progressed instead.

Reasons for poor product quality often focuses on the final structure of the mAb product, with fragmentation and aggregation being two important quality issues. Fragmentation refers to any product that is smaller than the desired mAb format, and can affect the isoelectric point (pI) of the mAb product which has been in turn shown to affect the binding activity of the mAb in humans (Torkashvand and Vaziri, 2017). Conversely, aggregation refers to any products that are larger than the desired format, often from incorrect folding causing binding of the mAb product together, and is important as aggregated mAb can cause immunogenic responses in humans (Ishii et al., 2014). Joubert et al. (2012), for example, showed that when aggregated formats of 3 different mAb products were introduced *in vitro* there was an increased secretion of cytokines related to innate and T-cell immune responses, in comparison to the introduction of their respective mAb monomer.

This issue of product quality and titre is exacerbated as biopharmaceutical companies begin to make the design of therapeutic antibody targets into more complex formats, increasing the burden on the CHO expression system. Novel mAb formats such as bispecifics, single domain formats and protein

conjugates (described in Section 1.2.6.) are coming into the forefront of therapeutic design- with two bispecific mAbs already gaining FDA approval in 2014 and 2017 (Mullard, 2021). Bispecific mAbs can target two different epitopes of target antigens – these can be the same epitopes of the same antigen or two different antigens. Bispecific mAbs therefore have advantageous qualities as a drug target, such as the ability to induce an immune effector response, by using one mAb epitope to redirect immune cells to problematic antigens on the other epitope, as well as increasing the half-life of the mAb drug and dual-targeting the same antigen target (Zhukovsky et al., 2016; Kontermann, 2011; Kontermann, 2012).

Blinatumomab, a bispecific mAb fragment approved in 2014, binds to cancerous B cell targets via CD19 receptor binding as well as simultaneously engaging cytotoxic T cells using CD3 mediated binding (Przepiorka et al., 2015; Topp et al., 2008). The second approved bispecific mAb, Emicizumab, is a full length bispecific that binds to coagulation factor IX and X and is approved for use in patients with Haemophilia A (Center for Drug Evaluation and Research, 2018). Haemophilia A is characterised by the loss of coagulation factor VIII, which is crucial for supporting the interaction of factor IX and X which in turn activates the rest of the coagulation cascade, that is required for successful blood clotting. Emicizumab therefore mimics the role of factor VIII in Haemophilia A patients preventing their need for exogenous factor VIII infusion (Shima et al., 2016; Kitazawa et al., 2012). These more complex designs bring their own challenges for CLD, as expressing a bispecific molecule for example can result in up to 9 different chain combinations as well as the desired format, drastically reducing the percentage of desired product (Carter, 2001). These potential chain combinations can be highlighted in Figure 1.6.

Whilst fragmentation and aggregation can have extracellular causes such as pH (Vlasak and Ionescu, 2011), literature has shown a link between product quality and endoplasmic reticulum (ER) folding capacities (Le Fourn et al., 2014; Ishii et al., 2014) and thus it was hypothesised that clones expressing poorer quality mAbs had impaired protein folding. Protein Disulphide Isomerase (PDI) is an enzyme that catalyses the formation of disulphide bonds and is a key enzyme in the folding of mAbs, with one study showing the overexpression of PDI resulted in an improved product secretion rate (Borth et al., 2005). In fact, the Endoplasmic Reticulum (ER) follows a strict folding pathway for mAbs (Section 1.2.3.), so when protein folding becomes impaired a signalling cascade known as the Unfolded Protein Response (UPR) attempts to return the ER folding pathway to homeostasis. The UPR is a complex, multi-armed pathway that is inhibited by Binding Immunoglobulin Protein (BIP) in homeostatic protein folding conditions (Hetz, 2012) (see Section 1.6. for the full pathway). When a build-up of misfolded protein occurs, BIP dissociates from the initial sensors of the UPR and instead binds to the misfolded proteins, thus signalling the initiation of the UPR. The UPR then activates transcription factors to

upregulate expression of genes involved in protein folding, and temporarily attenuate genes involved in protein translation (Patil and Walter, 2001; Prashad and Mehra, 2015). CHO clones with higher mAb titre, have been shown to have higher mRNA concentrations of key UPR markers such as BIP and spliced X-Box Binding Protein 1 (sXBP1) (Kober et al., 2012). In a second study, the mRNA of BIP and a host of other UPR proteins was more highly expressed in a high producing mAb clone compared to a low producing clone (Prashad and Mehra, 2015). This data suggested that higher producing clones are either inherently better at initiating the transcription of the UPR when a build-up of misfolded protein is present in the cell, or that there is a higher presence of the UPR proteins naturally in the clone without a stress stimuli.

Unfolded or misfolded protein has also been shown to be a cause of aggregated and fragmented protein in the CHO cell, when protein folding demands out balance the quality control processing capacity (Kiese et al., 2010; Torres *et al.*, 2022). Aggregation has been negatively correlated to free light chain in the media, which is easily secreted out of the ER whilst free heavy chain often is retained inside the clone (Bhoskar et al., 2013; Borth et al., 2005).

3.1.1. Chapter Aims

The aim of this Chapter was to determine how the ER and the UPR respond to the expression of bispecific mAb in a panel of CHO clones, with particularly stark product quality and titre issues. Multiple experimental techniques were trialled for their effectiveness, reliability and ease of use. The bispecific clonal lines analysed in this Chapter were previously generated by GSK and had undergone product quality analysis before the beginning of this thesis. From here, if any correlations were found in the bispecific lines, the tests could be extended to other mAb types to confirm if the effects were universal. A bispecific molecule was chosen for preliminary investigation in the hopes that these obvious product quality issues could be a basis for more typical mAb formats.

3.2. Results

3.2.1. Designing a clonal cell line panel for testing techniques

A panel of clonal CHO cell lines expressing a GSK proprietary bispecific mAb molecule was used for initial phenotype marker detection. 10 clones were chosen with desirable and undesirable characteristics relating to product titre, fragmentation and aggregation (Table 3.1). Titre and product quality were determined during Upstream and Downstream processing of the clonal cell line culture by scientists at GlaxoSmithKline prior to the start of the project.

Cell Line	SPR (pg/cell/day)	Fragment (%)	Aggregate (%)
Clone A	High	High	High
Clone B	Low	High	Low
Clone C	High	High	Low
Clone D	Low	High	High
Clone E	High	Acceptable	Low
Clone F	High	Low	Low
Clone G	High	High	High
Clone H	Low	High	Low
Clone I	High	Acceptable	Low
Clone J	High	High	Low

Table 3.1. The mAb product characteristics of a clonal cell line panel used to investigate the relationship between UPR proteins and mAb product and quality.

Clonal lines have been anonymised and are all expressing the same bispecific molecule. Specific Productivity Rate (SPR) (pg/cell/day) was used as a measure of titre. Aggregate (%) and Fragment (%) was measured by High Performance Liquid Chromatography (HPLC). Green highlights clones within the desirable production range, whilst orange shows properties that are out of the desirable criteria. Data was produced by GSK scientists.

3.2.2. Using a live ER Tracker Cell Stain to measure whole ER content

Initial examination of the clones protein processing capacity was measured by the live cell ER stain, ER Tracker (Invitrogen). ER Tracker allows monitoring of the intensity and size of the ER (Sahay et al., 2010). ER-Tracker was tested preliminarily on the CHO host, as well as clones A and B from the clone panel. Live, fluorescence imaging confirmed that the ER was clearly visible and quantifiable (Figure 3.1). Quantification was measured as the geometric mean of the fluorescence intensity (gMFI) in the sample population. There did not appear to be any visible difference in the amount of ER between the CHO host and the two clones (Figure 3.1.A), and this was reflected in the quantification of the stain (Figure 3.1.B). The standard deviation was calculated as the variability in the cell population, therefore large error bars were seen in the quantification due to heterogeneity in the size of the individual cells and the growth phase they were in at the time. As the staining intensity and quality of the ER Tracker was optimised for stain concentration prior to the experiment, as well as optimisation of the microscopy imaging technique, it was not thought to play a factor in this variability. Although live stains are advantageous due to their ease in use, ER Tracker is a cell permanent dye and cytotoxicity caused by the BODIPY dye has been cited (Laine et al., 2017). ER Tracker cytotoxicity was therefore tested by incubating the Clone A culture with 100 nM and 1 μ M ER-Tracker over a 4 day passage. Viable cell count, total cell count and viability did not appear to be affected by the addition of ER-Tracker compared to the negative control (Figure 3.1.C.) indicating there was no negative impact to the cells when using the ER tracker.

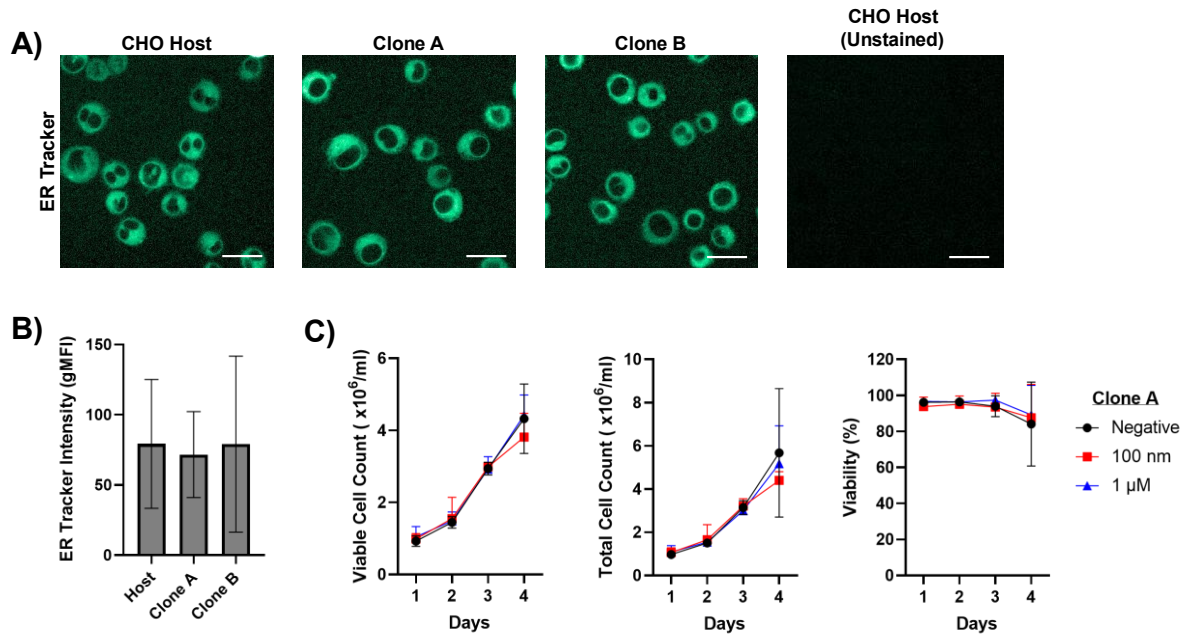


Figure 3.1. The intensity of the ER Tracker staining was similar between the CHO clones.

A) ER Tracker (Invitrogen) staining on three live cell populations: the CHO host and bispecific mAb Clone A and Clone B. 500,000 cells were taken from culture and incubated with 1 μM ER Tracker for 30 minutes before being washed and imaged on a Yokogawa CV8000 microscope. A CHO host negative control that was not incubated with ERTracker was also imaged. Scale bar = 20 μm . **B)** Quantification of ER Tracker intensity inside the cell populations (~ 1000 cells per cell line) by geometric mean fluorescence intensity (gMFI). ER Tracker intensity was measured at similar intensities in all three populations. Large error bars may be due to the heterogeneity of population sizes and the process of cell division ($N=1$). Error bars = ± 1 SD.

C) Viable cell count, total cell count and viability in Clone A cultures incubated with varying concentrations of ER Tracker over 4 days in culture. Samples were measured on the ViCell XR. ER Tracker did not appear to have any cytotoxic effects. Negative (black), 100 nM (red) and 1 μM (blue) ($N=3$). Error bars = ± 1 SD.

3.2.3. Human mAb staining showed distinct phenotypes in a high and low producer CHO clone when measured with immunofluorescence microscopy

As the size of the ER itself did not appear to be different between the CHO host and the mAb expressing clones, measuring UPR specific targets were considered rather than the ER organelle as a whole. BIP was chosen as it showed the high correlative relationships with titre in previous studies (Kober et al., 2012) (Prashad and Mehra, 2015). BIP is also the master regulator of the UPR, and thus any induction of BIP would likely suggest that there was an induction of the UPR due to a build-up of mis-folded protein present in the cell (Prashad and Mehra, 2015).

Immunofluorescence microscopy on fixed cells was first performed on the CHO host, Clones A and B to determine the localisation and levels of BIP and human IgG (Figure 3.2.). In addition, DAPI was used to stain the nucleus of the cells. As expected, no staining by the anti-human IgG antibody was observed in the CHO host as IgG was not present in the CHO host (Figure 3.2.A.). IgG staining was present in both clones. However, in Clone A the staining was largely present outside of the cells in structures which potentially resemble extracellular aggregates. In contrast, the IgG was present predominantly inside the cells of Clone B, as seen in the quantification of intracellular IgG (Figure 3.2.C.). Intracellular IgG was in fact 2.77 fold higher in clone B than clone A. Extracellular IgG could not be quantified. Clone A has been defined as a high titre producer, however the IgG it produces is prone to aggregation and fragmentation. The exact form the fragment takes cannot be confirmed as it was not measured in the previous study, however as all of the clones did produce measurable mAb it can be speculated that the product does contain secreted heavy chain as the protein A binding used by the Octet HTX (ForteBio) in CLD binds to the Fc region of mAbs (Fischer et al., 2017). Thus, it appears likely that the clones are able to produce heavy chains, and may be present in the fragmented product. Clone B is classified as a low titre producer, with low aggregate but high fragmentation. Thus, the large masses of IgG observed outside of the cells in the Clone A could be aggregated IgG.

BIP expression showed a localised ER staining pattern as expected. The staining appeared heterogenous within the populations, with the strongest visual expression in clone B. This was confirmed by microscopy quantification (Figure 3.2.C), with clone B showing a 2.08 fold increase in staining intensity compared to the CHO host. Surprisingly, the CHO host and clone B had very similar staining intensity's, suggesting that the UPR was not being upregulated due to the addition of the second plasmid. This may hint that the clone is very good at producing the high quantity of mAbs being translated, but is not necessarily folding them successfully enough that they maintain their monomer form following secretion.

As the quantification of the imaging was only tested over one biological replicate (~ 500,000 cells imaged per cell line), this result cannot be confirmed as statistically significant however. Of course, heterogeneity across the cells in each population may also play a part in this variation. The cells in the sample may be in different growth phases, and thus are not all necessarily focusing on protein production. As the intensity of the stain was normalised to the size of the cell, the effects of cell division have been mitigated where possible, however a tool that can quantify the staining intensity of individual cells may be beneficial.

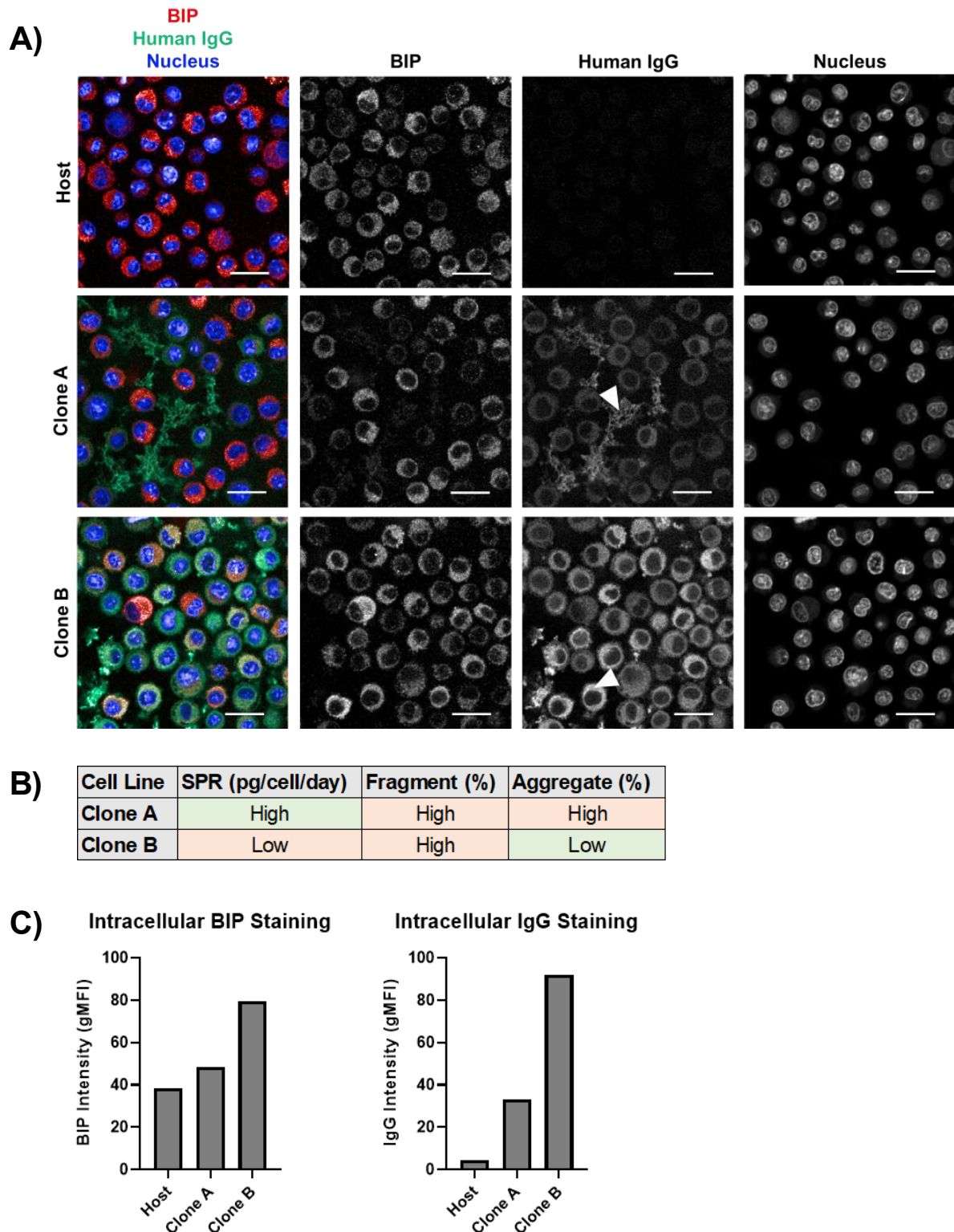


Figure 3.2. Large amounts of extracellular IgG was seen in clone A, a highly aggregated clone.

A) Fluorescence microscopy images on three fixed clonal cell line populations, measured on a Yokogawa CV8000 microscope. 500,000 cells from each culture was fixed and stained for BIP and human IgG. BIP shown in red, human IgG in green and DAPI nuclear staining in blue. Clone A has greater extracellular mAb staining, and clone B has greater intracellular mAb staining, indicated by white arrows (N=1). Scale bar = 20 μ m.

B) Product quality table showing mAb titre and product quality for Clones A and B. **C)** Quantification of the intracellular BIP and IgG staining in the three clones as measured by Columbus software, version 2.9.1 (N=1). A minimum of 1000 cells were used for quantification per sample.

3.2.4. Quantification of UPR targets with PrimeFlow RNA

The microscopy-based experiments suggested that there may be differences in the folding and expression levels of the IgG molecules between each clone. Thus, it may be of interest to determine what is happening in these clones at the molecular level. Thus, it was decided to quantify the UPR pathway and intracellular IgG levels using a transcriptomic based approach.

PrimeFlow RNA was used to measure intracellular IgG, BIP and PDI transcripts. PrimeFlow RNA is based around fluorescence *in situ* hybridisation (FISH) and flow cytometry. A probe is designed to a specific mRNA target which is then hybridised to the fixed cells and the signal amplified by a series of branched DNA structure steps followed by the addition of a fluorescent label to the probe (schematic in Figure 3.3.A.). BIP and PDI probes were obtained directly from ThermoFisher, whilst a custom made IgG probe was designed to a conserved region of the IgG heavy chain specific to GSK's proprietary mAb sequences (see Table 2.8.). The technique was confirmed to be binding specifically to the targets by the addition of increasing concentrations of the chemical stressor Tunicamycin to CHO host culture. Tunicamycin inhibits N-linked glycosylation, resulting in mis-folded protein folding that becomes blocked in the ER (Tordai et al., 1995). Tunicamycin was incubated in the cultures for 4 hours before performing BIP RNA quantification via PrimeFlow RNA. The concentration of BIP RNA showed to increase as the amount of Tunicamycin (and therefore ER stress) increased, suggesting that the response was specifically binding to the BIP RNA (Figure 3.3.B.).

RNA transcripts of BIP, PDI and human IgG in the panel of bispecific cell lines were measured in the cell lines 1 day post passage, in biological triplicate (Table 3.1.). PDI and BIP transcripts were labelled in separate experiments. The binding of IgG probe was shown to be specific to the IgG target RNA as the CHO host control was negative for IgG RNA compared to the expressing clones (Figure 3.3.C.). Results were performed in biological triplicate. PrimeFlow RNA quantification was measured by the geometric mean fluorescence intensity (gMFI) of the bound fluorescent label probes, however when the intensity values were compared across the triplicates the values were inconsistent (Figure 3.3.D.). IgG RNA transcript staining intensity (gMFI) ranged from 2,711 - 1,750,000 across the experiment, with replicate 2 having the greatest average fluorescence intensity out of all of the replicates. The average replicate 2 intensity was in fact almost 50 x fold greater than replicate 2, and over 400 x fold increase than replicate 3. To account for this variability in intensity scores at different replicates the values were normalised to the CHO host.

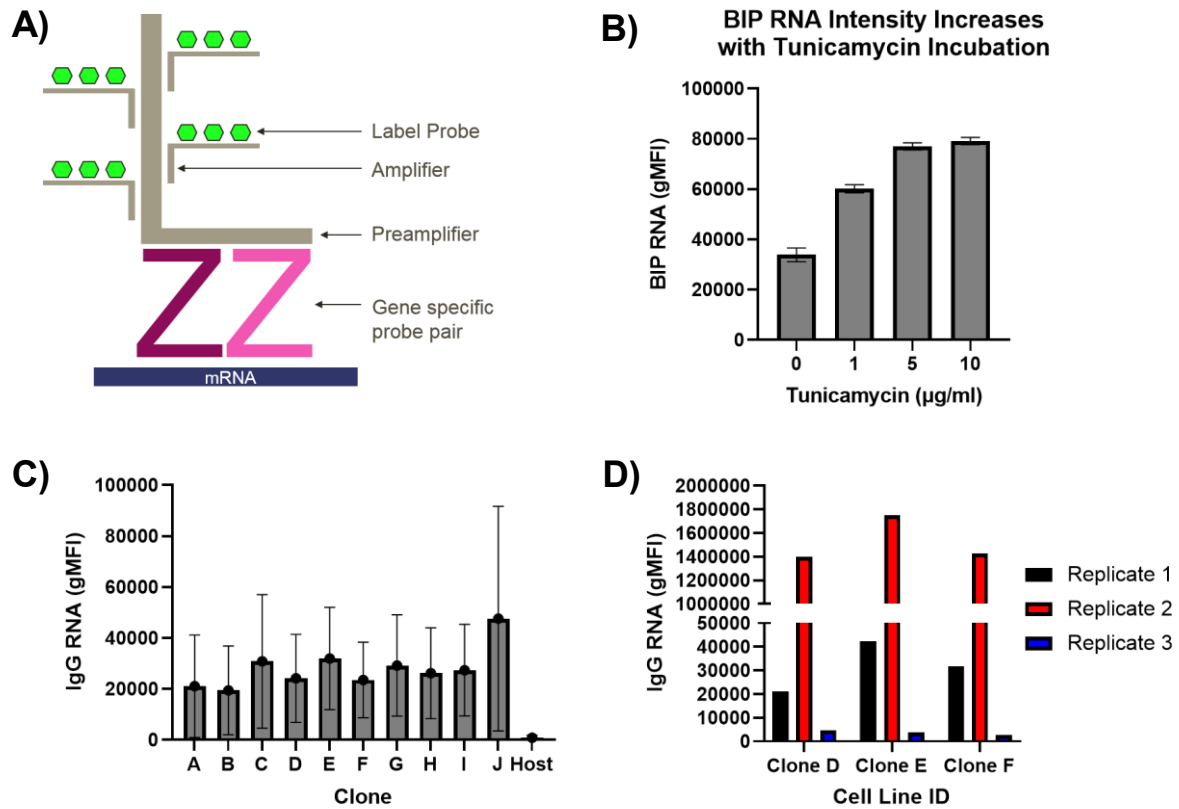


Figure 3.3. PrimeFlow RNA was able to successfully detect IgG RNA transcripts although the biological reproducibility was very low.

A) Schematic diagram showing the principles of PrimeFlow RNA. A pair of gene specific probes are added to the sample, followed by complementary pre-amplifiers and amplifiers to increase the signal. A final label probe is added containing AlexaFluor specific dyes that can be measured by flow cytometry. Diagram adapted from Invitrogen, 2017. **B)** BIP RNA transcripts were increased in the CHO host with increasing Tunicamycin incubation as measured by PrimeFlow RNA on the iQue flow cytometer (N=3). Error bars =+/- 1SD. **C)** IgG RNA gMFI intensity in all Clones A-J and the CHO host. IgG RNA was at background levels for the CHO host suggesting that the IgG PrimeFlow probe was specific (N=3). Error bars = +/- 1SD. Quantified on the iQue flow cytometer. **D)** IgG RNA transcript gMFI intensities of Clone D, Clone E, and Clone F (N=3). The three replicates vary greatly between each other indicating this technique is not reproducible. Quantified on the iQue flow cytometer.

After normalisation the RNA transcripts of PDI, BIP and IgG in the samples were correlated to the previously calculated SPR (pg/cell/day), Fragment (%) and Aggregate (%) (See Section 3.2.1.). Pearson's rank analysis was used for all correlation analysis as the data passed a Shapiro-Wilk normality test. BIP showed a significant, strong correlation with fragment (%) ($r = 0.902$, $p < 0.01$) (Figure 3.4.A.). Neither SPR (pg/cell/day) nor aggregate (%) showed any correlation with BIP RNA expression. PDI transcript expression however was moderately negatively correlated to the fragment (%) in the final mAb product ($r = -0.644$, $p = 0.045$, Figure 3.5.A). A correlation matrix heat map highlighted all of the non-significant correlations not discussed for the BIP and PDI RNA studies against product titre and quality (Figure 3.4.B. and Figure 3.5.B respectively). No correlation was seen with aggregate (%) in the final mAb product, as well as a non-significant SPR positive correlation. This suggests that PDI has a correlative link to the product being fragmented, where an increased PDI reduces the likelihood of fragmentation. As the chaperone activity of PDI to catalyse disulphide bonds is important to ensure fully folded product (Weissman and Kimt, 1993), this led to the hypothesis that low PDI activity results in a high population of fragmented or LMWS.

Interestingly, the correlation between IgG RNA and SPR over the two separate experiments (measuring BIP and PDI respectively) varied, despite using the same probe sets for measuring IgG. IgG RNA was only significantly correlated to the SPR (pg/cell/day) in the BIP study (r of 0.89, $p < 0.05$). The PDI study in comparison had only a moderate positive, and non-significant correlation for IgG RNA against SPR ($r = 0.53$, $p = 0.119$). Whilst variation is expected over different experiments it was surprising that the two correlations were so dissimilar from each other. This combined with the inconsistency of the measured concentrations from each biological replicate, threw the reliability of PrimeFlow RNA as a technique into doubt. Instead, a different RNA quantification technique could be used to confirm that the PrimeFlow trends towards BIP and PDI transcripts to predict titre and product quality.

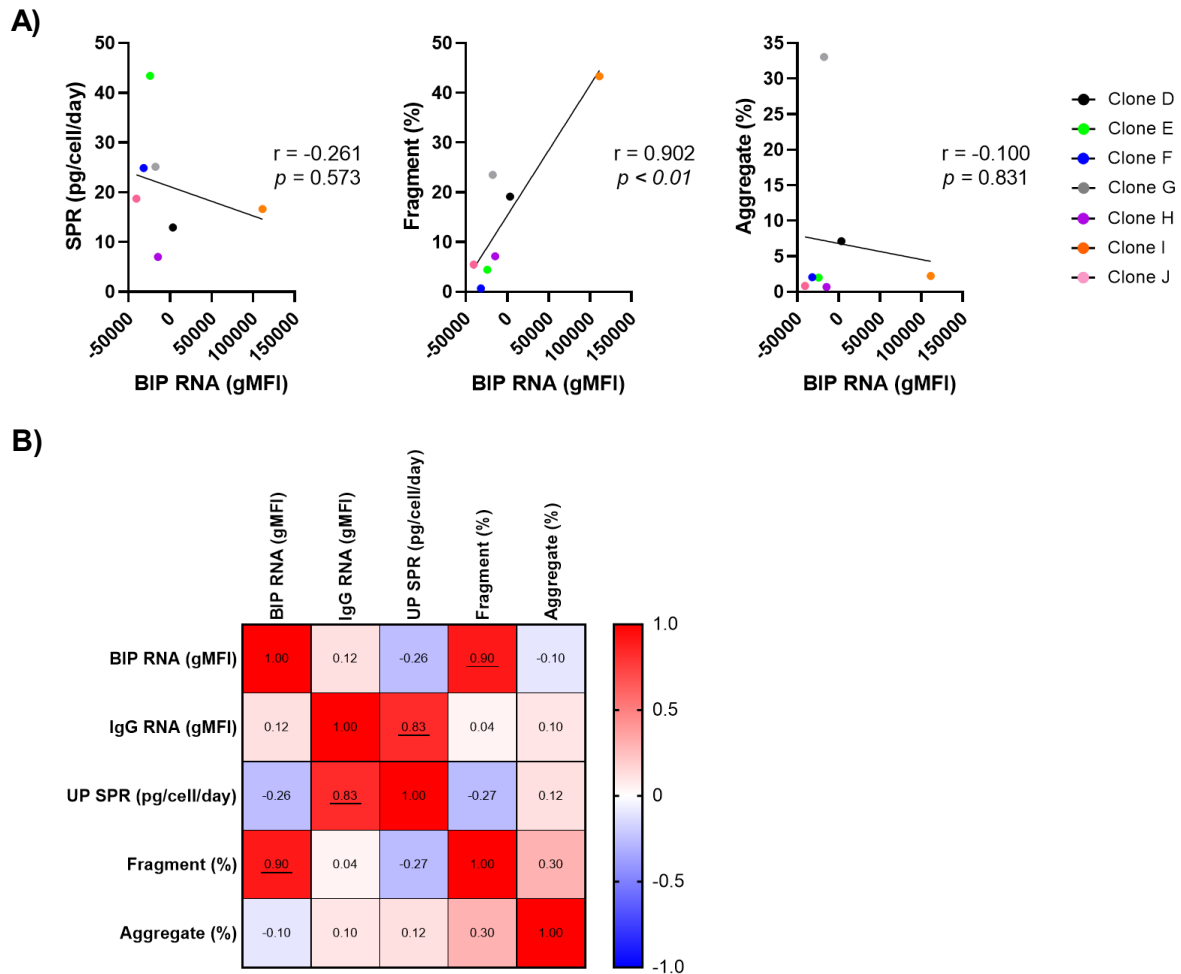


Figure 3.4. The levels of BIP RNA are positively correlated to fragment (%) when measured using PrimeFlow RNA in the clonal cell panel.

5×10^6 viable cells/ml were fixed for PrimeFlow RNA experimental conditions (N=2). The final samples were measured on an iQue flow cytometer. Clones have been coloured to be representative over each graph in figure 3.4-3.6. **A)** BIP RNA transcript intensities normalised to the CHO host in each triplicate, and correlated to SPR (pg/cell/day), fragment (%) and aggregate (%). Pearson’s rank analysis was used to measure the correlation. Statistical significance $p < 0.05$. **B)** Correlation matrix monitoring the BIP and IgG RNA transcripts against all three mAb product variables. Red= Perfect 1.0 positive correlation, blue = perfect -1.0 negative correlation. Statistically significant correlations were set at $p < 0.05$, and underlines in the matrix.

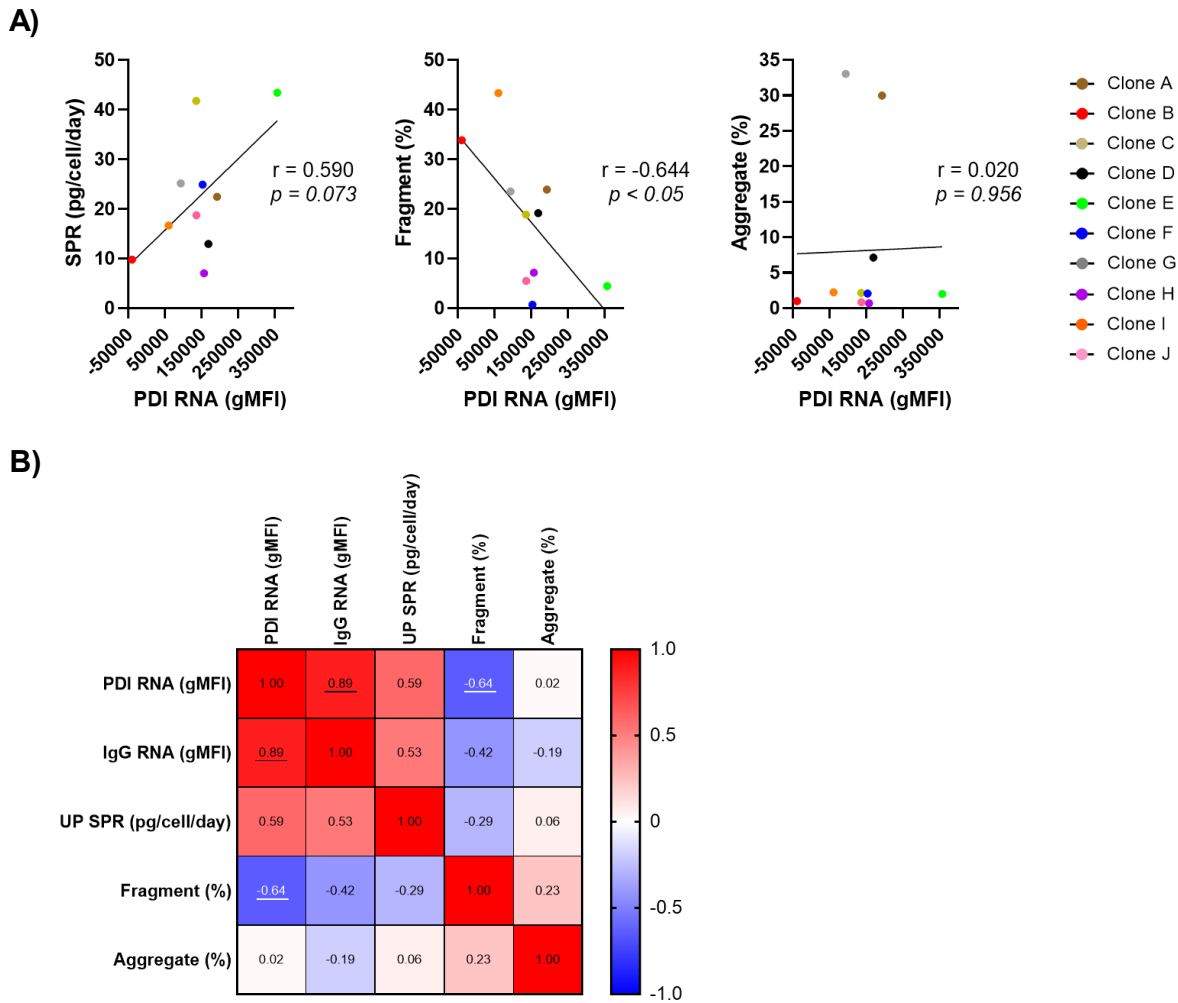


Figure 3.5. The levels of PDI mRNA are negatively correlated to fragment (%) using PrimeFlow RNA in the clonal cell panel.

5×10^6 viable cells/ml were fixed for PrimeFlow RNA experimental conditions (N=3). The final samples were measured on an iQue flow cytometer. Clones have been coloured to be representative over each graph in figure 3.4-3.6. **A)** PDI RNA transcript intensities normalised to the CHO host in each triplicate, and correlated to SPR (pg/cell/day), fragment (%) and aggregate (%). Pearson’s rank analysis was used to measure the correlation. Statistical significance $p < 0.05$. **B)** Correlation matrix monitoring the PDI and IgG RNA transcripts against all three mAb product variables. Red= Perfect 1.0 positive correlation, blue = perfect -1.0 negative correlation.

3.2.5. Quantification of UPR RNA targets with Droplet Digital PCR

Due to the significant variability in the PrimeFlow experiments, digital droplet Polymerase Chain Reaction (ddPCR) was employed as an alternative technique to investigate UPR RNA targets in the bispecific clone panel. ddPCR is a branch of quantitative PCR (qPCR) that has the ability to calculate absolute quantification of nucleic acids, without the need of standard curves. In ddPCR the sample is fractionated into ~20,000 droplets using an oil emulsion, before performing PCR with a fluorescent probe that binds to the target of interest (Hindson et al., 2013). The fractionated sample ddPCR is beneficial over PrimeFlow RNA as a housekeeper gene such as β -Actin can be used to normalise the data using a second fluorescent label (Dhiman et al., 2020). Here, RNA was isolated from the cultured samples in biological triplicate (samples were collected from the same cultures over consecutive passages) and converted to cDNA for use in ddPCR (Section 2.5.). The concentration of the target transcript was normalised to the concentration of the reference transcript, in technical and biological triplicate.

As ddPCR is a higher throughput method, two additional UPR targets were also investigated using these samples: XBP1 and ATF6. Both targets are directly activated during the UPR pathway (Section 1.3.2.) and thus any response seen could be indicative of a UPR response. In addition, the levels of the ER-resident Ceramide Synthetase 2 (CERS2) was also measured. This protein may be predictive of undesirable CHO clones as it was shown to increase mAb titre in CERS2 knocked down clones (Pieper et al., 2017). CERS2 was also tested by ddPCR here therefore to see if non-UPR based targets may be useful as a tool for identifying clones with desirable quality characteristics.

The expression of the target genes normalised to the β -Actin reference, showed a clear difference in the host compared to the bispecific mAb producing clones (Figure 3.6.A and B). Transcripts of all of the targets were between 1.22 and 2.75 fold higher in the host than in the averaged clones, and with much larger error bars. This was likely due to the nature of the CHO host, compared to the clones that were derived from one progenitor cell. The CHO host was derived from a single progenitor cell when it was first generated, however the natural plasticity of the CHO genome means that mutations within the CHO host are likely to have occurred since cloning. CERS2, XBP1 and ATF6 transcripts had fewer copy numbers per μ l compared to the BIP and PDI group - as can be seen by the scale bars of the graphs (CERS2, XBP1 and ATF6 ranged between 0.00-0.05, whilst BIP and PDI ranged between 0.00-0.25). This could suggest that overarching chaperones and folding enzymes such as BIP and PDI were more abundantly transcribed than specific components of the UPR. Zhang et al. (2016) highlights this plasticity using RNA-Seq, whereby over 80 mutations reached the accepted confidence level for significance in a mAb expressing CHO clones after 150 population doublings. When considering the CHO host is not cloned in the same manner, it would explain why such a difference in expression was

seen in this study. Of course, it is not known whether the RNA expression seen in this study is necessarily representative of final protein expression levels for all of these chaperones, and this would have to be further analysed via western blot.

The values obtained from the ddPCR were then plotted in a correlation matrix, where their r value was calculated (Figure 3.6.C.). Four of the Pearson's r correlative tests showed a statistical significance ($p < 0.05$, underlined in the correlation matrix figure). Three of which were stating a positive correlation between two different transcript analyses. XBP1 strongly, positively correlated to BIP and ATF6 expression ($r = 0.85$ and 0.83 respectively), as well as ATF6 and BIP ($r = 0.80$). Further to this, the correlation matrix showed a moderate positive correlation (> 0.40) r value for all of the transcript combinations, albeit not significantly, with the exception of CERS2 that on the whole showed little correlation to the other ER markers. CERS2's main function is to catalyse the synthesis of very long chain ceramides (Yamaji et al., 2016), and as such is not directly regulated by the unfolded protein response. A lack of correlation in CERS2 expression to titre and quality therefore suggests that overall transcription in the clones is not causing the correlations with the UPR, and instead the UPR is up-regulated specifically.

The final correlation seen within the ddPCR data was between PDI and Fragment (%) ($r = -0.625$, $p < 0.05$, Figure 3.6.D.). This was almost identical to that of the PrimeFlow technique (Figure 3.5., $r = -0.644$). This data therefore bolstered the idea that PDI could potentially monitor fragmentation of the product during CLD, under the hypothesis that high PDI activity or transcription is required to catalyse the disulphide bonds necessary for fully folded mAb as previously stated.

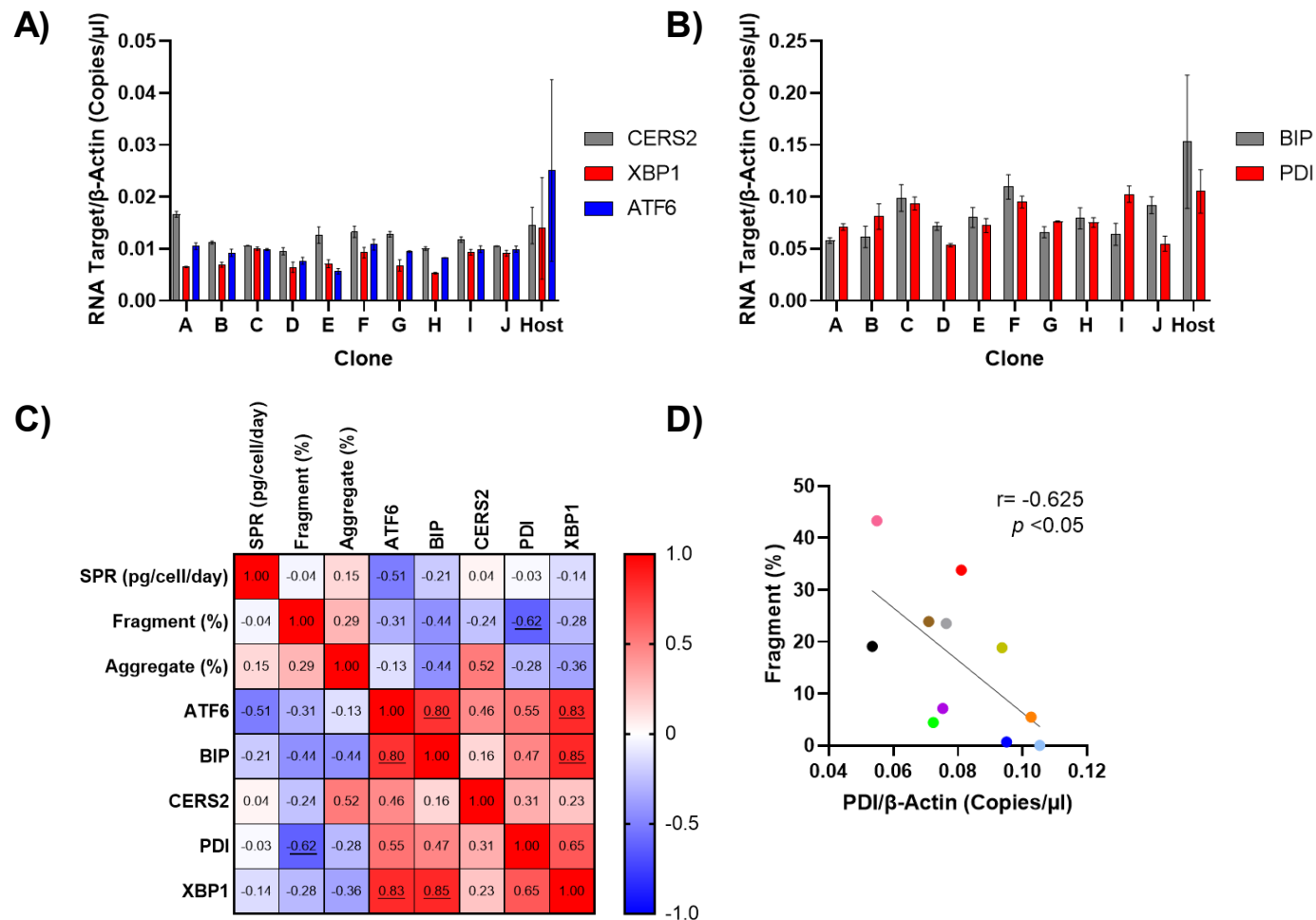


Figure 3.6. RNA transcripts for markers of the UPR pathway were successfully quantified by ddPCR.

A) RNA transcript quantification of CERS2 (Grey), XBP1 (red) and ATF6 (blue) transcripts, after normalisation to a β -Actin reference transcript (N=3). Error bars = +/- 1 SD. **B)** RNA transcript quantification of BIP (grey) and PDI (red), measured as per A. The two graphs were separated to highlight the y axis. **C)** Correlation matrix, plotting each of the RNA transcripts against the product quality and titre data previously obtained from GSK. Coloured on a scale with a perfect positive correlation in red, to a perfect negative correlation in blue. Highlighted correlations were statistically significant ($p < 0.05$). **D)** Correlation plot showing the negative relationship between PDI copies/ μ l and Fragment (%) of Clones A-J of the resulting population. Clones have been coloured to be representative over each graph in figure 3.4-3.6.

3.3. Discussion

mAb expressing CHO cell clones are well-known for their heterogenic nature (Kaas et al., 2015; Vcelar et al., 2018), and much literature has been published characterising clones for desirable mAb quality and quantity characteristics such as titre, aggregate (%) and fragment (%). To this end this thesis aimed to generate a reporter assay or biosensor that could be used to quickly identify clones with a desirable phenotypic fingerprint which correlated with the quality and quantity mAb they produced. This Chapter aimed to first identify what clonal phenotypes show desirable characteristics, with an emphasis on the correct folding of proteins in the ER, and the UPR response when this folding is not completed properly. The folding of the protein was focused on as a wealth of literature shows a correlative link between a clones protein folding capacity and its ability to produce high titre clones. There has been very little evidence however to its link to producing high quality clones, and thus this study aimed to see if quality such as aggregate and fragment could be monitored by the ER's folding capacity and the UPR, as well as titre. To do this a panel of CHO clones expressing a bispecific mAb with particularly stark aggregate and fragment percentages were measured for their ER capacity and folding transcripts, until a final selection of potential targets could be found for reporter construct design.

Initial investigation focused on the size of the ER, using an ER Tracker live cell stain. Professional mAb expressing plasma cells have a well characterised expansion of the ER (Goldfinger et al., 2011), and thus it was suggested that high producing CHO clones may show the same expansion of the ER compared to the CHO host. The results of the ER Tracker study however showed that the size of the ER alone is not indicative of mAb titre, in fact the ER size is not increased in mAb expressing lines compared to the CHO host (Figure 3.1.). ER Tracker was tested in a previous study, and similarly showed no difference in ER tracker intensity between a CHO host and two mAb expressing cell lines when measured by flow cytometry (Reinhart et al., 2014). This suggests that merely the size of the ER is not a suitable tool for monitoring antibody production, and the addition of the mAb plasmid does not increase the size of the CHO's ER. The use of ER Tracker as a tool for CLD could also be problematic as a cell permanent dye. The ER tracker did not show any cytotoxic effects in the shake flask cultures (figure 3.1.C.), unlike a previous study had stated. The cell type used, as well as the concentration and incubation of ER Tracker used in this study was much lower than that of the Laine et al. (2017) study that reported cytotoxicity when using BODIPY present dyes. However, despite the CHO cells appearing to be unaffected by the ER Tracker in culture, the cells used in CLD are often much more fragile than those that have already undergone the CLD process, where transfection and single cell cloning techniques are often performed in small cell volumes within a high stress environment. Due to the inability to identify desirable clones and the potential for cytotoxicity in early clonal populations

therefore, the ER Tracker was not pursued as an option for monitoring mAb titre and quality in early CLD.

An alternative method for measuring the folding and biosynthetic capacity of the ER is to measure specific protein targets, rather than monitoring the organelle as a whole. This is potentially advantageous as more molecular and mechanistic understanding of the pathways can be investigated. Immunofluorescence microscopy was employed to monitor BIP, a master regulator of the UPR. The fixed immunofluorescence imaging of BIP and IgG showed differences between the CHO host and two different mAb expressing clones (Figure 3.2.A). IgG was present in both clones, with intracellular staining being more intense in the low-producer cell line. One possible explanation for this observation is IgG was being produced but not being efficiently secreted, highlighting a potential bottleneck in the ER. BIP staining was also greater in this cell line, further suggesting that there may be an increased stress phenotype in the poor expressor. As it has been shown that heavy chain is retained within the ER (Lee et al., 1999; Bole et al., 1986), it could be hypothesised that this build up is predominantly heavy chain that is yet to be paired to the light chain, although further study would be required to confirm this. Whilst both clones in this study were bispecific mAbs, the clonal differences may indicate a similar production bottleneck at the ER for the lower producing cell line. This data was similar to an imaging study that compared a standard format IgG and a bispecific mAb, where the bispecific clone had an exacerbated ER phenotype compared to the standard format IgG clone. Co-localisation of the mAbs to the Golgi apparatus was also measured in the study, and was heavily reduced in the bispecific line compared to the standard IgG format, again suggesting that the mAb was not progressing through the secretory pathway as efficiently as the conventional mAb (Mathias et al., 2018). The Clone A mAb product was also known to be highly aggregated, and the immunofluorescence image showed high concentrations of extracellular IgG staining which potentially indicated mAb aggregates. If confirmed as aggregates this could be a useful predictor tool for aggregate, where a sample of culture media could be easily fixed and stained with a directly conjugated anti-human IgG antibody before reading on a high-throughput plate reader. In order to do this more cell lines with known aggregation propensity would have to be investigated using this technique. The extracellular staining seen in the figure would have to be confirmed as aggregates however, with one method used in the literature being the BIS-ANS stain. BIS-ANS is a fluorescent probe that changes its emission spectra upon interaction with hydrophobic sites of proteins (Bothra et al., 1998), and has been shown to measure to the same order of aggregate as the gold-standard HPLC technique (Paul et al., 2015; Paul et al., 2018). Of course, hydrophilic aggregates have been identified by HPLC (Meyer et al., 2021), meaning that the BIS-ANS stain may not reliably identify all of the aggregate accurately as an assay used in CLD.

As the BIP staining appeared to be related to IgG expression in the fixed cell imaging, BIP and IgG RNA transcripts were quantified in the full clone panel using PrimeFlow RNA. PDI was also explored as a key enzyme that folds the disulphide bonds of IgG (Borth et al., 2005). The results in this Chapter showed that the PrimeFlow RNA could specifically measure the targets as a concentration dependent expression of BIP was seen in the CHO host after incubation with Tunicamycin, a known chemical ER stressor (Figure 3.3.B). The target designed for IgG was also shown to be specific as no fluorescent signal was observed in the host negative control (Figure 3.3.C.). A significant negative correlation was seen between PDI staining intensity and fragment (%), as well as a significant positive correlation between BIP staining intensity and fragment (%). Similar trends have been seen previously, with low PDI mRNA being a characteristic property of clones producing high levels of fragment (Ishii et al., 2014).

The reliability of the PrimeFlow RNA technique was brought into question when comparing the staining intensity of the immediate biological replicates in the IgG stained samples - an average 400 x fold change was seen between the samples of replicate 2 and 3 for example (figure 3.3.D.). It is not fully understood why such variation was seen with the technique; however it is hypothesised that the sheer number of wash steps and manual pipetting in the protocol affected the number of cells in each sample, resulting in an inconsistent concentration of probes and fluorescent labels present across samples and therefore the availability for binding was not consistent. Despite being a relatively new technique PrimeFlow RNA has shown a wide variety of uses in the literature from the detection of bovine viruses in bovine lymphoid cells (Falkenberg et al., 2017), to detecting specific miRNA disparities in human innate lymphoid cells dependent on sex (Malmhäll et al., 2020). Only one journal article has cited the use of PrimeFlow RNA in CHO cells however, where it was used to monitor heavy and light chain RNA transcripts (Pekle et al., 2019). The paper correlated product titre of a panel of CHO clones with heavy chain expression by four different quantification methods: PrimeFlow RNA, western blotting, intracellular protein staining by flow cytometry and qRT-PCR. All four of the techniques showed a similar positive trend with titre, and when PrimeFlow RNA quantification was compared to the flow cytometry protein staining quantification there was a correlation. This paper suggests that the PrimeFlow was as reliable as more traditional techniques. It did not however show the margin of error for each technique, or suggest whether the protocol was undertaken manually or automatically and as qPCR is a tried and tested method for RNA quantification it was decided that this project would try to replicate the results seen in the PrimeFlow experiment via ddPCR.

ddPCR did successfully replicate the negative correlation between PDI RNA expression and fragment (%) measured in the PrimeFlow experiment (Figure 3.5.D.). The positive BIP correlation was not replicated however, with ddPCR instead showing a non-significant relationship with fragment (%). The

repetition of the PDI result, and in a more robust technique (ddPCR), suggested that PDI could be useful for monitoring mAb fragment (%) at an early stage in CLD without the need to wait for HPLC studies. Further UPR markers, ATF6 and XBP1, as well as the non-UPR marker CERS2 were also investigated. A correlation matrix was then performed on the quantified transcript and product quantity and quality data. It was interesting to note that out of the four significant correlative results seen, three of them were stating a positive correlation between different transcript analyses. XBP1 strongly and positively correlated to BIP and ATF6 expression ($r= 0.85$ and 0.83 respectively), as well as ATF6 and BIP expression ($r= 0.80$). This was not surprising, as the XBP1 regulates BIP levels, and ATF6 is regulated by BIP in the UPR pathway (Hetz, 2012), and thus an increased BIP expression would result in an increased UPR response. This has been shown in the literature by (Prashad and Mehra, 2015) with a higher producer cell line having greater BIP and XBP1 expression than a lower producer clone (Prashad and Mehra, 2015). Despite the overall up-regulation of the UPR, the copy number of BIP and PDI was greater than CERS2, ATF6 and XBP1 in the clones, even after Beta-Actin normalisation (Figure 3.6.A. and B.). The over-arching folding enzymes and chaperones (BIP and PDI) may therefore be preferentially up-regulated in the clones compared to the downstream UPR effectors. A similar picture was seen previously by Kober et al. (2012) using RT-PCR, which showed that BIP mRNA concentration had an approximate 400 % maximum increase in expression compared to CHO DG44 host cells, whilst spliced XBP1 maxed out at a much lower ~250 % increase.

ddPCR proved to be much more reliable than PrimeFlow RNA when measuring biological replicates. The suggested relationship between PDI and fragment (%) made the UPR an attractive option for designing a reporter assay or sensor for predicting quality in the CHO clones. As ddPCR requires a substantial sample size to isolate enough RNA for quantification (5×10^6 viable cells per sample), and requires cDNA manufacture before running the ddPCR, it is not a suitable technique for quick screening during the earliest stages of CLD when cultures are scaled up from only a singular progenitor cell. Similarly the time restrictions for screening cell lines would also be impacted using this technique, therefore a simpler and more retained technique is required for use during CLD when considering later steps.

3.3.1. Limitations of the study and future work

The data presented in this chapter suggests that PDI and potentially BIP may be useful markers of product titre and quality in relation to this Bispecific molecule. However, there are some limitations of this work which must be considered. Firstly, only one mAb type was analysed, which already showed more extreme product quality phenotypes than a standard mAb format. Most of the literature in the

field also follows this pattern, with studies often testing multiple clones expressing the same mAb. It is crucial to test different mAb constructs in CHO cells if this project aims to design an assay or reporter for use in CLD over different projects, where the mAb structure or format may heavily differ. The second limitation to this study is that the mAb chosen was a bispecific molecule. The use of a bispecific mAb could be argued to be a good starting molecule as it shows a more extreme quality phenotype than a standard format mAb due to the number of chain combinations possible (Carter, 2001) and therefore give a more obvious UPR phenotype that could be refined when testing standard mAb formats. Bispecific are also becoming more prevalent in the literature, as they become more commercial. The phenotypes they present with are unlikely to be representative of other mAb formats, however. In the panel used here for example, two of the clones showed over 25% of the mAb product to be aggregated. These two data points heavily swing the correlation plots. This figure is much higher than that of other proprietary standard format mAbs tested at GSK, where > 3 % aggregate would not be tolerated and thus is not necessarily representative of the current mAb pipeline for CLD.

Designing a panel of cell lines expressing mAbs with different product quality characteristics could overcome these limitations and result in a more novel and in-depth study compared to the current literature. In Chapter 4 multiple clones for each mAb type will be produced and ddPCR RNA transcripts monitored for them all, ultimately enabling identification of genes involved in the UPR in cell lines producing high quality mAbs, which could then be used to develop a tool to aid with cell line selection of those desirable clones.

4. Monitoring the Unfolded Protein Response (UPR) in CHO clones expressing a panel of different mAb constructs

4.1. Introduction

After determining which experimental techniques were most suitable for monitoring potential targets for predicting product titre and product quality, the next aim was to test these results and techniques with a greater number of mAb constructs. The Unfolded Protein Response (UPR) was focused on as the target pathway for mAb titre prediction, as evidence from Chapter 3 suggested there to be a link between the two. A substantial amount of the literature has also shown that the expression of certain UPR components such as Binding Immunoglobulin Protein (BIP) and Calreticulin (CALR) are correlated to high titre clone identification (Kober et al., 2012; Prashad and Mehra, 2015). Despite this, little evidence is available to link UPR expression to high quality clones.

All prior experimental techniques used in Chapter 3 had been studied in cell lines expressing one single bispecific mAb format. Whilst expression of this mAb was of use due to the 'extreme' phenotypes seen with regards to poor quality and low titre, it was not relevant to the classical monospecific mAb format which are currently the most commonly seen mAb format to pass through cell line development (CLD). Further to this, any reporter construct or assay that may be produced from this thesis must be reproducibly accurate regardless of the mAb target or format type. Most of the current literature in the field typically use CHO clones expressing only one, or a handful of mAb constructs. As these studies then show correlations with varying strengths in their relationship between marker expression and titre it raises questions as to whether these relationships are generalisable enough over many different mAb constructs.

mAbs also typically have their own inherent product quality issues. Whilst efforts are made to choose CHO clones that express the least amount of poor quality mAb possible with the best production characteristics, sometimes the presence of poor quality mAb product, such as truncated or aggregated product, cannot be completely removed from the CHO clones. These characteristics are also typically impossible to measure at such an early stage as CLD, due to the low concentration of mAb product available to measure.

As this thesis aimed to generate a reporter assay that could be used to quickly identify clones producing high quality and high titre product regardless of the mAb construct expressed, it was crucial

to test different mAb constructs during the process of testing which UPR target would be suitable for reporter design. To this end, the structure and target of the mAbs needed consideration. mAbs can be classified dependent on the type of heavy and light polypeptide chain that is expressed, and which determines the functional activity of the antibody (Schroeder Jr et al., 2010). The light chain can be present in two classes: Kappa (κ) or lambda (λ). The heavy chain on the other hand can be present in five classes: Alpha (α), Delta (δ), Epsilon (ϵ), Gamma (γ) and Mu (μ) (Harkness, 1970). All current therapeutic mAbs express the Gamma heavy chain as they have a well-characterised effector function and prolonged half-life compared to other heavy chain types (Wang et al., 2007), although the light chains can be either Kappa or Lambda. The Gamma heavy chain can then be broken down into further sub-classes (IgG 1-4), which differ in the length of the hinge region and the number of disulphide bonds generated during mAb folding (Vidarsson et al., 2014; Wang et al., 2007). Thus even similar standard format mAbs can be different from each other, let alone different format mAbs, and present specific challenges to the CHO host. This has been highlighted in Hussain *et al.*, (2021), which compared the expression of three full-length IgG1 molecules in a proprietary CHO host with the expression of three corresponding Fab molecules. Following transfection fewer pools recovered, albeit non-significantly, in each of the full-length molecules in comparison to their respective Fab fragments suggesting that the expression of the Fab fragments posed less of a burden on the cells. The average productivity of the top 12 recovered pools per molecule were significantly higher in all of the full-length IgG1 pools compared to their Fab comparators however. Despite this, when the productivity was normalised to the number of molecules produced by each cell per day, two of the Fab pools produced significantly higher product than their corresponding full length IgG1. Taken together the Hussain *et al.*, (2021) paper therefore potentially suggested that the size of the molecule, alongside the complexity of its folding and post-translational modification requirements can all impact the efficiency of protein production, and highlighted how any tool generated in this thesis needed to be robust enough to consider these affects.

In order to predict these characteristics, clonal CHO cell lines expressing a panel of different mAb constructs had to be generated. These mAbs were all of a standard, monomer format but targeted different antigens and had different product quality issues inherent in their mAb structure. Further information about these mAbs can be found in Table 2.2. The process was performed as per a typical CLD platform process (Introduction 1.1.5.). Briefly, the CLD platform is the first time in which mAb is expressed in the CHO host. As the CLD platform varies greatly between biopharmaceutical companies it is difficult to determine an exact CLD protocol, and often are not readily publishable. An example protocol of the CLD platform at GlaxoSmithKline can be found in Section 2.4. Briefly, following transfection of the mAb into the CHO host and recovery, the cells are isolated into single cell clones

to establish a cell population arising from a single progenitor cell. During single cell cloning, the top producing cell lines are selected for further progression ensuring that only mAb expressing cell lines are used in the production process. As a result of random integration during transfection, the clones each have specific titre and growth characteristics. The highest mAb producing clones with the most suitable growth profiles for bio-reactor culture are therefore selected for as the clonal populations are scaled up.

Single cell cloning was performed on the Berkeley Lights Beacon, as per GSK's typical platform protocol. The Beacon is a microfluidics culture platform that uses opto-electropositioning (OEP), combined with microscopy to manipulate and assay single cells on a nanofluidic chip (Berkeley Lights, 2022; Le et al., 2020). The addition of the Beacon to the CLD platform not only results in a much enhanced ability to select for high producing clones at an early time point, but the capability to use fluorescent imaging provides an opportunity to select clones based on additional properties. Thus, it makes it a potential place to test the reporters that were designed in this thesis.

4.1.1. Chapter Aims

To monitor the effects of the UPR on mAb titre, the UPR was quantified in the clones generated in this Chapter and correlated to the titre of the clones to confirm whether they had predictive capabilities. Unfortunately, most product quality characteristics cannot be measured at such an early stage during CLD due to the fragility of the clones following export and the small concentrations of mAb that is produced by low cell numbers. This indeed shows how important a predictive capability of product quality would be at an early CLD stage, and thus product quality will be measured in the generated clones in later Chapters of the thesis.

This Chapter aimed to generate a panel of clonal cell lines, each expressing one of 8 different mAb constructs with different titre and quality issues, found inherently in their mAb structure during the design process. Upon the successful production of the clonal lines, ddPCR would be used to monitor the UPR pathway to understand whether it can predict the best possible clones for use in CLD. Whilst this chapter focuses on titre, which is already easily monitored during cell culture, the ability to predict titre as well as quality in later chapters will give CLD a second confirmatory titre technique to use for clone selection.

4.2. Results

4.2.1. The mAb panel was successfully transfected into the CHO host, but showed varying recovery following MSX selection

Stable cell lines were generated in order to monitor the levels of the UPR in CHO clones expressing different mAb constructs (See Section 2.1.5. for mAb constructs). To do this, the mAb plasmids were individually transfected into the CHO host via lipid-based transfection. The resulting transfected pools were then selected for by the addition of methionine sulphoximine (MSX) to the media 48 hours post transfection, whereby only cells that had successfully integrated glutamine synthetase (GS) gene would survive (Section 2.4.2.). The addition of MSX selection did successfully select for the mAb expressing lines as the PBS transfected negative control, and the GFP positive control transfections did not recover as noted by their drop in viability and viable cell count (Figure 4.1.A. and 4.1.B.). The GFP positive control was obtained from the Lonza nucleofection kit (Section 2.4.1.), and did not contain a GS selection gene. The mAb panel transfected clones all recovered. Following the expected drop in viabilities between 12 and 16 days post transfection, all clones fully recovered by approximately week 4 post transfection (average 96.8 % viability and a 1.08×10^6 cells/ml viable cell count across the mAb expressing populations).

The pre-clonal pools were measured for their growth and viability 29 days post transfection to ensure successful recovery of the cultures. The viable cell count ($\times 10^6$ cells/ml) and viability (%) of the pre-clonal pools was measured on the ViCell XR. The viability was similar across the pre-clonal pools which showed at least 90 % viability (Figure 4.1.C.), whilst the viable cell count varied across the clones more substantially (Figure 4.1.D). The pools expressing mAbs 4 and 8 had lower cell counts than the rest of the pools, with the mAb 4 pool in fact having a 1.3 fold lower cell count than mAb 6 which had the highest counts. mAb expression was also confirmed and quantified using the Octet HTX and showed that all 8 pre-clonal pools were expressing at varying concentrations (Figure 4.1.E.). Interestingly mAbs 3 & 4 showed much higher titres than the other clones, and mAb 8 was particularly low in titre. To curtail the effects of cell counts, the productivity (pg/cell) was measured; calculated by normalising titre to the viable cell count (Figure 4.1.F.). Here, the patterns seen in the titre data were generally maintained, with mAb 3 and 4 still showing a much higher productivity than the other pre-clonal pools. Table 4.1. shows the mAb constructs expressed, and highlights that mAb 4 was used as a good expressor control molecule which may explain why its titre and productivity was high, of course this does not explain why mAb 3 also had high titre and productivity as it was chosen for its poor developability. As the populations were pre-clonal at this stage it was difficult to determine whether

this was solely caused by the molecule expressed itself or if there was a transcriptional cause for this as well.

As these pools were obtained by random integration the cells did not have a uniform expression of the mAb due to variation in gene copy number, integration location into the genome and whether the full plasmid was present. It is possible that only the GS gene on the plasmid was successfully introduced into the CHO genome, and so titre was not measurable as the heavy and/or light chains not expressed. Due to this population heterogeneity, little could be inferred from this data in regard to the effect of the mAb type on the CHO host. Experimental techniques like single cell imaging could also be used to infer more about the pre-clonal pools, such as whether the expression of UPR chaperones can be a predictor of titre. In this study, the pre-clonal pools were instead cloned to investigate this, in attempts to follow the CLD platform protocol.

mAb Construct	Problematic Quality Rationale
mAb 1	Prone to aggregation
mAb 2	High molecular weight species present in Acetate and Phosphate
mAb 3	Poor developability
mAb 4	Control mAb used during final structure selection of project molecules
mAb 5	Poor expressor
mAb 6	Engineered variant of mAb 5, aiming to increase expression titres
mAb 7	Engineered variant of mAb 5, aiming to increase expression titres
mAb 8	Prone to dimerising and aggregation

Table 4.1. Anonymised mAb panel naming convention, and the rationale as to why they were chosen as poor quality mAbs (repeated from table 2.2).

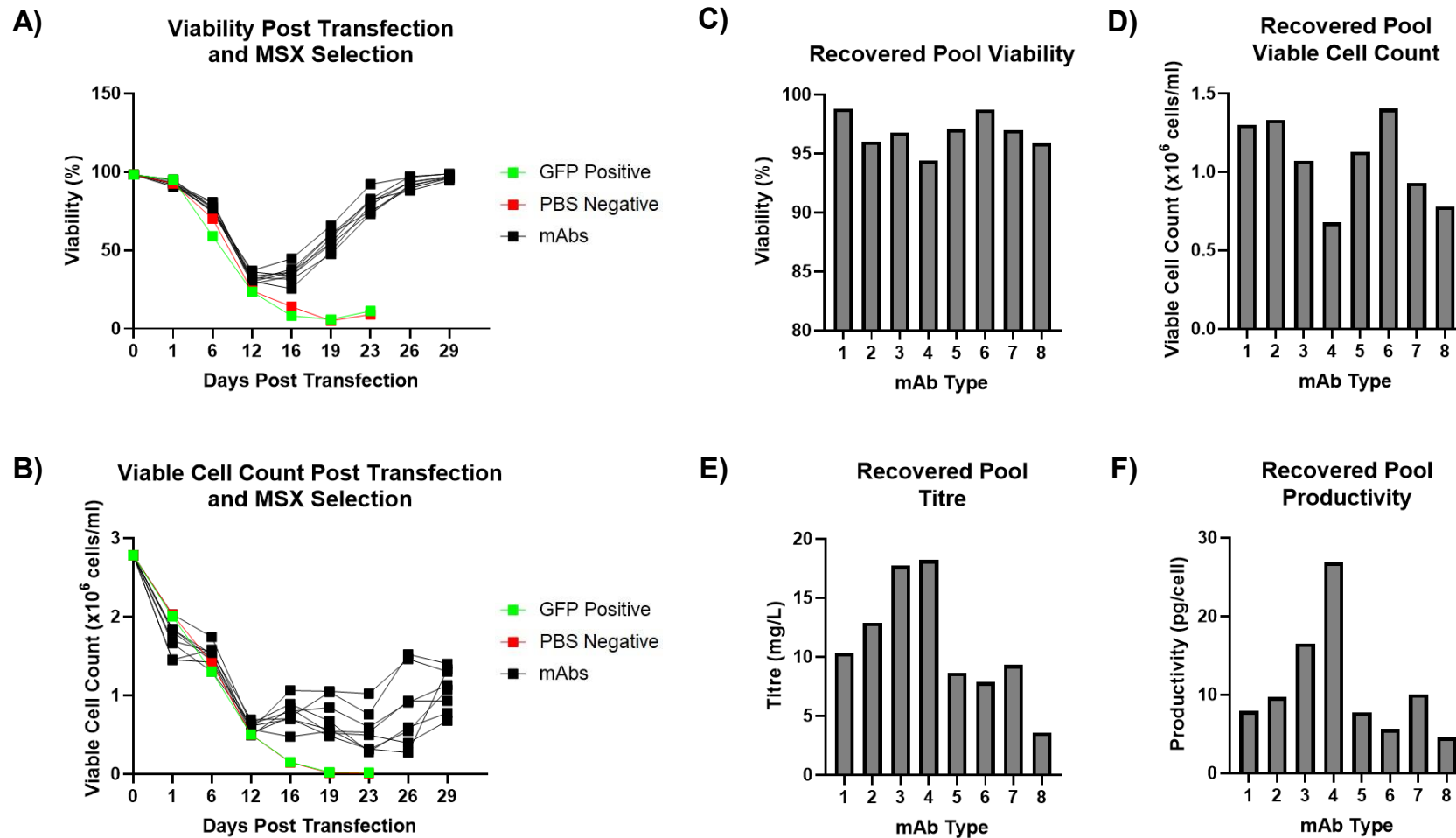


Figure 4.1. Recovered mAb pool titre and productivity were different dependent on the mAb type expressed.

A) Viability (%) and **B)** viable cell count ($\times 10^6$ cells/ml) of the pre-clonal CHO pools post transfection with the mAb panel as measured on the ViCell XR. Selection was added 2 days post transfection. A GFP positive control (green) and PBS negative control (red) did not recover following selection as expected, as neither transfections contained a GS selection gene. **C)** Viability (%) **D)** Viable Cell count ($\times 10^6$ cells/ml) **E)** Titre (mg/L) and **F)** Productivity (pg/cell) of the pre-clonal pools following recovery 29 days post transfection. Cell counts were measured on the ViCell XR and mAb titre on the Octet HTX (N=1).

4.2.2. Single cell clones were monitored for titre on the Beacon, and showed similar average titres to their pre-clonal pool titres

Following successful recovery post-transfection, the pre-clonal pools generated were single cell cloned on the Beacon System (BLI), to obtain clonal populations derived from one single progenitor cell. The pre-clonal reporter cell lines were loaded and cultured as per Section 2.4.3. Briefly, the cell cultures were loaded onto a nanofluidic chip containing 1750 nanopens (Figure 4.2.A.). A single cell was loaded into each individual pen to ensure that the resulting clonal population that grew on the Beacon were derived from one single cell. Following 4 days culture on chip, the cell lines were assayed for growth and mAb titre. The cell numbers were counted, and mAb titre was measured using BLI's proprietary Spotlight assay. The resulting clone productivity could then be calculated from the results (Pen Productivity = Spotlight Au Score / Cell Count). The average number of cells per pen varied depending on the mAb construct expressed in the CHO host (Figure 4.2.B.), and ANOVA analysis showed there to be a significant difference across the means ($F = 16.5$, $p < 0.0001$). Growth was particularly affected by the expression of mAb 8, which showed a significant difference in means compared to every other mAb type expressed following a post-hoc Tukey test ($p < 0.0029$ in relation to all other mAb type expressed).

The average Spotlight assay score (Au Score) per mAb type expressed (Figure 4.2.B.) was again significantly different across the mAb types as determined by ANOVA ($F = 140.0$, $p < 0.0001$), and the multiple comparisons post-hoc Tukey test showed a significant difference between each mAb comparison apart from between mAbs 1, 5, 6 and 7 which all had very similar means. As expected from the use of transfection by random integration, some individual clones expressing mAbs 2, 3 and 8 showed the occasional clone that had particularly high Au scores, suggesting they were expressing much greater titres of mAb than the rest of the clones.

When the titre was normalised to the number of cells in the pen to obtain productivity, a different picture emerged across the clones. The productivity was still significantly different across the means when measured by ANOVA ($F = 8.479$, $p < 0.0001$), but the clonal distribution was split into two different groups. One population within each mAb type expressed showed a high productivity, and a second population showed a much lower productivity (Figure 4.2.B.). The differentiation between the two populations was shown in the growth of the clones, with the top group having high titres but very poor cell outgrowth and thus despite initially appearing more desirable, suggested that these clones would not grow in culture after Beacon export. This highlighted the importance of looking at all three measurements (Spotlight Au score, cell number and productivity) when selecting cells for export.

To understand whether the Beacon Au score was sufficiently accurate at monitoring mAb titre during single cell cloning, the average titre from the pre-clonal pools (Figure 4.1.E.) were correlated to the average Beacon Au score for each mAb type expressed (Figure 4.2.C.). A positive, but non-significant correlation was seen ($r = 0.647$, $p = 0.083$) suggesting that the two titre techniques were relatively comparable with each other as expected. The data appeared to be mostly skewed by mAb 8, which had a much higher pre-clonal titre than Spotlight score. mAb 8 also had the poorest out-growth and titre on the Beacon and one of the poorest during pre-clonal scale up suggesting that there may be difficulty in expression due to the inherent mAb 8 sequence. mAb 8 was chosen for the panel as it had shown a propensity to dimerise and aggregate in early culture studies, and thus this may have had an effect on the CHO cell growth and mAb expression.

10 cell lines per mAb type were selected for export off the Beacon for static scale up and future experimental work. CLD scientists at GSK would typically not choose a clone for export if it contained less than 15 cells in the pen, as clones with any less tend to not recover during static scale up. Those clones were removed from selection. As such interesting grouping of phenotypes were seen in the productivity data it was decided that 7 of the lines per mAb type with the best Au scores, and 3 of the clones with the worst Au scores would be chosen for export. By exporting 3 non-producing clones it could also be confirmed as to whether the Spotlight assay could accurately predict mAb titre during static scale up.

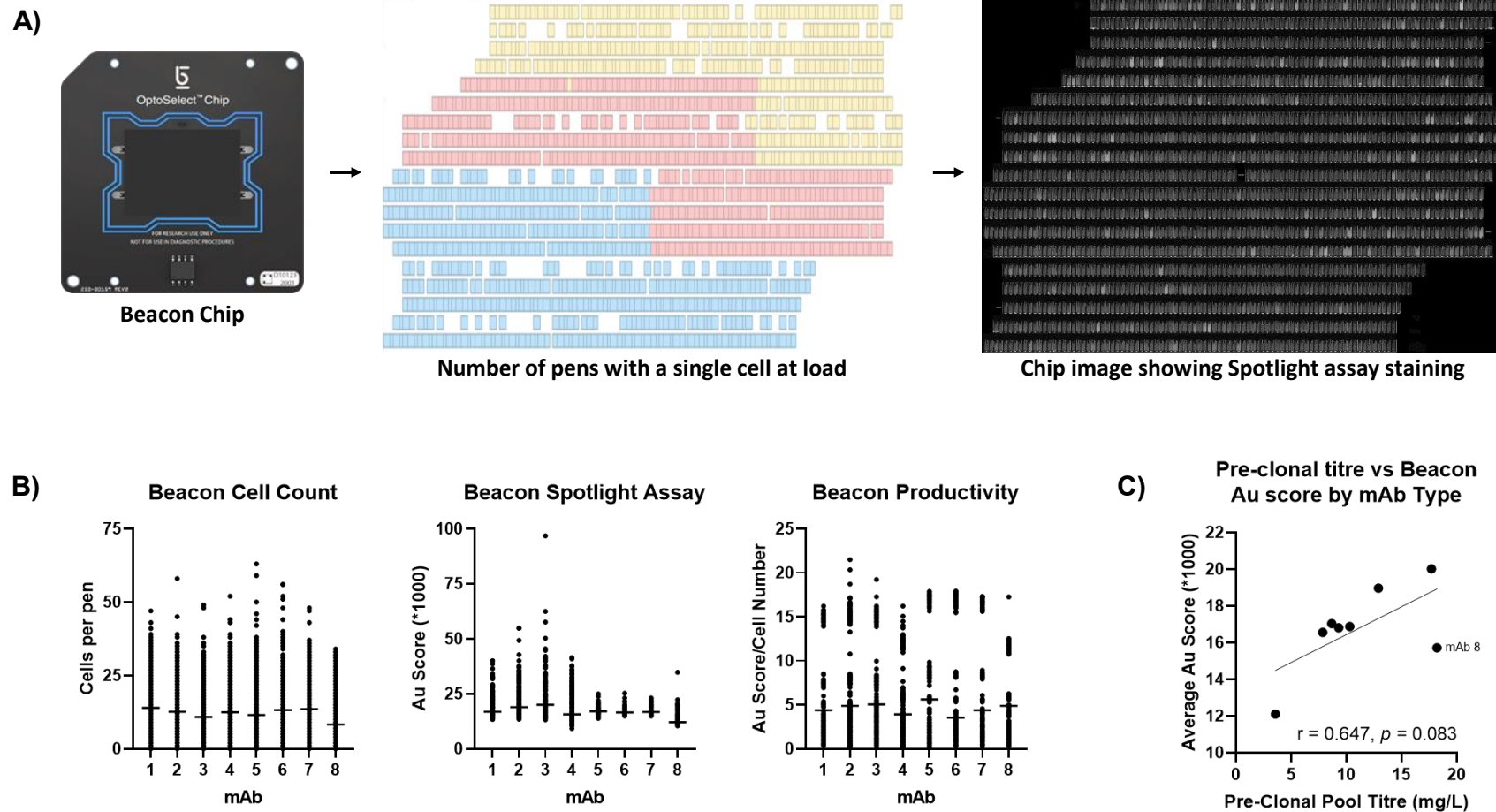


Figure 4.2. Titres of the clones varied dependent on the mAb type during single cell cloning on the Beacon, but still correlated to pre-clonal titres.

A Left) Image of the Berkeley Lights Beacon OptoSelect nanofluidic chip. Beacon chip image obtained from Berkeley Lights (Berkeley Lights, 2022). **A Middle)** Representative schematic showing the number of pens that contained a single cell during Beacon loading, pens have been coloured by the mAb type they are expressing mAb 5 (blue), mAb 6 (red) and mAb 7 (yellow). Gaps represent pens with no cells at load. **A Right)** Representative Beacon chip image of the Spotlight assay. More intense Spotlight staining highlights a higher titre in the pen. **B)** Results of the Beacon Spotlight assay performed prior to cell selection and export. The cell count, Spotlight titre assay score (Au Score) and subsequent productivity of each pen has been shown, separated by mAb type. The mean per mAb type has been added to each graph as a horizontal line. **C)** Correlation plot showing the relationship between the pre-clonal pool titres and the mean resulting Spotlight Au score following culture on the Beacon. Pearson's r analysis $r = 0.647, p = 0.083$

4.2.3. Clone productivity was affected by the static scale up stage

Following Beacon export, the cells were taken through static scale up from 96 well plates to 24 well plates, 12 well plates and finally to 6 well plates before inoculating into T25 flasks for shaking incubation (Section 1.1.5.). The number of clones per mAb type were further triaged to 6 clones from the original 10 as some clones did not recover following export. The 6 clones were chosen by titre during early static culture scale up and consisted of the 4 highest titre clones, 1 clone that was not producing any measurable mAb and 1 clone that was expressing the lowest amount of titre above 0.

The growth and productivity of the clones from early to late static scale up was investigated. The average viable cell count of the clones varied by mAb type at both the 24 well scale up stage and the shake flask stage (Figure 4.3.A.) suggesting the effect of the mAb itself may need to be considered when making decisions based on cell growth at the earliest time point of scale up. The productivities (titre normalised to viable cell count) was also varied across the mAbs at both stages, however mAb 4 was consistently the most productive mAb type (Figure 4.3.B.).

It was of interest to see whether the titres and productivities of the clones measured on the Beacon by the Spotlight assay then correlated to the titres and productivities at the end of scale up (Figure 4.3.C.). The titres and productivities at these two CLD stages showed a strong positive correlation to each other ($r = 0.713$ and $r = 0.715$ respectively, $p < 0.0001$ for both). This suggested that the Beacon Spotlight assay could reliably predict high producing clones at the end of CLD, giving confidence to the method. As the productivity looked to be correlated at both time points, it was then questioned whether this productivity varied at all over the scale up process. The productivity of all 52 clones was plotted over time (Figure 4.3.D.) and showed a surprising change. Although the 24 well and shake flask stage were similar in productivities, there was actually an increase between the 24 well and 6 well stage. After the 6 well stage, the productivity then plummeted to its lowest value at the T25 stage before recovering at shake flask. This phenotype was retained in all of the clones, regardless of the mAb type. It was hypothesised that the initial increase at 6 well stage was caused by the cells recovery following export from the Beacon, and then the sudden drop caused by the cells movement from static culture to shake flask culture where the cells had to re-adapt. In this study the Beacon titre and productivities were most predictive of the shake flask culture stage of CLD which was unexpected as the Beacon represents a low cell number, static culture condition, similar to that of the 24 well scale up stage.

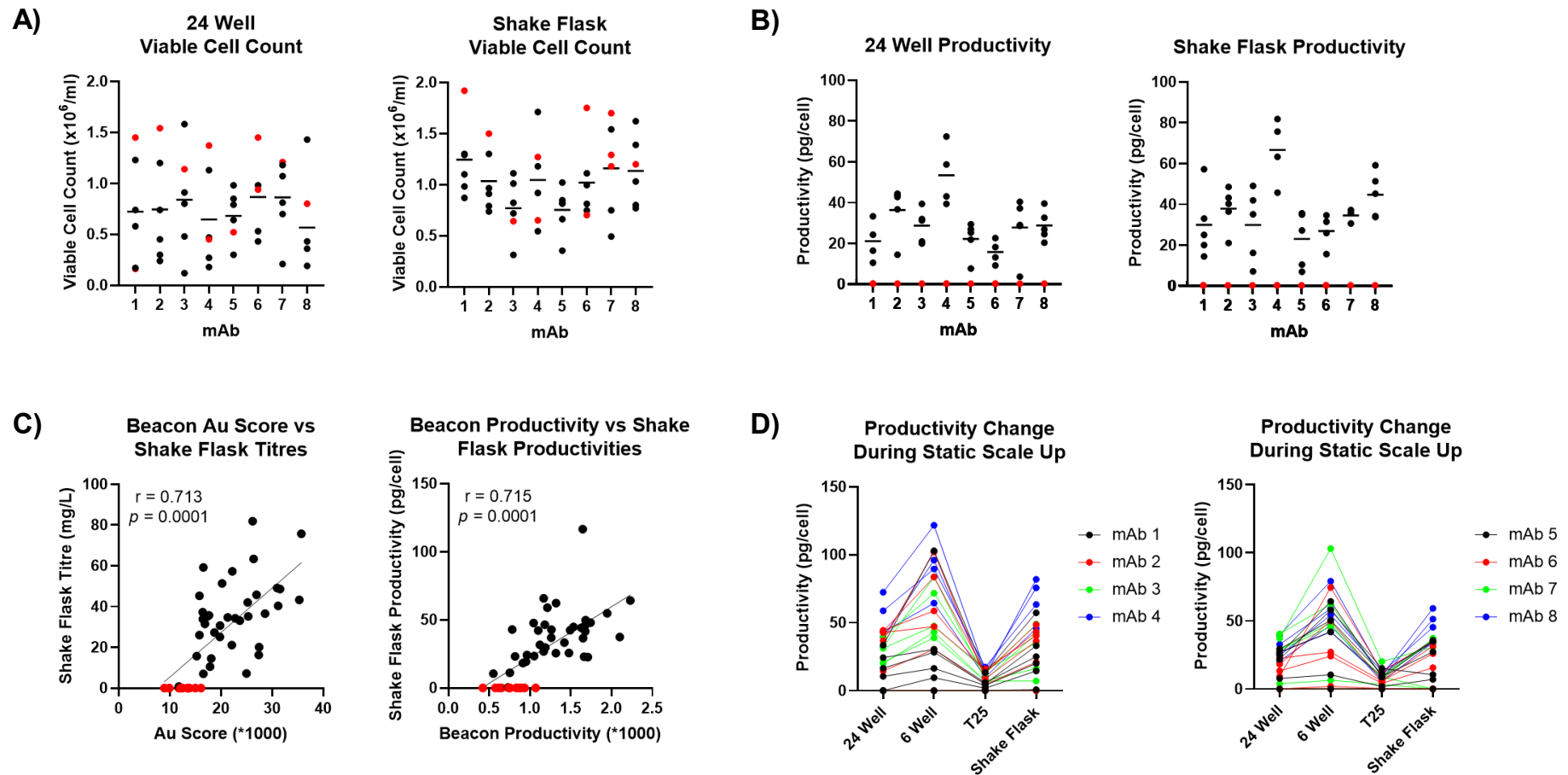


Figure 4.3. Clone productivity fluctuated over each scale up time points, but remained relatively similar to the Beacon Au score.

A) Viable cell count ($\times 10^6$ cells/ml) of the clones at the 24 well and shake flask stage of scale up, split by mAb type measured on the ViCell XR. Average values are included as horizontal lines. Non-producing cell lines are highlighted in red. **B)** Productivity (pg/cell) of the clones at the 24 well and shake flask stage of scale up, split by mAb type. Average values were included as horizontal lines. Productivity was measured by normalising the titre, as measured on the Octet HTX by the viable cell count. Non-producing cell lines are highlighted in red. **C)** Correlation plot measuring the relationship between the Beacon Au Score and shake flask titre (mg/L), and the Beacon and Shake Flask productivity (pg/cell). Non-producing cell lines are highlighted in red. Correlation was measured by a Spearman r test. Significance was set at $p < 0.005$. **D)** Productivity (pg/cell) change of the clones throughout scale up stages, as coloured by mAb type. Graphs were split into two for clarity between the 8 mAbs.

4.2.4. A negative correlation was seen between titre and the expression of pro-recovery UPR chaperones, but no correlation was seen with pro-apoptotic chaperones.

As the sub-culture of 52 cell lines and their subsequent collection of cell lysates for the ddPCR experiments were labour intensive, the number of clones progressed for further study were reduced to 24. The progressed clones were those expressing mAbs 1-4, as these had the most diverse range of product quality issues and expressed the widest panel of mAb targets. Unfortunately one of the 24 clones expressing mAb 3 became contaminated and thus only 23 clones were investigated.

Results of Chapter 3 showed that there had been a negative relationship with clone titre and UPR chaperone expression, and the most reliable methods of monitoring the UPR was via digital droplet PCR (ddPCR, BioRad)– specifically mRNA quantification. The 23 clones expressing mAbs 1-4 were therefore quantified for their expression of UPR stress markers as per Section 2.5, during shake flask sub-culture, post static scale up and correlated with the titres that they produced. Four markers of the protein folding pathway and the UPR were measured specifically: BIP, CALR, PDI and ATF4. These markers were chosen based on the data obtained in Chapter 3 and for their specific role in the protein folding pathway. PDI was chosen for the significant correlation it showed with fragment (%) (Chapter 3.6.D.), as well as BIP due to its role as the master regulator of the UPR. CALR, was also investigated here for the first time in the study, to investigate whether the protein quality chaperone expression also affected mAb titre and quality. Finally, the pro-apoptotic UPR transcription factor, ATF4, was investigated as it was of interest to see whether the UPR was exhibiting a specific UPR response phenotype geared towards folding recovery, or if a more non-specific phenotype was activated that would result in ATF4 having a similar relationship to other UPR components.

The 23 clones were cultured over a 4 day passage, and every 24 hours the samples were counted for their cell growth and viability, their titre obtained and a sample of culture taken for RNA isolation. The isolated RNA was then converted to cDNA and the transcripts of the UPR chaperones were measured using ddPCR following normalisation with a β 2M reference transcript (Section 2.5.). The relationship between the UPR chaperone transcripts and the titre of the clones on the fourth day in culture can be seen in Figure 4.4, as measured by Spearman rank analysis.

A significant, moderate negative correlation was immediately apparent between the clone titre with the three pro-recovery chaperones: CALR (Figure 4.4.A., $r = -0.514$, $p = 0.012$), BIP (Figure 4.4.B., $r = -0.486$, $p = 0.019$) and PDI (Figure 4.4.C., $r = -0.522$, $p = 0.011$). No relationship was seen however with the pro-apoptotic transcription factor ATF4 (Figure 4.4.D., $r = -0.053$, $p = 0.809$). This suggested that the clones capable of producing the highest titres of mAb have a lower transcription of the UPR components compared to those producing low titres. This was somewhat surprising, as the previous

literature describes opposing evidence to the relationship between UPR expression and mAb titre. Le Fourn et al. (2014) for example, have shown a similar relationship to the results here, whereby cell lines expressing low titres of a mAb construct have a higher expression of BIP during cell culture than a high producing clone counterpart. Kober et al. (2012) on the other hand, showed that BIP mRNA was positively correlated to mAb titre in clonal CHO lines, whereby the low producing clones had low BIP expression.

The strength of the negative correlation was moderate, and thus whether this is a strong enough correlation to confirm a biological relationship could be questioned. Increasing the number of clones would help to answer this, particularly if clones with higher titres than those recorded already could be included to increase the diversity of the sampling. This negative correlation was less clear when the clones were split by mAb type, with some mAb types retaining the negative correlation throughout ddPCR study e.g. mAb 1 and 4 (green and purple respectively, Figure 4.4.). Others showed fluctuations, such as the expression of PDI in the mAb 3 (blue) clones. This may be due to the small sample sizes per mAb type, or it may suggest that the mAb type, and thus its product quality attributes, may affect UPR expression.

The second observation was that the UPR elicits a very specific response to ER stress in the clones, rather than a blanket expression of all three pathways, as the ATF4 pro-apoptotic pathway did not show the same relationship as the pro-recovery markers. This was expected as the clones all grew in culture, as shown by the high viable cell counts in the clones during scale up (Figure 4.3.A.). It would be interesting to repeat the experiment in cell lines that are not growing well in culture to see if ATF4 is indeed then activated.

Nevertheless, it is important to note for biopharmaceutical production that clones that direct themselves towards ATF4 mediated apoptosis would not be suitable for large scale mass-manufacture. It was also interesting to see that the pro-recovery markers measured did not appear to have a big influence on the strength of the correlation and suggests that each component is as important to consider as the others. This data therefore suggests that any of the BIP, CALR or PDI markers would be suitable candidates for reporter construct design as they all showed a significant, negative correlation with titre in the mAb panel.

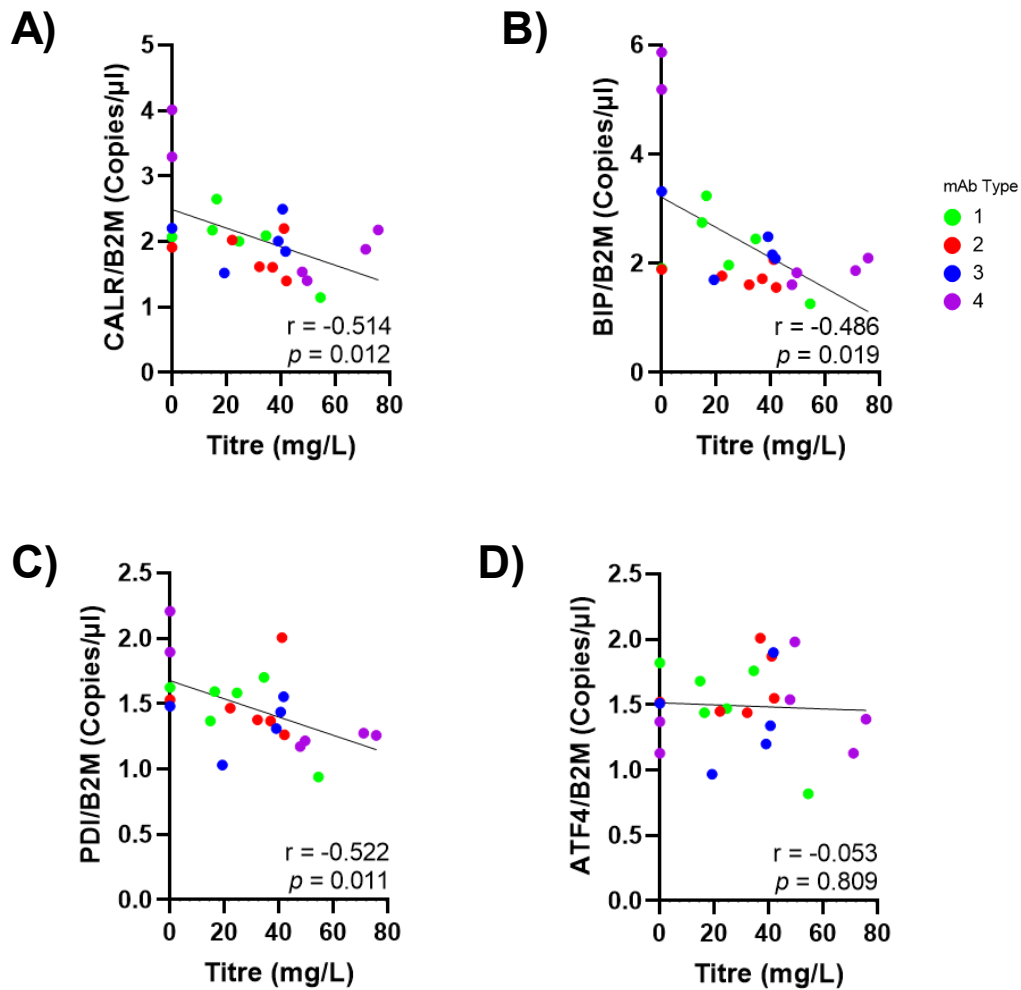


Figure 4.4. CALR, BIP and PDI mRNA transcript expression was negatively correlated to mAb titre in the 23 mAb expressing clones, but ATF4 mRNA transcript expression was not correlated.

A) CALR B) BIP C) PDI and D) ATF4 mRNA expression was measured in the 23 mAb expressing clones using digital droplet PCR (ddPCR) after 4 days in culture in technical and biological triplicate. The transcripts were correlated with their respective titres, measured on the Octet HTX (N=3). Clones were coloured by mAb type expressed: mAb 1 (green), mAb 2 (red), mAb 3 (blue) and mAb 4 (purple). Spearman rank analysis was performed to monitor the relationship significance. Significance was set at $p < 0.05$.

4.2.5. The non-producing CHO clones showed varying phenotypes of ER stress levels over 4 day sub-culture

Despite this overall negative correlation between mAb titre and pro-recovery UPR targets suggesting that the UPR would be a good target for reporter construct design, when the ddPCR data was interpreted over each time point of the 4 day sub-culture some interesting phenotypes in the non-producing clones were observed.

As mentioned above, of the 23 clones progressed for ddPCR assessment, 5 of the clones were not-producing any measurable mAb titre. These clones were found in each of the mAb type expressed, and were kept on for further study to ensure that within the panel of clones there was a range of expression profiles included in the quantification of the UPR components. The inclusion of non-producing clones therefore would incorporate the most extreme titre phenotypes into the study and could be used to help progress the reporter construct. Their non-expression was confirmed when the clones did not produce measurable titre during scale up, highlighted by a single clone in each mAb type (Figure 4.3.B.).

When the non-producing clones were measured via ddPCR for their UPR mRNA transcript quantity alongside the high-producing clones, interesting phenotypes were seen. The expression of BIP, PDI, CALR and ATF4 mRNA transcripts were measured every 24 hours across the 4 day passage study, and split by mAb type expressed (Figure 4.5). The non-producing clones of mAb 1 and 2 (named mAb 1-B and mAb 2-B: named after their mAb type expressed followed by their order of export alphabetically), showed expression levels in line with those of their respective high-producing clones for all four UPR transcripts measured. The remaining non-producing clones of mAb 4 and to a lesser extent in mAb 3 (mAb 3-D, mAb 4-B and mAb 4-F) on the other hand showed elevated concentrations of BIP, PDI and CALR in comparison to their high producing clone counterparts. This suggested that these three non-producing clones that have consistently shown no expression were undergoing high levels of ER stress, despite not producing mAb. It was hypothesised therefore that these 3 clones may actually be producing single or fragmented chains. To confirm this an imaging study was performed on all 23 of the CHO clones, staining for intracellular human IgG.

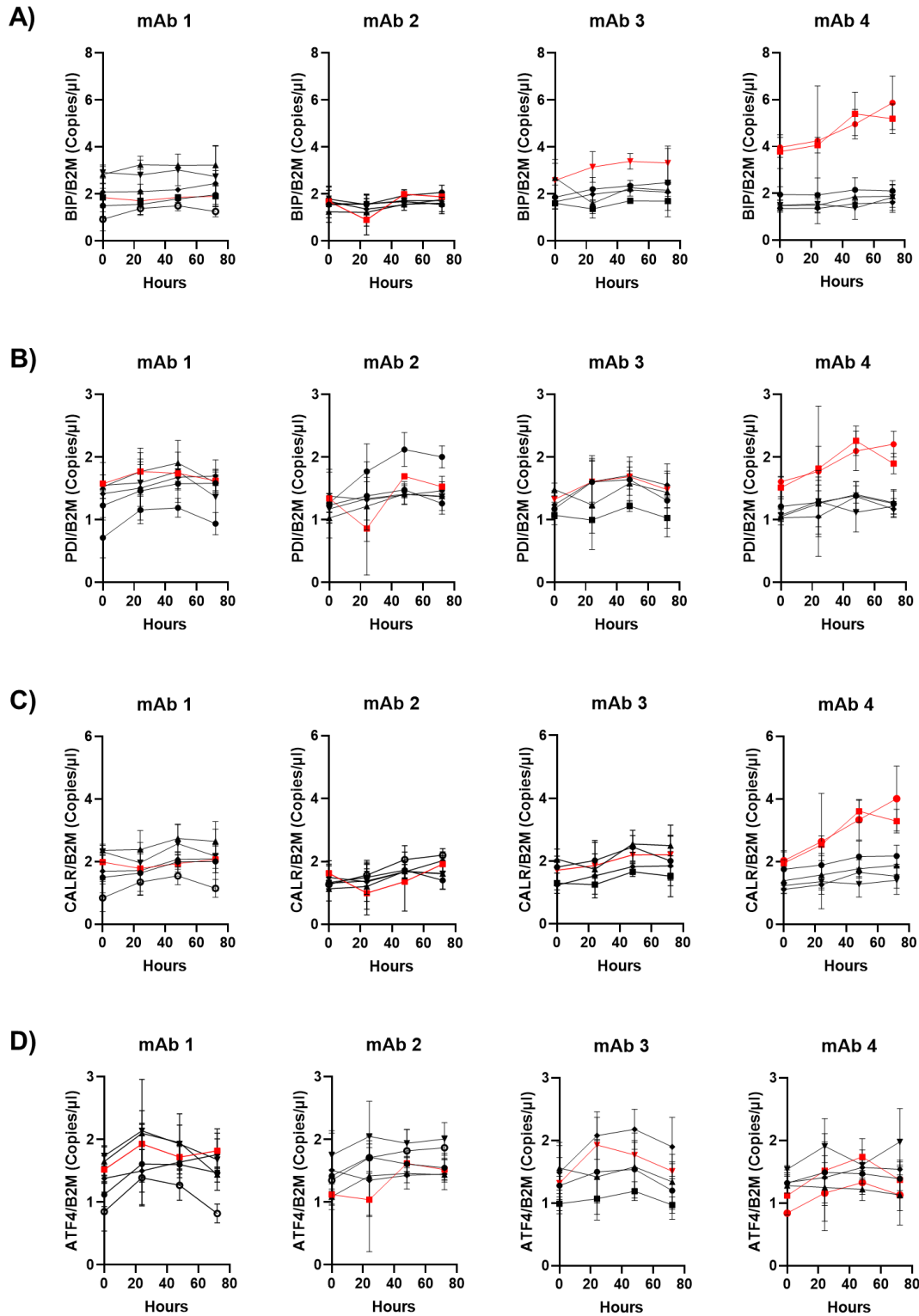


Figure 4.5. Variation in the expression of UPR component transcript quantities were seen over 4 days in the non-producing CHO clones.

A) BIP B) PDI C) CALR and D) ATF4 mRNA transcript expression in the 23 clonal mAb lines over the 4 day passage, as measured by ddPCR (BioRad). Non-producing clones were highlighted in red, whilst producing clones were shown in black. Transcripts were normalised to a $\beta 2M$ reference transcript. BIP, PDI and CALR were more highly expressed in the non-producers expressing mAb 4 than their equivalent high producing clones (N=3). Error bars = ± 1 SD.

4.2.6. The highly-stressed non-producing CHO clones had mAb present inside the cell

The 5 non-producing lines were investigated further to understand why 3 of the clones were showing a heavily increased UPR stress response, whilst the other 2 were not. Despite the clones not producing any measurable titre, they did survive the whole CLD process in media containing MSX selection. It was hypothesised therefore that these clones had successfully integrated the plasmid into their genome and were expressing the Glutamine Synthetase (GS) gene required to survive MSX selection (Chapter 1.1.3.) but the integration of the mAb heavy and/or light chain had not been successful or was truncated and was therefore causing translational and protein-folding stress on the clone.

Fixed cell immunofluorescence imaging was employed to confirm this hypothesis (Section 2.7.2). The 23 clonal lines were fixed and stained for anti-human IgG (specific to both the heavy and light chain) to predict whether the gene sequences were integrated into the genome and were being made into protein. An anti-BIP antibody was also employed to confirm the increased UPR phenotype seen in the ddPCR study. The intensity of the intracellular IgG and BIP staining was quantified for each of the 23 clones using Columbus data analysis software (version 2.9.1.), and the two intensity's correlated against each other using Pearson R analysis (Figure 4.6.A.). The cell lines that were chosen off of the Beacon for their high titre phenotypes showed a very strong positive correlation for intracellular IgG and intracellular BIP expression ($r = 0.918$, $p < 0.0001$). The 5 non-producer clones also showed the same positive correlation between intracellular BIP and IgG expression ($r = 0.955$, $p < 0.05$), but with a shift in increased BIP expression. A second graph showing the same data, but coloured by the mAb type expressed was also plotted to consider whether the mAb type expressed had an effect on the correlation (Figure 4.6.B.). Here, the same negative correlation appeared to be retained in all of the clones expressing the same mAb type. As hypothesised, 3 of the clones stained positive for intracellular IgG expression (Figure 4.6.C.). The intracellular staining was also quantified (Figure 4.6.D). These 3 clones were the same clones that had high ddPCR expression of the pro-UPR markers BIP, PDI and CALR. As the anti-human IgG antibody used was directed against heavy and light chain, it could not be confirmed whether the clones were expressing both chains, individual chains or truncated proteins and thus further study was required as to what was causing the UPR increase.

Of course, the fact that these clones were not producing measurable titre on the Beacon and during scale up meant that they would unlikely ever be encountered by CLD as they would not be selected for in the first place. However, the fact that they stained positive for IgG was interesting as it suggests that any form of intracellular imaging of mAb using an antibody non-specific to either chains would be an inefficient tool for CLD as it would note false-positive mAb expressing clones, and thus should not be considered as an assay tool in the future.

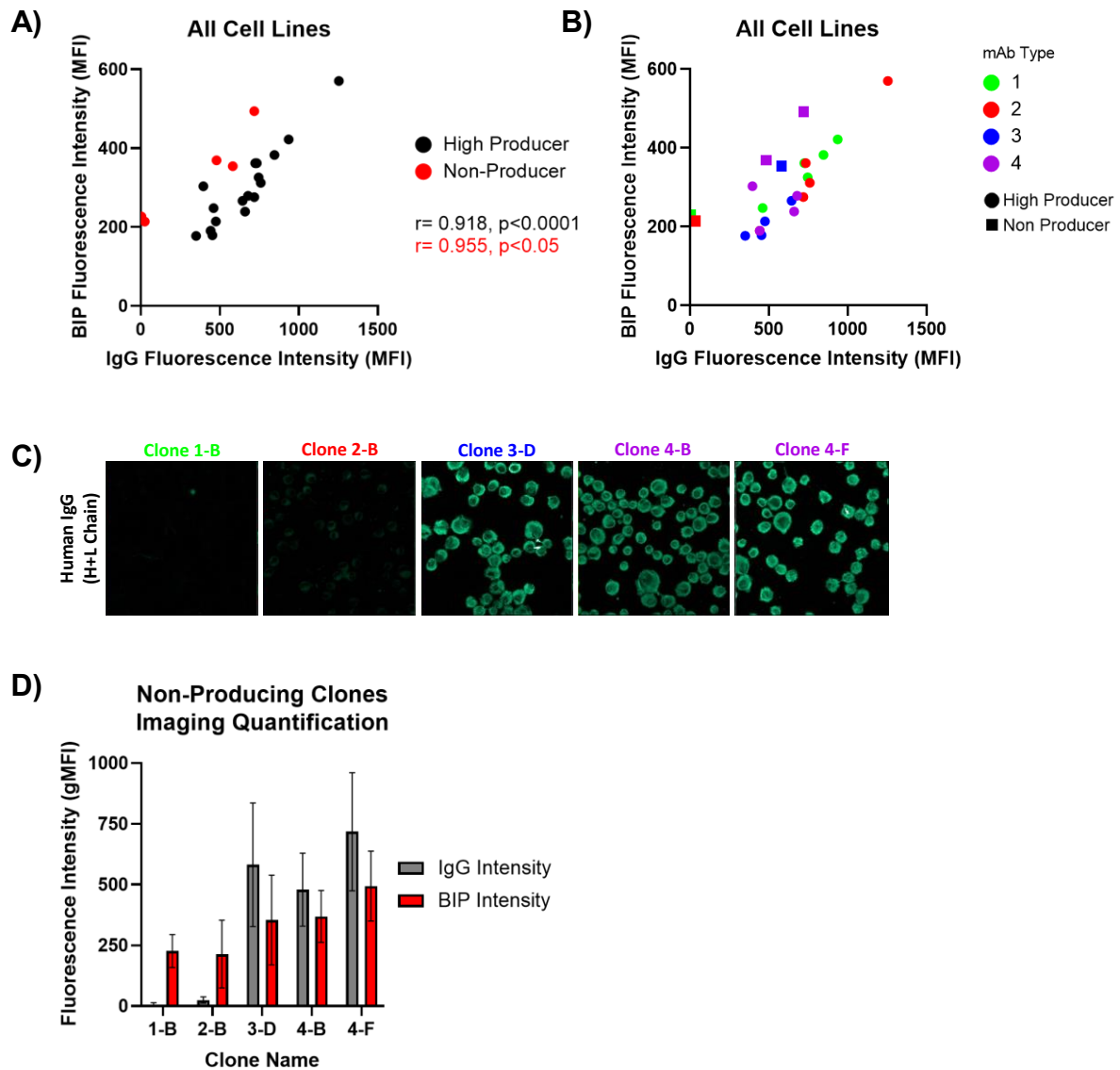


Figure 4.6. A strong positive correlation was seen between BIP and IgG fluorescence in the high producing clones, whilst some non-producing clones showed positive IgG expression.

Clones secreting antibodies tended to have higher levels of intracellular IgG and BIP. The 23 clonal, mAb expressing cell lines were fixed and stained for human BIP and IgG. The clones were then imaged on a Yokogawa CV8000 microscope and quantified for their intensity staining of each marker using Columbus software (version 2.9.1.). **A)** Correlation between the BIP and IgG intracellular staining. Clones were highlighted black if they showed measurable titre during scale up, and red if they were non-producing. Pearson R correlation was used to analyse the relationship between the two staining intensities, and statistical significance was set at $p < 0.05$. **B)** The same correlative data as panel A, but coloured by mAb type and shaped to non-producing and high producing clones to highlight the effect of different mAb expression on the correlation. **C)** Anti-human IgG staining of the 5 non-producing clones, coloured by their mAb type expressed **D)** the quantified intracellular intensity of BIP (grey) and IgG (red) staining of the non-producing clones. Error bars = $\pm 1SD$.

4.2.7. The highly stressed, non-producing mAb clones only express the mAb heavy chain

The 3 clones that showed intracellular IgG staining despite not producing measurable titre (Figure 4.7.A.), were confirmed to be producing only a single mAb chain via a multitude of further confirmatory tests. Fixed imaging was repeated on the lines but this time using anti-human heavy chain and anti-human kappa light chain specific antibodies in attempts to distinguish between the chain types. The quantification of the imaging study showed that the three non-producing clones with high BIP stress (Clones 3-D, 4-B and 4-F) had high staining concentrations for mAb heavy chain but not light chain (Figure 4.7.A.). The two non-producing, non-stressed clones on the other hand showed no positive staining for either chains. This suggested that the stressed non-producers therefore were successfully producing heavy chain protein, but had no light chain protein to form fully folded and secreted mAb product. As heavy chain cannot be secreted from the ER without the attached light chain (Hendershot et al., 1987), this may explain why the clones were highly stressed. As imaging quantification was previously shown to produce large error margins (Section 3.2.2.), the staining study was repeated and quantified by flow cytometry and showed the same increase in heavy chain in the stressed non-producers (Figure 4.7.B.). Interestingly, the non-stressed 2-B clone did appear to also have positive light chain expression compared to the other clones. The same patterns were again seen during western blotting of the non-producing clones under reduced conditions (Figure 4.7.C.).

As these studies were directed at the protein level it was questioned whether these stressed non-producing clones actually had any light chain present inside them and may have just never been folded correctly and thus the final mAb product could not be folded correctly. To test this, ddPCR was employed as per Section 2.5. to quantify mRNA expression of the heavy and light chain in the non-producing clones (Figure 4.7.D.). The number of heavy chain mRNA copies/ μl in the stressed cell lines was 2.83 fold higher than in the non-stressed clones (10.2 and 3.61 copies/ μl respectively). These quantities were still much lower than any of the 18 high producing clones that were also measured for heavy chain mRNA (97.55 mRNA copies/ μl on average, data not shown). A second observation from the ddPCR study, reiterated that the high copies of light chain present in the non-stressed clone 2-B seen after flow cytometry analysis, with 39.05 copies/ μl of mRNA quantified by ddPCR in the clone compared to all of the other non-producer lines (average 2.74 copies/ μl). Again, the copy numbers were still relatively low compared to the high producer clones (average 161.08 copies/ μl , data not shown). Interestingly the fold increase in heavy chain quantification for RNA was not as great as the heavy chain quantification for the DNA quantification, suggesting that the effect on production may be bottlenecked more greatly at the protein expression stage. All of these studies taken together provide solid evidence that the light chain has been lost in all of the non-producing clones apart from clone 2-B, and the heavy chain expression has been lost in clones 1-B and 2-B.

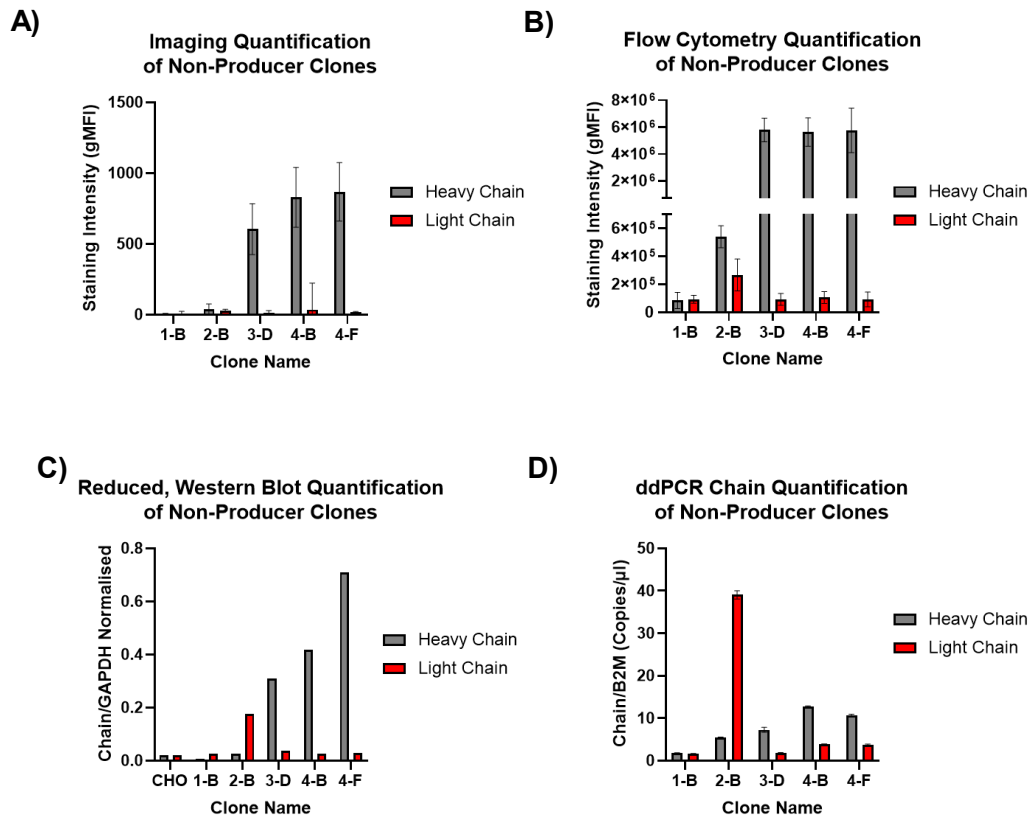


Figure 4.7. Multiple experimental methods confirm that only clones 3-D, 4-B and 4-F are expressing the heavy chain, whilst clone 2-B may express low copy numbers of the light chain.

Heavy (grey) and light chain (red) protein expression in the non-producing clones was measured and quantified by **A)** immunofluorescence imaging, **B)** flow cytometry and **C)** western blotting under reduced conditions. The CHO host was also tested in this study for reference. **D)** mRNA transcripts of heavy and light chain were measured by ddPCR following normalisation to a β 2M housekeeping transcript (N=1). Error bars where present = \pm 1 SD.

4.2.8. The heavy chain only producing clones still attempt to fold the heavy chain as evidenced by heavy chain homodimer presence in the cell lysate

As the non-producing clones appeared to be surviving and growing alongside the high-producing clones without any negative effect on growth, it was questioned as to whether the UPR was activated by the heavy chain expressing clones to cope with the protein that could not be secreted. It was also questioned as to whether the clones producing individual chains remained in monomer form, or if the clone was attempting to fold the mAbs where possible. To do this, western blots were performed on all 23 of the clone lysates under non-reducing conditions as per Section 2.6. Non-reducing conditions were used as to not disturb any disulphide bonds holding the folded mAbs together. A GAPDH protein reference was used.

The resulting western blots performed under non-reducing conditions showed that all of the high-producer clones contained the fully-folded mAb (~150 kDa) and various intermediate formats of the heavy and light chain that had yet to complete folding (Figure 4.8). The non-producers on the other hand did not show bands in the 150 kDa region as expected. Clone 1-B that showed neither chain expression with only the GAPDH control band. Clone 2-B, that expressed only the light chain, contained a single 25 kDa light chain band. The three non-producer clones with heavy chain expression (mAb 3-D, 4-B and 4-F) however showed a 50 kDa heavy chain monomer band, and surprisingly a ~100 kDa heavy chain dimer band. This result was interesting as it showed that these clones were still attempting to fold the mAb product despite having no light chain to bind to the homodimer. mAb folding starts with the bonding of two heavy chains into a homodimer configuration, before the addition of the two folded light chains to the homodimer (Chapter 1.2.3.). This suggests therefore, that the clones are still attempting to make this mAb despite not having the light chain to do so. This heavy chain homodimer cannot be exported from the ER like the light chain can be (Hendershot et al., 1987), and thus may explain why the clones are under stress as referenced by the increased UPR chaperone expression (summarised for the non-producers in Figure 4.9.). The light chain only expressing clone (mAb 2-B) does not undergo this stress however as the light chain can be freely secreted from the cell without the heavy chain.

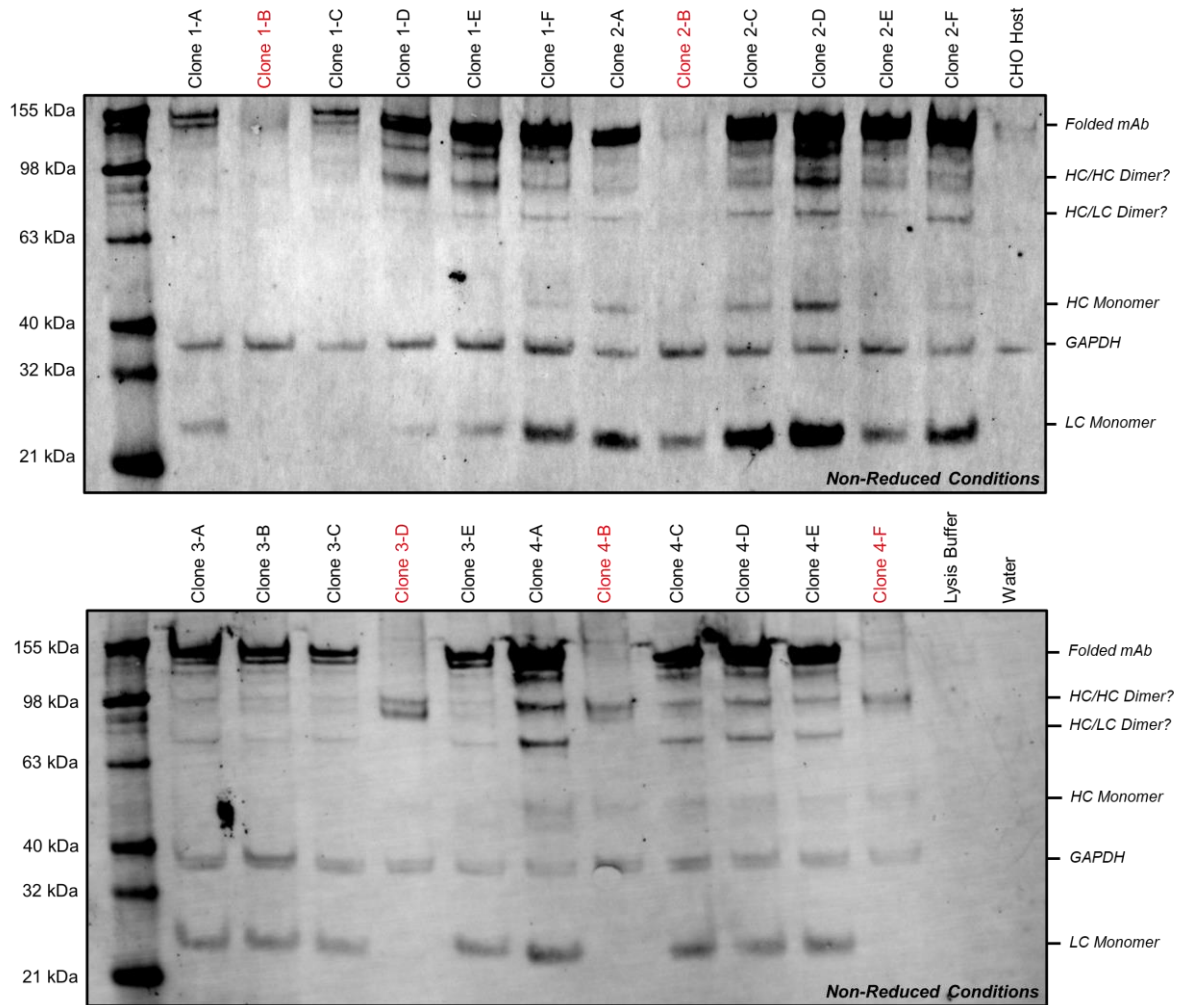


Figure 4.8. Western blots showed variation in expression of heavy chain and light chain across the 23 clonal cell lines.

Western blots were performed under non-reducing conditions on a 4-12 % BIS-Tris 1.0 mm protein gel following cell lysate extraction using RIPA lysis buffer. A fully folded mAb monomer should be ~ 150 kDa (comprised of 2x 25 kDa light chains and 2x 50 kDa heavy chains). The non-producing clone 1-B did not express either chain, whilst clone 2-B expressed only the light chain. Non-producer clones 3-D, 4-B and 4-F expressed only the mAb heavy chain. Heavy chain dimerisation is also apparent in these three clones as seen by the ~100 kDa band, despite the lack of light chain.

ddPCR UPR Marker Quantification in Non-Producers

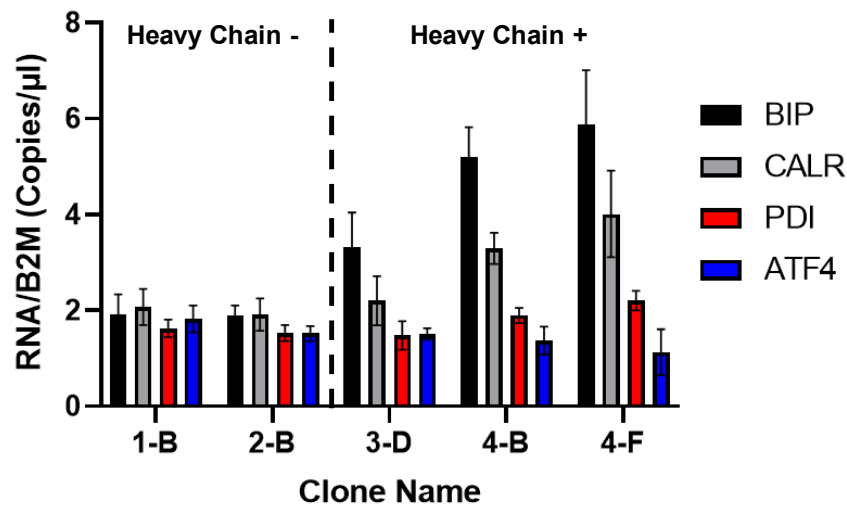


Figure 4.9. Summary of the expression of UPR transcripts in the non-producing clones measured by ddPCR. Pro-recovery UPR chaperones are more highly expressed after 4 days in culture, in the non-producing clones that are expressing the heavy chain only (mAb 3-D, 4-B and 4-F) than the clones not expressing either chains (mAb 1-B) or only the light chain (mAb 2-B). mRNA expression of UPR chaperones was measured and quantified by ddPCR (BioRad) and day 4 quantification has been shown here (Figure 4.6). PDI and ATF4 mRNA expression was consistently expressed across the non-producing clones, regardless of whether they were expressing mAb chains or not. BIP mRNA expression however was increased in all 3 of the clones expressing only the mAb heavy chain. CALR was also increased to a lesser extent in clones 4-B and 4-F, but not 3-D (N=3). Error bars = \pm 1 SD.

4.3. Discussion

Significant progress has been made in the literature to identify gene and transcript targets that can help to identify good quality and quantity mAb expressing CHO clones. Most analysis has been performed on the CHO host expressing only one, or a handful, of typical format mAb constructs, however. These studies then often find correlations with varying strengths in their relationship between marker expression and titre. This raises significant questions therefore regarding whether these relationships are reproducible across many different mAb constructs, which are always adapting in their target and design. Further to this, mAb constructs are also becoming more atypical in their format, with the additions of fusion proteins and different chain arrangements not seen in nature becoming common place and potentially causing extreme folding stress phenotypes. These complex mAb formats bring about additional product quality issues with them such as their propensity to aggregate and fragment. To combat these limitations, this chapter has aimed to monitor some of the markers that may be predictive of titre and quality identified in chapter 3, across a panel of mAb constructs that each inherently have 'problematic' titre and quality phenotypes. As product quality cannot be measured at such an early stage during CLD this Chapter has focused on the titre of the clones, before discussing quality in later Chapters. Any correlations that were seen with quality and titre could then be safely expected to be predictive regardless of the mAb type expressed.

The expression of the mAb constructs in the CHO host at the pre-clonal stage showed an interesting variation in titres and productivity related to the mAb type expressed (Figure 4.1. C-F.). This suggested that the mAb sequence, and thus what it is targeting, itself may have an impact on the titre values likely to be seen over the clones, and the viable cell growth of the pre-clonal pools following recovery from selection. The mAb titre at the pre-clonal stage and the average Spotlight assay by subsequent cloning on the Beacon then showed an interesting correlation. It was reassuring to note that a strong correlation was seen between the two, as it confirmed the efficiency of the Spotlight assay as a marker of titre during single cell cloning. One outlier was mAb 8 that did not share an equal relationship between the two techniques. The pre-clonal titres appeared much higher than the Beacon Spotlight assay, suggesting that either the clones expressing mAb 8 were not producing during single cell cloning, potentially due to stress, or that one of the techniques was inaccurate. It is hypothesised that this is due to a lack in mAb binding affinity in the Spotlight assay or in the Protein A Octet sensors. This could be due to the sequence of mAb 8 in particular, and how it interacts with the assays. This may need to be taken into consideration when using these techniques in the future but is out of the scope of this thesis due to the proprietary nature of the mAb constructs. Another interesting observation regarding the productivities of the mAb constructs was between mAbs 5, 6 and 7. mAb 6 and 7 had been engineered by GSK scientists from the parental mAb 5 construct in an attempt to see increased

titres when expressed in CHO cells. No sustained pattern of increased titre was seen in either engineered variant across the pre-clonal pool titres, the Beacon Spotlight assay or the clonal cell line titres. Thus any changes made from the parental molecule did not improve productivity.

Once the clonal lines had been generated, the correlation between the UPR and titre was investigated. The results of the correlation between titre and BIP and PDI mRNA transcripts in this chapter had a similar negative trend of the PrimeFlow and ddPCR data in Chapter 3. This suggested that the relationship seen between the UPR and titre covered a plethora of different mAb constructs and could be a reliable tool for monitoring mAb titre regardless of the mAb type. As the same relationship was observed between BIP, PDI and the newly investigated CALR after ddPCR quantification (Figure 4.4.), it appears that the response is an overall increase in UPR in poor producing clones. As there was no relationship between titre and ATF4 however, this is likely specific to the 'recovery' arms of the UPR, as opposed to the apoptotic arm. It does suggest that whichever specific UPR marker is used for the design of the reporter construct is not necessarily important as long as it is within the recovery response pathway of the UPR. As a result, a difficult decision would be needed when deciding which final marker would be used for the reporter construct/assay. As BIP plays multiple roles in the folding of protein, from binding to nascent polypeptides that are produced in homeostatic conditions, to binding to incorrectly folded protein during the UPR response, it may be less suitable as a reporter construct (Feige et al., 2010; Cao and Kaufman, 2012).

4.3.1. The negative relationship between UPR expression and titre was the opposite of that seen in the literature

The negatively correlated relationship seen between the UPR markers and titre via ddPCR was surprisingly the opposite to what the majority of the literature has so far shown. One study showed the same relationship as this study; with Le Fourn et al. (2014) measuring high BIP protein expression in poor expressing clones than in higher expressing clones, via western blot. Whilst this gave confidence to the data shown here, the study did not measure RNA transcripts. Other studies that have measured the mRNA transcripts of UPR markers, in a similar fashion to this study, have then shown the opposite relationship to this study - a positive correlation between the UPR and titre (Kober et al., 2012; Prashad and Mehra, 2015). Why this study therefore shows the opposite to this is unknown and would require further study to understand why this has occurred. As there appears to be conflicting evidence in the literature about the relationship, it may suggest that the true relationship is actually affected by different factors. Examples of the differences in the experiment between this study and the Prashad and Mehra (2015) and the Kober et al. (2012) studies include the

type of CHO lineage and selection pressure used, the length of the culture, the type and number of mAb constructs used and the number of CHO clones investigated. All of the factors that may have had an effect on the difference in results between this study and the literature has been discussed fully in Chapter 7.

4.3.2. Measuring mAb titre and mAb mRNA expression resulted in a different relationship with BIP

An unexpected outcome of this study was seen when imaging was employed to measure the relationship between intracellular BIP and intracellular IgG - whereby an inverse relationship was seen between mAb titre and BIP mRNA transcript expression via ddPCR (Figure 4.4.B.), and intracellular BIP protein and intracellular IgG (Figure 4.6.A.). It is hypothesised that this change in relationship is due to the mAb form that was measured in each study. In the ddPCR study the mAb was measured in the form of secreted titre (mg/L), whilst in the imaging study the quantification of intracellular IgG was measured. It is hypothesised therefore that noticing large quantities of intracellular IgG is actually suggestive of bad titre characteristics in the clones, as it suggests that the mAb is not being secreted efficiently from the cell and thus a high expression of BIP occurs from the resulting ER stress. This relationship was also shown in Chapter 3 (Figure 3.2.) whereby a known high producing CHO clone had lower quantities of intracellular mAb, compared to a known low producer that had a 2.08 fold increase in intracellular mAb staining. Similarly, Mathias et al. (2020) showed that when a 'difficult to express' mAb was transfected into a CHO host the ER morphology was heavily altered, showing more individual, spherical structures rather than the diffuse staining of the ER of a CHO clone expressing a standard format mAb. These spherical structures localised to mAb light chain staining suggesting that the ER phenotype seen was caused by the presence of mAb. The staining intensity of the clones expressing the difficult to express mAb was not compared to the standard format mAb clone, but it does give further evidence to suggest that the morphology of the ER and the presence of mAb inside the clone may be a useful diagnostic tool for clonal selection, as well as highlighting how this problem may be exacerbated as more complex mAb formats arise. If the hypothesis that high intracellular mAb staining is an indicator of poor expression is correct it may give an interesting argument for the role of the secretome in the CHO clones, as well as successful protein folding. The secretome has been previously suggested to be implicated in clonal productivity, with Kol et al. (2020) showing that reducing secreted host cell proteins improved CHO productivity and growth characteristics.

Questions could be asked as to whether the ddPCR technique itself is causing this inverse relationship rather than it being a biological response, whereby the analysis is incorrect or not specific enough to

accurately measure the transcripts. This has been confirmed to not be the case however, at least in part, by an extended investigation into the technique. This was first confirmed with the data from the study of heavy and light chain via ddPCR (Figure 4.7.D.). When the values of heavy and light chain measured by ddPCR were correlated together, a strong positive correlation ($r = 0.881$, $p < 0.001$) was seen between the two (Appendices Figure 1.A.), which would be expected as the heavy chain and light chain were expressed at a 1:1 ratio on the same plasmid, and thus as long as successful integration had occurred in the clones there should have been a positive linear relationship between the two. This was further confirmed when the ddPCR quantified heavy and light chain values were correlated to the observed titre of the clones, also measured during the study (Appendices Figure 1.B.). Two positive correlations were observed against titre ($r = 0.7885$ and $r = 0.805$ for heavy and light chain respectively, both $p < 0.0001$). This result gave further evidence to ddPCRs accuracy as a technique, as it was predictive of a secondary technique (mAb titre measured on the Octet HTX).

Following the confirmation that ddPCR did appear to be specific and accurate as a technique it was then questioned as to why such an opposite relationship was seen between the quantification of BIP and intracellular IgG in the imaging study (Figure 4.6.A.) and BIP ddPCR quantification and mAb titre in the same cell lines (Figure 4.4.B.). It was hypothesised that it was due to regulation occurring in the ER post RNA translation. To explore this, the values of the ddPCR heavy and light chain expression were plotted against the concentrations of intracellular IgG imaging in the clones (Appendices Figure 2.), as well as ddPCR quantified BIP and intracellular imaging quantified BIP (Appendices Figure 3.A.). Neither heavy nor light chain ddPCR expression correlated to the quantification of intracellular IgG imaging by microscopy ($r = 0.268$, $p = 0.216$ and $r = 0.112$, $p = 0.612$ for heavy and light chain respectively). BIP expression did moderately positively correlate on the other hand ($r = 0.655$, $p = 0.0009$). The imaging quantification was also shown to be accurate and reliable, as when quantification was repeated using flow cytometry, a positive relationship was seen between the two studies (Appendices Figure 4.).

As a result of these brief studies it does suggest that both the ddPCR and imaging quantification are reliably quantifying transcripts and proteins, as seen by the correlations with BIP, but the difference seen between measuring intracellular IgG and secreted product was causing the inverse relationship seen in this thesis. This can be confirmed by correlating the mAb titre and IgG imaging values obtained in the study, showing no relationship between the two techniques (Appendices Figure 3.A., $r = 0.149$, $p = 0.499$).

4.3.3. Non-producing clones often expressed individual mAb chains

Whilst the results of the non-producing cell lines are not useful for the development of a reporter for CLD as they would not typically be exported from the Beacon in the first place, their expression of mRNA transcripts related to protein folding do hint at the complexity of the UPR and protein stress in CHO cells. The fact that BIP, CALR and PDI are all more highly expressed in the non-producing clones that do have evidence of single heavy chain expression (Figure 4.9.) shows how CHO cells initiate the UPR to adapt with stress. It also shows how the cells are unaffected by the expression of the light chain singularly, which can be freely secreted out of the ER (Bhoskar et al., 2013). Of the three UPR markers, PDI showed the least fold change in expression between the non-producers with mAb heavy chain only (mAb 3-D, mAb 4-B and mAb 4-F) and the non-producers with no mAb heavy chain (mAb 1-B and mAb 2-B). It could be speculated therefore, that PDI is not necessarily recruited in the UPR as heavily as other markers or that there are less disulphide bonds present that need catalysing. Despite the increases of CALR, BIP and PDI, the complete lack of ATF4 expression in these clones suggests that even this heavy chain build up is not enough to elicit an apoptotic or reduced growth response, and asks the question of how much sustained, mis-folded protein is actually required to initiate apoptosis. Single cell cloning on the Beacon requires cells to have grown within the culture time it used for, and therefore it could be suggested that clones with slower growth have not been included in this study to prove this. As clones with slower growth are not desirable for mass manufacture however, and this thesis attempted to remain relevant to CLD, this theory has not been explored further here.

The study of the non-producers for their expression of the heavy and light chain was also useful for confirming the specificity of the ddPCR experimental technique. The heavy and light chain expression in the clones was measured by four techniques - ddPCR, immunofluorescence imaging, flow cytometry and western blot (Figure 4.7.). All four techniques showed very similar expression characteristics in the non-producing clones. Particular clarity of expression was seen in the western blotting under non-reduced conditions (Figure 4.8.), which showed the expression of the mAb heavy chain in its unfolded and homodimeric folded form in the non-producers expressing only the heavy chain. The ddPCR data showed the same result as the western blot image and its subsequent quantification, showing that the ddPCR data obtained was reliable and specific to the target of interest following normalisation to the β 2M housekeeping transcript. This is particularly important in the context of the ddPCR studies measuring for UPR components, which did not have a knockout control, as the data obtained was used to make decisions based on the future reporter construct due to their high throughput nature and more quantitative results.

As there is now clear evidence to show that the UPR is up-regulated in poorly expressing CHO clones in this study, chapter 5 will focus on the design and expression of a UPR-based reporter construct for

use in CHO lines expressing the same panel of mAbs used in this study. The reporter construct will then be tested for its ability to predict mAb titre and quality in clonal mAb expressing cell lines throughout the CLD process.

5. Designing an ER resident fluorescent organelle reporter to monitor mAb production throughout Cell Line Development (CLD)

5.1. Introduction

Historically, cell line development (CLD) has been synonymous with vast numbers of mAb expressing CHO cell lines scaled up from low culture volumes, triaging at each scale-up stage based on growth and productivity. Intense experimental procedures such as the transfection of a host cell line with a gene of interest (GOI), followed by single cell cloning often leaves these cells extremely fragile and sensitive to disturbance during recovery. Subsequent static scale-up involves low numbers of cells as the cell lines are expanded until they reach larger volumes in shake flasks. It is therefore critical that the screening techniques used to triage cell lines during scale-up uses either the least volume of cells manageable or can be performed on cultures without the need for sampling. Suitable screening techniques are also required to be rapid and high-throughput to allow a multitude of cell lines to be analysed and selected within short timeframes. As previously demonstrated in Chapter 3, this makes sampling techniques such as PrimeFlow RNA and ddPCR that can take multiple days to run and analyse, impossible to use as a screening tool in CLD.

In order to develop a tool to monitor mAb titre and product quality throughout CLD, which enables rapid screening at early stages, a fluorescently tagged unfolded protein response (UPR) reporter construct was designed. The use of a fluorescent reporter allows cells to be monitored live throughout all stages of CLD from imaging static culture plates post transfection and post Beacon export, single cell cloning on the Beacon or sampling during shake flask culture by flow cytometry. By having the opportunity to monitor this as early as possible, the best cell lines can be chosen quickly, reducing costs and resource, with a greater range of higher quantity and quality clones at the same time. Similarly, fluorescence could be monitored further into Upstream processes, where 15 day production studies are performed, as well as shake flask cultures that monitor stability in cultures of increasing generations. Transient fluorescence techniques like the ER Tracker dye tested in Chapter 3 are not able to monitor mAb titre or quality over a long period of time. Instead, it was decided that a fluorescence based reporter construct would be more beneficial for CLD as it would be continuously expressed and monitored throughout CLD.

As the data in Chapter 3 and 4 highlighted that the unfolded protein response (UPR) is correlated with product titre and quality, it was decided to design a reporter construct which may respond to the UPR. Fluorescently tagged UPR reporters have been described previously in the literature. For example, a dual RFP/GFP fluorescent reporter construct was generated which is alternatively spliced by XBP1 under conditions when IRE1 is activated by chemical stressors (Roy et al., 2017).

Chemical stressors can induce stress along the secretory pathway, mimicking the effects of mAb expression and as such are often used in the literature. Examples of chemical stressors include Tunicamycin and Brefeldin A. Tunicamycin is a mixture of homologous nucleoside antibiotics that were first isolated from *Streptomyces lysosuperificus*. Tunicamycin inhibits N-linked glycosylation, preventing core oligosaccharide addition to nascent polypeptides. Protein folding therefore becomes blocked in the ER, and as such Tunicamycin has become a common drug used to elicit and monitor ER stress (Tordai et al., 1995; Roy et al., 2017). Brefeldin A on the other hand inhibits protein transport from the ER to the Golgi apparatus by inhibiting vesicle COP-I association to the Golgi membrane (Chardin and McCormick, 1999). Thus, here proteins are folded correctly but cannot translocate past the ER.

The Roy et al. (2017) reporter study focused on transient transfection of the reporters into mAb expressing cell lines however, which results in differences in reporter copy number transfected into cells across the population. Thus, the intensity of the reporter, and the availability of UPR components to interact with varying numbers of reporter levels can impact on the quantification abilities of the reporter. The effect of different mAb constructs, each with different problematic characteristics is also not well represented in the literature.

To generate a novel reporter tool that investigates the ER, calreticulin (CALR) was chosen to be fluorescently tagged. Calreticulin is an ER luminal protein, retrieved by the ER by the presence of a KDEL retention signal. It has many recognised functions, but one of its earliest discovered roles was its ubiquitous storage of Ca^{2+} in the ER (Krause and Michalak, 1997). CALR has also shown to function as an N-linked glycosylation chaperone in the ER. CALR binds to proteins that have yet to be trimmed of their glucose residues that were added during N-linked glycosylation. CALR binding prevents these proteins from being translocated to the Golgi until the glucose has been trimmed, or alternatively marking it for degradation, if the glucose is not removed (High et al., 2000; Ellgaard et al., 2003; Molinari and Helenius, 1999). Calreticulin was chosen namely for this function in ensuring N-linked glycosylation, with which incorrect N-linked glycosylation can have a negative effect on product quality, from Fc effector function and mAb binding to the mAbs pharmacokinetics (PK) (Boune et al., 2020). It was also one of the markers identified by the ddPCR data to be correlated to mAb titre, and

was increased in clones with an imbalanced heavy chain: light chain ratio (Figure 4.5.). Finally, Calreticulin has also been successfully tagged with GFP in other organisms such as *Dictyostelium* and rat pancreas (AR42j) cells (Müller-Taubenberger et al., 2001; Avezov et al., 2015), giving confidence that CALR could be tagged in CHO cells without effecting the proteins form or function. Calreticulin was chosen over BIP due to its singular UPR role as a quality-control chaperone. Whilst BIP is increased in response to ER stress it also inhibits the UPR in homeostasis and binds to nascent protein and thus the multi-purpose role of the reporter meant that the results of the expression could not be solely based on the UPR.

A mitochondrial reporter was also designed to confirm localisation could be measured in smaller organelles and to see whether the reporter response was specific to the ER. Whilst many studies have focused on the ER, one study has also shown that the membrane potential of mitochondria in high producing clones is higher than in low producing clones (Chakrabarti et al., 2019). Translocase Of Outer Mitochondrial Membrane 20 protein (TOM20) was selected as the protein to tag as it is localised to the mitochondrial membrane and has been successfully tagged previously in Normal Rat Kidney Cells (NRK) and rat neuronal cells (Wang et al., 2015; Cho et al., 2017). Both CALR and TOM20 were tagged with GFP via two, quadruple glycine-serine linkers (GGGGS) (Figure 5.1) and cloned into one of GSK's proprietary expression plasmids containing a geneticin resistance gene. CALR was also tagged to mOrange, to give a second wavelength option for the Beacon, and to give the option of transfecting both reporters together.

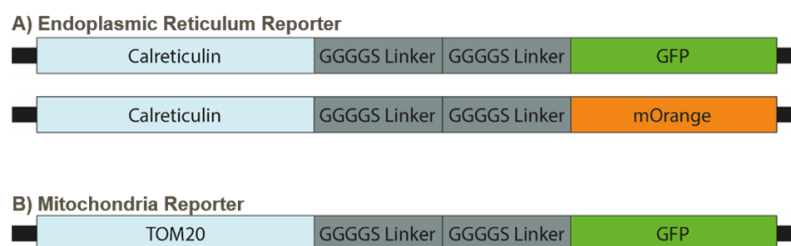


Figure 5.1. Schematic of the fluorescent organelle reporter constructs prior to being cloned into a proprietary GSK plasmid.

The organelle specific protein was tagged to GFP or mOrange via a double Glycine, Serine (GGGGS) linker. The sequences were synthesised by Thermofisher's DNA Gene Strings service. The fragments were inserted into a GSK proprietary plasmid containing a Geneticin selection marker. **A)** The Endoplasmic Reticulum reporter was based on the Calreticulin protein. **B)** The Mitochondrial reporter was based on the translocase of the outer mitochondrial membrane 20 (TOM20) protein.

5.1.1. Chapter Aims

The aim of this Chapter was to design and test a fluorescently tagged UPR based reporter construct that could be used to generate a reporter host cell line. The reporter cell lines should express the reporter consistently across the population of cells and the intensity of the reporter respond to changes in biosynthetic capacity (e.g. when cells were expressing mAb). In addition, the potential of using a mitochondrial membrane based reporter construct was explored, to determine if mitochondrial activity affects mAb production in CHO clones and to be used as an ER-specific control.

The reporter host was then transfected with the same panel of mAbs used in Chapter 4, to understand whether the reporter can be used to monitor titre of different mAbs, with different problematic characteristics and product quality issues (Table 2.2.). This Chapter focuses on the ability to predict mAb titre during CLD, as quality cannot be determined until greater concentrations of mAbs have been obtained - typically after the clones are cultured in a production study for 15 days. This product quality analysis will therefore be performed in Chapter 6.

5.2. Results

5.2.1. The fluorescently tagged reporter proteins are localised to the Endoplasmic Reticulum and Mitochondria following transfection into the CHO Host

The three reporter constructs were transfected separately into the CHO host, and selected for using Geneticin (Section 2.4.1. and 2.4.2.). Following recovery the pre-clonal pools were confirmed for successful stable integration of the reporter constructs into the CHO host genome by live cell imaging (Figure 5.2.). The cells were transferred to a Poly-Lysine coated 96 well plate, and spun down to ensure flat imaging (Section 2.7.3.). Expression of the CALR-GFP and TOM20-GFP reporter plasmid was localised to the ER and mitochondria respectively, shown by organelle specific fluorescence (Figure 5.2.A.). CALR-mOrange was also successfully localised to the ER. As expected, cells transfected with the reporter construct grew successfully under geneticin selection whereas the negative control, not transfected with DNA, did not recover and was discarded after 18 days (Figure 5.2.B.). This successful localisation and growth following selection recovery indicates that the cells were not impacted by the addition of the constructs.

Despite undergoing selection, the population had a diverse range of reporter expression intensities (Figure 5.2.A.), and many of the cells in each population were not positive for reporter expression, perhaps as a result of gene silencing of the exogenous reporter construct DNA. In order for these reporter constructs to be used as a tool for cell line selection it is imperative that differences in fluorescence intensity reflect characteristics of mAb titre and product quality and are not simply inherent within the host population. To ensure this, the pre-clonal lines stably expressing each reporter construct were single cell cloned to create three clonal host cell lines expressing each of the reporters homogeneously. From this mAb could be transfected into the newly generated host. Figure 5.3 shows a schematic of this experimental plan.

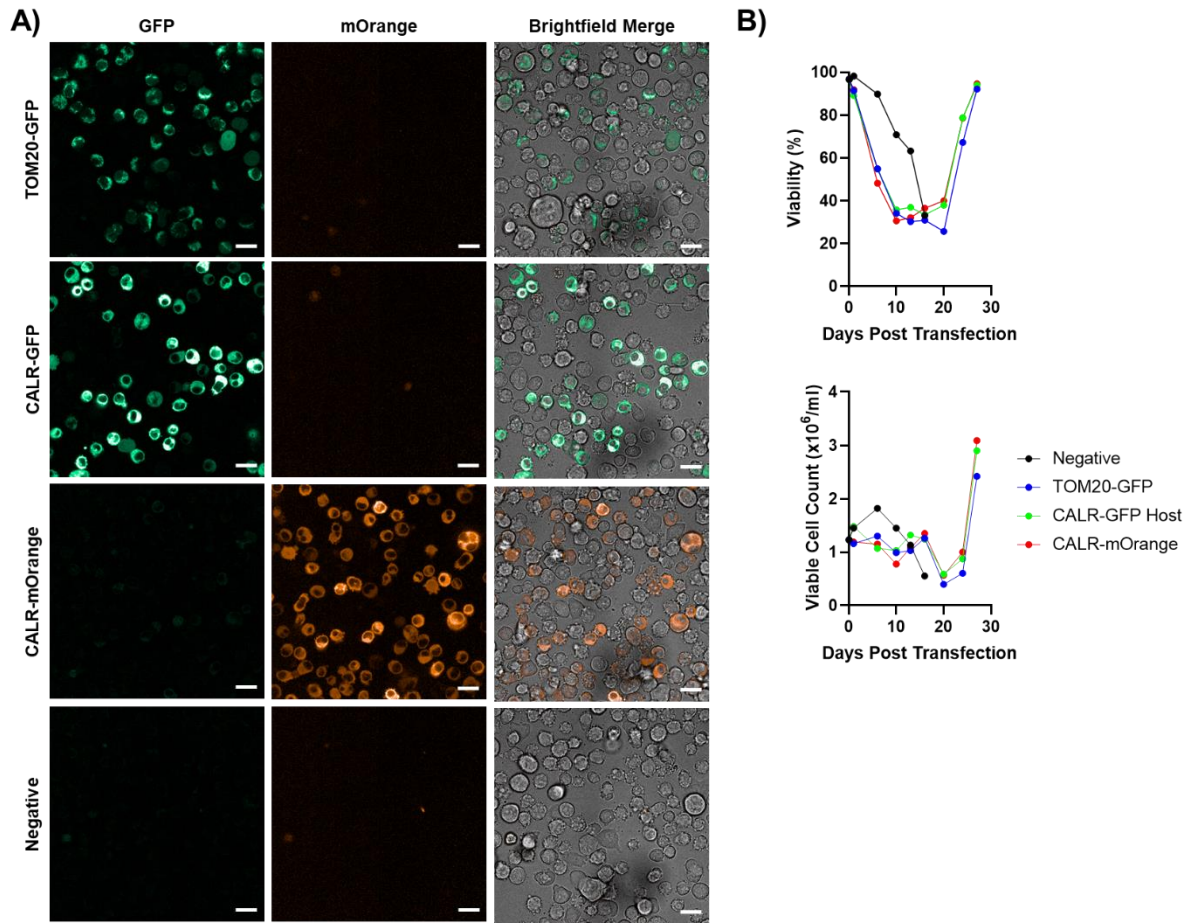


Figure 5.2. CALR-GFP, CALR-mOrange and TOM20-GFP all fluoresced in the CHO host, and localised to the ER and mitochondria respectively.

A) Live cell imaging of the CHO host showed successful reporter transfection following recovery from stable transfection. Pre-clonal populations were positive for each reporter; however expression was heterogenous in the population. 500,000 cells were sampled 31 days post transfection, after the cultures had recovered to > 95% viability. Images were taken on the Yokogawa CV8000. Scale bar = 20 μ m.

B) CHO clones transfected with the reporter constructs dropped in viable cell count (cells $\times 10^6$ /ml) and viability (%) following the addition of geneticin selective media. The population increased over time as successfully transfected clones recovered in the presence of the selective media. Viability and viable cell count was measured on the ViCell XR, up to 30 days post transfection with the fluorescent organelle reporters. Negative control transfected with PBS only. Selection was added 2 days post transfection.

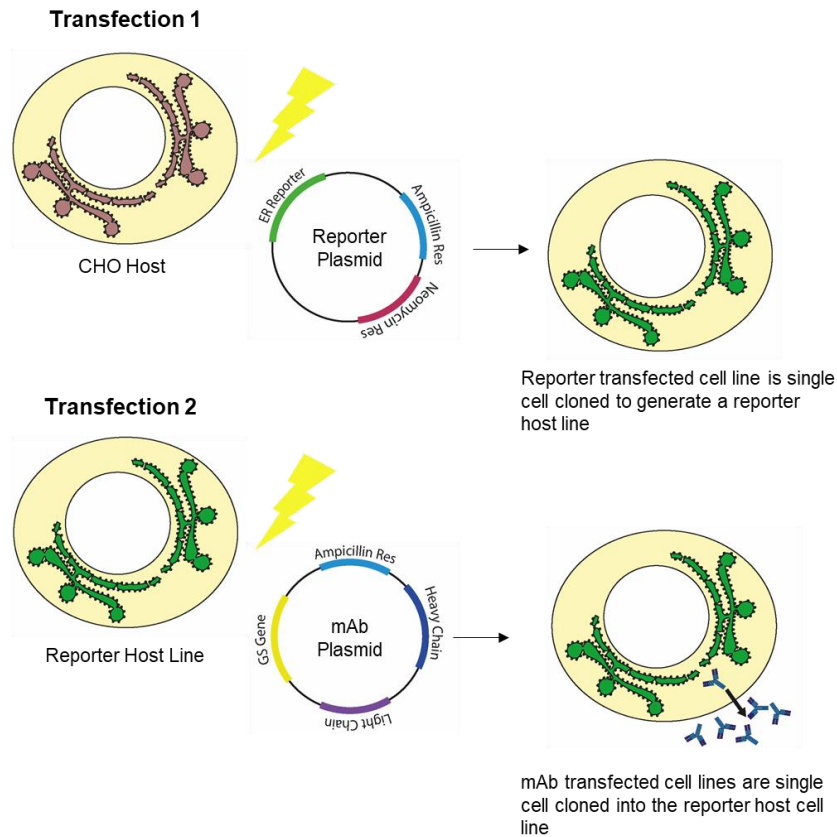


Figure 5.3. Experimental plan for the development of host cell lines expressing the fluorescent reporters.

As the reporters needed to be expressed at the same copy number, and location within the CHO host genome, the reporter was stably transfected (transfection 1) and single cell cloned on the Beacon. A single, positive clone for each reporter construct was chosen during scale up to generate a reporter host cell line. DNA sequences expressing mAbs of interest could then be transfected into the new reporter host cell line, that was expressing the same reporter consistently throughout the population (transfection 2). These pre-clonal pools could then be single cell cloned to obtain stably transfected mAb reporter cell lines.

5.2.2. Generation of clonal CALR-GFP, CALR-mOrange and TOM20-GFP expressing host lines

Following successful recovery post-transfection, the pre-clonal reporter pools generated were single cell cloned on the Beacon System (BLI), to obtain clonal populations derived from one single progenitor cell. The pre-clonal reporter cell lines were loaded and cultured as per Section 2.4.3.

Following four days culture on the Beacon, images of the reporter cell lines were taken on the Beacon using the FITC (GFP) and TexasRed (mOrange) filters. Expression of the CALR-GFP reporter was very clear, with the GFP signal concentrated in the perinuclear region of the cell in the majority of the pens (Figure 5.4. A). As seen previously (Figure 5.2.A), there was a range in expression levels of the reporter constructs in the pre-clonal pool across the pens on the Beacon. GFP intensity and cell size varied across the pens, as well as within the pens themselves in some clones. The TOM20-GFP signal was more difficult to see and the average staining intensity was much lower than the equivalent CALR-GFP populations, apart from in one pen where the mitochondrial targeting had possibly been lost and the GFP expression was cytoplasmic (third pen in the TOM20-GFP reporter, Figure 5.4. A; bottom row). This lack of distinction between the TOM20-GFP expressing cell lines is likely due to the smaller nature of the mitochondria, as localised imaging was seen in the higher resolution pre-clonal imaging (Figure 5.2.A). Unlike the CALR-GFP, the CALR-mOrange signal was far weaker and appeared almost diffuse (Figure 5.4. A; middle row). This may have been due to the mOrange not emitting and exciting at the exact same wavelength required for the TexasRed filter available on the Beacon.

16 pens for each prospective host cell line were selected for export based on growth and homogenous expression within the clonal population. Following export and recovery, the reporter cell lines were scaled up and based on growth and continuing expression of the reporter construct, a final cell line was selected for each reporter: CALR-GFP host, CALR-mOrange host (not shown) and TOM20-GFP host. As mentioned above, the images obtained from the CALR-mOrange cell lines on the Beacon were not optimal. Furthermore, the Beacon Spotlight assay, which enables an on-chip titre assay to be performed, requires use of the TexasRed filter. Use of the CALR-mOrange host would therefore prevent this titre assay being run if this host were to be included as a selection tool during cell line development. Given this, the CALR-mOrange host was not progressed further as a potential selection tool. The two clones chosen for the CALR-GFP and TOM20-GFP host line had consistent expression on the Beacon (* pens in Figure 5.4.A.), and showed considerable growth on the Beacon. The reporter was measurable during static scale up by live, fluorescence microscopy (Figure 5.4.B.), although expression was variable as cultures still had low viabilities during recovery (Figure 5.4.C.).

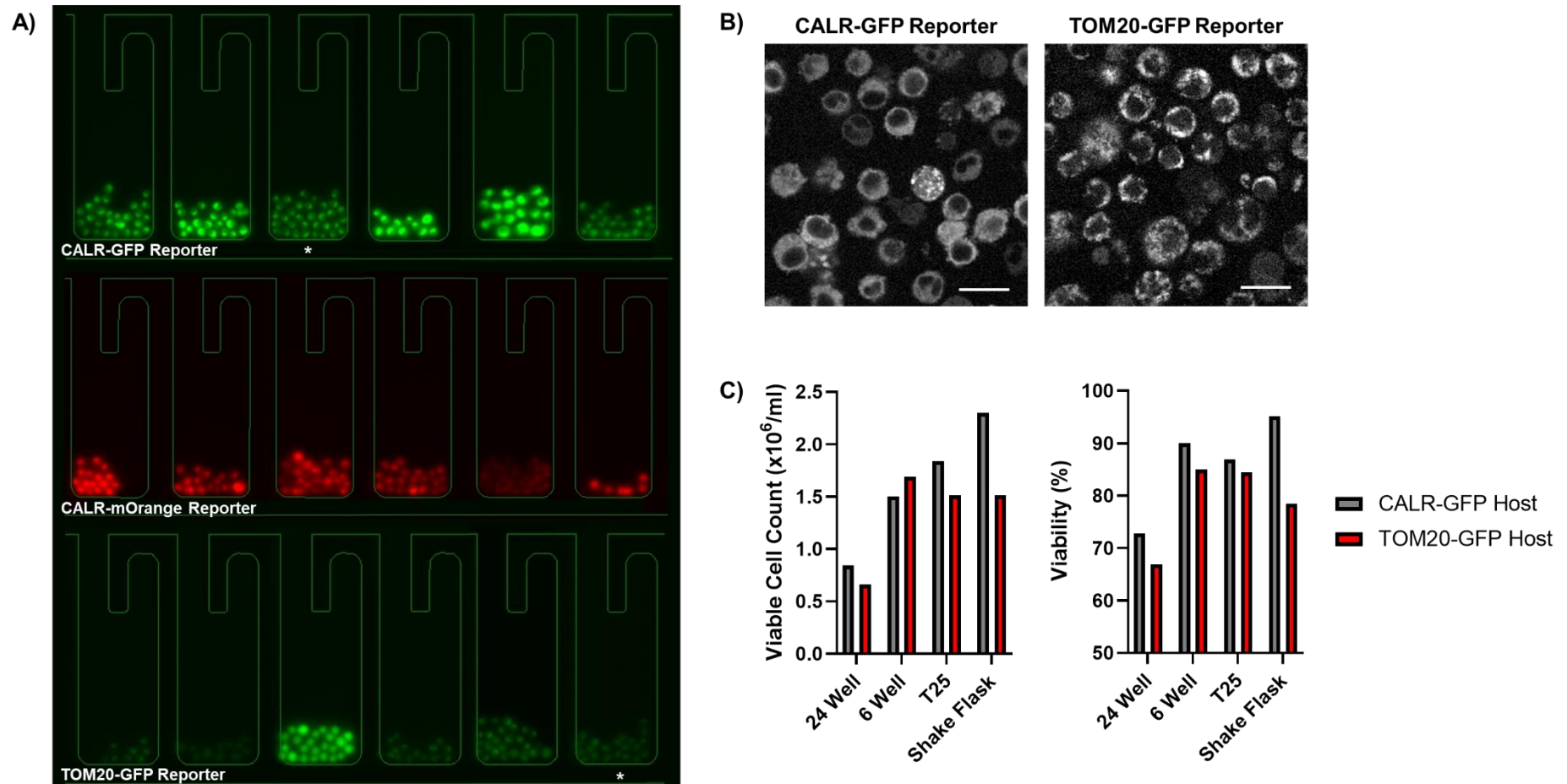


Figure 5.4. The generation of clonal reporter host lines on the Beacon, and the subsequent scale up of the CALR-GFP and TOM20-GFP host cell lines.

A) Example of beacon pen images taken using the FITC filter (GFP reporters) and TexasRed filter (mOrange reporter) after 4 days culturing on the Beacon. * pens = final clone chosen to be the reporter host cell lines. **B)** Live, fluorescence imaging of the CALR-GFP and TOM20-GFP reporter host cell lines during static culture recovery using a Yokogawa CV8000 microscope, taken at the 24 well stage. Scale bar = 20 μm . **C)** Viable cell count ($\times 10^6/\text{ml}$) and viability (%) of the CALR-GFP and TOM20-GFP reporter host cell lines during static and shaking culture recovery measured with a ViCell XR. Viable cell count and viability increased consistently with increased scale up volumes for the CALR-GFP reporter host line. The TOM20-GFP reporter host line increased until 6 well scale up, before dropping slightly as cultures were moved from static culture to T25 shaking culture.

5.2.3. The expression of the reporters is retained during culture and does not impact the health of the CHO host

In order for the CALR-GFP host or the TOM20-GFP host to be a feasible tool for use in cell line selection it is necessary that expression of these reporters does not impact the performance of the CHO host cell line which may later impact expression of mAb proteins. During the selection of the reporter host cell lines, geneticin was required for selection of cell lines which had integrated the reporter plasmids into their genome during transfection and subsequent stable cell line generation. The presence of geneticin however would be an extra stress on the cell lines that would not be present in GSK's platform CHO host, and thus when comparing the suitability of the reporter host this would have to be taken into consideration. Ideally, the geneticin would be removed from the culture media to keep the cell lines without impacting expression of the reporters. To investigate this, the CHO host, CALR-GFP host and TOM20-GFP host were grown in the presence or absence of geneticin selection and the subsequent impact on growth and GFP expression monitored.

Live cell imaging of the reporters in culture at passage 1 and passage 8 showed that the GFP reporter was still consistently expressed in both the CALR-GFP and TOM20-GFP reporter host cell lines and thus removal of geneticin did not cause the loss of the reporter expression (Figure 5.5.A. and B).

The effect of geneticin removal was then analysed in the CHO host and the reporter hosts. The removal of geneticin also did not have a negative effect on the growth of either of the reporter host cell lines. The viable cell count of the CHO host was consistently lower when in presence of geneticin, and the viability was also much lower (between 79-93%) compared to the CHO host in non-selective conditions (>99%) (Figure 5.5.C). This was expected as the CHO Host did not contain a geneticin resistance gene. However, despite the lack of a geneticin resistance gene, the CHO host was still able to survive and multiply under selection, albeit at a much reduced viability (Figure 5.5.C). This may have contributed to the earlier finding that some of the reporter cell lines were able to grow on the Beacon but did not exhibit any fluorescence. The removal of selection to both the CALR-GFP and TOM20-GFP reporter lines had a positive effect on viability, with the average viability increasing by 2.33% and 2.71 % for the CALR-GFP and TOM20-GFP reporters respectively. Similarly, the viable cell count was increased in both reporter cell lines in the absence of geneticin. Overall, these results indicated that removal of geneticin from the reporter host media may increase, albeit marginally, both growth rate and viability of these hosts.

The growth of the reporter host cell lines without geneticin was also compared to the CHO Host, to confirm that the addition of the reporter did not affect cell growth. The viable cell count, viability and doubling time over 8 passages did not show any clear differences between the 3 cell lines. The TOM20-

GFP reporter host did have a consistently larger diameter compared to the CHO Host, with an average diameter over the 8 passages being 15.3 and 14.9 microns respectively (Figure 5.5.D). It was unclear as to why the TOM20-GFP reporter host was larger, particularly as it did not appear to be visually larger than the CALR-GFP reporter host on the Beacon (Figure 5.4.A.). It was suspected therefore to be a phenotype of the particular clone chosen following scale up as cells recovered back into suspension culture.

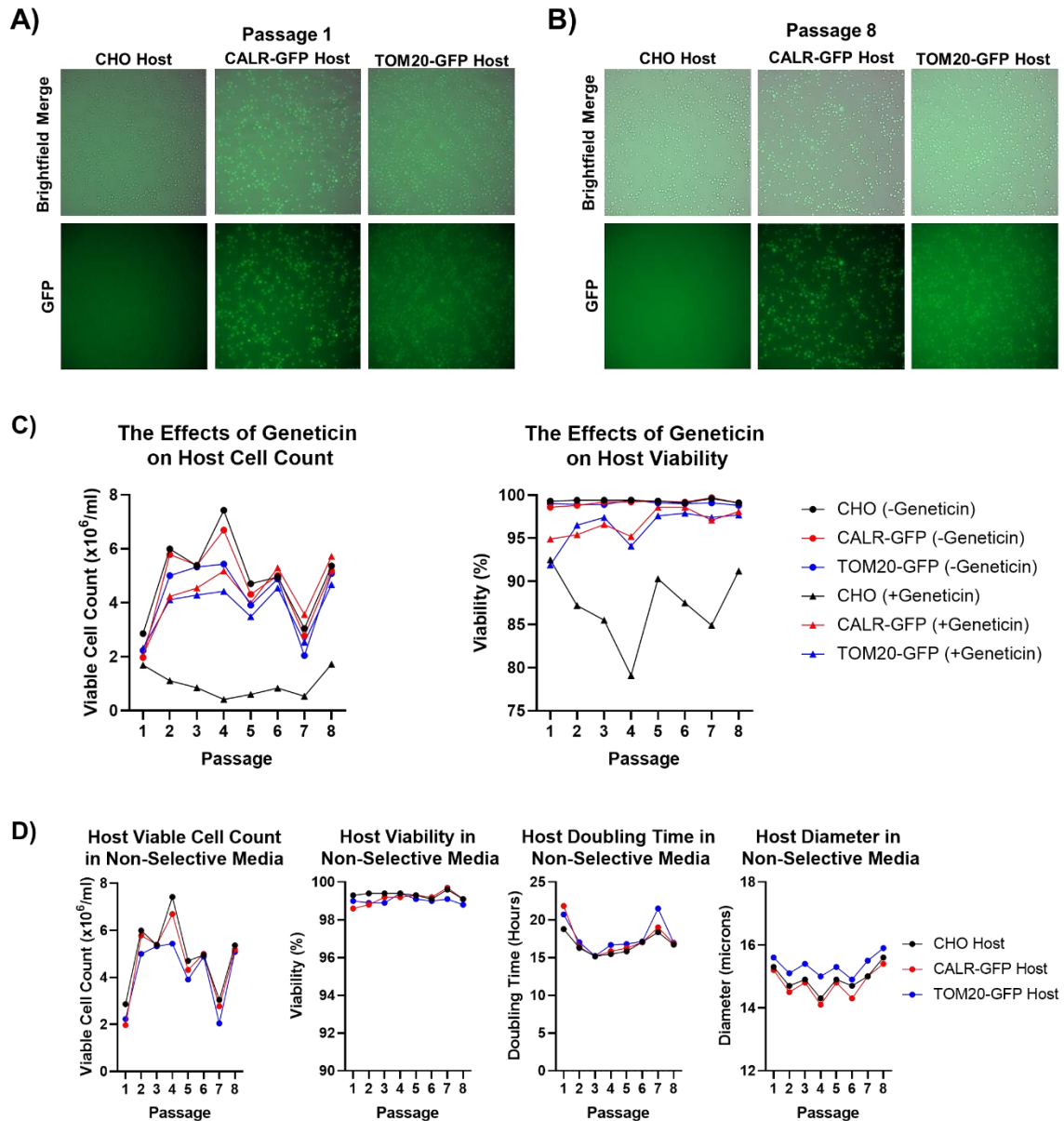


Figure 5.5. Removal of geneticin selection does not impact the expression of CALR-GFP or TOM20-GFP but improves the growth of the reporter cell lines.

GFP and brightfield live cell imaging of the cultures after **A)** 1 passage and **B)** 8 passages without geneticin selection. GFP is still present in all of the reporter cells despite removal of selection. Images were taken on a NyONE Scientific plate reader. **C)** Viable cell count and viability of the CHO host (black), CALR-GFP host (red) and TOM20-GFP host (blue) with (triangle) and without (circle) the presence of geneticin selection. The CHO host did not contain the geneticin resistance gene, and showed a reduced viable cell count as a result. **D)** Growth characteristics of the reporter hosts compared to the CHO host, in non-selective media. Coloured as per panel B. L-R: Viable cell count ($\times 10^6/\text{ml}$), viability (%), doubling time (hours) and diameter (microns). Counts were measured on the ViCell XR.

5.2.4. CALR-GFP reporter expression is retained, and can be seen during mitosis

Although reporter expression was confirmed to be retained in culture with low resolution live imaging on a NyOne plate reader (Figure 5.5.A), high resolution imaging was also performed to confirm that the reporter expression would continue in cells undergoing mitosis in non-selective media. For this fluorescence time lapse imaging was used on the live cell populations at 10 minute intervals, and the images further confirmed the retention of the CALR-GFP reporter expression throughout mitosis (Figure 5.6.A.). Three cells actively underwent mitosis during the ~5 ½ hour time lapse experiment. The process of mitosis took approximately 20 minutes. The CALR-GFP reporter can still be seen during anaphase in one cell line (Figure 5.6. B). TOM20-GFP reporter mitosis was not captured during the time lapse imaging, although expression of the reporter was still evident (data not shown).

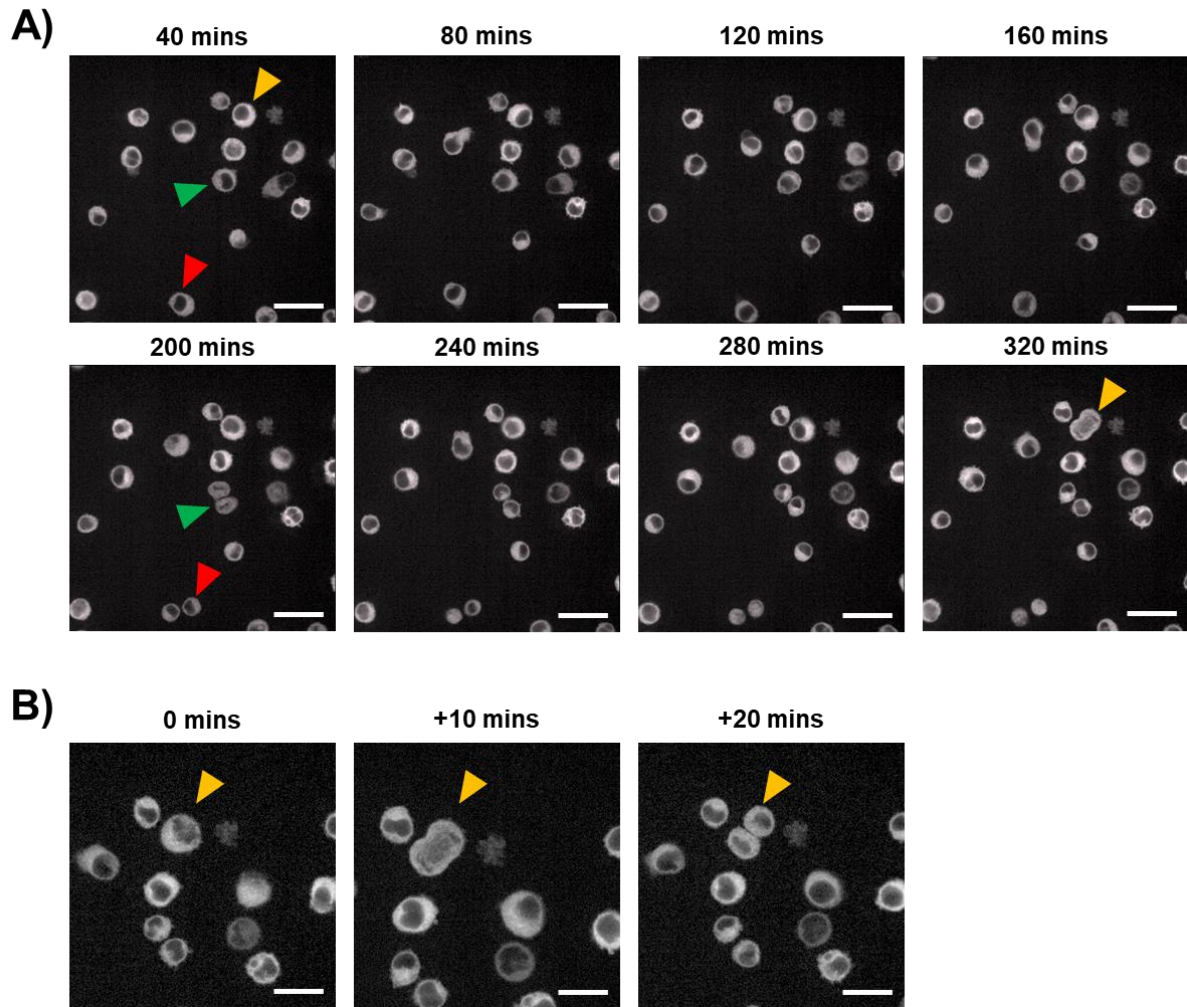


Figure 5.6. CALR-GFP reporter expression is retained in the host cell line during mitosis.

A) Time lapse images taken on a Yokogawa CV8000 microscope. Scale bar = 20 μm . Images were taken at 10 minute intervals. Images from every 4th interval has been shown here for the ease of visualisation. Dividing cells are highlighted in the first image taken 40 minutes after initial incubation in the microscope. Corresponding arrows show the time point at which they undergo mitosis. **B)** Time lapse images of the CALR-GFP host shown here after 20 minutes; one cell undergoes mitosis within the 20 minute time period. GFP expression is still seen during anaphase.

5.2.5. Reporter host responds to chemically induced ER stress

Following confirmation that the CALR-GFP and TOM20-GFP hosts were successfully being expressed within the host cell line without impacting its performance, it was necessary to assess their use as a reporter in detecting stress within the cells. To understand whether the expression of a mAb resulted in an ER stress response, the GFP phenotype in response to ER stress had to be first characterised. The chemical stressors Tunicamycin and Brefeldin A were employed for this, these two chemical stressors were chosen as they affect different parts of the protein folding and secretory pathway.

To determine whether the CALR-GFP and TOM20-GFP reporter host cell lines respond to UPR stress, the cell lines were incubated in the presence or absence of Tunicamycin or Brefeldin A for 24 hours in GSK's proprietary CHO host culture media. Live fluorescence images of the cultures were taken after 6 and 24 hours incubation, as well as quantification of the GFP intensity by flow cytometry.

Within 24 hours, the effects of Tunicamycin and Brefeldin A could be seen (Figure 5.7.A. and B.). Under normal culture conditions the reporter cells were similar in size with typical blebbed or ruffled cell membranes in the majority of the population. The GFP expression was also co-localised to the organelle targets. The addition of Tunicamycin did not stop reporter organelle co-localisation, but GFP was also present within the membrane ruffles unlike the normal conditions, in both cell lines. GFP fluorescence intensity did appear to be greater in the CALR-GFP reporter host compared to the normal culture conditions, whereas the TOM20-GFP reporter host looked the same.

The addition of Brefeldin resulted in the complete loss of the blebbed membrane in the majority of the population as seen in the brightfield images. Again, the CALR-GFP reporter host had a much more intense GFP expression compared to the cultures in the absence of Brefeldin A, and whilst it was co-localised to the ER, it appeared distorted with a heavy halo shaped presence around the cell membranes (Figure 5.7.A.). The GFP expression from the TOM20-GFP reporter host however did not look obviously different to the normal conditions (Figure 5.7.B).

The visual observations were confirmed quantitatively using an iQue flow cytometer (Figure 5.7.C. and 5.7.D). The average intensity of the CALR-GFP reporter host was 2.22 fold higher than that of the TOM20-GFP host in the normal culture conditions at both time points, likely due to the larger surface area of the ER. There was no significant difference between GFP intensity in the TOM20-GFP reporter in the normal conditions compared to the populations kept in Tunicamycin or Brefeldin A after 6 hours incubation. Again, after 24 hours incubation there was no significant change in GFP intensity between the Tunicamycin incubated cells and the normal control culture. The addition of Brefeldin A did result in a significant reduction in GFP intensity compared to the normal conditions.

The CALR-GFP host had a significantly increased GFP intensity when incubated with Brefeldin A at both time points, compared to the normal conditions (Figure 5.7.C.). Interestingly however, the CALR-GFP reporter host showed an initial significant reduction in GFP intensity when incubated with Tunicamycin compared to the control, before increasing in GFP expression after 24 hours. As CALR's main function in the ER lumen is to bind to proteins that have a misfolded glycan profile during N-linked glycosylation, and Tunicamycin inhibits N-linked glycosylation the increase in GFP expression after 24 hours was not surprising. Further study would be required to confirm that the response was specific to the chemical addition, and not by means of another stress factor. Questions could also be asked as to whether a different mechanism of action was at work, as the CALR-GFP reporter was expressed over a constitutive promoter, rather than the protein specific promoter. Previous literature however has also shown that Calreticulin is upregulated in HeLa cells when incubated with Tunicamycin, both when looking at endogenous CALR expression and upon addition of an exogenous plasmid and promoter (Yang et al., 2019). Further analysis would be needed to further investigate this. The slight reduction in expression of CALR-GFP after 6 hours of Tunicamycin incubation was surprising however, as the UPR can temporarily attenuate translation via the PERK pathway (Figure 1.7.) (Walter and Ron, 2011), it is hypothesised that this initial reduction may have been an initial response to the addition of Tunicamycin. Despite this, the study does suggest that the CALR-GFP reporter host is capable of monitoring a stress response via the intensity of the reporter expressed, and whilst it may reduce in expression initially, the likely phenotype is to be an increased GFP intensity in the presence of constant stress.

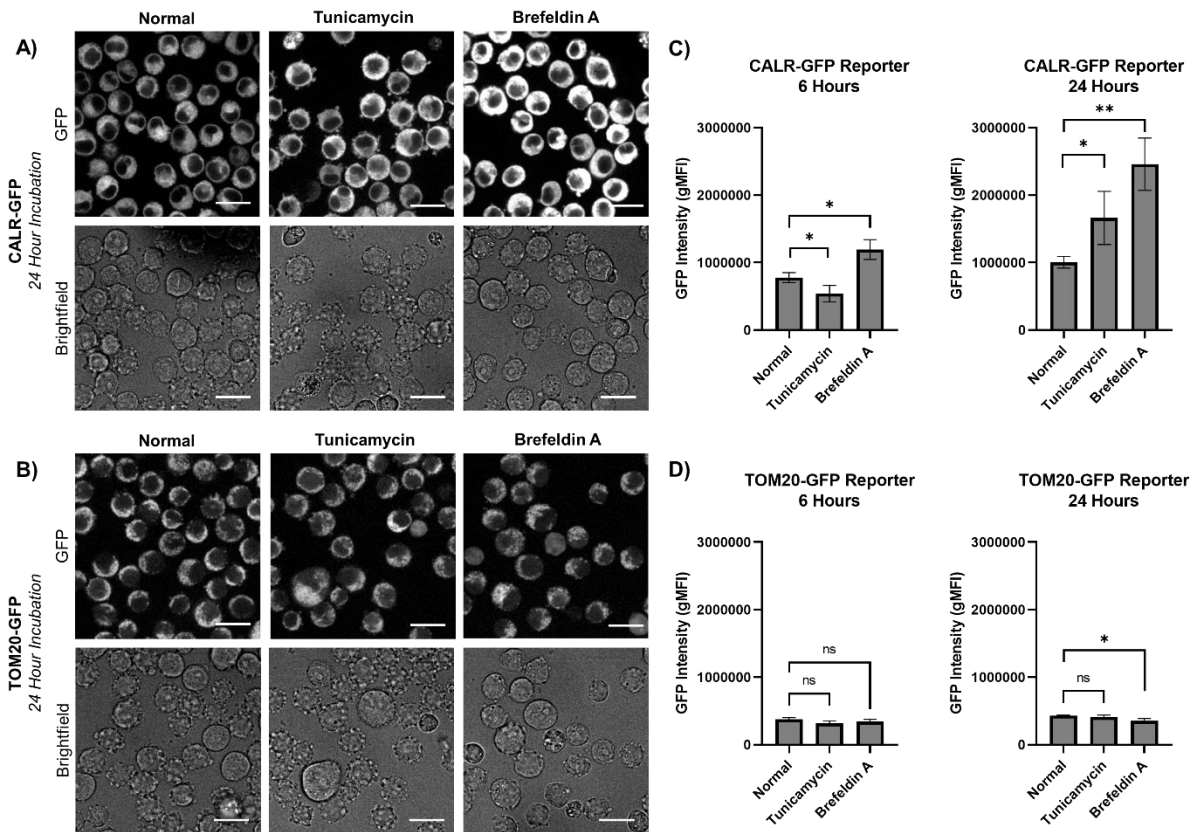


Figure 5.7. Effects of Tunicamycin and Brefeldin A on the CALR-GFP and TOM20-GFP reporter host cell lines. A-B) Fluorescence and brightfield imaging of CALR-GFP and TOM20-GFP host cell lines after 24 hours incubation in either media, media containing 1 μ g/ml tunicamycin, or media containing 1 μ g/ml brefeldin A. Images captured using a Yokogawa CV8000 microscope. Scale bar= 20 μ m. **C-D)** GFP intensity of the fluorescent reporter measured by flow cytometry (N=3), on an iQue flow cytometer. Student's t test was performed on the Tunicamycin and Brefeldin A cultures against the normal condition control. P value ns= non-significant, * <0.05 and ** <0.01. Error bars = \pm 1SD.

5.2.6. CALR-GFP and TOM20-GFP reporter expression increases after transient transfection with plasmids expressing antibody

Given that the CALR-GFP reporter host cell line could successfully be used to measure chemically induced ER stress using Tunicamycin and Brefeldin A, it was of interest to see whether mAb expression resulted in the same phenotype. The reporter expression would need to be measurable at any stage of the CLD pipeline to be a useful selection tool. This was therefore tested, by transiently transfecting the reporter hosts with mAbs 3, 4 and 7 from the mAb panel (Table 2.2). Two negative controls were also measured: a PBS transfected control and non-transfected control. The CHO host was also transfected with a constitutive GFP plasmid, and mAb 4 as positive control. mAb 4 was chosen as it is known to be a high expressor control mAb. The cells were then analysed on 1 day and 7 days post transfection for growth, reporter expression and mAb titre.

Cell viability (%) in all of the cultures remained high 1 day post transfection (95.6 % average), but dropped to 72.4 % after 7 days in culture (Figure 5.8.A.). As the untransfected controls also dropped in viability it most likely caused by the exhaustion of nutrients from the media or the toxic build-up of metabolites. To confirm this, the concentration of waste metabolites such as Lactate and Ammonia could have been measured. The CHO host had a higher viable cell count than the two reporter lines 1 day post transfection, but after 7 days left in 6 well culture, all cultures had over 1×10^6 /ml cells (Figure 5.8.B.). The mAb transfected cultures were all producing measurable titres by day 7 (0.74 – 1.62 mg/L), however some were measurable as early as 1 day post transfection (up to 0.36 mg/L, Figure 5.8.C.). mAb expression was further confirmed with positive IgG staining on the iQue flow cytometer, in all mAb transfections at both timepoints (Figure 5.8.D.).

As expected, GFP was not measurable in the CHO host, apart from the cultures transfected with the constitutive GFP plasmid. A trend was seen in GFP reporter intensity in both reporter hosts, with higher intensities in the mAb transfected cell lines, compared to the non-transfected and PBS transfected controls (Figure 5.8.E.) (an average 1.47 fold increase in CALR-GFP expression in the mAb transfected populations compared to the PBS control). Despite the TOM20-GFP reporter not significantly increasing in response to chemical stressors, an increase was observed in response to transient mAb transfection at the exact same fold increase as the CALR-GFP reporter populations (1.47 fold increase). The transfection procedure did not affect reporter intensity, as similar intensities were recorded in the non-transfected control, suggesting that the increase in GFP expression was caused by the expression of the mAb molecule and/or the plasmid it was expressed in. The type of mAb expressed also did not affect the intensity of the reporter, suggesting that the response could be monitored with any plasmid containing a mAb construct.

The reporter GFP intensities had large error bars across the replicates, making it difficult to accept the results seen in the experiment. The large error is thought to be due to the heterogeneity of the pre-clonal pools post transfection. Despite this, it did give early evidence that the sudden addition of a mAb construct that requires complex protein folding pathways causes stress to the cell immediately after its addition. To understand if this is a true biological reaction that is retained throughout culture, the reporter GFP expression will have to be monitored throughout a full CLD campaign, from the transfection to generation of single cell clones.

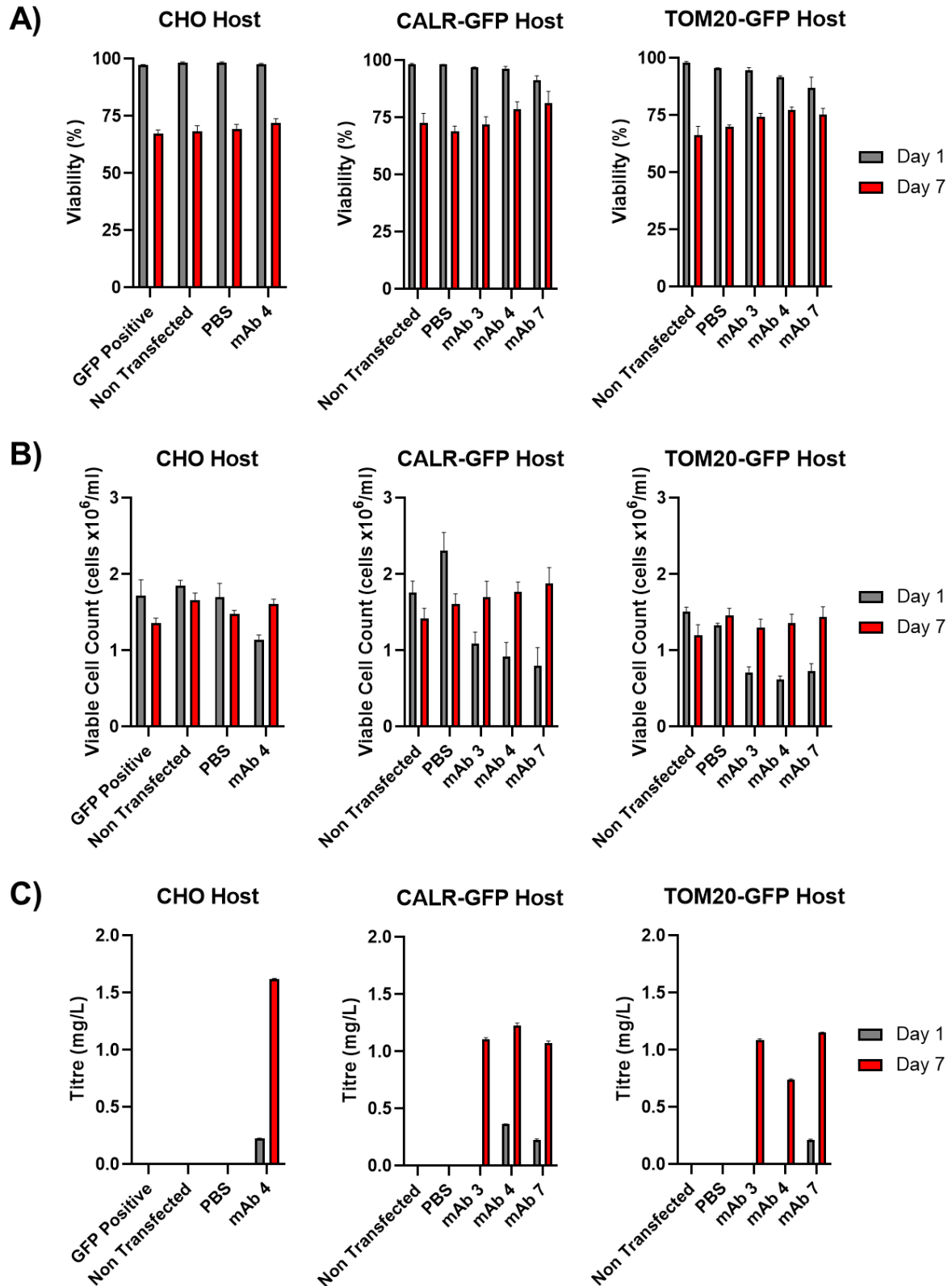


Figure 5.8. Reporter expression was increased 24 hours post transient transfection with mAb constructs.

The three host lines were transfected with mAb constructs via electroporation and monitored 1 day (grey) and 7 days (red) later (N=3). The transfected cells were measured on the ViCell XR for their **A)** Cell viability (%) and **B)** Viable cell count (cells x10⁶/ml). **C)** mAb titre (mg/L) was monitored on the Octet HTX. **D)** Reporter GFP expression (gMFI) and **E)** IgG Intensity (gMFI) were measured on the iQue flow cytometer. Error bars = \pm 1 SD.

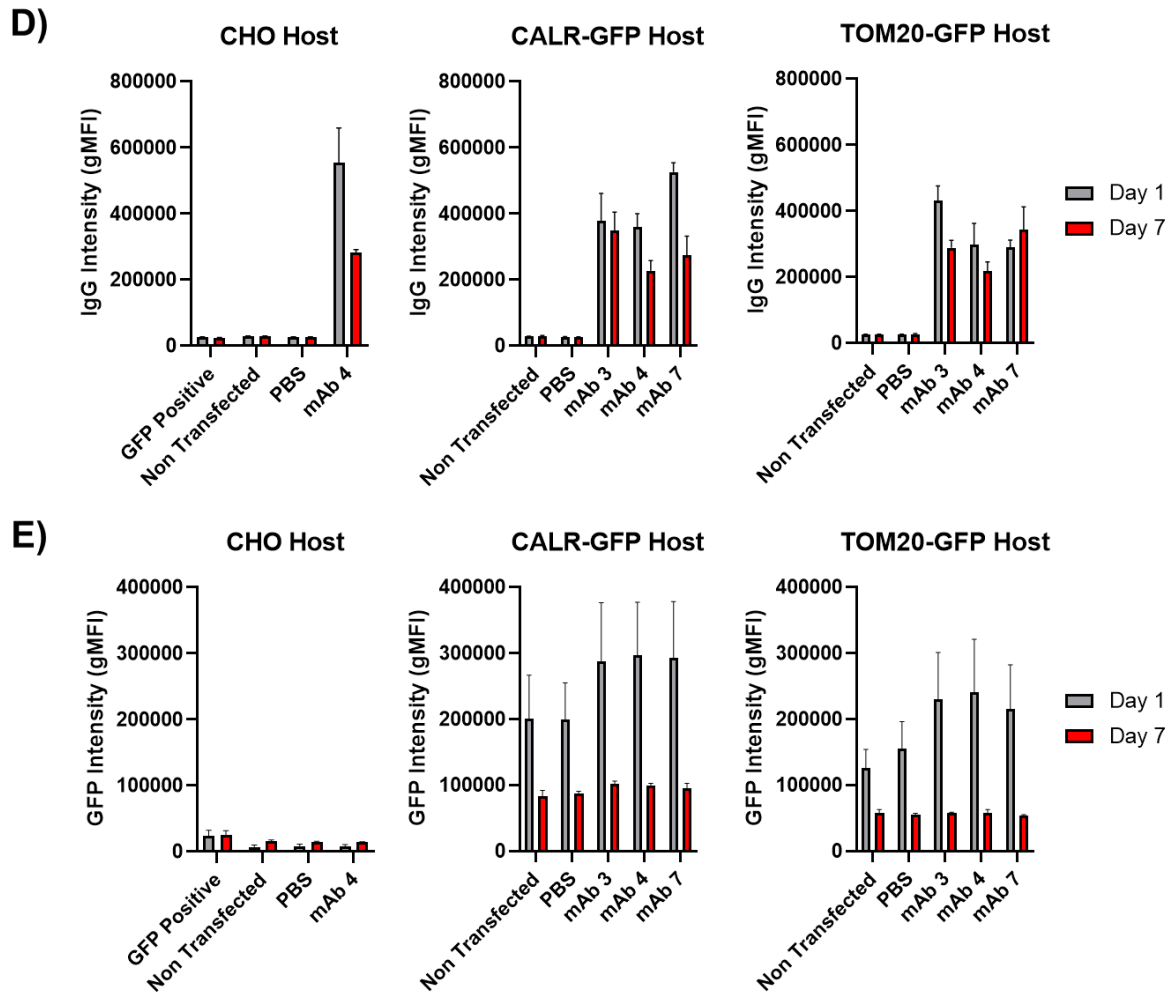


Figure 5.8. (Continued) Reporter expression was increased 24 hours post transient transfection with mAb constructs.

The three host lines were transfected with mAb constructs via electroporation and monitored 1 day (grey) and 7 days (red) later (N=3). The transfected cells were measured on the ViCell XR for their **A)** Cell viability (%) and **B)** Viable cell count (cells $\times 10^6/\text{ml}$). **C)** mAb titre (mg/L) was monitored on the Octet HTX. **D)** Reporter GFP expression (gMFI) and **E)** IgG Intensity (gMFI) were measured on the iQue flow cytometer. Error bars = ± 1 SD.

5.2.7. CALR-GFP and TOM20-GFP reporter localisation remains visible on the Beacon after mAb transfection

The CALR-GFP reporter expression was increased during chemical stress induction and immediately after transient transfection with mAb in the CALR-GFP reporter host, suggesting that it may be monitoring ER stress. To confirm that this prediction could be useful during a CLD pipeline the CALR-GFP reporter host had to be run through a typical CLD workflow where the CALR-GFP expression could be monitored throughout. As the TOM20-GFP reporter host did not show an increase in reporter expression during chemical stress induction it was decided to not take the TOM20-GFP reporter host line through the CLD pipeline.

The CALR-GFP host cell line was stably transfected with the mAb panel (Table 2.2.) and following recovery and selection these pre-clonal cell lines were loaded and cultured on the Beacon as per Section 2.4.3. Clonal cell lines showed an overall consistency in the localisation of the reporter and cell size (Figure 5.9.A.). However, the intensity of the reporter varied between different pens, suggesting that the CALR-GFP may be responding to differences in the folding environment of the ER potentially caused by differences in the levels of antibody expression between clones.

The Beacon titre measurement (Au score) and productivity (QP) cannot be directly compared with previous experiments, as variation is present between the chips, culture times and Spotlight assay reagent lots. The general trend here was the same as the Spotlight titre assay measured in the mAb expressing CHO clones in Chapter 4. mAbs 1-3 had the higher Au scores, whilst mAbs 5-7 had much lower Au scores. 96 cell lines were exported, ensuring that clones expressing a range of mAb types were chosen with a range of Au scores to obtain good and bad producing cell lines.

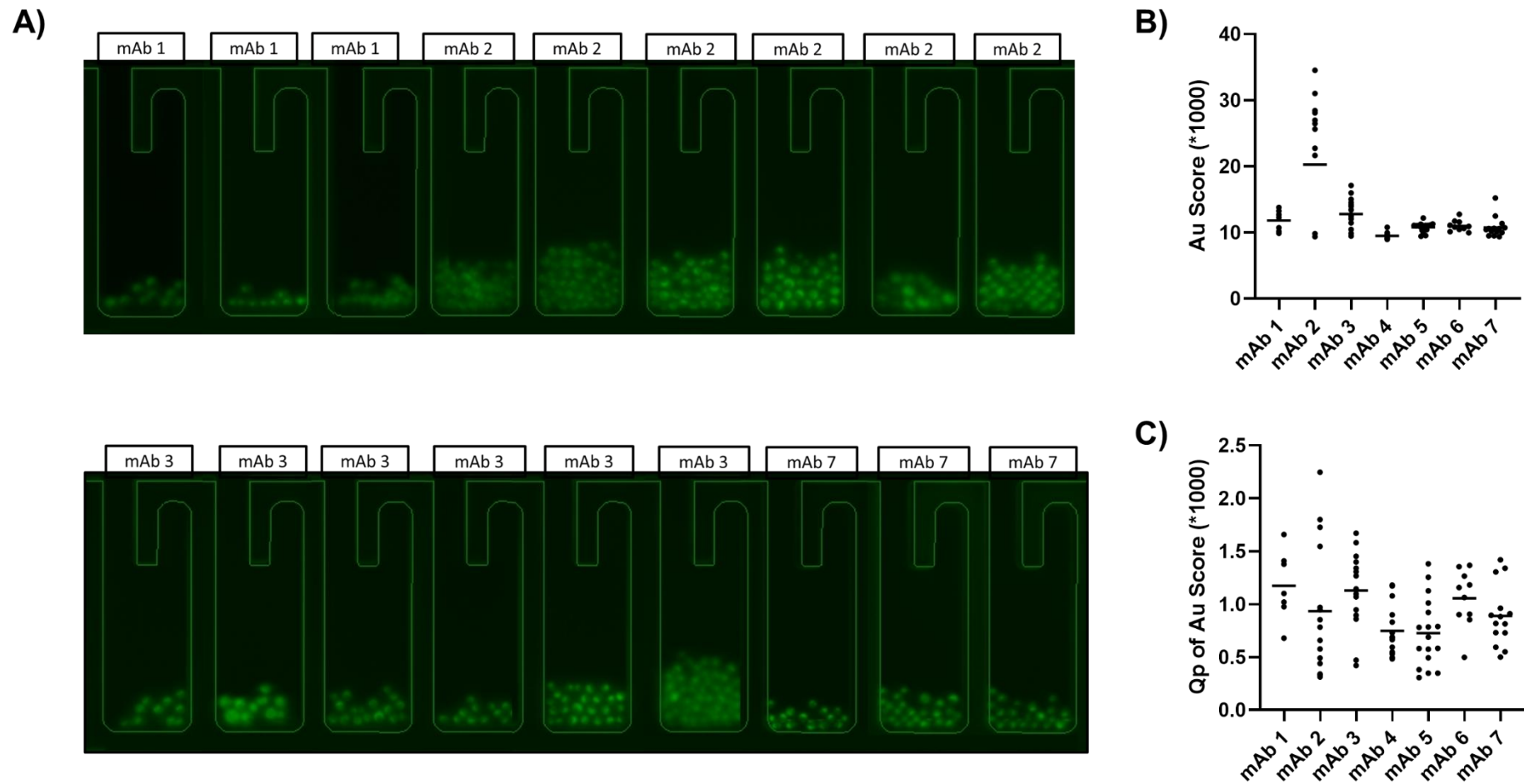


Figure 5.9. Single cell cloning of the CALR-GFP reporter host transfected with a panel of mAb constructs.

A) Selection of CALR-GFP reporter host line pens imaged on the Beacon 6 days after load on the FITC filter. Pens were expressing different mAb constructs. Reporter intensity, cell counts and cell sizes varied across the pens. **B)** Spotlight Au score (*1000) for each of the 96 exported mAb lines after 6 days in culture on the Beacon, divided into the mAb construct. Mean Au score also shown. **C)** Productivity (Qp, *1000) of the 96 exported mAb lines after 6 days in culture on the Beacon, divided into the mAb construct. Mean Qp also shown. Qp was obtained by dividing the Au score by the cell number.

5.2.8. CALR-GFP reporter host expression negatively correlates to titre during static scale up

After export from the Beacon, the 96 exported cell lines were scaled up as per the CLD platform process defined in the introduction of this thesis (Section 1.1.4.). Unfortunately, some cell lines did not recover following export, or were not expressing measurable mAb titres. These cell lines were removed from the panel of cell lines. Initially, 39 cell lines recovered following Beacon export and were scaled up to shake-flask culture. 30 of these cell lines were expressing measurable mAb titres on the Octet HTX and were kept for further investigation. The low number of clones producing measurable mAb was not surprising, or a reflection on the Beacons selective capabilities, as poor producing clones were chosen on purpose for export to obtain a range of clonal characteristics.

GFP intensity was monitored for all of the clonal cell lines that were expressing mAb during each stage of scale up from the 6 well stage. CALR-GFP was difficult to measure before this stage as the cultures were at such low cell volumes. The average CALR-GFP expression remained the same between the 6 well and T25 screen, before increasing in intensity at the shake flask stage where it stabilised again (Figure 5.10.A.). This increase may be due to the cultures becoming more viable as cell numbers and culture volumes increase (Figure 5.10.C), whilst it appears unlikely to be linked to the clones productivity during the scale up, as average titres remained similar throughout (Figure 5.10.D.).

There was a significant difference between the mAb type being expressed and the intensity of CALR-GFP expression at the shake flask bulk stage (One-way ANOVA analysis, $F = 3.949$, $p = 0.013$). A Tukey post-hoc test also showed that mAb 3 had a significantly lower CALR-GFP expression than mAb 6 (mean diff. -0.103 , $p < 0.05$) and mAb 7 (mean diff. -0.109 , $p < 0.05$) (Figure 5.10.B.).

The average log CALR-GFP intensity of the cell lines was then correlated to titre at each stage of static scale up (Figure 5.11.). The data showed to be non-parametric, and a resulting Spearman's rank analysis showed that titre was moderately negatively correlated with CALR-GFP expression at each time point ($p < 0.05$ at all stages apart from T25, actual p values can be seen in Figure 5.11.A.). The reduction in correlation at the T25 stage may be explained by the movement of cultures to static culture for the first time, where the increase in GFP intensity was seen to increase (Figure 5.10.A.).

This suggested that the higher the intensity of the GFP from the CALR-GFP reporter expression, the lower the resulting mAb titre in the clones. Spearman's rank analysis was performed on each of the mAbs individually at the shake flask bulk stage, with all mAbs apart from mAb 7 showing a similar negative correlation suggesting that the reporter would be reproducible over different projects and mAb designs (Figure 5.11.A.). None of these correlations were statistically significant, potentially affected by the small sample sizes (N number between 3-8). As CLD processes often base selection off

of cell rankings rather than specific values, the 30 mAb expressing cell lines at the shake flask bulk stage could be ranked for their GFP expression, titre and productivity scores individually. The cell lines ranked by GFP expression were still negatively correlated with the ranked titre and productivity scores (Figure 5.11.B.), to a similar strength as the non-ranked data. As shown by a Pearson's correlation coefficient of -0.640 and -0.637 for GFP intensity against productivity and titre respectively (both $p < 0.0005$). Taken together this data suggests that the CALR-GFP reporter host can predict the titre of clones expressing various mAbs with a moderate reliability at any time point apart from the T25 stage where cultures first enter shaking culture.

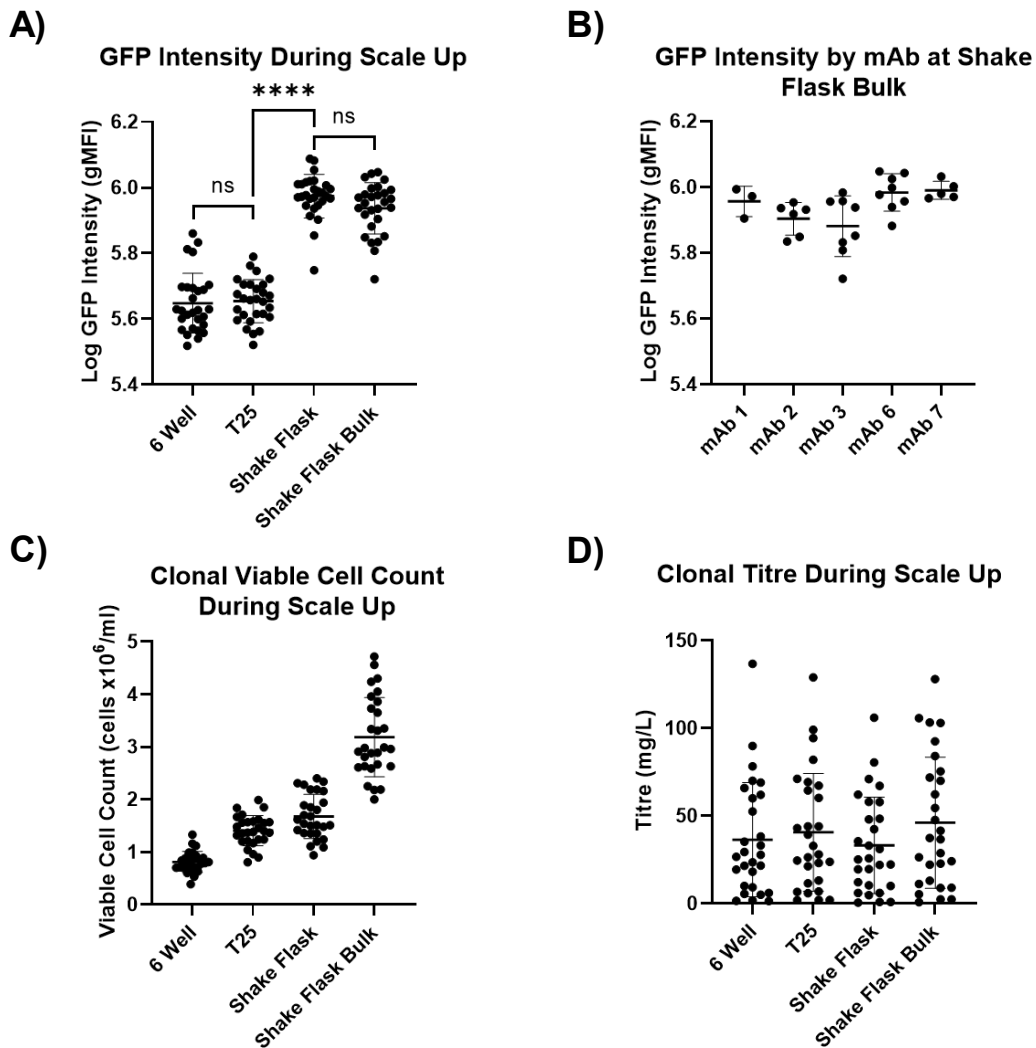


Figure 5.10. Monitoring CALR-GFP intensity in mAb expressing clonal lines during static scale up.

A) Log GFP intensity of each cell line at each scale up stage measured using an iQue Screener flow cytometer, alongside the mean ± 1 SD. Average GFP intensity increased in all cell lines, irrespective of mAb they're expressing, after movement to shake flask culture. Student's t test was performed between each scale up step. (6 well to T25 flask $p = 0.770$, T25 to shake flask $p < 0.0001$, shake flask to shake flask bulk $p = 0.062$). **B)** Log GFP intensity at the shake flask bulk stage, split by mAb type, alongside the mean ± 1 SD. One-way ANOVA analysis: $F=3.949$, $p < 0.05$. Tukey post-hoc test showed mAb 3 GFP intensity was lower than mAb 6 (mean diff. -0.103 , $p < 0.05$) and mAb 7 (mean diff. -0.109 , $p < 0.05$). **C)** Viable cell count (cells $\times 10^6$ /ml) and **D)** titre (mg/L) of each clonal cell line at each scale up stage measured using the ViCell XR and Octet HTX respectively, alongside the mean ± 1 SD.

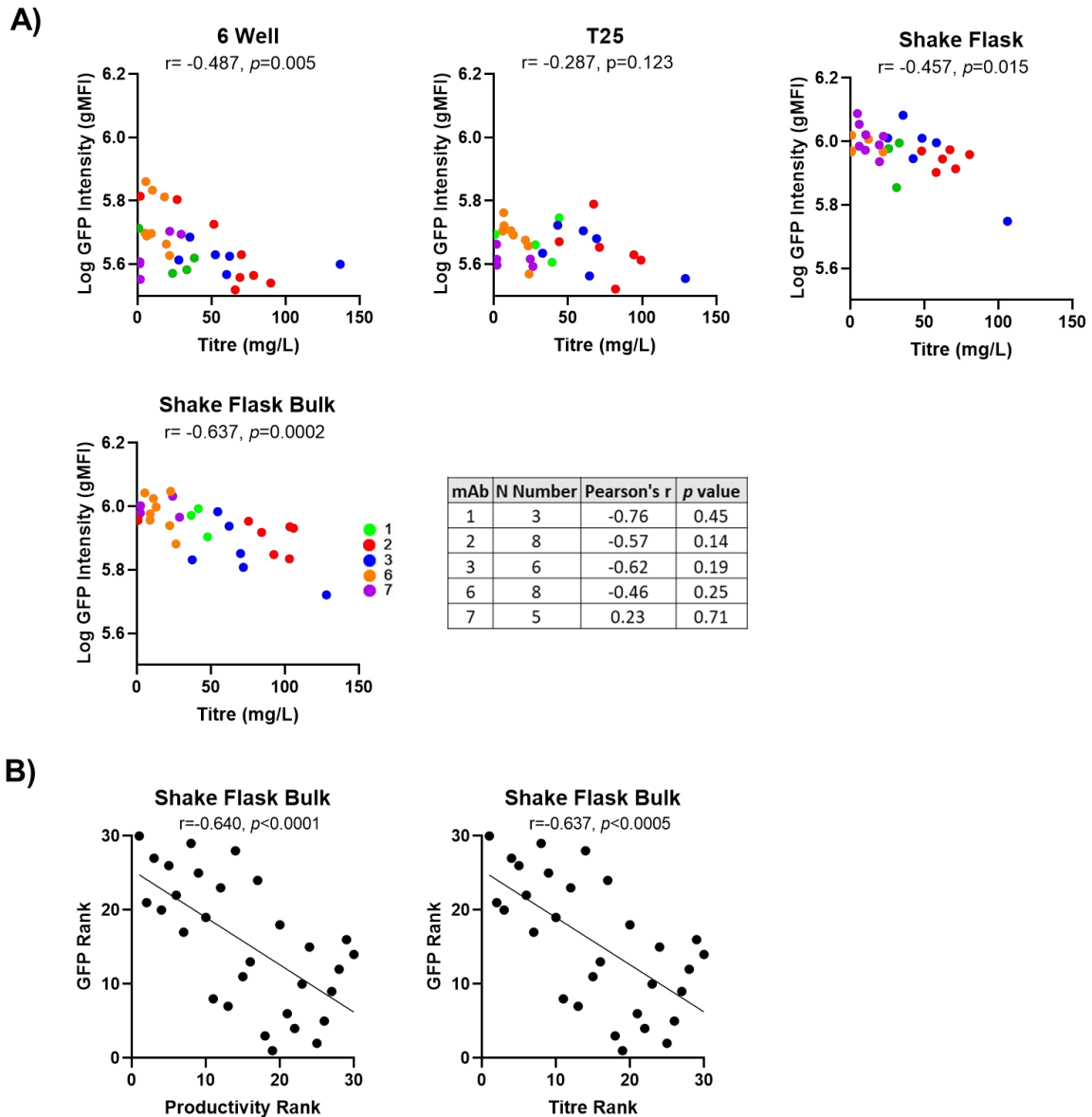


Figure 5.11. CALR-GFP intensity negatively correlated to mAb titre during each stage of static scale up in mAb positive clones.

A) Log GFP intensity measured using an iQue Screener flow cytometer, of the clonal cell lines correlated to titre, as measured by the Octet at each time point. Cell lines are coloured by mAb expressed. Correlation measured by Spearman's rank analysis. Statistical significance $p < 0.05$. **B)** GFP intensity ranked at the shake flask bulk time point, correlated to the ranked productivity and titre of the cell lines respectively. Correlation measured by Pearson's rank analysis. Statistical significance $p < 0.05$.

5.3. Discussion

The expression of an exogenous mAb expressing plasmid in CHO cells requires usage of the host cell's transcription and translational machinery, reducing the amount available for normal cell functions (Davies et al., 2013). Adding to this, the complex folding process of the mAb construct can result in stress to the ER, and ultimately result in a build-up of mis-folded proteins (Hetz, 2012). Previous literature has shown that some clones are able to cope with mAb folding better than others, and often have an elevated number of RNA transcripts dedicated to protein folding (Kober et al., 2012; Prashad and Mehra, 2015). This Chapter has focused on exploring whether a UPR based fluorescent reporter assay can identify clones that are more adaptable to high protein expression so that they can be detected at the earliest stages of CLD. Here, we expressed an exogenous fluorescent reporter tagged to the ER folding chaperone Calreticulin (CALR). A second mitochondrial based reporter was also expressed to determine whether the mitochondria played a role in high protein expression using the Translocase Of Outer Mitochondrial Membrane 20 (TOM20) protein. CALR was successfully tagged with GFP and mOrange, and TOM20 was successfully tagged with GFP. All of the reporters showed localised expression to their respective organelle and could be used to monitor during the cell line development process when transfected into the CHO host. The CALR-GFP host in particular showed the expression of the reporter was stable and uniform in culture, and could respond to antibody expression and chemical mediated stress.

The use of fluorescence reporters on the Beacon system has previously been reported, however this was only used to assess clonality where single cell clones were imaged for their fluorescence. Le et al. (2020) used the Beacon to single cell clone a mixture of cells constitutively expressing either RFP or GFP. The resulting clones were scaled up and imaged for either their GFP or RFP expression to confirm the clonality capabilities of the Beacon. The paper showed that the Beacon had an export purity of 100 % out of 112 exported clones (only the correct fluorescence was seen in the populations as in the respective pen loaded). To date, the use of an organelle-localised fluorescence based reporter as a selection tool on the Beacon has not been reported. Following confirmation that the organelle reporter constructs were correctly expressed within the CHO host, and GFP and mOrange could be visualised (Figure 5.2.A.) the cell lines were single cell cloned on the Beacon system. This system enables single cells to be cloned and cultured on chip and provides imaging at selected stages throughout. The FITC and TexasRed filters within the Beacon allowed the expression of the reporter constructs to also be imaged. When the pre-clonal pool was loaded on the Beacon to generate a clonal reporter host cell line the variation in the intensity and the co-localisation of the reporter construct was apparent (Figure 5.4.A.). Heterogeneity in reporter expression was seen across the pens; and within the pens themselves suggesting clonal instability in some instances. These observations suggest

that the Beacon can successfully determine subtle differences in reporter intensity which would be useful for identifying clones with 'good' and 'bad' production characteristics. Less variability in reporter expression was observed between cells once a final CALR-GFP cell line had been established (Figure 5.9.A.).

One potential limitation of this current approach is that these differences in expression would have been only possible to measure on the Beacon visually, as quantitative expression intensity values are not currently available for GFP expression. The ability to use CALR-GFP expression to select cell lines expressing mAb on the Beacon therefore was limited by the lack of quantification of fluorescence per pen. The Spotlight assay uses fluorescence quantification to monitor clone titre and to allow export selection, thus a similar quantification tool for the FITC filter would be beneficial to select for cells based objectively on the reporter expression. The mOrange variant of the CALR reporter showed co-localised staining but at a much poor resolution than the GFP variant making it difficult to gage staining intensity across the pens, this was most likely due to the mOrange excitation/emission spectra (547/561) not sufficiently aligning to the Beacon's TexasRed filter (562/624) (Jorgolli et al., 2019). The Spotlight Assay used to monitor titre also uses the TexasRed filter, and thus generating a second permanent assay with TexasRed as the detection filter could distort both assay results, making the FITC filter a more reliable choice for reporter expression, hence the CALR-GFP host and TOM20 host were selected for further analysis.

The addition of the CALR-GFP and TOM20-GFP reporter plasmids did not affect cell growth or viability when the two reporter hosts were compared to the CHO host in non-selective conditions. Cell growth is a crucial factor to consider in CLD, with a fine balance between having high cell growth to sustain long periods of culture in large scale manufacture, and high protein productivity the key to generating the ideal CHO clone (Nolan and Lee, 2012). Improvements in cell growth were immediately seen when the geneticin selection was removed from the culture media, and thus the removal of the unnecessary selection marker from the plasmid itself following the successful recovery of plasmid containing cells after transfection, could further improve titre. Ribo-Seq analysis has shown that ~15 % of all ribosomes in a mAb expressing CHO cell line were actively translating mRNAs attributed to the recombinant protein plasmid (heavy chain, light chain and neomycin resistance gene) during cell culture, with over 5 % overall attributed specifically to the neomycin resistance gene. Further to this, when the neomycin gene was knocked down by 87 %, titres rose by ~18%, highlighting the benefits of a non-selective system (Kallehauge et al., 2017). Whilst a selection based system for the reporter plasmid design does ensure that only GFP-reporter positive plasmids are progressed, the appeal to not select during transfection, and single cell clone on the Beacon at random does look to be beneficial to improve

product titres and cell growth. This effect is then doubled when considering mAb plasmid selection is also typically achieved by using a selective marker.

Despite the addition of a secondary plasmid containing a secondary selection marker, the staining intensity of the reporter showed a significant, moderate negative correlation with titre in the CALR-GFP reporter host, when transfected with a panel of different mAbs during static scale up. The panel of mAbs chosen each had a problematic production characteristic inherently within their protein sequence, caused by changes to the DNA sequence (Table 2.2.). As a proof of concept study our preliminary data suggests that it may be possible to use this reporter system to identify clones with high titres, as it showed a moderate negative correlation, specifically by selecting for those that had lower CALR-GFP expression. A blind study whereby clones with previously unknown titres could be measured for titre and RNA expression via ddPCR to see whether the correlation remains even when cells are not selected on titre. In support of these findings, the correlation was the same as that seen with the endogenous CALR RNA transcript in the mAb expressing CHO host cell lines, whereby higher CALR concentrations were found in low titre clones (Figure 4.4.). Interestingly, the strength of the correlations from the endogenous and exogenous CALR expression compared to the titre were similar ($r = -0.514$ and -0.637 respectively) suggesting that regardless of whether the CALR expression is endogenous or exogenous the relationship to titre is the same. A hypothesis for why this relationship looks so similar would be that the high producing clones potentially have a better adapted biosynthetic pathway so are under less stress, which results in the UPR not being initiated. Whereas the low producing clones are maladapted to high levels of protein expression and have upregulated UPR markers such as CALR to cope with the stress they are experiencing. It is unclear why the levels of the exogenous CALR then also follows this pattern, however it is likely that it is related to the post-translational and folding activity of CALR and thus it is hypothesised that the lower producer clones actually utilise and retain the exogenous CALR-GFP to deal with the stressed conditions, resulting in higher GFP intensities whilst the higher producers do not require the CALR-GFP and it can be marked for degradation. This link between expression and function can be further evidenced with the response of the reporter following incubation with Tunicamycin and Brefeldin A. If the tagged exogenous protein did not have a function within the culture then the TOM20-GFP reporter would have equally seen an increase in expression when incubated with Tunicamycin and Brefeldin A.

The ability to predict titre that was seen during the static scale up of the clonal lines was not seen during initial transient transfection however. Following the transient transfection of the TOM20-GFP and CALR-GFP reporter host with a panel of mAbs the TOM20-GFP reporter expression was increased to the same fold as the CALR-GFP reporter when transiently transfected with mAb. It did appear that the increase in reporter intensity was caused by the addition of the mAb rather than the transfection

protocol itself, as the PBS transfected control did not show as elevated reporter expression, however the study was limited as an empty plasmid control transfection was not included, and thus it cannot be confirmed that the increase in expression was caused directly by the mAb construct or the large secondary plasmid.

5.3.1. Potential improvements to the reporter construct design

As a proof of concept study, the CALR-GFP reporter host behaved in a manner which suggested that an ER specific reporter can monitor mAb titre. However, whether CALR is the best ER marker for monitoring mAb titre is not fully understood and further reporter constructs tagging other ER proteins would be required to determine this. Calnexin (CANX), a membrane bound homolog of CALR, may be advantageous over CALR for example, as CALR has been cited to translocate to the nucleus in multiple cell types meaning that quantification may not be consistently measuring for the ER folding specific mechanism that CANX does (Roderick et al., 1997). The question as to what protein marker may be more predictive, however, is difficult to answer. Previous literature has shown sXBP1 and BIP related reporter constructs correlated strongly to titre in mAb expressing CHO clones (Kober et al., 2012; Roy et al., 2017), suggesting they could potentially be better at predicting titre than CALR. In the Ribo-seq study by Kallehauge et al. (2017) mentioned above, of the 15919 endogenous mRNA transcripts successfully identified during the profiling experiments, XBP1 was the 2102nd most highly expressed transcript, suggesting that it was not highly utilised in the mAb expressing cells. Conversely, BIP and CALR registered as 1st and 9th on the list respectively. BIP was the most highly sequestered protein by the ribosomes of a mAb expressing CHO population after 6 days of culture, followed by a host of proteins primarily focused on folding, sorting and degradation, biosynthesis and translation. This suggests that these proteins are crucial for the CHO cell and bolsters the choice of CALR as the reporter construct. Of course, it also highlights that BIP could also be a more predictive choice.

A second question also arises when investigating potential improvements in the reporter construct- is exogenous CALR expression representative of endogenous CALR capacities? This could be addressed by instead tagging the endogenous CALR gene with GFP using techniques such as CRISPR. This way the expression measured is directly under an endogenous promoter and thus any fluorescence response is a specific physiological response of the UPR. However, whether the addition of a large fluorescent tag onto the end of an ER resident chaperone such as CALR would affect its function and binding affinity to nascent protein would need to be interrogated. One opportunity to curtail this affect would be to take advantage of a split GFP system, whereby the 11th GFP motif is tagged to the CALR, and a secondary recombinant plasmid containing GFP motifs 1-10 expressed alongside (Kamiyama et al.,

2016). GFP would therefore only fully fold in CALR localised areas. This small size of the GFP11 tag makes it much easier to perform knock in experiments (Blakeley et al., 2012), and potentially may be less disturbing to the folding of the attached protein in comparison to a full size GFP marker (Nguyen et al., 2013). Multiple ER resident proteins have been successfully tagged in HEK293T cell using a CRISPR based approach. The most interesting of which in consideration to this project being Calnexin, Calreticulin's membrane bound homolog (Leonetti et al., 2016).

A preliminary study in GSK's CHO host was performed to test the splitGFP system against an exogenous BIP-GFP¹¹ protein. Two recombinant plasmids- one containing the splitGFP¹⁻¹⁰ motifs and one containing a BIP-GFP¹¹ sequence were co-transfected into the host and fluorescence microscopy used to check for ER localised GFP expression. Unfortunately, no GFP expression was observed (data not shown). The splitGFP¹⁻¹⁰ protein may not have been retained within the ER for a period of time long enough to cause binding to the BIP-GFP¹¹ protein, with previous literature obtaining a localised Calreticulin signal in *Drosophila S2* cells when an ER retention sequence was added to the splitGFP¹⁻¹¹ (Kamiyama et al., 2016).

Whilst a CRISPR based endogenous marker system would be desirable in understanding why the ER may correlate to mAb titre in a technical sense, it still requires an additional second plasmid for the splitGFP system which would require a second selection pressure and present as much translatory stress as the exogenous reporter plasmid used here. The endogenous system fluorescence could also be poorly monitored when considering that the two separate GFP sequences need to bind together between the 10th and 11th motif in the ER lumen following individual translation. If the splitGFP¹⁻¹⁰ construct was expressed differentially to the BIP-GFP¹¹ protein then there could be a build-up of incorrectly folded protein that creates a greater stress on the cell. The exogenous CALR construct is already bound to the full GFP format, which allows us to be confident in its correct expression and folding as long as there is GFP expression present and localised to the ER. Thus there are merits to the use of an exogenous tag for monitoring mAb titre.

5.3.2. What are the most important predictive capabilities for CLD to be able to measure?

Of course, the mAb titre relationship measured here can already be easily measured throughout CLD using equipment such as the Spotlight assay on the Beacon and the Octet HTX. The Octet HTX can be used during each scale up stage in CLD, and was used in this study to measure titre. This presents a major limitation to the necessity of a reporter construct. The CALR-GFP reporter construct therefore is not a particularly useful tool for CLD if it is only able to predict mAb titre, as current technologies already exist to do this. To be able to predict product quality at an early culture stage would be a much

more useful tool for CLD as static scale up following single cell cloning is defined by its small culture volumes, and as such sampling must be kept to a minimum to ensure successful recovery. Monitoring for product quality using traditional methods at this stage is therefore impossible, as media containing mAb products at concentrations of up to 2 mg/ml are required for the gold-standard HPLC based product quality assessments. The collection of this media is typically obtained after a 15 day fed-batch production study of each of the clones, which is followed by a filtration and purification protocol. To be able to predict the product quality of the clones based on their reporter expression alone would therefore be an invaluable tool to reduce the number of poor quality clones progressing to production study stage. Chapter 6 explores this concept, whereby the clones generated in this chapter will be product quality assessed, namely for product size and product charge. As the CALR-GFP reporter host has already shown to be able to moderately predict mAb titre, then the ability to predict product quality aspects would make the tool invaluable for CLD. This is especially interesting for the CALR-GFP reporter as CALR has a function in N-linked glycosylation, of which incomplete or dis-regulated glycosylation can have an effect of mAb product quality. Further to this, CALR directly associates with PDI to form the disulphide bonds for mAbs, and this thesis has already shown a correlation between PDI and fragment (Figure 3.6.D.). Product size typically focuses on measuring for fragmented and aggregated product, whilst product charge explores whether the charge on the proteins acid have a high percentage of acidic or basic charges on them. These product quality aspects will be described and explored in detail in Chapter 6.

6. The CALR-GFP reporter host may be able to predict product titre and quality in a production study

6.1. Introduction

After the preliminary data generated in this thesis suggested that CALR-GFP expression in the CALR-GFP reporter host cell line was indicative of mAb titre during the static scale up process of cell line development (CLD) (Figure 5.11.), the next aim was to investigate if the addition of the reporter negatively impacts the clones further down the biopharmaceutical pipeline, and to see whether it could continue to predict mAb titre following CLD selection. If the expression trend was continued past CLD then the reporter could reliably be used as a selection tool for titre at the earliest stages of CLD. Production studies are typically the first stage in which product quality data can be obtained as it is only at this stage that enough material can be collected for analysis. This chapter also aimed to evaluate if the CALR-GFP reporter could be used to assess product quality at a time point much earlier than is currently possible. 'Product quality' can be used as an umbrella term for many different mAb property characteristics, and this study has focused on two of the main quality characteristics: product size and product charge. These characteristics were measured using gold-standard, High Performance Liquid Chromatography (HPLC) techniques (Section 2.11.). Whilst performing the production study and product quality analysis it was also crucial to measure the effect of the CALR-GFP reporter on the Chinese hamster ovary (CHO) host, and thus a comparison to the standard CHO host was completed alongside and the two hosts compared.

6.1.1. Production Studies

Once a panel of clones are successfully scaled up, they are traditionally transferred to an Upstream processing team where the clones are typically tested for their production capabilities in small scale bioreactors. This is used as a predictive tool to see how the clones behave at a larger manufacturing scale, and can be used to select clones with the best production characteristics (Klaubert et al., 2021; Chen et al., 2018). During a typical production study, the cells are cultured for 15 days, and are often performed in a fed-batch format where the cultures are fed nutrient rich media on specific sample days to ensure the cultures are provided with enough energy for sustained growth. On the sample days the cultures are measured for their cell growth, titre and key energy and waste metabolites (Yahia et al., 2021; Klaubert et al., 2021). In a typical experiment it takes the cells 2-3 days to adapt to their new culture conditions. An exponential growth phase then occurs as the cells undergo rapid growth,

and is followed by a stationary phase where the rate of cell growth and death is equal to each other causing a plateau in the viable cell count. Finally, as nutrients are used up and waste products increase, the culture will enter a death phase (Pan et al., 2017). Small-scale production studies are important for biopharmaceutical production as they represent a gateway model between clonal behaviours during CLD and large scale manufacture (Bareither and Pollard, 2011). Cultures are kept in very different conditions in comparison to the CLD static scale up process (Section 2.4.4.), and so the small scale production study can identify any problematic phenotypes in clones and remove them from the selected panel before spending time and consumables on large scale manufacture. Large scale bioreactors are also not feasible for the large number of clones that remain at the beginning of Upstream processing (Bareither and Pollard, 2011; Hsu et al., 2012).

Whilst titre and cell growth may be the most crucial characteristics to measure during fed-batch production studies, the metabolite profiles of the cultures are also important as they show evidence of the clones growth profiles. Glucose and glutamate are key energy sources for CHO cells (Wahrheit et al., 2014). Other metabolite factors to consider are ammonia and lactate, both of which are waste products of cell culture and can have inhibitory consequences on the CHO cell growth (Wahrheit et al., 2014). Shake flask cultures have been traditionally used to perform fed-batch production studies, and will be used in this Chapter. However, the biopharmaceutical industry is increasingly turning to high throughput and cost-effective automated systems to perform production studies on CHO clones for their mAb biotherapeutic assets. Systems such as the Ambr15 (Sartorius) are at the forefront, which miniaturises the production process, using only 15 ml of culture whilst still retaining comparable results to those of large scale production. Each Ambr15 system can run 24 cultures in parallel and samples can be easily removed from the system for cell growth, titre and metabolite analysis at any time using the automated system (Kelly et al., 2018). Janakiraman et al. (2015) showed that the Ambr15 system culturing CHO lines expressing a therapeutic protein could monitor critical culture parameters at a comparable level to an experimental 3 L bench scale bioreactor, as well as a 15,000 L manufacturing scale case study following mathematical modelling. Whilst, the Ambr15 has not been used in this study, the same sampling principle could be applied to the Ambr system to measure the fluorescence intensity of the CALR-GFP reporter, further showing the reporter's flexibility within the biopharmaceutical pipeline.

6.1.2. Product Quality Analysis: Product Size

The size of the mAb product is one of the most important product quality attributes for safety and efficacy in patients. mAb product that is greater than the size of the monomeric mAb protein is known as aggregated product, and aggregated species have shown to cause highly immunogenic reactions in models (Hermeling et al., 2004). It is crucial therefore to ensure that aggregated mAb product is not present in the final drug formulation, as this could have extremely dangerous effects on patients especially if the product has to be administered over a long-term basis (Singh, 2011). Aggregates can be formed as a result of biological causes such as the folding of the protein in the CHO clones (Ishii et al., 2014), or physical causes such as thermal stress or freeze-thawing (Hassell et al., 1991; Cromwell et al., 2006) and has been fully discussed in Section 1.2.5.

mAb product can also be smaller in size than its monomeric form, and is described as fragmented product (Wang et al., 2018). Similarly to aggregated product, fragmentation can be caused by environmental and biological factors during culture as discussed in Section 1.2.5. In one particular study, the levels of Protein Disulphide Isomerase (PDI) mRNA levels, a chaperone that catalyses disulphide bond formation prevalent in the mAb structure, negatively correlated with high fragmentation (Ishii et al., 2014), and the same relationship between PDI and fragmentation was seen in this thesis on a panel of bispecific clones (Section 3.2.).

Studies monitoring fragmentation due to CHO clonal variation are fewer overall than that of aggregation however. This may be due to difficulty in determining between the fragmented product that has formed as a result of only partial assembly during initial protein folding, or if the mAb has been fully folded but has been since degraded. For example, CHO cells can secrete the light chain in the absence of the heavy chain (Reinhart et al., 2014; Borth et al., 2005). Whilst these mAb size issues have been addressed by stringent monitoring and purification, the problem of product size is beginning to resurge in the literature as newer, more complex mAb constructs that are more prone to degradation are being developed, which ultimately results in a higher amount of aggregation and fragmentation (Gomez et al., 2020). The bispecific mAb panel in Chapter 3 highlighted this, here 60 % of the clones used had over 10 % of the total product fragmented, whilst 20 % of the clones had over > 25 % of their total product aggregated (Table 3.1.). Similarly, mispairing of the desired heavy chain and light chain can also reduce product quality. In one study, a tri-specific molecule was expressed in a panel of 38 CHO clones, and the percentage of product that contained the desired format ranged between 10-90 % of the total product across the clones (Tousi et al., 2020). These figures highlight the necessity for the development of novel tools which can be used to predict product size as early as possible, particularly as all of the clones from the bispecific mAb panel had successfully passed through CLD and a subsequent production study.

6.1.3. Product Quality Analysis: Product Charge

The variation in mAb product charge is another crucial product quality that has to be addressed when designing drugs. mAb charge can be caused by a plethora of biological processes and modifications such as deamidation, glycation and a reduction in disulphide bonds (Du et al., 2012; Perkins et al., 2000; Quan et al., 2008) as discussed in Section 1.2.5. The variation of charge may substantially affect the antibodies effectiveness as a drug target; with target binding, tissue distribution and tissue penetration all being potentially affected by variation from the main isoform. The effects of the acidic and basic isoforms depends greatly on the specific modifications and their locations (Du et al., 2012). Analysis of the specific modifications seen in the mAbs used in this study were not determined here however, thus further speculation of the product charge mechanisms cannot be inferred, although the overall amount of product lost from acidic and basic isoforms can be investigated.

6.1.4. Cell Lines Investigated In This Chapter

This Chapter describes the results of a 15 day shake flask fed-batch production study performed on a panel of 32 mAb expressing cell lines, with the aim to understand whether GFP expression continued to correlate with product titre, and whether the reporter correlated with product quality after CLD and without the reporter having a negative impact on titre and growth, and thus whether selection decisions can be made at the earliest point of CLD. 16 mAb expressing cell lines in the CALR-GFP reporter host and 16 mAb expressing cell lines in the proprietary CHO host were analysed. The clones were the same as those used in previous Chapters to be able to compare their characteristics during CLD. The CHO host clones were obtained from cell lines of Chapter 4, and the reporter host clones from Chapter 5. The clones were chosen based on their confirmed mAb expression, and to ensure that all four of the different mAb types with different 'problematic production characteristics' were considered. One exception to this was mAb 4, which failed to generate any clones with measurable titre in the CALR-GFP reporter host. This lack of recovery is predicted to be due to a failed transfection event and thus the cells did not survive selection. This is suggested as mAb 4 was successfully expressed in the CHO host and the CALR-GFP host also successfully expressed all of the other mAbs in the panel. The effect of the mAb type expressed could therefore be taken into account during analysis, and be used to confirm that any correlation seen with the CALR-GFP reporter host in the production study could be reliability reproduced regardless of whichever mAb constructs the CHO clones were expressing in the future. Following the production study, the culture media was harvested, filtered and purified to prepare the samples for product quality analysis. Size Exclusion Chromatography (SEC) and Cation Exchange Chromatography (CEX) were used for product quality analysis of the samples; mAb size and mAb charge respectively (Section 2.11.).

6.2. Results

6.2.1. Addition of the CALR-GFP reporter did not affect cell growth characteristics during the production study

The production study was first analysed for culture growth and viability. Viable cell count ($\times 10^6$ cells/ml), total cell count ($\times 10^6$ cells/ml) and viability (%) were measured over the 15 days of culture, and plotted by the host type (Figure 6.1). The viable cell counts showed that all of the cultures followed a typical cell growth curve with a lag phase until day 3 (Figure 6.1.A.), followed by an exponential growth phase, the duration of which varied across the cultures, finishing between days 6 and 8. A stationary phase was then seen until \sim day 10 before the number of viable cells began to drop during the death phase until day 15. This was reflected in the total cell count (Figure 6.1.B), with an overall increase in cell counts seen progressively before flattening at approximately day 8 as the rate of cell growth and cell death equalise in the stationary phase and then ultimately declining. These insights can again be confirmed by the viability (%) recorded (Figure 6.1.C.) as the viability does not reduce below 95 % until \sim day 8 in the majority of the cell lines.

The samples on the graphs were coloured by the mAb type they expressed. The viable and total cell count did not show any obvious patterns in either of the host types or in the mAb type expressed. To confirm this, the average viable cell count, total cell count and viability was calculated for each host type and plotted by the mAb type expressed (Figure 6.2.). The addition of the CALR-GFP reporter did also not appear to have any effect on viable cell count (Figure 6.2.A.) or total cell count (Figure 6.2.B.), and was not affected by the mAb type expressed. The viability of the cultures was also similar between the two host types in all of the mAb types expressed, with the exception of mAb 2 that showed an improved viability towards the end of the study in the CALR-GFP reporter host (Figure 6.2.C.).

By the end of the culture log phase (day 8) the average viable cell counts across all cultures for the CHO host and CALR-GFP reporter host were 27.52 and 29.32 $\times 10^6$ viable cells/ml respectively (a 6.54 % increase from the CHO host to CALR-GFP host). In fact, the percentage change at each time point between the two host types was never more than \pm 7.50 %, with the exception of day 15 where a 15.99 % change was seen, where the CHO host cultures had reduced in viability much more quickly. As the percentage change was higher in the CALR-GFP host than the CHO host at some points but lower in the others, and the standard deviation overlapped across the averages it suggests that the CALR-GFP reporter addition is neither beneficial nor detrimental to cell growth.

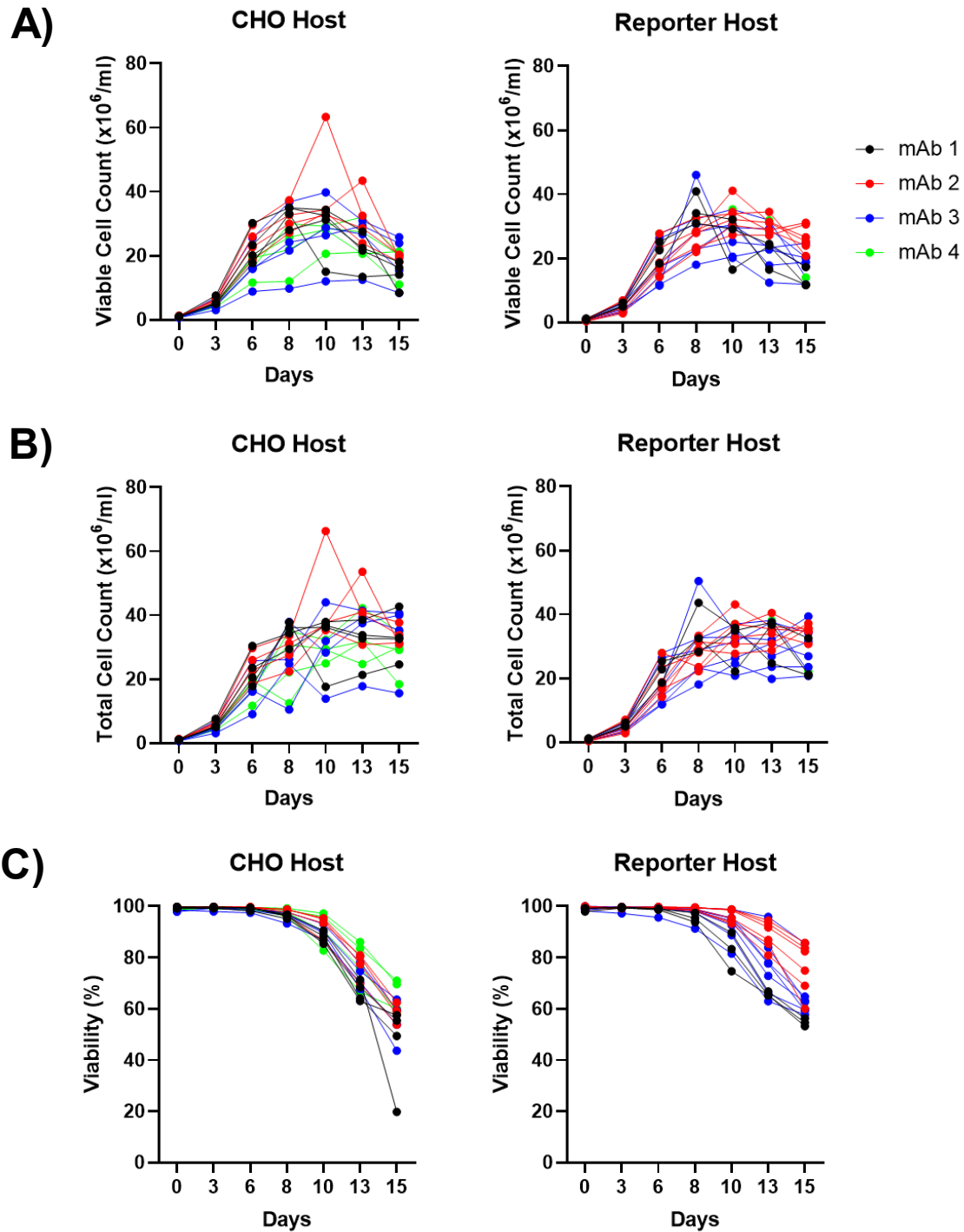


Figure 6.1. Cell growth and viability were not affected by the addition of the CALR-GFP reporter during the production study.

A) Viable cell count (cells $\times 10^6$ cells/ml) **B)** total cell count (cells $\times 10^6$ cells/ml) and **C)** viability (%) of each clone over the 15 day production study run, separated by the host type they were expressed in. mAb 1 (black), mAb 2 (red), mAb 3 (blue) and mAb 4 (green). As measured on the ViCell XR. The growth and viability of the clones did not appear to be negatively impacted by the addition of the reporter to the host. There was also no obvious trend in cell growth and viability dependent on the mAb type expressed.

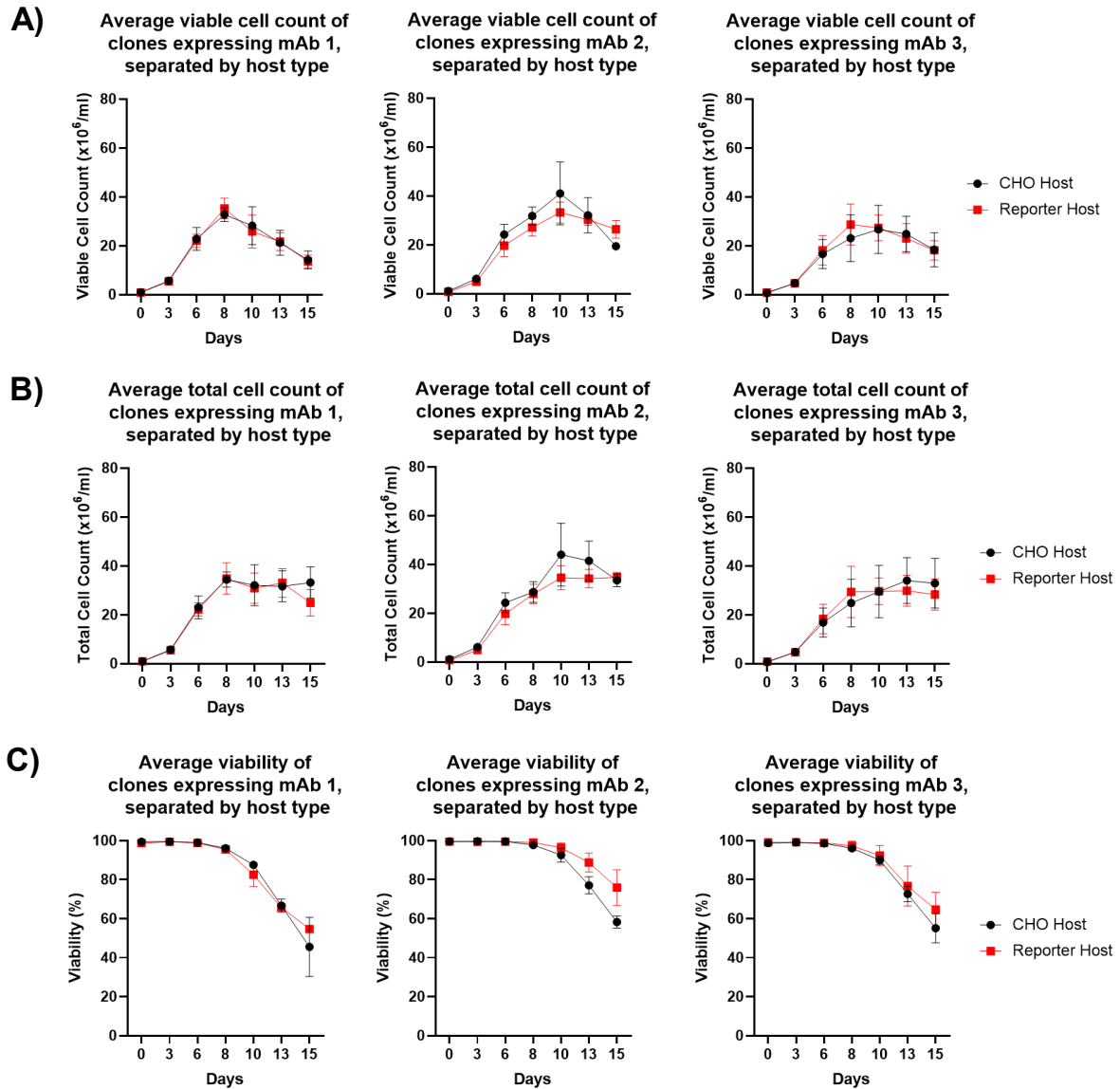


Figure 6.2. Cell growth and viability were not affected by the type of mAb expressed during the production study.

Average **A)** Viable cell count (cells $\times 10^6$ cells/ml) **B)** total cell count (cells $\times 10^6$ cells/ml) and **C)** viability (%) of clones, divided by the mAb type expressed and the type of host they are expressed in as measured on the ViCell XR. mAb 4 was omitted from this figure as there were no clones expressing mAb 4 in the reporter host. CHO host (black) and CALR-GFP reporter host (red). Error bars = \pm 1SD. The average viable cell counts and total cell counts were similar in the two hosts regardless of the mAb type expressed. The average viability of the clones was also similar in the two hosts regardless of the mAb type expressed, except from the clones expressing mAb 2 at the end of the production study (days 13-15).

6.2.2. Titre was higher on average in the CALR-GFP reporter host cell lines compared to the CHO host lines

Titre (mg/L) was measured using the CEDEX assay (Roche) on each sampling day and was found to be clearly linked to the type of mAb expressed. For example, the lowest producer was mAb 1 (black) in both host types, followed closely by mAb 3 (blue) (Figure 6.3.A). The highest producer was mAb 2 (red) for the CALR-GFP reporter host. mAb 2 was also the highest producer in the CHO host, excluding one cell line expressing mAb 4. mAb 4 (green) was only measured in the CHO host as mAb 4 did not produce any clones with measurable titre after transfection in the CALR-GFP reporter host (Section 5.2.8.). The order of titres of each mAb type expressed was maintained when normalised to the cell count to obtain specific productivity (pg/cell/day) (Figure 6.3.B.). Productivity did drop over time, most likely due to the reduction in viable cells in the culture but the overall pattern of expression does suggest that whilst the CHO clone does result in clones with varying titres, there is an inherent barrier for high titres based on the mAb structure itself and so that must always be taken into consideration when undergoing clonal selection in each mAb construct project and using the CALR-GFP reporter host as a predictor.

Importantly, the addition of the CALR-GFP reporter again did not appear to have a negative impact on titre. This was shown when the clones were separated by the mAb type they expressed, and the reporter host they were expressed in and then averaged (Figure 6.3.C. and D.). In fact, by day 15 the average titres across the clones expressing mAb 2 were higher in the CALR-GFP host (2710.28 mg/L) than in the CHO host (1802.40 mg/L). Similarly, the productivity was higher in mAb 2 expressing clones in the CALR-GFP host (9.05 pg/cell/day) than in the CHO host (5.39 pg/cell/day). As the addition of the CALR-GFP reporter increased the titre in only some of the mAb types expressed it is thought that the addition of the reporter is not necessarily beneficial to titre, any is more likely to be a random occurrence. Taking this data together with the cell growth and viability data (Figure 6.1. and 6.2.) the CALR-GFP reporter host however is at least as good at producing mAb as the CHO host, and in some instances it is actually better.

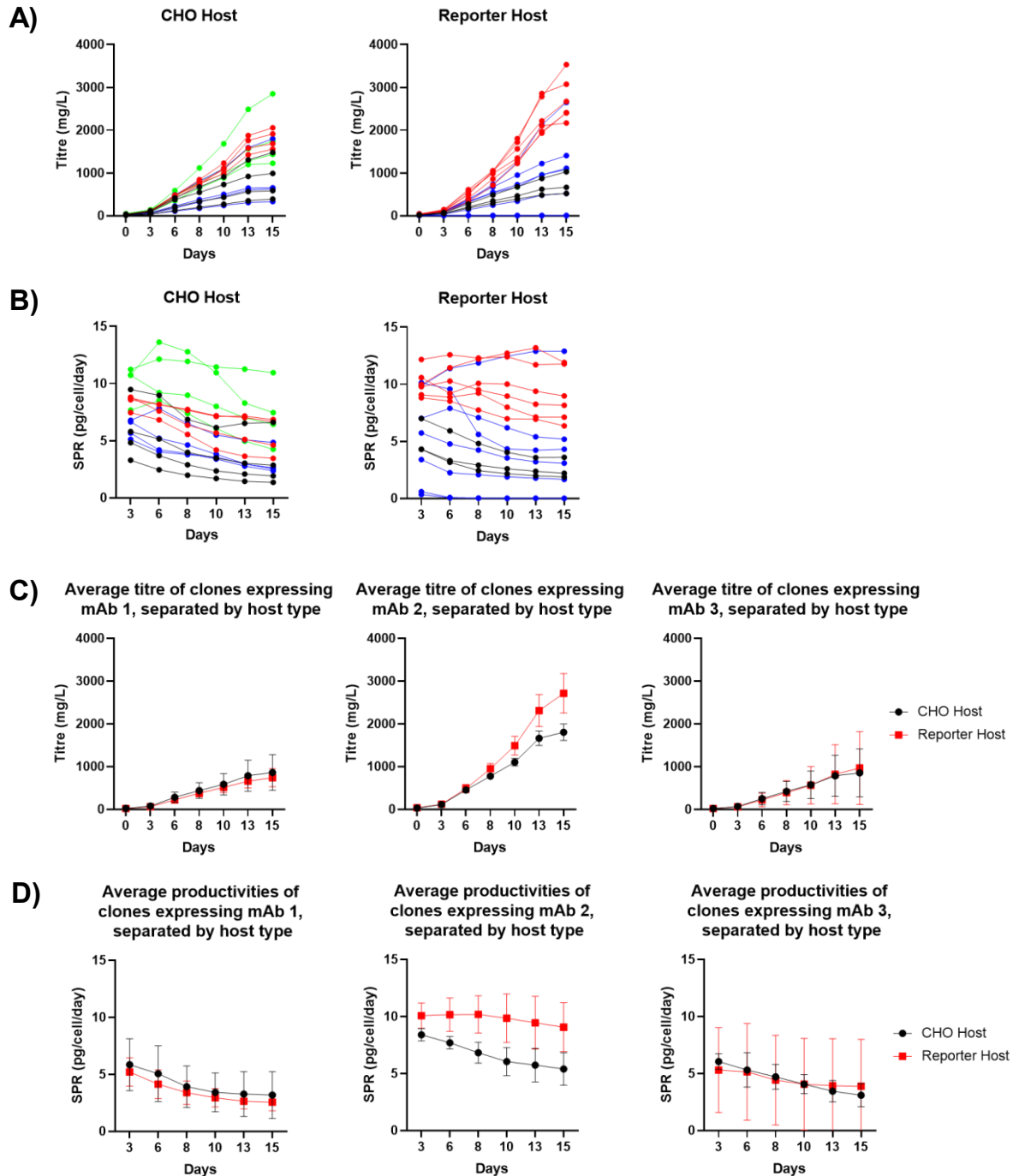


Figure 6.3. mAb titre and productivity were not affected by the addition of the CALR-GFP reporter during the production study.

A) Titre (mg/L) as measured by CEDEX (Roche) and **B)** Specific productivity (pg/cell/day), calculated from mAb titre, of each of the clones measured during the production study and split by the host type they are expressed in. Clones are coloured by the mAb construct expressed: mAb 1 (black), mAb 2 (red), mAb 3 (blue) and mAb 4 (green). **C)** Average titre (mg/L) and **D)** average productivity (pg/cell/day) of clones divided by the mAb type expressed and the type of host they are expressed in. Error bars ± 1 SD. The average titre of clones expressing mAb 1 and 3 were similar between the two host types for titre and productivity, whilst mAb 2 was more highly expressed in the CALR-GFP reporter host compared to the CHO host. As the addition of the reporter improved titres in some mAb types expressed but not in others it is thought that the effect is random, rather than the reporter presence being a beneficial attribute for titre.

6.2.3. Metabolite consumption was comparable across the hosts during fed-batch culture

A plethora of metabolites and metabolic enzymes were measured throughout the production study. Glucose, glutamate, glutamine, ammonia, lactate and lactate dehydrogenase (LDH) were all studied as a measurement of energy consumption and waste build up. None of the metabolite profiles observed over the production study were affected by the addition of the CALR-GFP reporter (Figures 6.4. and 6.5.).

Glutamate (mmol/L) interestingly dropped heavily between days 6 and 13 in half of the clones, whilst continued to increase in the other cell lines. The cultures that dropped tended to be the higher producing cell lines expressing mAb 2 (red) in the CALR-GFP reporter host (Figure 6.4.B.).

As glucose (mmol/L) was maintained by a supplementation feed it was never depleted in the cultures apart from in the highest producers of mAb 2 (red) when expressed in the CALR-GFP reporter host. Depletion of glucose in the highest producing cell lines was not surprising as mammalian cultures use both glucose and glutamine as their major energy sources (Lao and Toth, 1997; Wahrheit et al., 2014), and those cultures producing more product require more energy. Whilst the glucose can be catabolised by a complex set of metabolic pathways, the most prevalent use in CHO cells is by the process of glycolysis resulting in the waste product lactate (Hassell et al., 1991). This is exhibited by the build-up of lactate being highest in the highest producers of mAb 2 (red) (Figure 6.5.A.). LDH is also increased as a result during the culture, and did not appear to be affected by the mAb type expressed or the addition of the reporter (Figure 6.5.B.). Ammonia, another waste product similarly increased as the production study increased, however it was less clear that this was linked to titre and appeared to increase in a biphasic manner. Ammonia increased until day 6 before reducing until day 10, where it exponentially increased until the end of the production study (Figure 6.5.C.). This biphasic patterned decline of Ammonia has been shown in the literature before (Chung et al., 2003; Xing et al., 2010).

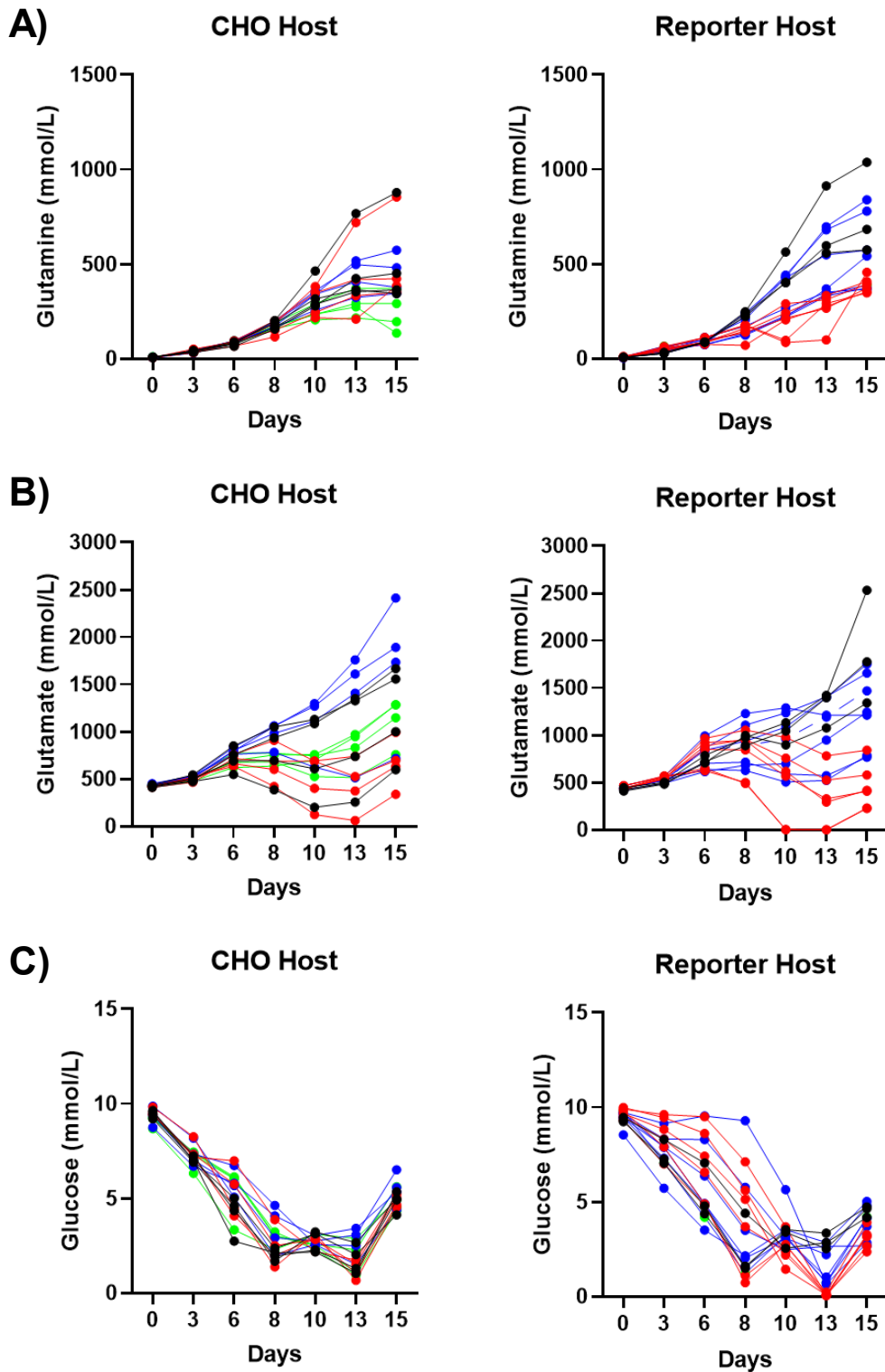


Figure 6.4. Glutamine, glutamate and glucose concentrations varied across the production study dependent on the mAb type expressed.

A) Glutamine (mmol/L) **B)** Glutamate (mmol/L) and **C)** Glucose (mmol/L). All data measured on the CEDEX (Roche). Clones are coloured by the mAb construct expressed: mAb 1 (black), mAb 2 (red), mAb 3 (blue) and mAb 4 (green).

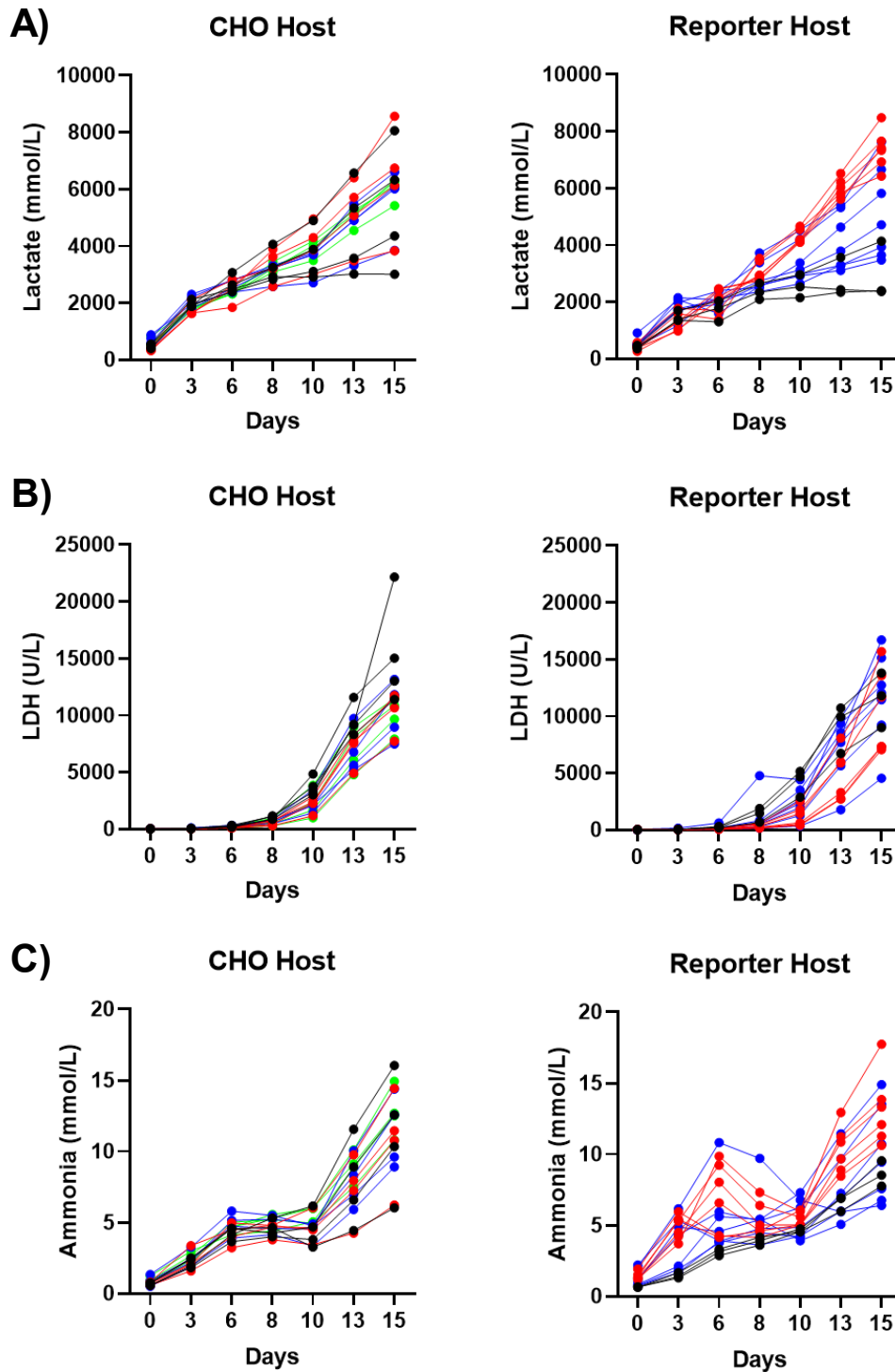


Figure 6.5. Lactate, Lactate Dehydrogenase and Ammonia concentrations varied across the production study dependent on the mAb type expressed.

A) Lactate (mmol/L), **B)** Lactate Dehydrogenase (LDH) (U/L) and **C)** Ammonia (mmol/L). All data measured on the CEDEX (Roche). Clones are coloured by the mAb construct expressed: mAb 1 (black), mAb 2 (red), mAb 3 (blue) and mAb 4 (green).

6.2.4. CALR-GFP reporter expression varied during fed-batch culture

GFP expression was monitored in the CALR-GFP reporter host cell lines during the production study by flow cytometry (Figure 6.6). The intensity of the GFP showed a similar trend across all 16 of the lines, regardless of the mAb type expressed. GFP expression initially increased between day 0 and day 3, before dropping to its lowest GFP intensity at day 8. On average the GFP intensity remained low until day 10, after which the GFP expression increased again to around the same intensity as day 0. This trend was almost the inverse pattern of the cell growth curve seen via the viable cell count (Figure 6.1.A.). The reporter expression was at its highest at the end of the lag phase (day 3), before plummeting to its lowest expression during the log and stationary phases (day 3-10). This may be related to the cell growth, as relatively little cell growth is occurring at the lag phase as the population is focusing on acclimatising to the culture and undertaking intense periods of metabolic activity (Salzman, 1959). It may also be explained by the function of CALR, which prevents incorrectly folded protein from leaving the ER by binding to terminal glucose moieties (Section 1.2.4.) (Jiang et al., 2014). When the reporter expression is low e.g. during the stationary phase, where little cell growth is occurring, the cells can focus energy consumption on protein production and thus less stress may be present in the ER. It could be argued therefore that the exogenous CALR-GFP construct may not be utilised by the ER and is degraded more quickly than in a high stress environment, where the CALR-GFP construct may be retained for longer in the ER as it binds to the unfolded protein.

Further to this, although the pattern remained the same regardless of the mAb, the intensity of the expression showed a trend with the mAb type (Figure 6.3.). The highest average titre mAb type, mAb 2 (red), had the lowest CALR-GFP expression. Whilst the two lower producers, mAb 1 (black) and mAb 3 (blue) had higher CALR-GFP expression. This general trend was similar to the correlation between CALR-GFP and titre during static scale up, where reporter intensity was negatively correlated with titre (Figure 5.11.).

This correlation was also seen during the production study at certain sample points. The CALR-GFP expression at a time point representative of each stage of the cell growth curve was plotted against the accumulated titre measured at the same time point (Figure 6.7). Despite the specific productivity remaining relatively stable throughout the experiment (Figure 6.3.B.), two methods of measuring titre were evaluated for correlation to the CALR-GFP expression. Firstly, the titre accumulated throughout the production study at each time point was measured (Figure 6.7. Left panel). The second titre measurement focused on the sole increase in titre since the previous sampling point (Figure 6.7. Right panel). Both were studied to understand whether the relationship between the reporter expression and mAb titre was consistent throughout the production study, or if the reporter expression was specific to certain phases of growth. Pearson's rank analysis was used as the data was normally

distributed, and determined that the titre was significantly negatively correlated with CALR-GFP reporter expression at 3 out of the 4 time points investigated. The strength of the correlation was also relatively unchanged between the two types of titre variables measured (i.e. accumulated titre over the production study, and the titre specifically gained between the previous sampling point), with the exception of day 15. The strongest correlation between CALR-GFP expression and titre was on day 0 of the production study ($r = -0.701$, $p < 0.003$), which as previously mentioned may be related to the cells focus on protein synthesis during the lag phase of culture. A second strong correlation was seen on day 15 between the accumulated titre and CALR-GFP expression ($r = -0.646$, $p = 0.007$).

This data again therefore suggests that the CALR-GFP reporter host can effectively monitor clonal titre during cell culture, and that it can be measured at the earliest phase of culture, meaning selection can be performed during a standard culture passage in CLD before beginning the production study, saving time and labour.

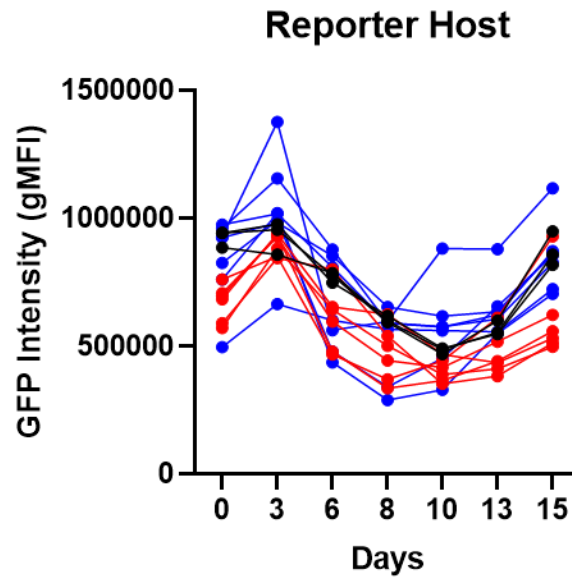


Figure 6.6. CALR-GFP reporter host fluorescence intensity (gMFI) changes over time in a similar pattern across all of the reporter clones.

GFP intensity was measured on an iQue Screener plus flow cytometer. Clones are coloured by the mAb construct expressed: mAb 1 (black), mAb 2 (red) and mAb 3 (blue).

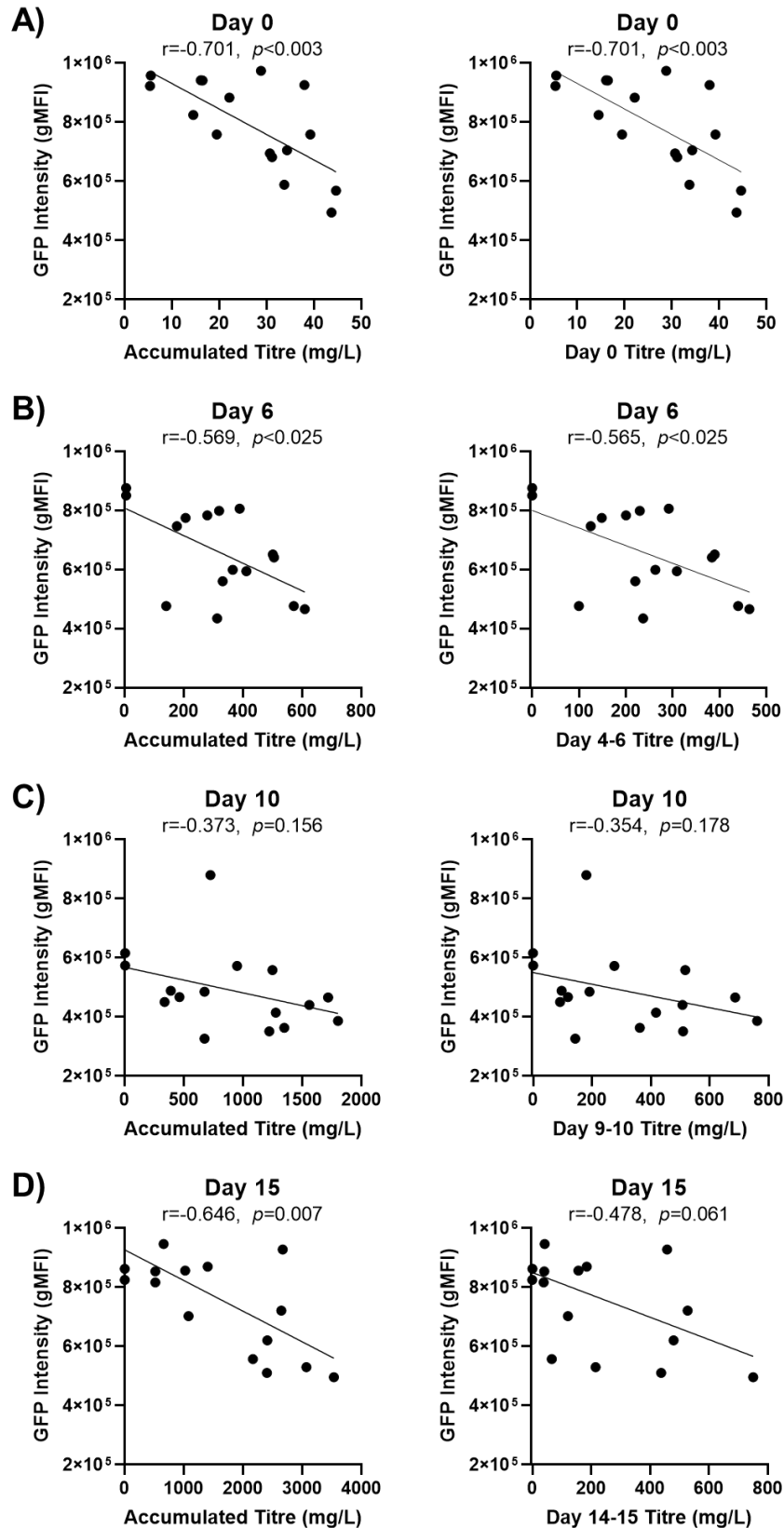


Figure 6.7. CALR-GFP reporter fluorescence intensity correlated to titre (mg/L) during the production study. Titre as measured by the CEDEX (Roche), and GFP intensity using an iQue Screener plus flow cytometer. Accumulated titre (left) and the titre increase from the previous time point (right) were both tested. Pearson r correlation was used for statistical analysis, and statistical significance was measured as $p < 0.05$. **A)** Day 0. **B)** Day 6. **C)** Day 10. **D)** Day 15.

6.2.5. Product size was not affected by the addition of the CALR-GFP reporter

Product quality was investigated by two variables: mAb product size and mAb product charge. Both of these variables have crucial effects on the mAb product as a drug target, and can result in immediate removal from the cell line selection process.

mAb product size was measured by size exclusion chromatography (SEC) and the product sizes were characterised into three categories. The first product size to elute off of the HPLC column was the aggregate (%), followed by the main peak of the monomeric protein (%) - the portion of product that contained the desired size product. The final peak contained the fragmented protein (%) consisting of mAb formats smaller than the desired size.

As expected, the mAb samples eluted over different retention times (mins) highlighting the differences in size between each mAb type (Figure 6.8). The largest product was mAb 4, followed by mAb 3, mAb 1 and finally mAb 2. As all of the mAb constructs were of the same sequence length (~ 18 bp maximum difference between the combined heavy and light chain sequences between the largest and smallest constructs) it was interesting that the peaks of each mAb product had distinct retention times. As the use of SEC was to focus on the presence of aggregates and fragments within the peaks however, the retention time of the peaks were not a concern. Interestingly, the product of one of the clones expressing mAb 3 eluted more quickly and with a slightly broader peak than the other clones. This suggested that the product was larger than expected. As further sequence and structure analysis was not performed on the product, so it could not be determined what was causing the difference. The clone producing this product was derived from the CALR-GFP host, however as the rest of the product peaks were consistent despite the type of host it was expressed in this did not suggest that the addition of the CALR-GFP reporter is affecting product quality.

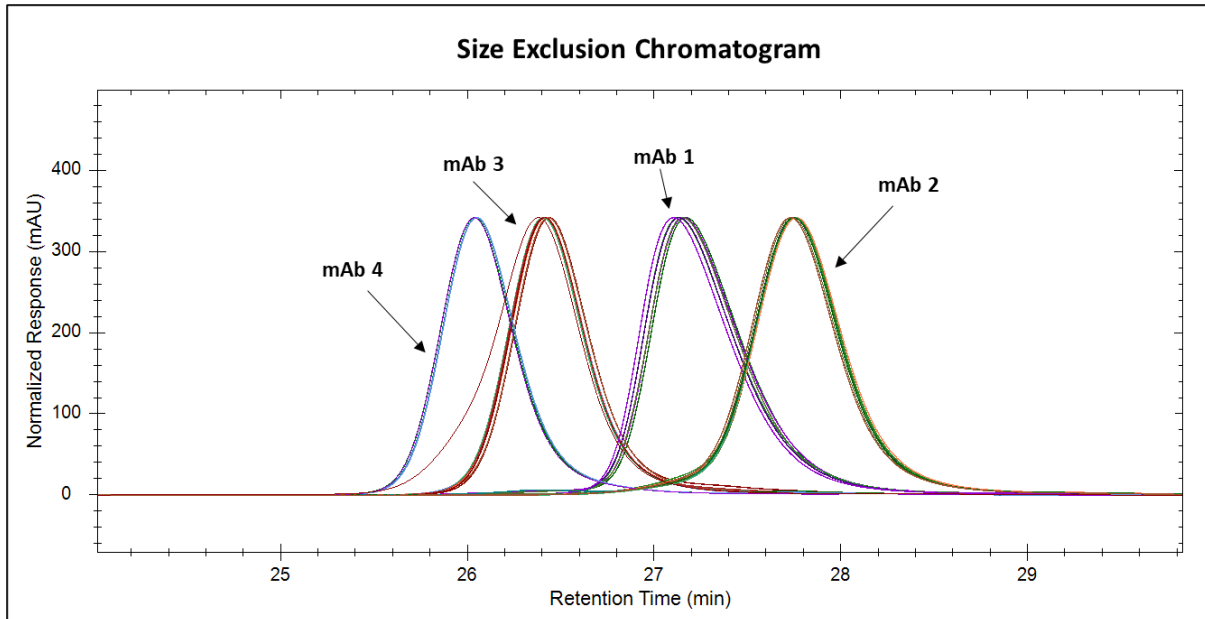


Figure 6.8. mAb product size was dependent on the mAb type expressed, and showed a largely monomeric population.

Product size was measured by Size Exclusion Chromatography on a 1260 Infinity II HPLC system (Agilent). The graph was produced by ChromView software (Version 2.4.3.). The retention time (min) shows the elution time of the samples. The responses were normalised to the highest response peak in ChromView, to highlight the shape and location of the peak in relation to retention time, rather than the concentration of the mAb.

6.2.6. Product charge was not affected by the addition of the CALR-GFP reporter

mAb product charge was measured by Cation Exchange Chromatography (CEX). Briefly, purified mAb samples are passed through a column coated with a negatively charged ion exchange resin. Molecules with a net negative surface charge are repelled by the resin charge and pass through the column quickly, whilst positive surface charge are attracted to the resin and pass through the column more slowly. The elution times of the proteins can then be used to calculate the percentage of the product with more negatively charged (acidic species) and more positively charged (basic species) than the main neutral isoform of the mAb (Jungbauer and Hahn, 2009; Ng et al., 2009).

The product charge could be isolated into three categories. The most prevalent peak is the main isoform and elutes between the charged variants. Acidic isoforms then elute before the main isoform, whilst the basic isoforms elute afterwards (Figure 6.9.). mAbs 2 and 3 eluted first and with similar charge profiles, followed by mAb 4 and mAb 1. Importantly, none of the mAb profiles varied between the CHO and CALR-GFP host, showing that the CALR-GFP reporter was not negatively impacting product charge. As the peaks had the exact same shape and retention time dependent on the mAb type expressed it was clear that the charge was greatly affected by the mAb expressed itself. This was not surprising; however it does highlight the importance of considering different mAb types when designing a reporter system for monitoring mAb production that will be reused over many projects.

As mAb 1 and 2 expressed the same target it was surprising that their resulting CEX profiles were so different from each other. However upon further investigation of the DNA sequences of the heavy and light chains the two mAbs only had 74.59 % and 61.16 % sequence homology between the heavy and light chains respectively. This suggests that the sequence differences can have a great impact on the charge of the product, much greater than any clonal variation caused by the CHO system itself. Instead, mAbs 2 and 3 had extremely similar profiles despite expressing different targets. It is hypothesised that these similarities in profiles are due to specific mutations put upon the mAb sequences during their design prior to CHO expression. mAbs 2 and 3 actually had a very similar sequence homology as to mAbs 1 and 2, despite targeting different targets (mAb 2 and 3 homology was 75.81 and 61.58 % for the heavy and light chain respectively).

Whilst it appeared that the profile shape was not affected by the clonal variation, but affected by the inherent mAb structure, this did not mean that the reporter could not be used to predict product charge, as the profiles that were present in the product may be influential on reporter expression. Therefore, once the charge and size of the mAb products had been identified the product quality could be quantified and used to see whether the expression of CALR-GFP could be predictive of product quality during the shake flask production study.

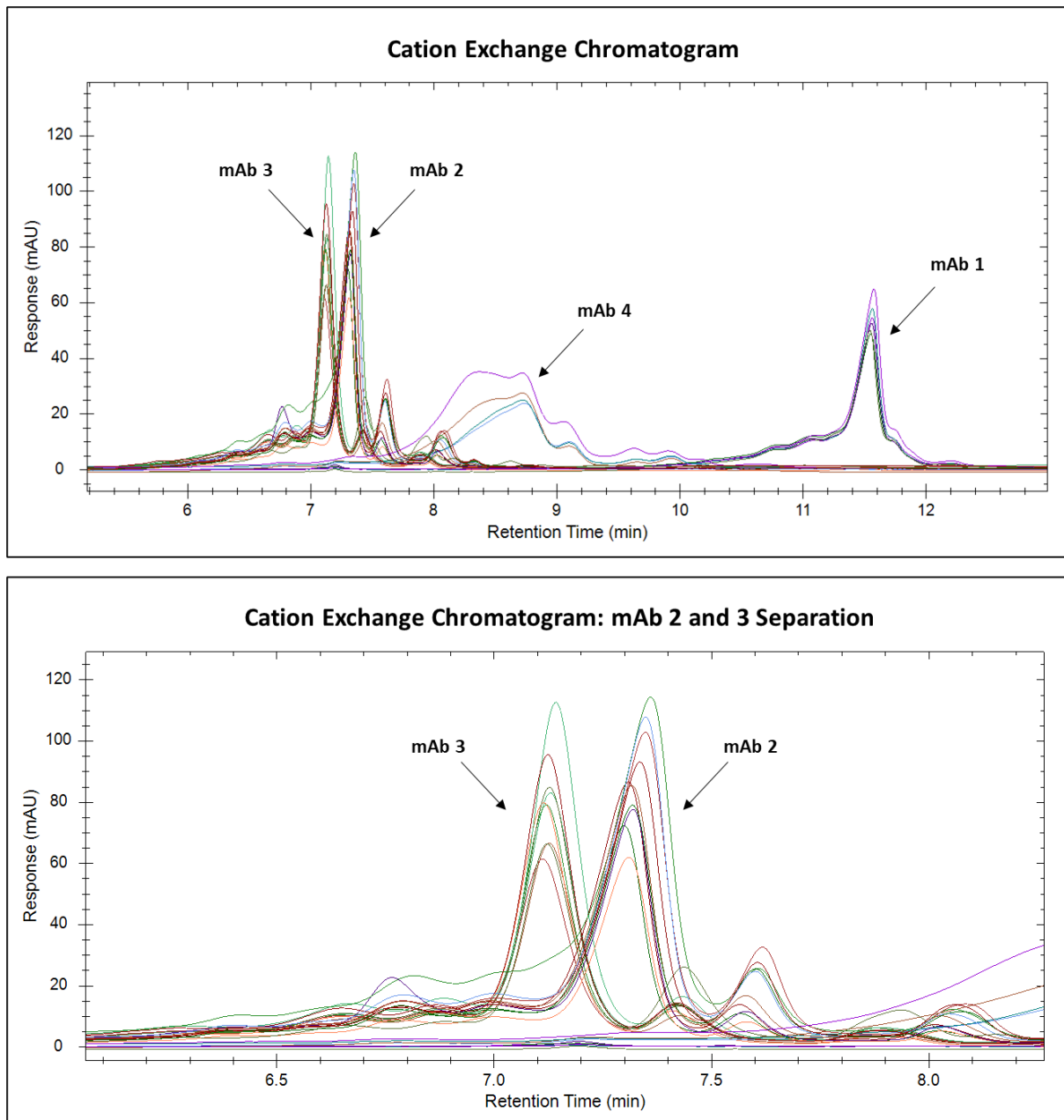


Figure 6.9. mAb charge variants were diverse and peaks depended on the mAb type expressed.

Product charge was measured by cation exchange chromatography (CEX) on a 1260 Infinity II HPLC system (Agilent). The graphs were produced by ChromView software (Version 2.4.3.). **A)** The profiles of all 29 measured samples. Retention time (min) and peak shape was dependent on the mAb type expressed as annotated. **B)** The same populations scaled to mAb 2 and 3 to highlight their similarities.

6.2.7. Product size was affected by the mAb expressed but not by the addition of the CALR-GFP reporter

Quantification of the SEC peaks were performed as per Section 2.11.4. The results of the quantification are shown in Table 6.1. Product quality criteria's in this thesis are set as requiring > 90 % monomer, < 2 % fragment and < 3 % aggregate. Clones featuring these undesirable characteristics would typically be removed from selection, and have been highlighted in red. SEC quantification confirmed that the addition of the CALR-GFP reporter in the CHO host did not result in an increased concentration of aggregated or fragmented protein in any of the mAb types. The average aggregate (%) and fragment (%) for the two hosts were plotted against each other, separated by mAb type and an un-paired student's t test showed no significant difference between the hosts in all scenarios (Figure 6.10.A. and B, $p < 0.05$). All of the clones contained acceptable aggregation percentages (< 3 %), which was interesting as mAb 1 had been chosen for the panel as it had shown aggregation tendencies during mAb design and development stage (Table 2.2.). Average aggregate % within the panel was calculated by mAb type (Figure 6.10.C.). The mAb type with the highest aggregate % in the product was mAb 3 (mean aggregate = 1.34 %, 1 SD = 0.43 %) that had showed an overall poor developability profile and propensity to oxidise during the mAb design, prior to this thesis. mAb 1 then showed the second highest average aggregate % from the clones (mean aggregate = 0.77 %, 1 SD = 0.91 %), although as highlighted with the SD value the variation across the clones was greater in mAb 1 than mAb 3 clones.

Conversely, 8 of the mAb products in the panel had a fragmented percentage higher than the 2 % cut off point. These products were derived from the CHO host and the CALR-GFP host, showing that the addition of the CALR-GFP reporter was not the cause of this fragmentation. Average fragment percentage was calculated by mAb type (Figure 6.10.C.) and was most prevalent in mAb 3, the clone with poor developability. The increases in aggregate and fragment (%) in the mAb 3 clones resulted in a significantly reduced average monomer percentage in comparison to the other 3 mAbs. The difference in product size dependent on the mAb type expressed was measured statistically (Figure 6.10.C.). One-way ANOVA analysis was performed on each product size parameter to compare whether the variance seen by the mAb type expressed was significant. The variance between the mAb types were significant across all of the product sizes (Aggregate $F = 3.542$, $p = 0.029$, Fragment $F = 11.54$, $p = 0.0001$ and Monomer $F = 13.01$, $p = 0.0001$). A post-hoc Tukey test was then performed to confirm whether significant variances could be seen between two specific groups, and are highlighted on the graphs. Despite this, none of the clones monomer percentage fell below the 90 % total objective and would not be removed from the clone selection based on monomer alone. This final size quality analysis was interesting as the mAbs had been chosen specifically for this thesis to show poor mAb quality, however this does not appear to have translated into the CHO cell system.

mAb	Host Type	Aggregate (%)	Monomer (%)	Fragment (%)
1	CHO	1.00	97.86	1.14
1	CHO	1.11	97.84	1.05
1	CHO	0.00	99.05	0.95
1	CALR-GFP	0.00	99.08	0.92
1	CALR-GFP	2.51	96.19	1.30
1	CALR-GFP	0.00	98.98	1.02
2	CHO	0.48	98.18	1.35
2	CHO	1.09	97.55	1.37
2	CHO	0.17	98.46	1.37
2	CHO	0.26	98.28	1.46
2	CALR-GFP	1.93	96.61	1.46
2	CALR-GFP	0.13	98.20	1.67
2	CALR-GFP	0.13	98.51	1.36
2	CALR-GFP	0.13	98.28	1.59
2	CALR-GFP	0.24	98.39	1.37
2	CALR-GFP	0.11	98.51	1.39
3	CHO	0.36	96.91	2.73
3	CHO	1.21	93.67	5.12
3	CHO	1.48	95.82	2.71
3	CHO	1.38	97.13	1.49
3	CALR-GFP	1.13	96.14	2.73
3	CALR-GFP	1.92	95.10	2.98
3	CALR-GFP	1.79	95.19	3.02
3	CALR-GFP	1.55	96.94	1.51
3	CALR-GFP	1.24	95.96	2.80
4	CHO	0.68	98.54	0.78
4	CHO	0.42	97.56	2.02
4	CHO	0.38	98.04	1.59
4	CHO	0.38	97.98	1.64

Table 6.1. Summary of the quantification of product size quality analysis in the clone panel.

Table shows the mAb type expressed, and which host cell line the clone was derived from. Fragment, aggregate and monomer (%) was measure by size exclusion chromatography (SEC). SEC was performed on a 1260 Infinity II HPLC system (Agilent). Cell lines were highlighted in red if the product size out with the selection criteria limits at GSK. GlaxoSmithKline typically denotes poor quality as < 90 % monomer, > 3% aggregate or > 2 % fragment.

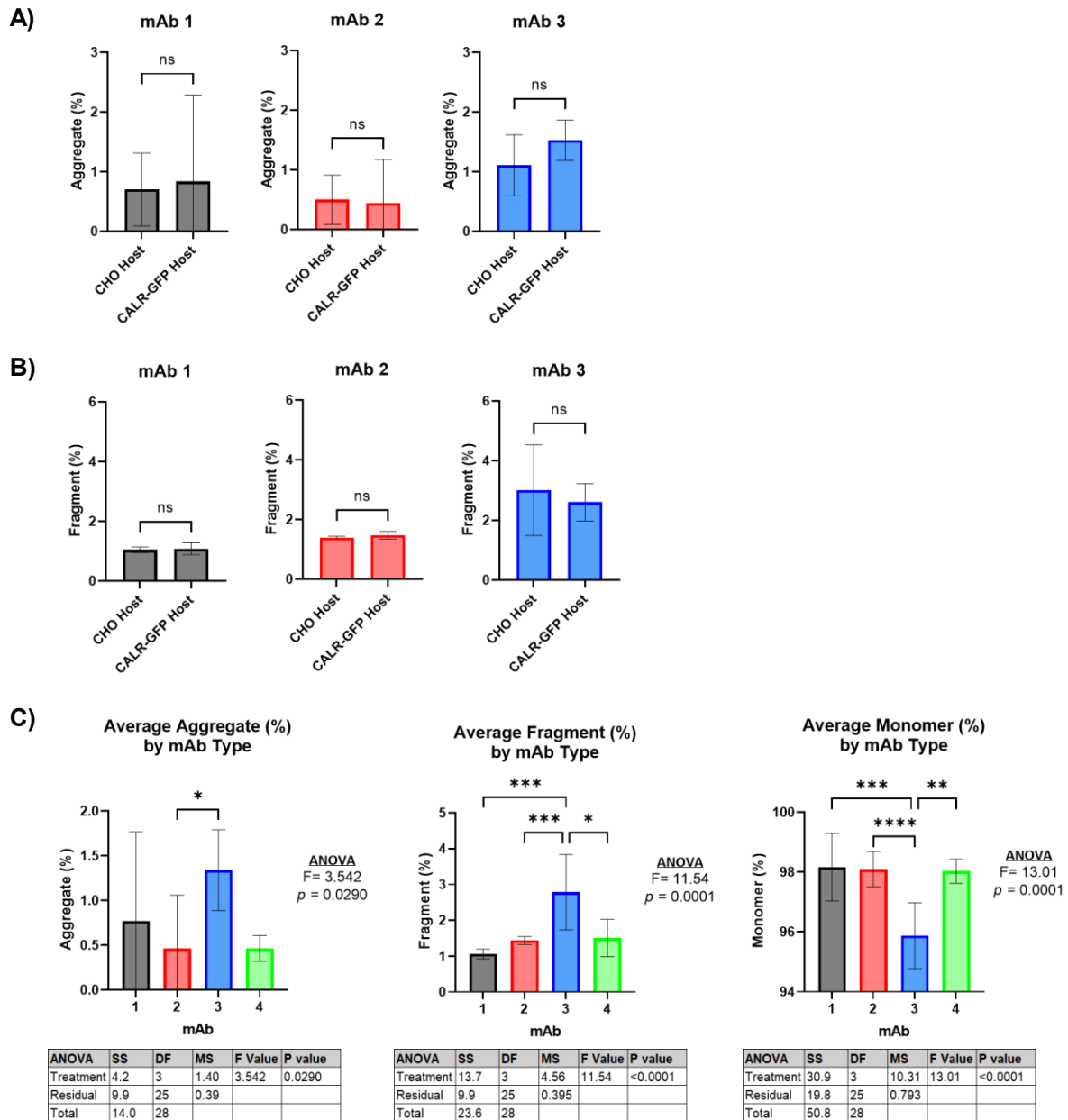


Figure 6.10. The CALR-GFP reporter did not affect the average product size in any of the mAbs when compared to the CHO host.

Measured by SEC, using a 1260 Infinity II HPLC system (Agilent). **A)** Average aggregate (%) and **B)** average fragments (%) in the CHO host and CALR-GFP host clones, split by mAb type expressed. mAb 4 could not be included as there were no CALR-GFP clones expressing mAb 4. Un-paired student's t test showed no significant difference in quality between the two hosts. **C)** Average aggregate (%), fragment (%) and monomer (%) in all clones, grouped by mAb type. A One-way ANOVA analysis showed the averages of each product characteristic was significant across the mAb types. A post-hoc Tukey test showed the averages that were significant between two specific mAb groups, and significant differences have been highlighted on the graphs. Significance set at ns=non-significant, * = <0.05, ** = <0.01, *** = <0.001 and **** = <0.0001. Error bars = +/- 1SD. mAb 1 (black, N=6), mAb 2 (red, N=10), mAb 3 (blue, N=9) and mAb 4 (green, N=4).

6.2.8. Product charge was varied between the clones expressing different mAb types

The quantification of the product charge analysis was measured between the host types in the same manner as the product size. Product charge quantification can also be seen in Table 6.2. As the charge profiles of mAb constructs are much less rigid than the size profiles, it is difficult to resolve specific acceptance criteria across different projects. A general principle for clone selection here is that at least 50 % of the product is within the main isoform peak as any variations of charge can affect the mAbs effectiveness as a drug target (Du et al., 2012).

The average percentage of acidic and basic isoforms, across the two host types, were plotted against each other, separated by mAb type (Figure 6.11.A and B.). An un-paired student's t test showed there to be no significant difference in the quality between the two host cell lines in the majority of the mAbs expressed. Two exceptions to this were seen. The CALR-GFP reporter host had a significantly higher acidic isoform (%) in clones expressing mAb 1 and had a higher basic isoform (%) in clones expressing mAb 2 ($p < 0.05$ in both). It is unknown as to why these significant results were seen, however for mAb 1 only three clones were analysed, and resulted in less than a 10 % difference in acidic isoforms. The change in mAb 2 basic isoform (%) was much greater in the CALR-GFP host than the CHO host however and further study would be required to understand whether this was due to the small sample size or if this is a biological response to the CALR-GFP host.

8 of the 29 mAb products had less than 50 % of their product falling within the main isoform peak and of those, 4 were close to the 50 % cut off point (> 47 %). The remaining 4 mAb products had a very low percentage of main isoform product at less than 30 %, and were all expressing the mAb 4 construct by the CHO host. As all 4 samples expressing mAb 4 had a low percentage of main isoform, and a high percentage of acidic isoform species it does suggest that this result is caused by the mAb structure itself. The difference in product charge was measured statistically (Figure 6.11.C.). One-way ANOVA analysis was performed on each product charge to compare whether the variance seen by the mAb type expressed was significant. The variance between the mAb types were significant across the acidic ($F= 34.22, p = 0.0001$) and main isoform groups ($F=84.14, p = 0.0001$), but not across the basic isoforms ($F=1.561, p = 0.224$). A post-hoc Tukey test was then performed to confirm whether significant variances could be seen between two specific groups. The majority of the acidic isoforms and main isoform mAb types were significant to each other, as highlighted on the graphs.

mAb	Host Type	Total Acidic Isoform (%)	Total Main Isoform (%)	Total Basic Isoform (%)
1	CHO	34.53	53.41	12.06
1	CHO	34.76	51.99	13.25
1	CHO	32.95	52.40	14.66
1	CALR-GFP	38.20	48.39	13.41
1	CALR-GFP	41.31	47.29	11.40
1	CALR-GFP	37.81	50.58	11.61
2	CHO	32.82	56.33	10.85
2	CHO	30.24	58.54	11.23
2	CHO	39.11	50.32	10.57
2	CHO	28.23	61.36	10.41
2	CALR-GFP	28.17	54.86	16.97
2	CALR-GFP	31.70	53.68	14.62
2	CALR-GFP	24.31	50.87	24.83
2	CALR-GFP	29.62	54.30	16.09
2	CALR-GFP	23.84	53.00	23.15
2	CALR-GFP	22.96	53.89	23.16
3	CHO	28.16	58.63	13.21
3	CHO	29.90	57.16	12.95
3	CHO	27.57	57.98	14.45
3	CHO	29.42	58.24	12.34
3	CALR-GFP	30.68	56.88	12.44
3	CALR-GFP	28.04	57.21	14.75
3	CALR-GFP	32.16	49.97	17.87
3	CALR-GFP	15.55	48.60	35.85
3	CALR-GFP	27.19	57.84	14.97
4	CHO	56.61	22.57	20.82
4	CHO	58.41	24.77	16.82
4	CHO	49.64	29.47	20.90
4	CHO	48.48	28.53	22.99

Table 6.2. Summary of the quantification of product charge quality analysis in the clone panel.

Table shows the mAb type expressed, and which host cell line the clone was derived from. Total acidic, basic and main isoform (%) was measured by cation exchange chromatography (CEX). CEX was performed on a 1260 Infinity II HPLC system (Agilent). Cell lines were highlighted in red if the product size out with the selection criteria limits at GSK. As product charge is often variable on the mAb type expressed it is less easy to designate strict cut-off points for the amount of acidic and basic isoforms. Instead a main isoform of >50 % is deemed ideal.

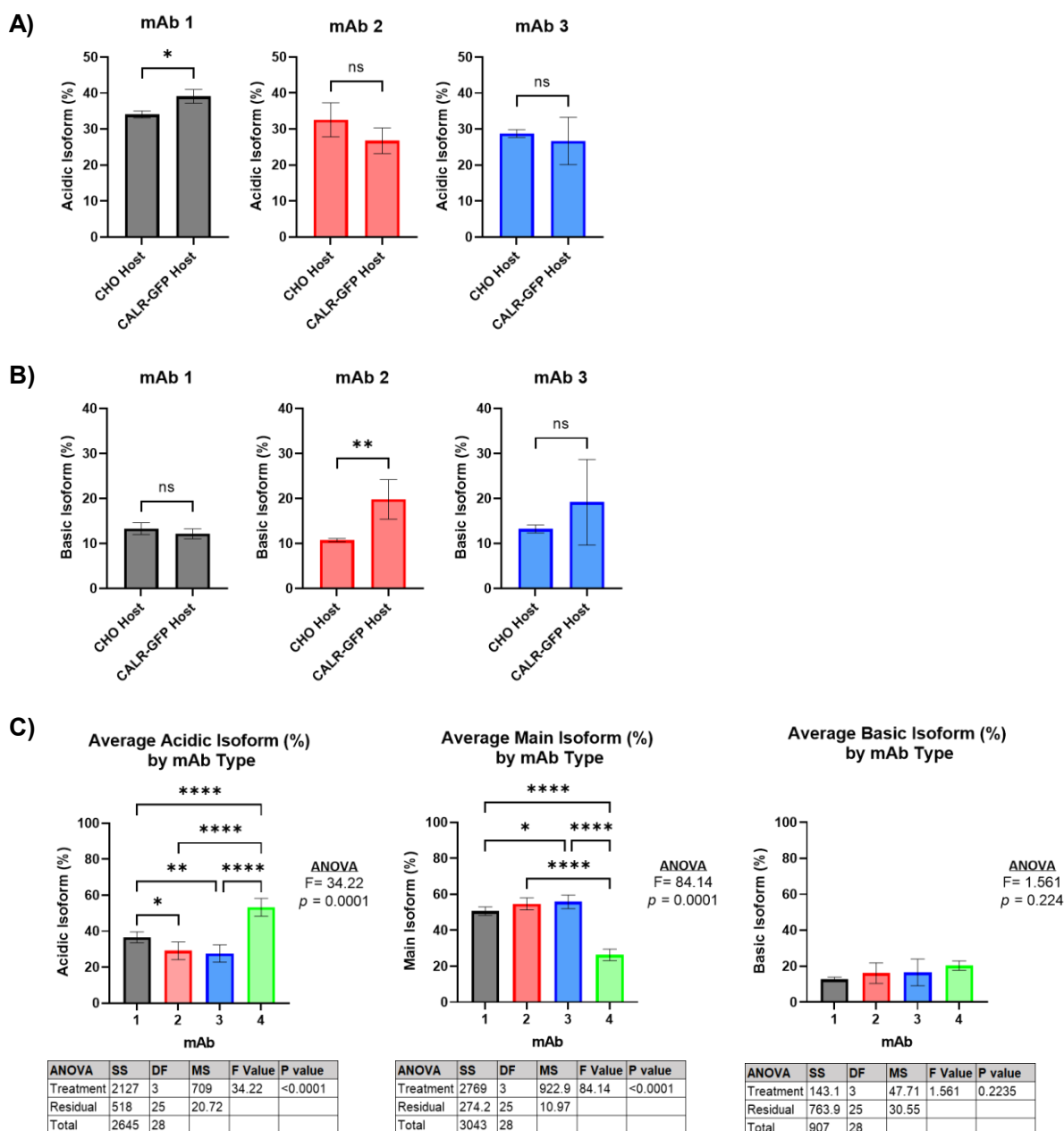


Figure 6.11. CALR-GFP reporter addition increased product charge variants in some mAb types.

Measured by CEX, using a 1260 Infinity II HPLC system (Agilent). **A)** Average acidic isoform (%) and **B)** average basic isoform (%) in the CHO host and CALR-GFP host clones, split by mAb type expressed. mAb 4 could not be included as there were no CALR-GFP clones expressing mAb 4. Un-paired student's t test showed a significant increase in acidic isoforms in the CALR-GFP host expressing mAb 1, and in basic isoforms in mAb 2, compared to the CHO host. **C)** Average acidic isoform (%), main isoform (%) and basic isoform (%) in all clones, grouped by mAb type. A One-way ANOVA analysis showed the acidic and main isoform averages were significant across the mAb types. A post-hoc Tukey test showed significant differences within the mAb types, and significant differences have been highlighted on the graphs. Significance set at ns=non-significant, * = <0.05, ** = <0.01, *** = <0.001 and **** = <0.0001. Error bars = ± 1SD. mAb 1 (black, N=6), mAb 2 (red, N=10), mAb 3 (blue, N=9) and mAb 4 (green, N=4).

6.2.9. CALR-GFP intensity showed predictive capabilities towards product quality during the production study

After it was confirmed that the addition of the CALR-GFP reporter did not cause obvious product quality issues, the reporter was tested for its ability to predict product quality. Initial investigation employed a correlation matrix using JMP software (version 15.2.0) between the GFP intensity at each time point during the production study run against the resulting product quality quantification (Figure 6.12.A.). As GFP was only measured in the CALR-GFP reporter host clones the CHO host samples could not be included in this analysis. The GFP intensity showed correlations to a variety of product quality attributes at different stages, of which seven were statistically significant ($p < 0.05$). Three of these correlations related to product charge, and the other four to product size.

The CALR-GFP intensity measured on day 3 could significantly predict for fragment percentage ($r = 0.645$, $p = 0.0128$) and monomer percentage ($r = -0.556$, $p = 0.0390$) (Figure 6.12.B. and 6.12.C.). Both correlations were moderate, with increasing GFP expression resulting in more fragmented and less monomeric product. The link between the two was expected as their relationship is inverse to each other, however it was interesting to see that the correlations with CALR-GFP and fragment was only seen on day 3 of the production study. The fragment percentage relationship was the inverse of what was seen in Chapter 3 when monitoring similar protein folding markers such as Protein Disulphide Isomerase (PDI) using digital droplet PCR (ddPCR) (Figure 3.6.). This could be due to the increased availability of the exogenous CALR being utilised by the clones that have less endogenous CALR. The correlation with GFP and both fragment and monomer percentage was again seen again on day 13 at a similar strength ($r = 0.606$, $p = 0.022$ and $r = -0.603$, $p = 0.0225$ respectively).

The CALR-GFP intensity was also correlated to the percentage of acidic and basic isoforms (Figure 6.12.D.), particularly at day 0 of the production study. These relationships were converse with each other as expected, with a strong positive correlation between CALR-GFP and acidic isoform percentages ($r = 0.821$, $p = 0.0003$) and a strong negative correlation with basic isoform percentages ($r = -0.805$, $p = 0.0005$). A final significant correlation was seen with the CALR-GFP intensity at day 8 and the final monomer (%) ($r = -0.708$, $p = 0.0046$).

The correlation matrix suggested therefore there are links between CALR-GFP expression and product quality, and gave credible evidence to the use of the reporter for predicting product quality. These correlations were looking at the linear relationship between two single variables however rather than considering how all of the variables measured during the production study over time may interact with each other to cause the specific product quality phenotypes. To take all of these factors into consideration predictive modelling was also explored.

A)

	Acidic Isoform (%)	Main Isoform (%)	Basic Isoform (%)	Aggregate (%)	Monomer (%)	Fragment (%)	Day 0 GFP Intensity	Day 3 GFP Intensity	Day 6 GFP Intensity	Day 8 GFP Intensity	Day 10 GFP Intensity	Day 13 GFP Intensity	Day 15 GFP Intensity
Acidic Isoform (%)	1.0	-0.273	-0.871	0.060	0.027	-0.124	0.821	0.407	0.216	0.124	0.120	0.318	0.516
Main Isoform (%)	-0.273	1.0	-0.235	-0.005	-0.302	0.582	-0.049	0.107	-0.407	-0.708	-0.396	-0.066	-0.179
Basic Isoform (%)	-0.871	-0.235	1.0	-0.058	0.128	-0.172	-0.805	-0.466	-0.011	0.236	0.081	-0.288	-0.429
Aggregate (%)	0.060	-0.005	-0.058	1.0	-0.888	0.483	0.301	0.343	-0.022	0.122	0.432	0.448	0.303
Monomer (%)	0.027	-0.302	0.128	-0.888	1.0	-0.831	-0.355	-0.556	0.227	0.094	-0.488	-0.603	-0.393
Fragment (%)	-0.124	0.582	-0.172	0.483	-0.831	1.0	0.312	0.645	-0.406	-0.326	0.407	0.606	0.381
Day 0 GFP Intensity	0.821	-0.049	-0.805	0.301	-0.355	0.312	1.0	0.624	0.261	0.231	0.424	0.626	0.755
Day 3 GFP Intensity	0.407	0.107	-0.466	0.343	-0.556	0.645	0.624	1.0	-0.144	0.050	0.614	0.687	0.522
Day 6 GFP Intensity	0.216	-0.407	-0.011	-0.022	0.227	-0.406	0.261	-0.144	1.0	0.819	0.100	-0.199	-0.001
Day 8 GFP Intensity	0.124	-0.708	0.236	0.122	0.094	-0.326	0.231	0.050	0.819	1.0	0.514	0.085	0.177
Day 10 GFP Intensity	0.120	-0.396	0.081	0.432	-0.488	0.407	0.424	0.614	0.100	0.514	1.0	0.824	0.707
Day 13 GFP Intensity	0.318	-0.066	-0.288	0.448	-0.603	0.606	0.626	0.687	-0.199	0.085	0.824	1.0	0.923
Day 15 GFP Intensity	0.516	-0.179	-0.429	0.303	-0.393	0.381	0.755	0.522	-0.001	0.177	0.707	0.923	1.0

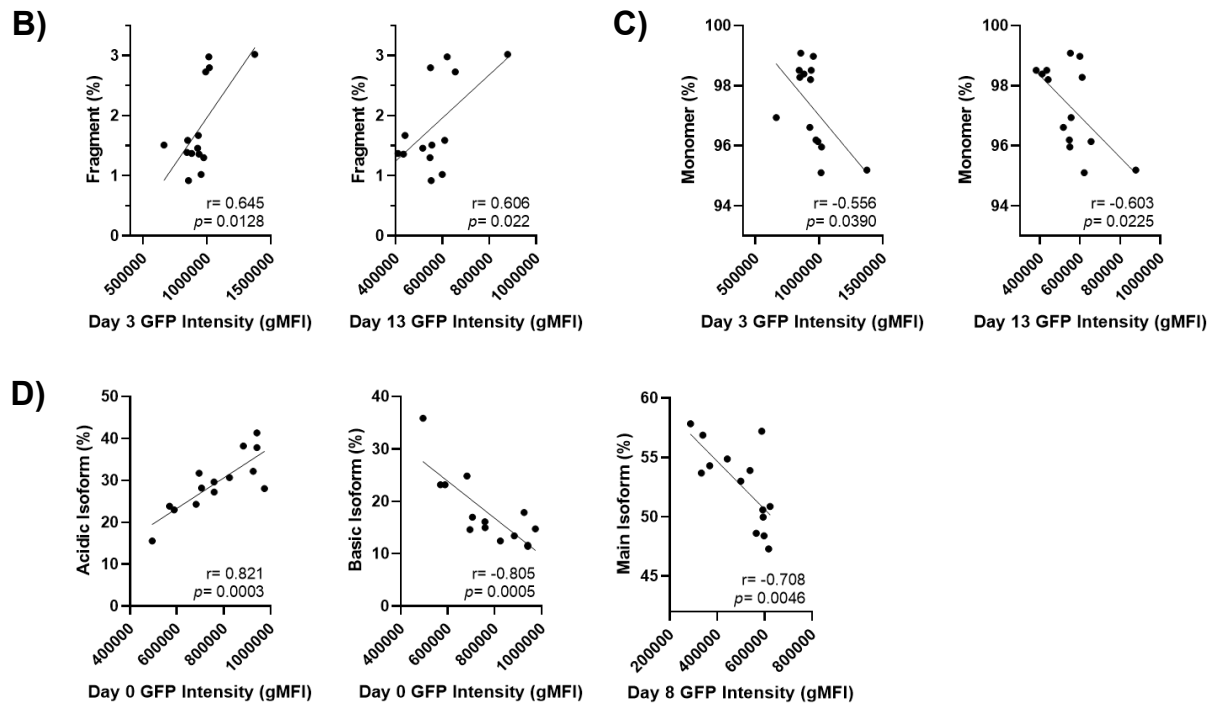


Figure 6.12. CALR-GFP intensity correlated to product quality phenotypes at different stages of the production study.

A) Correlation matrix for CALR-GFP intensity at each sample point for each clone with the resulting product quality analysis performed by SEC and CEX (performed in JMP software version 15.2.0) and transferred to excel (software version 2108) for colour scaling. Relationships were coloured on a scale by the strength of the correlation. A perfect correlation of +1 was highlighted in green, no correlation of 0 in yellow and a perfect negative correlation of -1 in red. Statistically significant relationships ($p < 0.05$) are shown in bold and underlined. **B)** Scatterplots of the statistically significant correlation between CALR-GFP intensity and fragment (%). **C)** Scatterplots of the statistically significant correlation between CALR-GFP intensity and monomer (%). **D)** Scatterplots of the statistically significant correlation between CALR-GFP intensity and product charge.

6.2.10. Modelling of the CALR-GFP reporter expression cannot predict all product quality measurements at the current sample size

Whilst the correlation between CALR-GFP and different aspects of product quality did appear to be strong at particular time points during the production study, the robustness of using the GFP data against one single variable is potentially questionable. For example, the correlation plots at day 0 showed the GFP intensity was strongly negatively correlated to titre and basic isoform species, whilst being strongly positively correlated to acidic isoform species. Then it wasn't until day 8 that the GFP intensity became negatively correlated to the main isoform species. These individual time point correlations make it incredibly difficult to make a reliable prediction of product quality overall.

Instead, a Partial Least Squares (PLS) regression model was employed to the 14 CALR-GFP reporter cell lines to see if the expression of the reporter throughout the culture could be predictive of the resulting mAb product quality. The GFP intensities of each individual clone, at each time point were modelled using the PLS model in Prism software against the 6 product quality percentages (Aggregate, Fragment, Monomer, Acidic Isoform, Basic Isoform and Main Isoform). The resulting model could predict 90.1 % of the variation in the measured variables during the production study and 54.8 % of the variation in the resulting product quality (3 factor model, $Q^2 = -0.45$, $R^2Y = 0.56$ and $R^2X = 0.92$). The negative Q^2 value suggested that the GFP intensities alone were not capable of predicting the resulting product quality and could not predict the product quality of unknown samples if the model was to be run on them. This was unsurprising due to the small sample size of CALR-GFP positive production study (N=14), and the dramatic changes in correlation of the product quality attributes with the CALR-GFP intensity over time. Hence, further study with a larger sample size would be required to truly confirm whether a model could be fitted to the GFP intensity.

6.3. Discussion

The CALR-GFP reporter host cell line had previously been transfected with a panel of mAb constructs with various product quality issues to generate clonal cell lines (Section 5.). The clonal lines were then be used to determine whether the addition of the reporter could monitor mAb product quantity (titre) and product quality during a typical CLD project process. The CALR-GFP reporter host had showed that there was a moderately significant correlation with mAb titre during static scale up of the clones (Section 5.11.). Whilst this was an interesting result, methods for monitoring mAb titre in clones during CLD are already readily available using equipment such as the Octet HTX. These techniques often use protein A binding and are highly accurate at measuring titre, and are reliably used to remove low producing clones (Huhn et al., 2021; Tejwani et al., 2021). To gain a further predictive aspect of clones in CLD, qualities that cannot currently be measured at such an early recovery stage is necessary. Product quality is one of these aspects and to this end this chapter has investigated whether the CALR-GFP reporter host negatively impacts product quality of the mAbs it expressed, and to see if it can be used to predict product quality. As product quality analysis currently requires 1-2 mg/ml of purified product for HPLC analysis, gained from a 15 day production study, the ability to predict product quality at a much earlier stage would be invaluable to CLD. To test the predictability of product quality, 16 of the scaled up CALR-GFP reporter host clones were put into a shake flask production study, measuring for GFP expression throughout. A further 16 mAb expressing clones expressed in the CHO host (Section 4.2.) were also run to confirm that the addition of the reporter did not have a negative effect on the clones during the production study and the mAbs product quality. The final product was then harvested and the product quality (product size and charge) was measured by HPLC. The expression of the CALR-GFP reporter was then retrospectively compared to the quality of the mAb produced to see if they could have been predictive during a production study.

The 32 clones that underwent the production study all showed a very typical growth curve for a fed-batch production study (Figure 6.1.A.). As a fed-batch study is defined by its consistent addition of fresh nutrients and culture media it was expected that the cultures would continue to divide until they reached a peak cell count, where they would then drop off as waste products built up and availability of nutrients diminished (Dean and Reddy, 2013). This was shown by the two waste products measured (lactate and ammonia) increasing over time. Similar CHO fed-batch production studies also show a general increase in the waste products over time (Hayter et al., 1991), with Xing et al. (2010) and Chung et al. (2003) showing the same characteristic increase of ammonia until the end of the log phase, before temporarily dropping during stationary phase and then increasing again. Whilst the fed-batch profile is not one of concern as the aim is to collect enough product for product quality analysis,

a perfusion culture system could be considered to further explore how long the clones can be cultured for and what the maximum titre could be. Perfusion culture is performed in a bioreactor, and fresh media is added at sampling time points as well as waste being removed meaning that the cultures are not negatively affected by waste build up (Pollock et al., 2013; Xie and Wang, 1997).

Perhaps one of the most important factors to consider about the production study was the effect of the addition of the CALR-GFP reporter to the clones final titres, productivity, growth and metabolite consumption. Reassuringly, the CHO host and CALR-GFP clones didn't appear to have any clear differences between any of these characteristics indicating that the addition of the CALR-GFP reporter would not negatively impact clones during CLD. The clonal titres and productivities were in fact higher on average in the CALR-GFP reporter host cultures that were expressing mAb 2 than in the CHO host, but were the same on average in the cultures expressing mAb 1 and 3 (Figure 6.3.C. and D). This suggested that in terms of titre alone the reporter host was at least as good at producing mAb as the CHO host or better, dependent on the mAb. This could be biologically linked to the fact that the CALR-GFP reporter host was cloned much more recently than the CHO host that was produced by GSK. As the CHO system is highly genetically plastic and the host was cloned much longer ago, the population is likely to be much more diverse than the CALR-GFP reporter host and thus a more diverse phenotype relating to product titre may be exhibited. This plasticity was highlighted by Zhang et al. (2016), who counted over 80 mutational events occurring in a CHO cell line following only 150 population doublings by RNA-seq (equivalent to a mutation ever ~2 doubling times).

Another variable that appeared to be heavily linked to product titre, as well as metabolites and growth characteristics was the mAb type expressed in the clones. Out of the mAbs expressed in both the CALR-GFP and the CHO host, the highest producing clones were expressing mAb 2 (Figure 6.3.C.), and the lowest producing clones were mAb 1. This was surprising as mAb 1 and mAb 2 were designed against the same target. It is hypothesised that the variation was caused by the substantial differences in the DNA sequences of the heavy and light chain sequences as mentioned above. This demonstrates that the variation between mutations in the mAb structures cause great effects on the host cells ability to express the mAb, even if they are targeting the same antigen. This was not investigated further however as this was out of the scope of the thesis, which focused on the predictability of the CHO clones rather than the improvement of the mAb structure itself.

The CALR-GFP reporter expression produced a similar pattern over sampling times across all of the samples, and produced an almost inverse pattern to the growth curve (Figure 6.6.). As this pattern was retained by all of the clones it is hypothesised that this is caused by the CALR-GFP host protein production machinery and the production conditions themselves. Whether this pattern of expression

would have been seen in the CALR-GFP reporter host without the addition of the mAb plasmid over a 15 day period was not investigated, and the further study of this may help to confirm this hypothesis. The CALR-GFP intensities at each time point were correlated to the respective titres measured, to see if the CALR-GFP intensity could predict the mAb titre. Correlations with mAb titre were seen on multiple sampling days, but at the highest strength on day 0. It was hypothesised that as the cells are undergoing intense protein and RNA synthesis during the lag phase (day 0) and are acclimatising to the culture conditions (Salzman, 1959) there may be high amounts of stress on the ER to correctly fold the greater volume of mAb product and CALR-GFP reporter construct and thus misfolding or unfolding is likely to be occurring. Further to this, the reporter construct may be utilised by the ER as a functioning CALR chaperone, and thus is being retained in the cell rather than being degraded due to the higher amounts of unfolded or misfolded protein at this time. A second hypothesis is that the CALR-GFP reporter fluorescence is impacted by the conditions of the ER lumen, such as the pH. The pH of the ER has been experimentally shown to be \sim pH 7.3 in mammalian cells (Jaworska et al., 2021). The Golgi apparatus on the other hand is \sim pH 6.0-6.7, and it is this shift in pH that ER chaperones containing a KDEL retention sequence, like CALR, use to return to the ER following delivery of their cargo to the Golgi (Jaworska et al., 2021; Samy et al., 2021). If this pH balance is lost therefore, this may affect the retention of the CALR-GFP reporter. Further work would be required to confirm this however, as little is known about pH change in the ER of the CHO cell, and whether it would be enough to elicit such a response. Finally, it could be questioned whether the reporter construct expression is regulated by a global upregulation of translation over the production study time frame under its constitutive promoter, or if the activation of the UPR is actually having an effect on the expression of the reporter plasmid. An increase in ER stress can result in the sudden incorrect translation, or translation attenuation of the reporter plasmid as controlled by the UPR (Harding et al., 1999). However, it would have been expected that if the CALR-GFP reporter expression on one plasmid was attenuated, so would the expression of the mAb chains on the second plasmid. Further work would be required to investigate this.

Despite the mAb structure not being investigated here, the mAbs themselves were chosen based on the product quality attributes that they had attributed during the final mAb design at GlaxoSmithKline to cover a range of mAb types. Here, the panel of mAbs chosen were used specifically to show mAbs that would cause 'problematic' quality phenotypes so that it was clear whether the CALR-GFP reporter host was able to monitor a whole range of poor quality aspects. The mAb types were chosen for the different issues they exhibited during mAb molecule design (As summarised in Table 2.2.), however when analysed by HPLC the results of the product size quality in this study were surprising and did not reflect these attributes. mAb 1 was prone to aggregation for example, but none of the clones

expressing mAb 1 had high levels of aggregation. In fact, none of the clones had an aggregation percentage of over the 3 % total product maximum selection criteria. In comparison, the bispecific mAb panel used in chapter 3 had an average 8.1 % aggregate. This may have been a biological result, as the mAb sequences are tested in HEK293T cells prior to choosing the final mAb. HEK293T cells are often used for protein production as also being a mammalian cell line they have similar protein folding and post-translational modifications to CHO cells, and in fact are often used in pharmaceuticals that require more stringent human-like modifications that cannot be performed in CHO (Khan, 2013; Tan et al., 2021). A second factor that could have affected the aggregation quantification is the purification and SEC method. Paul et al. (2014) showed that two samples of the same CHO culture media exhibited drastically different aggregate profiles using SEC when one was taken directly from the cell culture media and the other had been purified using Protein A columns. Of course, this is not an issue to patient safety if the downstream processing and analytical techniques have the ability to remove the aggregates from the product, however it does not resolve the aggregate formation in the first place. These highly aggregate prone clones could effectively be masked as good product quality when in fact better quality clones may exist. In this instance the HEK purified material used to determine if the molecule was poor quality prior to this thesis was also purified by Protein A and so any technique effects would not be affected in this study. The HEK purified material would not have undergone clonal selection on the Beacon, and thus the use of the Spotlight assay may actually indirectly select for clones that have higher product quality than by standard selection methods. Of course this has not been studied in this thesis, and evidence for this theory has not been shown by the Berkely Lights group. Taken together these factors highlight how important it is that the CALR-GFP reporter can overcome these differences in expression system and purification techniques to be universally applicable in CLD.

6.3.1. The CALR-GFP reporter host as a tool to predict product quality

The overall relationship between product quality and the CALR-GFP reporter intensity was measured by a correlation matrix, and showed significant relationships with all of the product quality attributes (excluding aggregate %) at at least one sampling time point. The correlation heatmap (Figure 6.12.A.) showed there to be a pattern to the relationships. The undesirable quality characteristics (aggregate, fragment, acidic and basic isoforms) were strongly correlated to the CALR-GFP intensity at the beginning of the culture, before becoming almost perfectly non-correlated to the CALR-GFP intensity at day 8, and then finally becoming correlated again towards the end of the study. The desirable characteristics (monomer and main isoform), unsurprisingly, was the inverse of this pattern. This showed that the earliest and latest time points of culture could identify poor quality clones, whilst the

middle time points could select the better quality clones. As cultures are not usually kept for longer than 7 days before passaging it is suggested that the best time point for CLD usage of the CALR-GFP reporter would be at the day 0 time points. This could capture the negative correlations with titre and basic isoforms (%), and the positive correlations with acidic isoforms (%). It has not been confirmed as to why the highest intensities were observed on day 0, however it is suggested that as the cells are adapting to new culture conditions, the process of protein production puts extra stress on the cell and thus more folding issues are observed. This theory was also speculated in regard to the strongest correlations with titre at the earliest stages of cell culture. This would also explain why the product charge correlations are much stronger than the product size correlations as CALR-GFP functions as a chaperone to ensure correct N-linked glycosylation by trimming glucose residues from protein (High et al., 2000; Ellgaard et al., 2003). Glycosylation has been shown to be an effector of product charge with Miao et al. (2017) showing the terminal Galactosylation index was higher in acidic isoforms compared to main isoforms. Whether this has any relation to CALR specifically that trims residual glucose is unknown, however. This could be confirmed by performing glycosylation analysis on the mAb product by a number of techniques, namely mass spectrometry (Yang et al., 2018). This theory then questions whether CALR is in fact the best marker for measuring product size (e.g. fragment, aggregate and monomer %), and whether a chaperone with a more functionally relevant response as a secondary fluorescent reporter on the same plasmid could better predict product size. As BIP and PDI were predictive in Chapter 3 these may be additional reporter options.

Of course, the correlations seen did not account for the variability across the time points and was complicated by the conflicts between the product quality and the addition of the titre correlation to contend with. It was therefore thought to be beneficial to try a modelling system that could take all of these factors into account. Despite the correlations showing evidence that the CALR-GFP reporter can predict product quality at certain time points this could not be confirmed by statistical modelling when investigating the reporter intensity over all sampling points. This may be due to the CALR-GFP reporter expression being more important at only single time points, or it may be that the sample size (N=14) was not great enough for the model to account for the variability in the sample. Further study, on a larger sample size would therefore be required.

This Chapter has therefore demonstrated that product quality and titre can be measured in CHO clones expressing a panel of mAbs using CALR-GFP fluorescence intensity as a quantitative marker. Questions still remain as to whether the CALR-tagged protein itself is playing a functional role in this relationship, and if a different marker could provide additional information relevant to monitoring product size. Further study would also need to focus on which time point would be best to monitor

CALR-GFP during CLD static scale up. Based on the production study this thesis suggests the best time point to monitor CALR-GFP intensity is as soon as possible after passage. CALR-GFP intensity was not measured in CLD static scale up until the cultures were ready to be scaled up. This meant that cultures were measured for CALR-GFP expression following 4-7 days in culture, which was where the weakest correlations were seen during the production study and so repeating the scale up at the more relevant time points that appear to be highly correlated (i.e. day 0, after passage) would be beneficial to confirm the product quality relationship at a static scale up level. As the relationship between the CALR-GFP reporter and titre was retained at a similar significant strength between static scale up in CLD (Figure 5.11.) and the subsequent production study (Figure 6.7.), it is predicted that the same could be said for product quality. This thesis therefore has shown preliminary evidence that the CALR-GFP reporter construct can predict mAb titre *and* quality in CHO cells, the likes of which have not been shown in the literature before.

7. Discussion

7.1. Introduction

Chinese Hamster Ovary (CHO) cells have been used for over 3 decades as an efficient expression system to produce biopharmaceutical proteins (Dahodwala and Lee, 2019). Due to their importance large amounts of research has been performed on the CHO host to identify high producing clones in an attempt to increase mAb titre (Kim et al., 2012), which has resulted in concentrations as high as 13 g/L to be seen in fed-batch culture conditions (Kelley, 2009). Thus, the field is now becoming interested in developing new approaches which can be used to improve and monitor the quality of the mAb as well as the quantity (Hong et al., 2018).

This thesis first aimed to identify a phenotypic fingerprint for CHO clones that produced large amounts of high quality mAb protein. The characteristics explored within this thesis focused on the role of protein folding, and in particular the role of ER stress and its response mechanism the Unfolded Protein Response (UPR). In order to do this a selection of CHO clones expressing mAbs with a variety of different product quality issues were investigated, and their relationship between these product quality characteristics were compared to the quantities of key protein folding chaperones. The study initially used a bispecific mAb construct (Chapter 3), before expanding this into a panel of mAb constructs with variety of known 'product quality issues' in later chapters (Table 2.2.). These studies suggested there was a negative relationship between the expression of ER chaperones with titre and product quality, which was in contrast to what has previously been observed in the literature.

The second aim of this thesis was to then generate a reporter cell line based off of a single protein folding marker that could ultimately be used as a selection tool within CLD to predict mAb titre and quality, using the data obtained in the first aim. Whilst many of the folding chaperones showed the same relationship with product quality and quantity the final chaperone chosen was Calreticulin (CALR). CALR was chosen as endogenous CALR RNA showed a negative correlation ($r = -0.514$, $p = 0.012$) with product titre in this thesis (Figure 4.4.A.), it had been successfully tagged in other organisms (Müller-Taubenberger et al., 2001; Avezov et al., 2015) and for its role preventing premature transport of proteins out of the ER (Jiang et al., 2014; Määttänen et al., 2010). CALR was also chosen over other folding related molecules such as Binding Immunoglobulin Protein (BIP) as BIP plays a dual role in binding to nascent protein in both homeostatic conditions (prior to folding) and in the re-folding of misfolded protein/unfolded protein that may make understanding the reporter expression mechanism difficult to pinpoint (Feige et al., 2010; Cao and Kaufman, 2012). A CALR

reporter CHO host cell line was generated which expressed exogenous CALR tagged with GFP (Chapter 5). The reporter host cell line was then transfected with the same mAb panel used for the first aim of the thesis, and tested for its predictive capabilities of titre during CLD static scale up. The negative correlation between CALR expression and titre was retained during the scale up (Figure 5.11.).

The clones were then taken through shake flask production studies to generate sufficient product to see if the reporter expression correlated with product quality i.e. product size and charge. The results of the product quality data measured by high performance liquid chromatography (HPLC) could then be compared to the CALR-GFP expression during cell culture for its predictive capabilities (Figure 6.12.). The size of the mAb product was significantly correlated to the CALR-GFP reporter expression at the earliest culture time points. Specifically, the percentage of the fully folded mAb product (monomer) was negatively correlated to the CALR-GFP reporter expression after 3 days in culture whilst a positive relationship was seen with the percentage of the undesired fragmented product (Figure 6.12.). The product charge analysis also showed there to be a strong positive correlation between the CALR-GFP reporter expression on day 0 in culture, and the amount of product that had an acidic charge or basic charge (Figure 6.12.). These significant correlations were the inverse of each other.

Based off of this data therefore a cell line with low CALR-GFP reporter expression between days 0-3 of cell culture would be desirable for selection on product titre and quality. This would be because it would be indicative of high titre, low fragment (%), high monomer (%) and low acidic isoform species (%). This thesis has therefore successfully designed, constructed and tested the use of a novel reporter construct system that can be used in CHO cells to monitor the production of high quality *and* quantity mAb product.

7.2. Using fluorescence imaging to monitor extracellular aggregates

In chapter 3, fluorescence confocal imaging was used to measure the levels of intracellular BIP and human IgG in two clones expressing a bispecific mAb construct, as well as the CHO host. An unexpected phenotype was seen when clone A (that had previously demonstrated high levels of aggregation) showed clear signs of extracellular aggregate staining (Figure 3.2.). Clone B on the other hand had very limited extracellular staining, and had not previously demonstrated any propensity to aggregate. The data suggests that this technique could be used to identify antibody aggregation and thus aggregate prone clones at a far earlier stage in the CLD process. However, these results are preliminary as only an N=1 was used and the clone imaged had an extreme aggregate profile. Whilst the imaging staining protocol is also relatively simple and easy to automate with many studies

measuring IgG in CHO cells (Mathias et al., 2018; Pekle et al., 2019), the quantification of imaging can be laborious and does not lend itself to a screening assay unless it can be automated to a plate reader. Thus, the technique may not be nuanced enough to be able to predict those with more moderate profiles and was not taken further in this thesis. Perhaps a simpler solution to these issues would be to incubate the cell media in a 96 well plate coated with Protein A. The plate could then be imaged and quantified to see if the aggregates remained bound to the plate. Not only would this be an easier protocol to quantify but it would also confirm that the staining shown was aggregated mAb and not cell debris or the remains of lysed cells.

7.3. The Beacon can successfully image the localised CALR-GFP reporter

The cloning of the CALR-GFP reporter CHO pools was essential to generate a reporter host cell line that contained the same copy number and integration location of the reporter in every single cell. This ensured that variations in GFP intensities between mAb expressing cell lines could be solely attributed to the effects of mAb expression. The Beacon (Berkeley Lights) was used for the cloning as it was both the standard platform option at GSK, and it was of interest to see if the organelle-localised GFP expression could be visualised on the Beacon during culture. Very little published literature is available for the Beacon due to it being a new technique. The few papers that do exist using the Beacon focus on clonality assurance, or evidencing its current Spotlight titre assaying capabilities (Le et al., 2020; Jorgolli et al., 2019). This thesis has demonstrated for the first time in the literature that the Beacon is capable of showing successful and clear imaging of the localised reporter to the ER, and to a much lesser degree the mitochondria, in cells during culture on the OptoSelect chip (Figure 5.4.A.). The quality of the images captured using the Beacon were high enough to be able to observe phenotypic differences in reporter expression between the pre-clonal reporter host pools. The mAb transfected CALR-GFP reporter host cell lines also showed phenotypic differences across the pens, albeit with lower diversity due to the clonal nature of the reporter host cell line (Figure 5.9.A.).

The Beacon currently does not have the ability to quantify the CALR-GFP reporter expression so only visual observations could be made in this thesis. As other fluorescent assays such as the Spotlight titre assay is quantifiable however, this observed reporter expression may present a new opportunity to develop an assay on the Beacon interface that could quantify reporter expression inside the clones, highlighting a new use for the Beacon that paves the way for further assay development. If quantification of the reporter on the Beacon was possible then clones could be dual selected based on reporter expression and the Spotlight titre assay. This would not only allow the CALR-GFP reporter to be tested for its predictability on the Beacon by comparing the quantification of the two techniques,

but it would give CLD a second tool for clonal cell selection over multiple fluorescent channels. Further to this, the reporter expression can be transferred to other single cell cloning devices with fluorescence capabilities that are available such as the CellenONE (Cellenion) and the F.Sight by (Cytana) (Vallone et al., 2020), further highlighting the potential for global CLD selection.

7.4. The Unfolded Protein Response negatively correlated with mAb titre in the CHO model

This thesis showed that the expression of UPR targets such as BIP, CALR and PDI were negatively correlated with mAb titre in a panel of clonal CHO cell lines expressing different mAb constructs (Figure 4.4.). This data suggested that the clones with the highest titres could be selected for using low UPR expression as a selection criterion. It was hypothesised that higher producing CHO clones were able to efficiently fold and secrete the mAb without the need to activate the UPR, whilst low producers possibly could not keep up with the demand of mAb production and folding and thus a UPR stress response is elicited. One exception to this rule in this study was Activation Transcription Factor 4 (ATF4), a pro-apoptotic factor in the UPR (Walter and Ron, 2011) which showed no correlation. It was hypothesised that the pro-apoptotic function of ATF4 was not being activated in the happily dividing cell cultures.

The literature has also studied the relationship between titre and the expression of various UPR chaperones, with Le Fourn et al. (2014) showing the same trend as this study with BIP via western blot, which was more highly expressed in poor expressing CHO clones than in high producing clones. Whilst this gave confidence to the data shown here, the study measured protein expression and not RNA transcripts. The general trend for RNA based quantification studies however suggested the opposite; with the higher the titre, the higher the expression of UPR-associated proteins. Prashad and Mehra (2015) for example compared the mRNA concentration of UPR chaperones in a high producer and a low producer CHO clone. Many of the factors studied such as BIP, growth arrest and DNA damage-inducible gene 34 (GADD34) and spliced X-box binding protein 1 (sXBP1) had elevated expression in the high producer clone than in the low producing clone. Similarly, Kober et al. (2012) showed a positive correlation between titre and BIP, sXBP1 and glucose-regulated protein 94 (GRP94) expression across a panel of mAb expressing clones. It was surprising therefore that the correlations seen in this thesis were the inverse of that seen in the literature. One theory as to why the opposite relationship was seen in this study is due to the differences between the experiments – the variables of which have been summarised in Table 7.1.

	Thesis Study	Kober et al. (2012) Study	Prashad and Mehra (2015) Study
CHO Host Used	CHO GS -/-	CHO DG44 (DHFR-/-)	CHO DG44 (DHFR-/-)
Number of mAb Constructs Used	4	1 ('Model IgG')	1 (Anti-Rhesus IgG)
Number of Clones Investigated	23 (5-6 per mAb type)	8	2
Selection Used	MSX	MTX	MTX
Age of Cell Lines	Approximately 3 passages post completion of CLD scale up.	Unknown – materials suggests the clones were scaled up and cultivated prior to the 11 day fed-batch study.	Unknown – first described in Chusainow et al. (2009).
Transfection Method	Lipofection	Unknown – electroporation was used for the reporter construct section of the paper however.	Electroporation
Cloning Method	Beacon	FACS	Limited Dilution
Culture Days Experimented	0-4 Days Post Passage in sub-culture	Day 11 of a fed-batch study	0-8 Days Post Passage in sub-culture
Titre Method	Octet	ELISA	ELISA
RNA Quantification Method	ddPCR	RT-PCR	qPCR
RNA House-Keeping Normalisation	β -2-Microglobulin	B-Actin	B-Actin
Titre Range	0 - 80 mg/L (in a 4 day sub-culture) * 330 - 3500 mg/L in subsequent fed-batch study (Chapter 6)	1100 - 3800 mg/L (in an 11 day fed-batch process)	~100 - 700 mg/L (in a 8 day sub-culture)
Feed Media Used?	No	Yes	No

Table 7.1. Comparison of the experimental controls and techniques used in this thesis and the Kober *et al.*, (2012) and the Prashad and Mehra (2015) studies.

The table highlights the differences in the RNA based experimental techniques such as the clone ages, and the number of clones and mAb constructs tested between the three studies. These differences may explain why an inverse relationship was seen between titre and UPR transcript expression in this study. *The cell lines used in this study produced titres between 0-80 mg/L during the 4 day sub-culture of which the ddPCR study was performed on. The subsequent 15 day fed-batch study of the same cell lines in chapter 6 went on to produce titres between 330 – 3500 mg/L.

Perhaps one of the most crucial differences between this study and the literature studies is the number of samples investigated. Prashad and Mehra (2015) used 2 cell lines, whilst Kober et al. (2012) used 8. This study instead included 23 cell lines in attempts to account for the vast clonal variation that is often seen following random integration transfection, suggesting that this study was more robust than the previous studies. With the lack of information of the mAbs available with industry sponsored projects, the mAb construct too can be a variable to consider for the differences seen between experiments.

The CHO host lineage and selection pressure was also different across the studies with the literature articles both using the DHFR ^{-/-} CHO DG44 system (Urlaub and Chasin, 1980) whilst this study used a proprietary GS^{-/-} CHO host. The CHO genome has been noted for its high plasticity with Davies et al. (2013) showing that when a single mAb expressing parental CHO cell was sub-cloned into 80 daughter cell lines there was obvious variation in proliferation and mAb titre. Whilst the DHFR ^{-/-} and GS ^{-/-} CHO host lines in this comparison were derived from the same single CHO line isolated nearly 70 years ago by Tjio and Puck (1958) (Figure 1.1.) the potential for substantial genomic change between these cell lines will therefore be high.

In regards to the design of the experiments, the cell lines in this study were only investigated over a 4 day passage in regular sub-culture in attempts to keep the cell lines relevant to a CLD process and thus any resulting trend that may be used to design a reporter construct was relevant for use in CLD. Prashad and Mehra (2015) similarly measured the two clones in sub-culture however they continued their monitoring for a total of 8 days, and thus it was surprising that a similar response was not seen between the studies over the first 4 culture days. As only two clones were studied however it is impossible to say whether the results seen in the paper were a trend, or were simply the difference between two clones regardless of their production capabilities. Kober et al. (2012) on the other hand performed a fed-batch production study on the clones and did not measure UPR expression until day 11 in culture, in which time their cultures were regularly subjected to nutrient addition and waste product build up and thus questions arise as to how comparable the conditions are. Du et al. (2013) has shown that production culture can increase UPR stress using a CHO cell line expressing a GFP-based, UPR inducible system. The induction of the UPR was compared between cultures kept in both sub-culture and production study. The sub-culture flasks showed background GFP induction, the same as that of a control line. The production study cultures however showed an obvious positive shift in GFP expression, suggesting that the conditions of the culture were causing ER stress to the cells. This theoretically could be a contributing factor for the increasing stress seen in the higher producing clones in the Kober et al. (2012) study. By measuring only one time-point the study cannot confirm whether the increased stress in the higher producing clones is as a result of UPR activation only seen

in the latter stages of production studies, or if it is consistently seen regardless of the culture time point. It would be of interest therefore to repeat the ddPCR studies from this thesis in a similar fed-batch production study to see if the UPR activation is much later. Of course, this may not be biologically relevant to the aims of this thesis which is looking to design a reporter construct for use in CLD. As CLD cultures are not left for as long as 11 days, any reporter that is designed based off of a later culture response may not be of relevance.

One final point to consider would be the effect of using the Beacon to actively select for the best producing cell lines. The Prashad and Mehra (2015) study obtained two clonal cell lines by the limited dilution method, and had chosen a high and low producer to study using ELISA to measure titre. Kober et al. (2012) on the other hand used a FACS based cloning approach to select for the best-producing CHO clones, also measuring titre via ELISA. This study purposefully selected the very best producing clones on the Beacon, in attempts to stay relevant to a typical CLD process at GlaxoSmithKline. The technique used therefore may be worth considering, as Le et al. (2018) showed that when the same cell pool was cloned on the Beacon and via a FACS cloning technique, the average mAb titre was greater in the exported Beacon clones than the FACS clones. The paper also showed that the top 3 producing clones from the Beacon had a consistently higher productivity than the top 3 FACS clones (Le et al., 2018). Thus, it could be suggested that by using the Beacon for clone selection, there is less of a range of titre across the clones and potentially a less obvious UPR expression spectrum. To confirm whether the results seen here and those in the literature are both reliable, repeating the ddPCR study in the cell lines used in the literature would be necessary. Of course, this would be difficult to pursue in an industrial setting, considering the various biopharmaceutical conflicts of interest at large in all these studies and this thesis. If the result seen in this thesis therefore suggested the opposite to the literature as more mAb variations were considered during the design and further evidence was built-up, then this could have a drastic effect on future knowledge of the subject.

7.5. Why do the levels of the CALR-GFP reporter change in response to titre and culture conditions?

An interesting question that has arisen from the exploration of the CALR-GFP reporter construct was what was the mechanism by which the exogenous CALR was up-regulated in lower producing clones than in higher producing clones (Figure 5.11.), and why an overall up-regulation of reporter expression was seen when the cultures were moved from static to shaking culture (Figure 5.10.). As the same negative relationship between CALR expression and mAb titre was seen in the endogenous monitoring (Chapter 4.5.) and in the CALR-GFP reporter expression (Chapter 5.11.) it is thought that the reporter

is working in the same manner as the endogenous CALR expression. As the reporter construct was expressed under a constitutive promoter, the expression should not have been driven by the promoter, or in response to a stimulus, however. Recent unpublished work from Andrew Peden's lab has shown that plasma cells can up-regulate the expression of exogenous reporter constructs despite being driven by a constitutive promoter, which may explain why such a response was seen in this study if CHO cells have the ability to induce promoter expression in the same manner. As B cells differentiate into plasma cells the transcription factors expressed by the cell changes, affecting the expression from the promoter (Lin et al., 1997; Reimold et al., 2001). Questions could therefore be asked as to whether something similar could be happening in the CALR-GFP reporter host in response to ER stress – whereby an increase of ER stress results in the upregulation of different transcription factors that changes the reporter expression. Therefore any changes in the CALR-GFP reporter expression may be caused by the changes in ER stress levels. This may explain why an increase in CALR-GFP expression was seen after the cells were moved from static to shaking culture during clonal scale up as the cells adapted to a new shaking culture condition (Figure 5.10.), and the negative relationship between titre and the CALR-GFP reporter expression (Figure 5.11.), as low producer clones had shown to be more highly stressed in chapter 4. Similarly, this could potentially explain the fluctuations in reporter expression seen during the 15 day production study, whereby the feeding regime and build-up of waste products could be affecting the levels of ER stress in the clones. The reporter construct and the mAb construct were expressed on separate plasmids containing different selection markers. Both of the plasmids were driven by the same type of promoter however, and thus the negative relationship between expression of the two plasmids was more perplexing and suggests a different mechanism of action for the reporter expression was occurring.

Instead of the expression being modulated in the clones, another suggestion to the mechanism of action is that the CALR-GFP conjugated protein is playing a functioning role in the ER lumen in the same manner as an endogenous CALR molecule and its levels are being post-translationally regulated. Here the expression of the reporter construct remains constitutive, but the CALR-GFP is being used and retained by the ER as a functioning chaperone, to retain the unfolded proteins in the ER lumen, ultimately chaperoning the formation of disulphide bonds by its relationship with PDI (Jiang et al., 2014; Määttä et al., 2010). As CALR has been shown to recycle from the ER to the Golgi and back to the ER again (Howe et al., 2009), an increased build-up of misfolded protein may contribute to the functional use of the CALR-GFP reporter. Further to this, the stability of the reporter may be improved when it is bound to the protein. This hypothesis could be confirmed by designing an exogenous CALR and PDI construct tagged for FRET analysis, whereby two fluorescent molecules would be attached to

the two constructs that only emit fluorescence after the binding of the two chaperones at close proximity (Sekar and Periasamy, 2003).

7.6. Would an endogenously tagged gene marker be better at predicting mAb titre and quality than an exogenous marker?

One way to potentially answer the questions that arise from the use of an exogenous reporter would be to consider tagging the CHO host's endogenous UPR proteins. By doing this the only fluorescence response measured would be that of the CALR naturally produced by the CHO clone and any response would be due to the clone changing its expression in reaction to ER stress. The availability of CRISPR has made the tagging of endogenous protein much more feasible, and evidence of its use in the literature is now emerging. Kyeong and Lee (2022) have used CRISPR to endogenously tag the UPR sensor BIP with GFP for example. The study confirmed that the tagging of BIP could measure UPR activation through the use of chemical ER stressors. mAb expressing clones were generated from the BIP tagged CHO host, and an almost perfect positive correlation was seen between BIP fluorescence and mAb titre ($R^2 = 0.9035$) – although the strength of the correlation may have been exacerbated by the addition of the non-transfected control mAb to the plot, which had a much lower BIP fluorescence intensity (~ 3 fold) than any of the mAb expressing clones tested.

Endogenous tagging does come with its own disadvantages and unknowns, however. In the Kyeong and Lee (2022) study that generated the endogenous BIP construct, untagged endogenous BIP was still measurable in the CHO cell lysate via western blot. This suggests that whilst this technique is measuring proteins in their natural state and reaction to stress, it does not necessarily mean it is monitoring every single BIP protein, and some expression may be missed. How the addition of a bulky GFP tag affects the endogenous protein function, and its correct folding is also another important factor to consider. This can be mitigated through the use of specific GFP variants. Kyeong and Lee (2022) for example showed successful reporter expression when fused using monomeric GFP (mGFP) but not when using a tetramer GFP variant (ZsGreen1). Cabantous et al. (2005) also showed that a mutated, super-folder GFP variant of GFP was also able to fluoresce in *E. coli* colonies much more effectively than other mutated GFP formats.

Alternatively, an even smaller, single GFP motif can be added to the protein instead of the full GFP tag, and transfected alongside the remaining 10 motifs of GFP on a separate plasmid. Thus only upon the localised binding of the two GFP sequences will fluorescence emit (Blakeley et al., 2012). This is performed via the splitGFP system and has previously successfully tagged Calreticulin in the ER

(Kamiyama et al., 2016), although it does require the presence of a secondary plasmid for the larger GFP motif unit, as well as an ER retention sequence. Taken together, the tagging of endogenous markers such as Calreticulin could be much more beneficial to CLD as it would reduce the stress of an additional plasmid and selection marker on the CHO cell, as well as not diverting the availability of ribosomes away from mAb polypeptide chains to the reporter.

Another alternative to using an endogenous reporter would be to continue to use an exogenous reporter but with an alternative design, potentially directed towards the CALR function. Roy et al. (2017) for example generated an XBP1 based reporter construct that expressed red fluorescent protein (RFP) in homeostatic ER conditions via an RFP sequence upstream of the XBP1 construct. Following the splicing of the XBP1 sequence by IRE1 during UPR activation a frameshift mutation then allowed the expression of GFP, meaning that any directly induced stress could be monitored by GFP.

7.7. Can the unfolded protein response be used to predict poor product quality?

One of the novelties of this project was its ambition to predict mAb product quality characteristics, as well as titre. Monitoring and improving mAb titre has been at the forefront of the literature, as highlighted by Hong et al. (2018) who showed in a comprehensive literature search that for the last three decades the majority of the literature has focused on improving productivity. In fact, in 2017 88 % of the studies investigated focused on productivity. However, the authors did find that the number of studies focusing on product quality and product stability, were beginning to increase.

As a result of this, there is little information available investigating whether mAb quality is affected by UPR expression. One of the few examples of this is Ishii et al. (2014) who showed that high levels of aggregate in mAb expressing CHO clones were associated with a high concentration of BIP and PDI mRNA following multiple linear regression analysis. They investigated BIP and PDI expression over three culture time points (between days 5 – 12). Interestingly, the strength of the relationship between aggregated protein and BIP or PDI expression decreased over time in culture. The R_s value of the aggregate vs BIP expression dropped from 0.823 to 0.397 between days 5 and 12 for example. This evidence suggested that the earlier expression characteristics of protein folding chaperones were more predictive of aggregate at that time. This could potentially be explained as an initial induction of the UPR by the cells as aggregated protein becomes more abundant. A similar pattern was seen in this thesis, whereby some product quality attributes such as acidic isoform (%), basic isoform (%),

monomer (%) and fragment (%) were strongest at the earlier time point of a fed-batch production study (Figure 6.12.).

Despite attempts to identify product quality it is now clear that some mAbs do have inherent issues within their genetic sequence that cannot be overcome through clonal selection alone. Guo et al. (2021) highlights this with a four-chain bispecific molecule, where its cognate chains have undergone charge mutations to encourage correct heavy and light chain binding. The purified mAb product obtained from CHO however contained a high percentage of incorrectly paired by-products, most frequently of which being a fully-folded mAb that contained two of the same light chains. It was found to be caused by the mutation added to one of the light chains, with the addition of the said mutation completely preventing the light chains export from CHO and HEK cells, whilst the wildtype variant was present in the culture media. This paper therefore highlights that no amount of CHO clones could be screened for to allow for this light chain to be secreted, and so the mAb sequence and type expressed are crucial to consider when comparing the literature. As a bispecific mAb this does present more of an extreme quality phenotype, but as these formats are becoming more prevalent it becomes even more relevant.

7.8. Does the constant improvement of the CLD platform hinder the use of reporter cell lines?

Potentially a general comment towards the limitations of the reporter construct as a screening tool could incorporate the constant, changing landscape of the biopharmaceutical industry itself. The improvement of the CLD pipeline is integral to the increase in the number of mAb projects that can be achieved per year per team and the increase in productivities of the CHO host itself, and thus the number of new products likely to be approved and available to patients (Priola et al., 2016; Hong et al., 2018). The transition from techniques performed by humans to automated liquid handling systems and single cell cloning machines like the Beacon are just one example of how this process has evolved over the last few decades. Some of these newer advances focus specifically on the engineering CHO host however, and thus may have an effect on the reporter expression and ultimately its capacity to predict high quality and quantity mAb product.

One very recent improvement in CLD globally is the availability of transposase technologies that have been designed to ensure integration of the mAb plasmid into pre-determined transcriptionally active genomic loci (Matasci et al., 2011). The emergence of transposase technologies has already seen its use within pharmaceutical companies such as Boehringer Ingelheim and Eli Lilly and Company

(Schmieder et al., 2022; Balasubramanian et al., 2018). The benefits of this technology being that the DNA will be integrated into highly productive locations, with a maintained stability throughout culture (Balasubramanian et al., 2015). Balasubramanian et al. (2018) for example, compared the use of transposase technologies with a random integration transfection technique and showed that despite the random integration transfections having a higher heavy and light chain gene copy number than the transposase-mediated cell lines, the expression of heavy chain and light chain mRNA transcripts were actually higher in the transposase-mediated cell lines. As this technology has the potential to revolutionise CLD transfection protocols globally and drive mAb titres to higher and more stable concentrations than seen before, the CHO clones are likely to be face increased levels of ER stress in response. Thus, the use of this CALR-GFP reporter construct in this setting has the potential to be even more beneficial. Of course, the reporter would have to be tested in any transposase system to confirm that it still works as per the random integration technique used here. But this is just one example of how the reporter construct, if it was decided to be used in a CLD platform with this technology, could be able to continue to be consistent in its response as the rest of the CLD platform evolves around it, and in fact be even more beneficial for clone selection.

7.9. Limitations to the study

One of the greatest questions to arise from this study is whether the CALR-GFP reporter construct will always have a 'one size fits all' predictability to it following the expression of different mAb formats. Therapeutic mAbs are now becoming increasingly available in a wide variety of formats and sizes, as well as different numbers of targets (Absolute Antibodies, 2022). This makes designing a reporter that is consistently able to predict mAb titre and quality extremely difficult. The use of a mAb panel with varying 'known product quality issues' and a bispecific construct has helped to alleviate this challenge, and suggests that overall the CALR-GFP reporter host can do this. The Pearson's r negative correlative value between GFP expression and titre for example was of a similar range across all of the mAb types expressed during static scale up in all but one mAb type (Figure 5.11.). The exception, mAb 7, instead showed a very weak positive correlation. These correlations were not significant however, potentially due to the same sample size (Clone N = 11). It is therefore difficult to determine if this is a biological response or not but it does warrant further questioning as to whether the CALR-GFP reporter construct will be as predictive as mAb constructs become increasingly complex. To confirm this, the bispecific construct and other complex formats of mAb would need to be transfected into the CALR-GFP reporter host and tested.

7.10. Future Studies

The immediate next step for this study would be repeating the CLD process using the CALR-GFP reporter host cell line with a new mAb construct of unknown quality. A large number of clones expressing this mAb could be taken through CLD and beyond for product quality analysis. This would determine whether selection could be made based off of the CALR-GFP reporter expression alone, which is particularly crucial for product quality prediction as it is not currently measurable in CLD.

The titre and quality predictability of the reporter could also be improved in iterative studies as it is likely that performing linear correlations between the reporter expression and each variable may not be the most efficient use of the CALR-GFP reporter. Instead future analysis could focus on predictive modelling that would account for the effects of all of these variables together, to help to streamline the reporter predictability. This was attempted (Chapter 6.2.10.) however the small sample size (N=14) meant that the model was not robust, and thus a larger sample size might help to improve this.

Another study to consider would be to increase the amount of product quality and titre attributes correlated with the reporter expression. The glycan profiles of mAb products are routinely measured due to the affect it can have on half-life, immunogenicity and stability (Kamoda and Kakehi, 2008). Glycan analysis was not available for this thesis but is becoming much easier to measure; with a range of techniques from the gold-standard mass spectrometry to lab bench based glycan assay plates to choose from (Yang et al., 2018; Giehring, 2020). Another attribute that could be explored would be the stability of mAb expression in the clones over time. This would typically be performed by ageing the cells until they have reached > 80 generations in sub-culture, and comparing the titres they are producing during a production study with cells of a much younger generation.

7.11. Concluding Remarks

A panel of antibody producing cell lines with well-defined antibody titre and product quality characteristics was designed and used to study the hosts ER stress response to antibody production. A Calreticulin based reporter tagged with GFP was then generated using the Beacon, and was shown to respond to ER stress using a range of pharmacological stressors. The reporter CHO cell line was shown to be a suitable expression host following transfection with the panel of the mAb constructs, generating titres at the same concentration as the CHO host. Product quality and titre data collected from the clonal cell lines expressing the panel of mAbs then showed that the CALR-GFP reporter was predictive of these characteristics during culture. This thesis has therefore successfully designed, constructed and tested the use of a novel reporter construct system that can be used in CHO cells to monitor the production of high quality *and* quantity mAb product.

8. Appendices

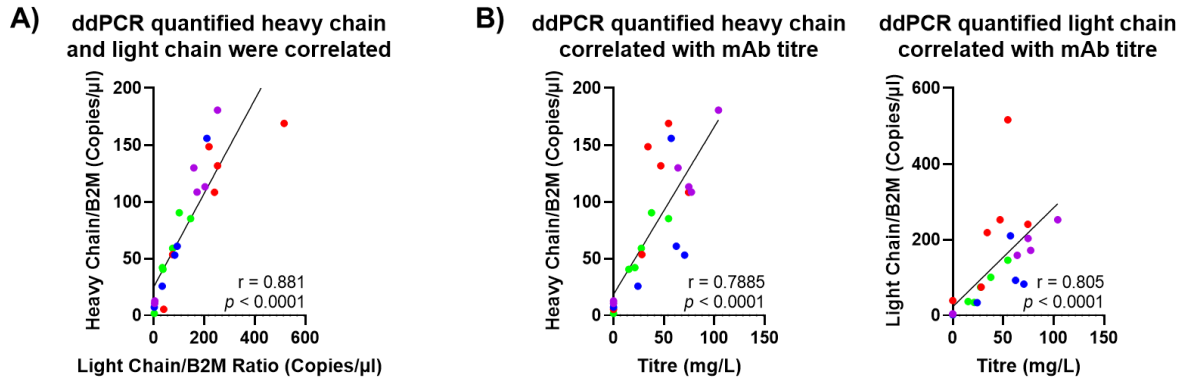


Figure 8.1. Heavy and light chain quantification via ddPCR positively correlated to mAb titre.

To confirm that the ddPCR quantification was specific to heavy and light chain expression in the CHO clones, they were correlated with themselves and mAb titre. Correlations were measured via Spearman rank analysis, and significance set at $p < 0.05$. Clones are coloured by mAb type expressed: mAb 1 (green), mAb 2 (red), mAb 3 (blue) and mAb 4 (purple) **A)** Heavy and light chain quantified via ddPCR were first correlated to each other. As the chains are expressed on the same plasmid, there should be a 1:1 ratio of heavy to light chain, a strong positive correlation suggested that the quantification was accurate. **B)** Heavy and light chain quantification were correlated to mAb titre, as measured on the Octet HTX, as an external test. A positive correlation was seen in both studies, suggesting that the ddPCR was as accurate as the mAb titre measurement.

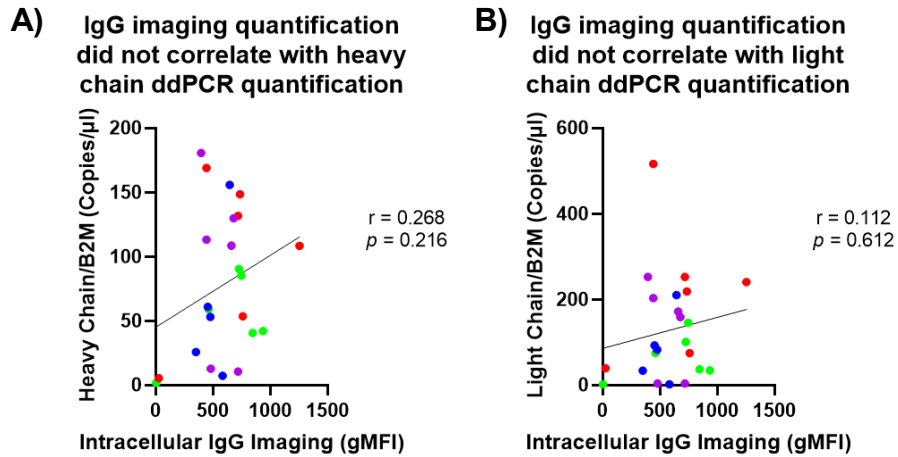


Figure 8.2. Heavy and light chain RNA expression as measured by ddPCR, did not correlate with intracellular IgG quantification, as measured by imaging.

Heavy and light chain RNA quantification measured by ddPCR was correlated to intracellular IgG staining, measured by microscopy. Correlations were measured via Spearman rank analysis, and significance set at $p < 0.05$. Clones are coloured by mAb type expressed: mAb 1 (green), mAb 2 (red), mAb 3 (blue) and mAb 4 (purple). Neither **A)** Heavy chain nor **B)** light chain ddPCR RNA expression correlated to intracellular IgG protein expression, suggesting that regulation of the chains was occurring in the ER following translation.

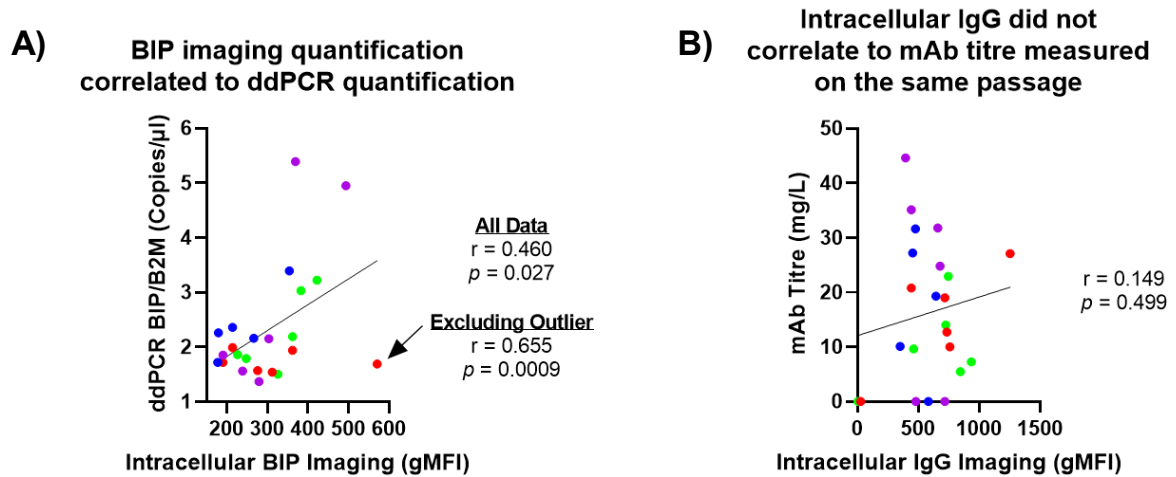


Figure 8.3. BIP RNA expression as measured by ddPCR correlated with intracellular BIP staining. mAb titre and intracellular IgG staining did not correlate, however.

Correlations were measured via Spearman rank analysis, and significance set at $p < 0.05$. Clones are coloured by mAb type expressed: mAb 1 (green), mAb 2 (red), mAb 3 (blue) and mAb 4 (purple). **A)** Intracellular BIP staining and BIP RNA expression were moderately positively correlated, suggesting that both techniques were specifically measuring BIP. **B)** Intracellular IgG staining and mAb titre did not correlate however, suggesting that the two were not predictive of each other.

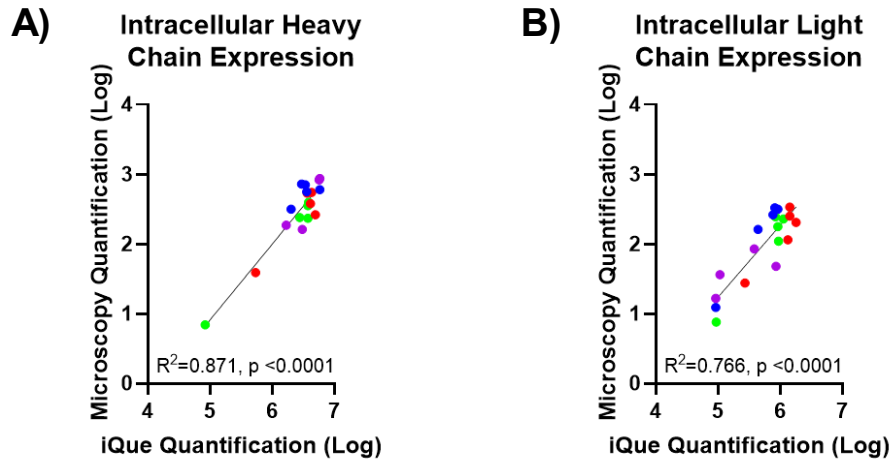


Figure 8.4. Light chain and heavy chain staining was correlated when measured by microscopy and flow cytometry.

Correlations were measured via Spearman rank analysis, and significance set at $p < 0.05$. Clones are coloured by mAb type expressed: mAb 1 (green), mAb 2 (red), mAb 3 (blue) and mAb 4 (purple). Intracellular **A)** heavy chain and **B)** light chain were measured in the clones via flow cytometry (using the iQue flow cytometer) and via microscopy. The two techniques were logged to the same scale and correlated together. Both chain quantifications showed a positive correlation between the two techniques.

9. References

- Absolute Antibodies (2022) *Bispecific and Trispecific Antibodies*. Available at: <https://absoluteantibody.com/custom-services/antibody-engineering/bispecific-and-trispecific-antibodies/> (Accessed: February 2022).
- Amzel, L.M. and Poljak, R.J. (1979). Three-dimensional structure of immunoglobulins. *Annual review of biochemistry*, 48(1), pp.961-997.
- Argon, Y. and Simen, B.B. (1999). GRP94, an ER chaperone with protein and peptide binding properties. In *Seminars in Cell & Developmental Biology*, 10(5), pp. 495-505.
- Avezov, E., Konno, T., Zyryanova, A., Chen, W., Laine, R., Crespillo-Casado, A., Melo, E.P., Ushioda, R., Nagata, K., Kaminski, C.F. and Harding, H.P. (2015). Retarded PDI diffusion and a reductive shift in poise of the calcium depleted endoplasmic reticulum. *BMC biology*, 13(1), pp.1-15.
- Bajaj, H., Sharma, V.K., Badkar, A., Zeng, D., Nema, S. and Kalonia, D.S. (2006). Protein structural conformation and not second virial coefficient relates to long-term irreversible aggregation of a monoclonal antibody and ovalbumin in solution. *Pharmaceutical research*, 23(6), pp.1382-1394.
- Balasubramanian, S., Matasci, M., Kadlecova, Z., Baldi, L., Hacker, D.L. and Wurm, F.M. (2015). Rapid recombinant protein production from piggyBac transposon-mediated stable CHO cell pools. *Journal of biotechnology*, 200, pp.61-69.
- Balasubramanian, S., Peery, R.B., Minshull, J., Lee, M., White, R., Kelly, R.M. and Barnard, G.C. (2018). Generation of high expressing Chinese hamster ovary cell pools using the Leap-In transposon system. *Biotechnology Journal*, 13(10), p.1700748.
- Bansal, R., Gupta, S. and Rathore, A.S. (2019). Analytical platform for monitoring aggregation of monoclonal antibody therapeutics. *Pharmaceutical Research*, 36(11), pp.1-11.
- Bareither, R. and Pollard, D. (2011). A review of advanced small-scale parallel bioreactor technology for accelerated process development: Current state and future need. *Biotechnology progress*, 27(1), pp.2-14.
- Berkeley Lights (2022) The Beacon® Optofluidic System. Available at: <https://www.berkeleylights.com/systems/beacon/> (Accessed: February 2022).
- Bertolotti, A., Zhang, Y., Hendershot, L.M., Harding, H.P. and Ron, D. (2000). Dynamic interaction of BiP and ER stress transducers in the unfolded-protein response. *Nature cell biology*, 2(6), pp.326-332.
- Beum, P.V., Lindorfer, M.A., Beurskens, F., Stukenberg, P.T., Lokhorst, H.M., Pawluczko, A.W., Parren, P.W., van de Winkel, J.G. and Taylor, R.P. (2008). Complement activation on B lymphocytes opsonized with rituximab or ofatumumab produces substantial changes in membrane structure preceding cell lysis. *The Journal of Immunology*, 181(1), pp.822-832.
- Bhoskar, P., Belongia, B., Smith, R., Yoon, S., Carter, T. and Xu, J. (2013). Free light chain content in culture media reflects recombinant monoclonal antibody productivity and quality. *Biotechnology Progress*, 29(5), pp.1131-1139.
- Blakeley, B.D., Chapman, A.M. and McNaughton, B.R. (2012). Split-superpositive GFP reassembly is a fast, efficient, and robust method for detecting protein–protein interactions in vivo. *Molecular BioSystems*, 8(8), pp.2036-2040.

- Bole, D.G., Hendershot, L.M. and Kearney, J.F. (1986). Posttranslational association of immunoglobulin heavy chain binding protein with nascent heavy chains in nonsecreting and secreting hybridomas. *The Journal of Cell Biology*, 102(5), pp.1558-1566.
- Bordes, F., Fudalej, F., Dossat, V., Nicaud, J.M. and Marty, A. (2007). A new recombinant protein expression system for high-throughput screening in the yeast *Yarrowia lipolytica*. *Journal of Microbiological Methods*, 70(3), pp.493-502.
- Bork, P., Holm, L. and Sander, C. (1994). The immunoglobulin fold: structural classification, sequence patterns and common core. *Journal of Molecular Biology*, 242(4), pp.309-320.
- Borth, N., Mattanovich, D., Kunert, R. and Katinger, H. (2005). Effect of increased expression of protein disulfide isomerase and heavy chain binding protein on antibody secretion in a recombinant CHO cell line. *Biotechnology Progress*, 21(1), pp.106-111.
- Bothra, A., Bhattacharyya, A., Mukhopadhyay, C., Bhattacharyya, K. and Roy, S. (1998). A fluorescence spectroscopic and molecular dynamics study of bis-ANS/protein interaction. *Journal of Biomolecular Structure and Dynamics*, 15(5), pp.959-966.
- Boune, S., Hu, P., Epstein, A.L. and Khawli, L.A. (2020). Principles of N-linked glycosylation variations of IgG-based therapeutics: pharmacokinetic and functional considerations. *Antibodies*, 9(2), p.22.
- Breedveld, F.C. (2000). Therapeutic monoclonal antibodies. *The Lancet*, 355(9205), pp.735-740.
- Brown, M.E., Renner, G., Field, R.P. and Hassell, T. (1992). Process development for the production of recombinant antibodies using the glutamine synthetase (GS) system. *Cytotechnology*, 9(1), pp.231-236.
- Brunelle, J.K. and Letai, A. (2009). Control of mitochondrial apoptosis by the Bcl-2 family. *Journal of Cell Science*, 122(4), pp.437-441.
- Buss, N.A., Henderson, S.J., McFarlane, M., Shenton, J.M. and De Haan, L. (2012). Monoclonal antibody therapeutics: history and future. *Current opinion in pharmacology*, 12(5), pp.615-622.
- Cabantous, S., Terwilliger, T.C. and Waldo, G.S. (2005). Protein tagging and detection with engineered self-assembling fragments of green fluorescent protein. *Nature biotechnology*, 23(1), pp.102-107.
- Cao, S.S. and Kaufman, R.J. (2012). Unfolded protein response. *Current biology*, 22(16), pp.R622-R626.
- Carter, P. (2001). Bispecific human IgG by design. *Journal of immunological methods*, 248(1-2), pp.7-15.
- Carter, P., Presta, L.E.N., Gorman, C.M., Ridgway, J.B., Henner, D., Wong, W.L., Rowland, A.M., Kotts, C., Carver, M.E. and Shepard, H.M. (1992). Humanization of an anti-p185HER2 antibody for human cancer therapy. *Proceedings of the National Academy of Sciences*, 89(10), pp.4285-4289.
- Center for Drug Evaluation and Research (2018) *New Drug Therapy Approvals*. Available at: <https://www.fda.gov/files/about%20fda/published/2017-New-Drug-Therapy-Approvals-Report.pdf> (Accessed: February 2022).
- Chakrabarti, A., Chen, A.W. and Varner, J.D. (2011). A review of the mammalian unfolded protein response. *Biotechnology and bioengineering*, 108(12), pp.2777-2793.
- Chakrabarti, L., Mathew, A., Li, L., Han, S., Klover, J., Albanetti, T. and Hawley-Nelson, P. (2019). Mitochondrial membrane potential identifies cells with high recombinant protein productivity. *Journal of immunological methods*, 464, pp.31-39.

- Chandrawanshi, V., Kulkarni, R., Prabhu, A. and Mehra, S. (2020). Enhancing titers and productivity of rCHO clones with a combination of an optimized fed-batch process and ER-stress adaptation. *Journal of Biotechnology*, 311, pp.49-58.
- Chardin, P. and McCormick, F. (1999). Brefeldin A: the advantage of being uncompetitive. *Cell*, 97(2), pp.153-155.
- Chatterjee, S., Basak, A.J., Nair, A.V., Duraivelan, K. and Samanta, D. (2021). Immunoglobulin-fold containing bacterial adhesins: molecular and structural perspectives in host tissue colonization and infection. *FEMS Microbiology Letters*, 368(2), p.fnaa220.
- Chen, C., Wong, H.E. and Goudar, C.T. (2018). Upstream process intensification and continuous manufacturing. *Current opinion in chemical engineering*, 22, pp.191-198.
- Chen, X., Shen, J. and Prywes, R. (2002). The Luminal Domain of ATF6 Senses Endoplasmic Reticulum (ER) Stress and Causes Translocation of ATF6 from the ER to the Golgi. *Journal of Biological Chemistry*, 277(15), pp.13045-13052.
- Chiu, M.L., Goulet, D.R., Teplyakov, A. and Gilliland, G.L. (2019). Antibody structure and function: the basis for engineering therapeutics. *Antibodies*, 8(4), p.55.
- Cho, B., Cho, H.M., Jo, Y., Kim, H.D., Song, M., Moon, C., Kim, H., Kim, K., Sesaki, H., Rhyu, I.J. and Kim, H. (2017). Constriction of the mitochondrial inner compartment is a priming event for mitochondrial division. *Nature Communications*, 8(1), pp.1-17.
- Chung, M.I., Lim, M.H., Lee, Y.J., Kim, I.H., Kim, I.Y., Kim, J.H., Chang, K.H. and Kim, H.J. (2003). Reduction of ammonia accumulation and improvement of cell viability by expression of urea cycle enzymes in Chinese hamster ovary cells. *Journal of Microbiology and Biotechnology*, 13(2), pp.217-224.
- Chusainow, J., Yang, Y.S., Yeo, J.H., Toh, P.C., Asvadi, P., Wong, N.S. and Yap, M.G. (2009). A study of monoclonal antibody-producing CHO cell lines: What makes a stable high producer?. *Biotechnology and Bioengineering*, 102(4), pp.1182-1196.
- Cooley, S., Burns, L.J., Repka, T. and Miller, J.S. (1999). Natural killer cell cytotoxicity of breast cancer targets is enhanced by two distinct mechanisms of antibody-dependent cellular cytotoxicity against LFA-3 and HER2/neu. *Experimental Hematology*, 27(10), pp.1533-1541.
- Cooper, J.K., Schilling, G., Peters, M.F., Herring, W.J., Sharp, A.H., Kaminsky, Z., Masone, J., Khan, F.A., Delanoy, M., Borchelt, D.R. and Dawson, V.L. (1998). Truncated N-terminal fragments of huntingtin with expanded glutamine repeats form nuclear and cytoplasmic aggregates in cell culture. *Human Molecular Genetics*, 7(5), pp.783-790.
- Corbascio, A.N., Kohn, H.I. and Yerganian, G. (1962). Acute X-ray lethality in the Chinese hamster after whole-body and partial-body irradiation. *Radiation Research*, 17(4), pp.521-530.
- Cordoba, A.J., Shyong, B.J., Breen, D. and Harris, R.J. (2005). Non-enzymatic hinge region fragmentation of antibodies in solution. *Journal of Chromatography B*, 818(2), pp.115-121.
- Cox, J.S., Shamu, C.E. and Walter, P. (1993). Transcriptional induction of genes encoding endoplasmic reticulum resident proteins requires a transmembrane protein kinase. *Cell*, 73(6), pp.1197-1206.
- Cromwell, M.E., Hilario, E. and Jacobson, F. (2006). Protein aggregation and bioprocessing. *The AAPS journal*, 8(3), pp.E572-E579.
- Dahodwala, H. and Lee, K.H. (2019). The fickle CHO: a review of the causes, implications, and potential alleviation of the CHO cell line instability problem. *Current opinion in biotechnology*, 60, pp.128-137.

- Davies, S.L., Lovelady, C.S., Grainger, R.K., Racher, A.J., Young, R.J. and James, D.C. (2013). Functional heterogeneity and heritability in CHO cell populations. *Biotechnology and Bioengineering*, 110(1), pp.260-274.
- De, A., Ansari, A., Sharma, N. and Sarda, A. (2017). Shifting focus in the therapeutics of immunobullous disease. *Indian Journal of Dermatology*, 62(3), p.282.
- Dean, J. and Reddy, P. (2013). Metabolic analysis of antibody producing CHO cells in fed-batch production. *Biotechnology and Bioengineering*, 110(6), pp.1735-1747.
- Dempsey, J. (2020). Cell line development for therapeutic proteins – current perspectives and future opportunities. Available at: <https://www.drugtargetreview.com/article/57784/cell-line-development-for-therapeutic-proteins-current-perspectives-and-future-opportunities/> (Accessed: February 2022).
- Desai, K.G., Pruett, W.A., Martin, P.J., Colandene, J.D. and Nesta, D.P. (2017). Impact of manufacturing-scale freeze-thaw conditions on a mAb solution. *BioPharm International*, 30(2), pp.30-36.
- Dhiman, H., Campbell, M., Melcher, M., Smith, K.D. and Borth, N. (2020). Predicting favorable landing pads for targeted integrations in Chinese hamster ovary cell lines by learning stability characteristics from random transgene integrations. *Computational and Structural Biotechnology Journal*, 18, pp.3632-3648.
- Diep, J., Le, H., Le, K., Zasadzinska, E., Tat, J., Yam, P., Zastrow, R., Gomez, N. and Stevens, J. (2021). Microfluidic chip-based single-cell cloning to accelerate biologic production timelines. *Biotechnology Progress*, p.e3192.
- DiMasi, J.A., Feldman, L., Seckler, A. and Wilson, A. (2010). Trends in risks associated with new drug development: success rates for investigational drugs. *Clinical Pharmacology & Therapeutics*, 87(3), pp.272-277.
- DiMasi, J.A., Grabowski, H.G. and Hansen, R.W. (2016). Innovation in the pharmaceutical industry: new estimates of R&D costs. *Journal of Health Economics*, 47, pp.20-33.
- Dovgan, T., Golghalyani, V., Zurlo, F., Hatton, D., Lindo, V., Turner, R., Harris, C. and Cui, T. (2021). Targeted CHO cell engineering approaches can reduce HCP-related enzymatic degradation and improve mAb product quality. *Biotechnology and Bioengineering*, 118(10), pp.3821-3831.
- Dritschilo, A., Piro, A.J. and Kelman, A.D. (1979). The effect of cis-platinum on the repair of radiation damage in plateau phase Chinese hamster (V-79) cells. *International Journal of Radiation Oncology-Biology-Physics*, 5(8), pp.1345-1349.
- Du, Y., Walsh, A., Ehrick, R., Xu, W., May, K. and Liu, H. (2012). Chromatographic analysis of the acidic and basic species of recombinant monoclonal antibodies. *mAbs*, 4(5), pp. 578-585).
- Du, Z., Treiber, D., McCoy, R.E., Miller, A.K., Han, M., He, F., Domnitz, S., Heath, C. and Reddy, P., (2013). Non-invasive UPR monitoring system and its applications in CHO production cultures. *Biotechnology and Bioengineering*, 110(8), pp.2184-2194.
- Durocher, Y. and Butler, M. (2009). Expression systems for therapeutic glycoprotein production. *Current Opinion in Biotechnology*, 20(6), pp.700-707.
- Ecker, D.M., Jones, S.D. and Levine, H.L. (2015). The therapeutic monoclonal antibody market. *mAbs*, 7(1), pp. 9-14.
- Ellgaard, L. and Frickel, E.M. (2003). Calnexin, calreticulin, and ERp57. *Cell Biochemistry and Biophysics*, 39(3), pp.223-247.

- Ellgaard, L., Molinari, M. and Helenius, A. (1999). Setting the standards: quality control in the secretory pathway. *Science*, 286(5446), pp.1882-1888.
- Eriksson, K.K., Vago, R., Calanca, V., Galli, C., Paganetti, P. and Molinari, M. (2004). EDEM contributes to maintenance of protein folding efficiency and secretory capacity. *Journal of Biological Chemistry*, 279(43), pp.44600-44605.
- Falkenberg, S.M., Dassanayake, R.P., Neill, J.D. and Ridpath, J.F. (2017). Improved detection of bovine viral diarrhoea virus in bovine lymphoid cell lines using PrimeFlow RNA assay. *Virology*, 509, pp.260-265.
- Fan, L., Kadura, I., Krebs, L.E., Hatfield, C.C., Shaw, M.M. and Frye, C.C. (2012). Improving the efficiency of CHO cell line generation using glutamine synthetase gene knockout cells. *Biotechnology and bioengineering*, 109(4), pp.1007-1015.
- Feige, M.J., Hendershot, L.M. and Buchner, J. (2010). How antibodies fold. *Trends in biochemical sciences*, 35(4), pp.189-198.
- Fernandez, M.J., Lopez, A. and Santa-Maria, A. (2003). Apoptosis induced by different doses of caffeine on Chinese hamster ovary cells. *Journal of Applied Toxicology: An International Journal*, 23(4), pp.221-224.
- Fischer, S., Marquart, K.F., Pieper, L.A., Fieder, J., Gamer, M., Gorr, I., Schulz, P. and Bradl, H., (2017). miRNA engineering of CHO cells facilitates production of difficult-to-express proteins and increases success in cell line development. *Biotechnology and Bioengineering*, 114(7), pp.1495-1510.
- Fradkin, A.H., Carpenter, J.F. and Randolph, T.W. (2009). Immunogenicity of aggregates of recombinant human growth hormone in mouse models. *Journal of Pharmaceutical Sciences*, 98(9), pp.3247-3264.
- Frye, C., Deshpande, R., Estes, S., Francissen, K., Joly, J., Lubiniecki, A., Munro, T., Russell, R., Wang, T. and Anderson, K. (2016). Industry view on the relative importance of “clonality” of biopharmaceutical-producing cell lines. *Biologicals*, 44(2), pp.117-122.
- Giehring, S. (2020) ‘High-Throughput Quantification and Glycosylation Analysis of Antibodies Using Bead-Based Assays’, in Pörtner, R. (ed.) *Animal Cell Biotechnology*. Fourth Edition. New York: Humana, pp. 271-284.
- Goldfinger, M., Shmuel, M., Benhamron, S. and Tirosh, B. (2011). Protein synthesis in plasma cells is regulated by crosstalk between endoplasmic reticulum stress and mTOR signaling. *European Journal of Immunology*, 41(2), pp.491-502.
- Gomez, N., Lull, J., Yang, X., Wang, Y., Zhang, X., Wieczorek, A., Harrahy, J., Pritchard, M., Cano, D.M., Shearer, M. and Goudar, C. (2020). Improving product quality and productivity of bispecific molecules through the application of continuous perfusion principles. *Biotechnology Progress*, 36(4), p.e2973.
- Gong, D., Riley, T.P., Bzymek, K.P., Correia, A.R., Li, D., Spahr, C., Robinson, J.H., Case, R.B., Wang, Z. and Garces, F. (2021). Rational selection of building blocks for the assembly of bispecific antibodies. *mAbs*, 13(1), p. 1870058.
- Grilo, A.L. and Mantalaris, A. (2019). The increasingly human and profitable monoclonal antibody market. *Trends in Biotechnology*, 37(1), pp.9-16.

- Gu, F., Nguyễn, D.T., Stuiblé, M., Dubé, N., Tremblay, M.L. and Chevet, E. (2004). Protein-tyrosine phosphatase 1B potentiates IRE1 signaling during endoplasmic reticulum stress. *Journal of Biological Chemistry*, 279(48), pp.49689-49693.
- Guo, C., Chen, F., Xiao, Q., Catterall, H.B., Robinson, J.H., Wang, Z., Mock, M. and Hubert, R. (2021). Expression liabilities in a four-chain bispecific molecule. *Biotechnology and Bioengineering*, 118(10), pp.3744-3759.
- Hansel, T.T., Kropshofer, H., Singer, T., Mitchell, J.A. and George, A.J. (2010). The safety and side effects of monoclonal antibodies. *Nature Reviews Drug discovery*, 9(4), pp.325-338.
- Harding, H.P., Zhang, Y. and Ron, D. (1999). Protein translation and folding are coupled by an endoplasmic-reticulum-resident kinase. *Nature*, 397(6716), pp.271-274.
- Harkness, D.R. (1970). Structure and Function of Immunoglobulins. *Postgraduate Medicine*, 48(6), pp.64-69.
- Hassell, T., Gleave, S. and Butler, M. (1991). Growth inhibition in animal cell culture. *Applied Biochemistry and Biotechnology*, 30(1), pp.29-41.
- Hayter, P.M., Curling, E.M.A., Baines, A.J., Jenkins, N., Salmon, I., Strange, P.G. and Bull, A.T., (1991). Chinese hamster ovary cell growth and interferon production kinetics in stirred batch culture. *Applied Microbiology and Biotechnology*, 34(5), pp.559-564.
- Haze, K., Yoshida, H., Yanagi, H., Yura, T. and Mori, K. (1999). Mammalian transcription factor ATF6 is synthesized as a transmembrane protein and activated by proteolysis in response to endoplasmic reticulum stress. *Molecular Biology of the Cell*, 10(11), pp.3787-3799.
- Hebert, D.N., Foellmer, B. and Helenius, A. (1996). Calnexin and calreticulin promote folding, delay oligomerization and suppress degradation of influenza hemagglutinin in microsomes. *The EMBO Journal*, 15(12), pp.2961-2968.
- Hebert, D.N., Garman, S.C. and Molinari, M., (2005). The glycan code of the endoplasmic reticulum: asparagine-linked carbohydrates as protein maturation and quality-control tags. *Trends in Cell Biology*, 15(7), pp.364-370.
- Hendershot, L., Bole, D. and Kearney, J.F. (1987). The role of immunoglobulin heavy chain binding protein: In immunoglobulin transport. *Immunology Today*, 8(4), pp.111-114.
- Hermeling, S., Crommelin, D.J., Schellekens, H. and Jiskoot, W. (2004). Structure-immunogenicity relationships of therapeutic proteins. *Pharmaceutical Research*, 21(6), pp.897-903.
- Hetz, C. (2012). The unfolded protein response: controlling cell fate decisions under ER stress and beyond. *Nature Reviews Molecular Cell Biology*, 13(2), pp.89-102.
- High, S., Lecomte, F.J., Russell, S.J., Abell, B.M. and Oliver, J.D. (2000). Glycoprotein folding in the endoplasmic reticulum: a tale of three chaperones?. *FEBS Letters*, 476(1-2), pp.38-41.
- Hindson, C.M., Chevillet, J.R., Briggs, H.A., Gallichotte, E.N., Ruf, I.K., Hindson, B.J., Vessella, R.L. and Tewari, M. (2013). Absolute quantification by droplet digital PCR versus analog real-time PCR. *Nature Methods*, 10(10), pp.1003-1005.
- Hong, J.K., Lakshmanan, M., Goudar, C. and Lee, D.Y. (2018). Towards next generation CHO cell line development and engineering by systems approaches. *Current Opinion in Chemical Engineering*, 22, pp.1-10.
- Howe, C., Garstka, M., Al-Balushi, M., Ghanem, E., Antoniou, A.N., Fritzsche, S., Jankevicius, G., Kontouli, N., Schneeweiss, C., Williams, A. and Elliott, T. (2009). Calreticulin-dependent recycling

- in the early secretory pathway mediates optimal peptide loading of MHC class I molecules. *The EMBO Journal*, 28(23), pp.3730-3744.
- Hsu, W.T., Aulakh, R.P., Traul, D.L. and Yuk, I.H. (2012). Advanced microscale bioreactor system: a representative scale-down model for bench-top bioreactors. *Cytotechnology*, 64(6), pp.667-678.
- Huber, R. (1976). Antibody structure. *Trends in Biochemical Sciences*, 1(8), pp.174-178.
- Huhn, S.C., Ou, Y., Tang, X., Jiang, B., Liu, R., Lin, H. and Du, Z. (2021). Improvement of the efficiency and quality in developing a new CHO host cell line. *Biotechnology Progress*, 37(5), p.e3185.
- Hussain, H., Patel, T., Ozanne, A.M., Vito, D., Ellis, M., Hinchliffe, M., Humphreys, D.P., Stephens, P.E., Sweeney, B., White, J. and Dickson, A.J. (2021). A comparative analysis of recombinant Fab and full-length antibody production in Chinese hamster ovary cells. *Biotechnology and Bioengineering*, 118(12), pp.4815-4828.
- Invitrogen (2017). *PrimeFlow RNA Assay*. Available at: https://assets.thermofisher.com/TFS-Assets/LSG/brochures/FC04290-PrimeFlow_RNA_1014_web.pdf (Accessed: January 2022).
- Ishii, Y., Murakami, J., Sasaki, K., Tsukahara, M. and Wakamatsu, K. (2014). Efficient folding/assembly in Chinese hamster ovary cells is critical for high quality (low aggregate content) of secreted trastuzumab as well as for high production: stepwise multivariate regression analyses. *Journal of Bioscience and Bioengineering*, 118(2), pp.223-230.
- Janakiraman, V., Kwiatkowski, C., Kshirsagar, R., Ryll, T. and Huang, Y.M. (2015). Application of high-throughput mini-bioreactor system for systematic scale-down modeling, process characterization, and control strategy development. *Biotechnology progress*, 31(6), pp.1623-1632.
- Jaworska, A., Malek, K. and Kudelski, A. (2021). Intracellular pH—Advantages and pitfalls of surface-enhanced Raman scattering and fluorescence microscopy—A review. *Spectrochimica Acta Part A: Molecular and Biomolecular Spectroscopy*, 251, p.119410.
- Jayapal, K.P., Wlaschin, K.F., Hu, W.S. and Yap, M.G. (2007). Recombinant protein therapeutics from CHO cells-20 years and counting. *Chemical engineering progress*, 103(10), p.40.
- Jiang, Y., Dey, S. and Matsunami, H. (2014). Calreticulin: roles in cell-surface protein expression. *Membranes*, 4(3), pp.630-641.
- Jing, Y., Borys, M., Nayak, S., Egan, S., Qian, Y., Pan, S.H. and Li, Z.J. (2012). Identification of cell culture conditions to control protein aggregation of IgG fusion proteins expressed in Chinese hamster ovary cells. *Process Biochemistry*, 47(1), pp.69-75.
- Johnson, K.A., Paisley-Flango, K., Tangarone, B.S., Porter, T.J. and Rouse, J.C. (2007). Cation exchange—HPLC and mass spectrometry reveal C-terminal amidation of an IgG1 heavy chain. *Analytical Biochemistry*, 360(1), pp.75-83.
- Jorgolli, M., Nevill, T., Winters, A., Chen, I., Chong, S., Lin, F.F., Mock, M., Chen, C., Le, K., Tan, C., Jess, P., Xu, H., Hamburger, A., Stevens, J., Munro, T., Wu, M., Tagari, P. and Miranda, L. (2019). Nanoscale integration of single cell biologics discovery processes using optofluidic manipulation and monitoring. *Biotechnology and Bioengineering*, 116(9), pp.2393-2411.
- Joshi, V., Shivach, T., Kumar, V., Yadav, N. and Rathore, A. (2014). Avoiding antibody aggregation during processing: establishing hold times. *Biotechnology Journal*, 9(9), pp.1195-1205.
- Joubert, M.K., Hokom, M., Eakin, C., Zhou, L., Deshpande, M., Baker, M.P., Goletz, T.J., Kerwin, B.A., Chirmule, N., Narhi, L.O. and Jawa, V. (2012). Highly aggregated antibody therapeutics can

- enhance the in vitro innate and late-stage T-cell immune responses. *Journal of Biological Chemistry*, 287(30), pp.25266-25279.
- Jungbauer, A. and Hahn, R. (2009). Ion-exchange chromatography. *Methods in Enzymology*, 463, pp.349-371.
- Kaas, C.S., Kristensen, C., Betenbaugh, M.J. and Andersen, M.R. (2015). Sequencing the CHO DXB11 genome reveals regional variations in genomic stability and haploidy. *BMC Genomics*, 16(1), pp.1-9.
- Kallehauge, T.B., Li, S., Pedersen, L.E., Ha, T.K., Ley, D., Andersen, M.R., Kildegaard, H.F., Lee, G.M. and Lewis, N.E. (2017). Ribosome profiling-guided depletion of an mRNA increases cell growth rate and protein secretion. *Scientific Reports*, 7(1), pp.1-12.
- Kamiyama, D., Sekine, S., Barsi-Rhyne, B., Hu, J., Chen, B., Gilbert, L.A., Ishikawa, H., Leonetti, M.D., Marshall, W.F., Weissman, J.S. and Huang, B. (2016). Versatile protein tagging in cells with split fluorescent protein. *Nature Communications*, 7(1), pp.1-9.
- Kamoda, S. and Kakehi, K. (2008). Evaluation of glycosylation for quality assurance of antibody pharmaceuticals by capillary electrophoresis. *Electrophoresis*, 29(17), pp.3595-3604.
- Kaplon, H., Muralidharan, M., Schneider, Z. and Reichert, J.M. (2020). Antibodies to watch in 2020. *mAbs*, 12(1), pp.1703531.
- Kelley, B. (2009). Industrialization of mAb production technology: the bioprocessing industry at a crossroads. *mAbs*, 1(5), pp. 443-452.
- Kelly, W., Veigne, S., Li, X., Subramanian, S.S., Huang, Z. and Schaefer, E. (2018). Optimizing performance of semi-continuous cell culture in an ambr15™ microbioreactor using dynamic flux balance modeling. *Biotechnology Progress*, 34(2), pp.420-431.
- Kemler, I. and Schaffner, W. (1990). Octamer transcription factors and the cell type-specificity of immunoglobulin gene expression. *The FASEB journal*, 4(5), pp.1444-1449.
- Khan, K.H. (2013). Gene expression in mammalian cells and its applications. *Advanced Pharmaceutical Bulletin*, 3(2), p.257.
- Khawli, L.A., Goswami, S., Hutchinson, R., Kwong, Z.W., Yang, J., Wang, X., Yao, Z., Sreedhara, A., Cano, T., Tesar, D.B. and Nijem, I. (2010). Charge variants in IgG1: isolation, characterization, in vitro binding properties and pharmacokinetics in rats. *mAbs* (Vol. 2, No. 6, pp. 613-624).
- Kiese, S., Pappenberger, A., Friess, W. and Mahler, H.C. (2010). Equilibrium studies of protein aggregates and homogeneous nucleation in protein formulation. *Journal of Pharmaceutical Sciences*, 99(2), pp.632-644.
- Kijanka, G., Bee, J.S., Korman, S.A., Wu, Y., Roskos, L.K., Schenerman, M.A., Slütter, B. and Jiskoot, W. (2018). Submicron size particles of a murine monoclonal antibody are more immunogenic than soluble oligomers or micron size particles upon subcutaneous administration in mice. *Journal of Pharmaceutical Sciences*, 107(11), pp.2847-2859.
- Kim, J.Y., Kim, Y.G. and Lee, G.M. (2012). CHO cells in biotechnology for production of recombinant proteins: current state and further potential. *Applied Microbiology and Biotechnology*, 93(3), pp.917-930.
- Kitazawa, T., Igawa, T., Sampei, Z., Muto, A., Kojima, T., Soeda, T., Yoshihashi, K., Okuyama-Nishida, Y., Saito, H., Tsunoda, H. and Suzuki, T. (2012). A bispecific antibody to factors IXa and X restores factor VIII hemostatic activity in a hemophilia A model. *Nature Medicine*, 18(10), pp.1570-1574.

- Klaubert, S.R., Chitwood, D.G., Dahodwala, H., Williamson, M., Kasper, R., Lee, K.H. and Harcum, S.W. (2021). Method to transfer Chinese hamster ovary (CHO) batch shake flask experiments to large-scale, computer-controlled fed-batch bioreactors. *Methods in Enzymology*, 660, pp. 297-320.
- Ko, P., Misaghi, S., Hu, Z., Zhan, D., Tsukuda, J., Yim, M., Sanford, M., Shaw, D., Shiratori, M., Snedecor, B. and Laird, M. (2018). Probing the importance of clonality: Single cell subcloning of clonally derived CHO cell lines yields widely diverse clones differing in growth, productivity, and product quality. *Biotechnology Progress*, 34(3), pp.624-634.
- Kober, L., Zehe, C. and Bode, J. (2012). Development of a novel ER stress based selection system for the isolation of highly productive clones. *Biotechnology and Bioengineering*, 109(10), pp.2599-2611.
- Kol, S., Ley, D., Wulff, T., Decker, M., Arnsdorf, J., Schoffelen, S., Hansen, A.H., Jensen, T.L., Gutierrez, J.M., Chiang, A.W. and Masson, H.O. (2020). Multiplex secretome engineering enhances recombinant protein production and purity. *Nature Communications*, 11(1), pp.1-10.
- Kontermann, R. (2012). Dual targeting strategies with bispecific antibodies. *mAbs*, 4(2), pp. 182-197.
- Kontermann, R.E. (2011). Strategies for extended serum half-life of protein therapeutics. *Current Opinion in Biotechnology*, 22(6), pp.868-876.
- Korennykh, A.V., Egea, P.F., Korostelev, A.A., Finer-Moore, J., Zhang, C., Shokat, K.M., Stroud, R.M. and Walter, P. (2009). The unfolded protein response signals through high-order assembly of Ire1. *Nature*, 457(7230), pp.687-693.
- Krause, K.H. and Michalak, M. (1997). Calreticulin. *Cell*, 88(4), pp.439-443.
- Kyeong, M. and Lee, J.S. (2022). Endogenous BiP reporter system for simultaneous identification of ER stress and antibody production in Chinese hamster ovary cells. *Metabolic Engineering*, 72, pp.35-45.
- Lai, T., Yang, Y. and Ng, S.K. (2013). Advances in mammalian cell line development technologies for recombinant protein production. *Pharmaceuticals*, 6(5), pp.579-603.
- Laine, M., Barbosa, N.A., Kochel, A., Osiecka, B., Szewczyk, G., Sarna, T., Ziólkowski, P., Wieczorek, R. and Filarowski, A. (2017). Synthesis, structural, spectroscopic, computational and cytotoxic studies of BODIPY dyes. *Sensors and Actuators B: Chemical*, 238, pp.548-555.
- Lao, M.S. and Toth, D. (1997). Effects of ammonium and lactate on growth and metabolism of a recombinant Chinese hamster ovary cell culture. *Biotechnology Progress*, 13(5), pp.688-691.
- Le Fourn, V., Girod, P.A., Buceta, M., Regamey, A. and Mermod, N. (2014). CHO cell engineering to prevent polypeptide aggregation and improve therapeutic protein secretion. *Metabolic Engineering*, 21, pp.91-102.
- Le, K., Tan, C., Gupta, S., Guhan, T., Barkhordarian, H., Lull, J., Stevens, J. and Munro, T. (2018). A novel mammalian cell line development platform utilizing nanofluidics and optoelectro positioning technology. *Biotechnology Progress*, 34(6), pp.1438-1446.
- Le, K., Tan, C., Le, H., Tat, J., Zasadzinska, E., Diep, J., Zastrow, R., Chen, C. and Stevens, J. (2020). Assuring clonality on the beacon digital cell line development platform. *Biotechnology Journal*, 15(1), p.1900247.
- Lee, A.H., Iwakoshi, N.N. and Glimcher, L.H. (2003). XBP-1 regulates a subset of endoplasmic reticulum resident chaperone genes in the unfolded protein response. *Molecular and Cellular Biology*, 23(21), pp.7448-7459.

- Lee, Y.K., Brewer, J.W., Hellman, R. and Hendershot, L.M. (1999). BiP and immunoglobulin light chain cooperate to control the folding of heavy chain and ensure the fidelity of immunoglobulin assembly. *Molecular Biology of the Cell*, 10(7), pp.2209-2219.
- Leonetti, M.D., Sekine, S., Kamiyama, D., Weissman, J.S. and Huang, B. (2016). A scalable strategy for high-throughput GFP tagging of endogenous human proteins. *Proceedings of the National Academy of Sciences*, 113(25), pp.E3501-E3508.
- Lewis, N.E., Liu, X., Li, Y., Nagarajan, H., Yerganian, G., O'Brien, E., Bordbar, A., Roth, A.M., Rosenbloom, J., Bian, C. and Xie, M. (2013). Genomic landscapes of Chinese hamster ovary cell lines as revealed by the *Cricetulus griseus* draft genome. *Nature Biotechnology*, 31(8), pp.759-765.
- Li, W., Prabakaran, P., Chen, W., Zhu, Z., Feng, Y. and Dimitrov, D.S. (2016). Antibody aggregation: insights from sequence and structure. *Antibodies*, 5(3), p.19.
- Lian, Z., Wu, Q. and Wang, T. (2016). Identification and characterization of a-1 reading frameshift in the heavy chain constant region of an IgG1 recombinant monoclonal antibody produced in CHO cells. *mAbs*, 8(2), pp. 358-370.
- Lin, Y., Wong, K.K. and Calame, K. (1997). Repression of c-myc transcription by Blimp-1, an inducer of terminal B cell differentiation. *Science*, 276(5312), pp.596-599.
- Linderholm, A.L. and Chamow, S.M. (2014). Immunoglobulin Fc-Fusion Proteins. *Bioprocess International*, 12, p.10.
- Liu, H. and May, K. (2012). Disulfide bond structures of IgG molecules: structural variations, chemical modifications and possible impacts to stability and biological function. *mAbs*, 4(1), pp. 17-23.
- Luo, D., He, Y., Zhang, H., Yu, L., Chen, H., Xu, Z., Tang, S., Urano, F. and Min, W. (2008). AIP1 is critical in transducing IRE1-mediated endoplasmic reticulum stress response. *Journal of Biological Chemistry*, 283(18), pp.11905-11912.
- Luo, H., Tie, L., Cao, M., Hunter, A.K., Pabst, T.M., Du, J., Field, R., Li, Y. and Wang, W.K. (2019). Cathepsin L causes Proteolytic cleavage of Chinese-hamster-ovary cell expressed proteins during processing and storage: identification, characterization, and mitigation. *Biotechnology Progress*, 35(1), p.e2732.
- Lutterotti, A. and Martin, R. (2008). Getting specific: monoclonal antibodies in multiple sclerosis. *The Lancet Neurology*, 7(6), pp.538-547.
- Määttänen, P., Gehring, K., Bergeron, J.J. and Thomas, D.Y. (2010). Protein quality control in the ER: the recognition of misfolded proteins. *Seminars in Cell & Developmental Biology* 21(5), pp. 500-511.
- Malmhäll, C., Weidner, J. and Rådinger, M. (2020). MicroRNA-155 expression suggests a sex disparity in innate lymphoid cells at the single-cell level. *Cellular & Molecular Immunology*, 17(5), pp.544-546.
- Masuda, K., Watanabe, K., Ueno, T., Nakazawa, Y., Tanabe, Y., Ushiki-Kaku, Y., Ogawa-Goto, K., Ehara, Y., Saeki, H., Okumura, T. and Nonaka, K. (2021). Novel cell line development strategy for monoclonal antibody manufacturing using translational enhancing technology. *Journal of Bioscience and Bioengineering*, 133(3), pp.273-280.
- Matasci, M., Baldi, L., Hacker, D.L. and Wurm, F.M. (2011). The PiggyBac transposon enhances the frequency of CHO stable cell line generation and yields recombinant lines with superior productivity and stability. *Biotechnology and Bioengineering*, 108(9), pp.2141-2150.

- Matasci, M., Hacker, D.L., Baldi, L. and Wurm, F.M. (2008). Recombinant therapeutic protein production in cultivated mammalian cells: current status and future prospects. *Drug Discovery Today: Technologies*, 5(2-3), pp.e37-e42.
- Mathias, S., Fischer, S., Handrick, R., Fieder, J., Schulz, P., Bradl, H., Gorr, I., Gamer, M. and Otte, K. (2018). Visualisation of intracellular production bottlenecks in suspension-adapted CHO cells producing complex biopharmaceuticals using fluorescence microscopy. *Journal of Biotechnology*, 271, pp.47-55.
- Mathias, S., Wippermann, A., Raab, N., Zeh, N., Handrick, R., Gorr, I., Schulz, P., Fischer, S., Gamer, M. and Otte, K. (2020). Unraveling what makes a monoclonal antibody difficult-to-express: From intracellular accumulation to incomplete folding and degradation via ERAD. *Biotechnology and Bioengineering*, 117(1), pp.5-16.
- Mease, P.J. (2007). Adalimumab in the treatment of arthritis. *Therapeutics and Clinical Risk Management*, 3(1), p.133.
- Merchant, A.M., Zhu, Z., Yuan, J.Q., Goddard, A., Adams, C.W., Presta, L.G. and Carter, P. (1998). An efficient route to human bispecific IgG. *Nature Biotechnology*, 16(7), pp.677-681.
- Merten, O.W. (2006). Introduction to animal cell culture technology—past, present and future. *Cytotechnology*, 50(1), pp.1-7.
- Meyer, R.M., Berger, L., Nerkamp, J., Scheler, S., Nehring, S. and Friess, W. (2021). Identification of monoclonal antibody variants involved in aggregate formation—Part 2: Hydrophobicity variants. *European Journal of Pharmaceutics and Biopharmaceutics*, 160, pp.134-142.
- Miao, S., Xie, P., Zou, M., Fan, L., Liu, X., Zhou, Y., Zhao, L., Ding, D., Wang, H. and Tan, W.S., (2017). Identification of multiple sources of the acidic charge variants in an IgG1 monoclonal antibody. *Applied Microbiology and Biotechnology*, 101(14), pp.5627-5638.
- Michalak, M., Parker, J.R. and Opas, M. (2002). Ca²⁺ signaling and calcium binding chaperones of the endoplasmic reticulum. *Cell Calcium*, 32(5-6), pp.269-278.
- Molinari, M. and Helenius, A. (1999). Glycoproteins form mixed disulphides with oxidoreductases during folding in living cells. *Nature*, 402(6757), pp.90-93.
- Muhammed, Y. (2020). The best IgG subclass for the development of therapeutic monoclonal antibody drugs and their commercial production: a review. *Immunome Research*, 16(1), pp.1-12.
- Mullard, A. (2021). FDA approves 100th monoclonal antibody product. *Nature Reviews. Drug Discovery*, 20(7), pp. 491-495.
- Müller-Taubenberger, A., Lupas, A.N., Li, H., Ecke, M., Simmeth, E. and Gerisch, G. (2001). Calreticulin and calnexin in the endoplasmic reticulum are important for phagocytosis. *The EMBO Journal*, 20(23), pp.6772-6782.
- Nakamura, T. and Omasa, T. (2015). Optimization of cell line development in the GS-CHO expression system using a high-throughput, single cell-based clone selection system. *Journal of Bioscience and Bioengineering*, 120(3), pp.323-329.
- Narhi, L.O., Schmit, J., Bechtold-Peters, K. and Sharma, D. (2012). Classification of protein aggregates. *Journal of Pharmaceutical Sciences*, 101(2), pp.493-498.
- Nelson, AL L. (2010). Antibody fragments: hope and hype. *mAbs*, 2(1), pp.77-83.

- Neve, R.M., Nielsen, U.B., Kirpotin, D.B., Poul, M.A., Marks, J.D. and Benz, C.C. (2001). Biological effects of anti-ErbB2 single chain antibodies selected for internalizing function. *Biochemical and Biophysical Research Communications*, 280(1), pp.274-279.
- Ng, P.K., He, J. and Snyder, M.A. (2009). Separation of protein mixtures using pH-gradient cation-exchange chromatography. *Journal of Chromatography A*, 1216(9), pp.1372-1376.
- Nguyen, H.B., Hung, L.W., Yeates, T.O., Terwilliger, T.C. and Waldo, G.S. (2013). Split green fluorescent protein as a modular binding partner for protein crystallization. *Acta Crystallographica Section D: Biological Crystallography*, 69(12), pp.2513-2523.
- Nolan, R.P. and Lee, K. (2012). Dynamic model for CHO cell engineering. *Journal of Biotechnology*, 158(1-2), pp.24-33.
- Novoa, I., Zeng, H., Harding, H.P. and Ron, D. (2001). Feedback inhibition of the unfolded protein response by GADD34-mediated dephosphorylation of eIF2 α . *The Journal of Cell Biology*, 153(5), pp.1011-1022.
- Ouellette, D., Alessandri, L., Chin, A., Grinnell, C., Tarcsa, E., Radziejewski, C. and Correia, I. (2010). Studies in serum support rapid formation of disulfide bond between unpaired cysteine residues in the VH domain of an immunoglobulin G1 molecule. *Analytical Biochemistry*, 397(1), pp.37-47.
- Pan, X., Streefland, M., Dalm, C., Wijffels, R.H. and Martens, D.E. (2017). Selection of chemically defined media for CHO cell fed-batch culture processes. *Cytotechnology*, 69(1), pp.39-56.
- Patil, C. and Walter, P. (2001). Intracellular signaling from the endoplasmic reticulum to the nucleus: the unfolded protein response in yeast and mammals. *Current Opinion in Cell Biology*, 13(3), pp.349-355.
- Paul, A.J., Handrick, R., Ebert, S. and Hesse, F. (2018). Identification of process conditions influencing protein aggregation in Chinese hamster ovary cell culture. *Biotechnology and Bioengineering*, 115(5), pp.1173-1185.
- Paul, A.J., Schwab, K. and Hesse, F. (2014). Direct analysis of mAb aggregates in mammalian cell culture supernatant. *BMC Biotechnology*, 14(1), pp.1-11.
- Paul, A.J., Schwab, K., Prokoph, N., Haas, E., Handrick, R. and Hesse, F. (2015). Fluorescence dye-based detection of mAb aggregates in CHO culture supernatants. *Analytical and Bioanalytical Chemistry*, 407(16), pp.4849-4856.
- Pekle, E., Smith, A., Rosignoli, G., Sellick, C., Smales, C.M. and Pearce, C. (2019). Application of imaging flow cytometry for the characterization of intracellular attributes in Chinese hamster ovary cell lines at the single-cell level. *Biotechnology Journal*, 14(7), p.1800675.
- Pento, J.T. (2017). Monoclonal antibodies for the treatment of cancer. *Anticancer Research*, 37(11), pp.5935-5939.
- Perkins, M., Theiler, R., Lunte, S. and Jeschke, M. (2000). Determination of the origin of charge heterogeneity in a murine monoclonal antibody. *Pharmaceutical Research*, 17(9), pp.1110-1117.
- Pieper, L.A., Strotbek, M., Wenger, T., Gamer, M., Olayioye, M.A. and Hausser, A. (2017). Secretory pathway optimization of CHO producer cells by co-engineering of the mitosRNA-1978 target genes CerS2 and Tbc1D20. *Metabolic Engineering*, 40, pp.69-79.
- Pollock, J., Ho, S.V. and Farid, S.S. (2013). Fed-batch and perfusion culture processes: economic, environmental, and operational feasibility under uncertainty. *Biotechnology and Bioengineering*, 110(1), pp.206-219.

- Porter, A.J., Dickson, A.J. and Racher, A.J. (2010). Strategies for selecting recombinant CHO cell lines for cGMP manufacturing: realizing the potential in bioreactors. *Biotechnology progress*, 26(5), pp.1446-1454.
- Prasad, V. and Kaestner, V. (2017). Nivolumab and pembrolizumab: Monoclonal antibodies against programmed cell death-1 (PD-1) that are interchangeable. *Seminars in Oncology*, 44(2), pp. 132-135).
- Prashad, K. and Mehra, S. (2015). Dynamics of unfolded protein response in recombinant CHO cells. *Cytotechnology*, 67(2), pp.237-254.
- Priola, J.J., Calzadilla, N., Baumann, M., Borth, N., Tate, C.G. and Betenbaugh, M.J. (2016). High-throughput screening and selection of mammalian cells for enhanced protein production. *Biotechnology Journal*, 11(7), pp.853-865.
- Przepiorka, D., Ko, C.W., Deisseroth, A., Yancey, C.L., Candau-Chacon, R., Chiu, H.J., Gehrke, B.J., Gomez-Broughton, C., Kane, R.C., Kirshner, S. and Mehrotra, N. (2015). FDA approval: blinatumomab. *Clinical Cancer Research*, 21(18), pp.4035-4039.
- Puck, T.T., Cieciura, S.J. and Robinson, A. (1958). Genetics of somatic mammalian cells: III. Long-term cultivation of euploid cells from human and animal subjects. *The Journal of Experimental Medicine*, 108(6), p.945.
- Puck, T.T., Sanders, P. and Petersen, D. (1964). Life cycle analysis of mammalian cells: II. Cells from the Chinese hamster ovary grown in suspension culture. *Biophysical Journal*, 4(6), pp.441-450.
- Pybus, L.P., Dean, G., West, N.R., Smith, A., Daramola, O., Field, R., Wilkinson, S.J. and James, D.C. (2014). Model-directed engineering of “difficult-to-express” monoclonal antibody production by Chinese hamster ovary cells. *Biotechnology and Bioengineering*, 111(2), pp.372-385.
- Quan, C., Alcala, E., Petkovska, I., Matthews, D., Canova-Davis, E., Taticek, R. and Ma, S. (2008). A study in glycation of a therapeutic recombinant humanized monoclonal antibody: where it is, how it got there, and how it affects charge-based behavior. *Analytical Biochemistry*, 373(2), pp.179-191.
- Rayner, L.E., Hui, G.K., Gor, J., Heenan, R.K., Dalby, P.A. and Perkins, S.J. (2015). The solution structures of two human IgG1 antibodies show conformational stability and accommodate their C1q and FcγR ligands. *Journal of Biological Chemistry*, 290(13), pp.8420-8438.
- Reimold, A.M., Iwakoshi, N.N., Manis, J., Vallabhajosyula, P., Szomolanyi-Tsuda, E., Gravallesse, E.M., Friend, D., Grusby, M.J., Alt, F. and Glimcher, L.H. (2001). Plasma cell differentiation requires the transcription factor XBP-1. *Nature*, 412(6844), pp.300-307.
- Reinhart, D., Damjanovic, L., Kaisermayer, C., Sommeregger, W., Gili, A., Gasselhuber, B., Castan, A., Mayrhofer, P., Grünwald-Gruber, C. and Kunert, R. (2019). Bioprocessing of recombinant CHO-K1, CHO-DG44, and CHO-S: CHO Expression hosts favor either mAb production or biomass synthesis. *Biotechnology Journal*, 14(3), p.1700686.
- Reinhart, D., Sommeregger, W., Debreczeny, M., Gludovacz, E. and Kunert, R. (2014). In search of expression bottlenecks in recombinant CHO cell lines—a case study. *Applied Microbiology and Biotechnology*, 98(13), pp.5959-5965.
- Ritacco, F.V., Wu, Y. and Khetan, A. (2018). Cell culture media for recombinant protein expression in Chinese hamster ovary (CHO) cells: history, key components, and optimization strategies. *Biotechnology Progress*, 34(6), pp.1407-1426.

- Roberts, C.J. (2014). Protein aggregation and its impact on product quality. *Current Opinion in Biotechnology*, 30, pp.211-217.
- Roche (2019) *Human IgG Assay for Cedex Bio and Bio HT Analyzers*. Available at: https://custombiotech.roche.com/content/dam/acadia/brochure/575/17/CustomBiotech_Cedex_IgG_Assay.pdf (Accessed: February 2022).
- Roderick, H.L., Campbell, A.K. and Llewellyn, D.H., (1997). Nuclear localisation of calreticulin in vivo is enhanced by its interaction with glucocorticoid receptors. *FEBS letters*, 405(2), pp.181-185.
- Rosenberg, A.S. (2006). Effects of protein aggregates: an immunologic perspective. *The AAPS Journal*, 8(3), pp.E501-E507.
- Roth, R.A. and Pierce, S.B. (1987). In vivo cross-linking of protein disulfide isomerase to immunoglobulins. *Biochemistry*, 26(14), pp.4179-4182.
- Roy, G., Zhang, S., Li, L., Higham, E., Wu, H., Marelli, M. and Bowen, M.A. (2017). Development of a fluorescent reporter system for monitoring ER stress in Chinese hamster ovary cells and its application for therapeutic protein production. *PLoS ONE*, 12(8), p.e0183694.
- Sahay, G., Gautam, V., Luxenhofer, R. and Kabanov, A.V. (2010). The utilization of pathogen-like cellular trafficking by single chain block copolymer. *Biomaterials*, 31(7), pp.1757-1764.
- Salzman, N.P. (1959). Systematic fluctuations in the cellular protein, RNA and DNA during growth of mammalian cell cultures. *Biochimica et Biophysica Acta*, 31(1), pp.158-163.
- Samy, A., Yamano-Adachi, N., Koga, Y. and Omasa, T. (2021). Secretion of a low-molecular-weight species of endogenous GRP94 devoid of the KDEL motif during endoplasmic reticulum stress in Chinese hamster ovary cells. *Traffic*, 22(12), pp.425-438.
- Schmieder, V., Fieder, J., Drerup, R., Gutierrez, E.A., Guelch, C., Stolzenberger, J., Stumbaum, M., Mueller, V.S., Higel, F., Bergbauer, M. and Bornhoeft, K. (2022). Towards maximum acceleration of monoclonal antibody development: Leveraging transposase-mediated cell line generation to enable GMP manufacturing within 3 months using a stable pool. *Journal of Biotechnology*, 349, pp.53-64.
- Schroeder Jr, H.W. and Cavacini, L. (2010). Structure and function of immunoglobulins. *Journal of Allergy and Clinical Immunology*, 125(2), pp.S41-S52.
- Sekar, R.B. and Periasamy, A. (2003). Fluorescence resonance energy transfer (FRET) microscopy imaging of live cell protein localizations. *The Journal of Cell Biology*, 160(5), p.629.
- Shatz, W., Chung, S., Li, B., Marshall, B., Tejada, M., Phung, W., Sandoval, W., Kelley, R.F. and Scheer, J.M. (2013). Knobs-into-holes antibody production in mammalian cell lines reveals that asymmetric afucosylation is sufficient for full antibody-dependent cellular cytotoxicity. *mAbs*, 5(6), pp. 872-881.
- Shima, M., Hanabusa, H., Taki, M., Matsushita, T., Sato, T., Fukutake, K., Fukazawa, N., Yoneyama, K., Yoshida, H. and Nogami, K. (2016). Factor VIII-mimetic function of humanized bispecific antibody in hemophilia A. *New England Journal of Medicine*, 374(21), pp.2044-2053.
- Singh, S.K. (2011). Impact of product-related factors on immunogenicity of biotherapeutics. *Journal of Pharmaceutical Sciences*, 100(2), pp.354-387.
- SinoBiological (2022) *Antibody Structure, Function, Classes and Formats*. Available at: <https://www.sinobiological.com/resource/antibody-technical/antibody-structure-function> (Accessed: January 2022).

- Tan, E., Chin, C.S.H., Lim, Z.F.S. and Ng, S.K. (2021). HEK293 Cell Line as a Platform to Produce Recombinant Proteins and Viral Vectors. *Frontiers in Bioengineering and Biotechnology*, 9:796991.
- Tejwani, V., Chaudhari, M., Rai, T. and Sharfstein, S.T. (2021). High-throughput and automation advances for accelerating single-cell cloning, monoclonality and early phase clone screening steps in mammalian cell line development for biologics production. *Biotechnology Progress*, 37(6), p.e3208.
- Telikepalli, S., Shinogle, H.E., Thapa, P.S., Kim, J.H., Deshpande, M., Jawa, V., Middaugh, C.R., Narhi, L.O., Joubert, M.K. and Volkin, D.B. (2015). Physical characterization and in vitro biological impact of highly aggregated antibodies separated into size-enriched populations by fluorescence-activated cell sorting. *Journal of pharmaceutical sciences*, 104(5), pp.1575-1591.
- Tjio, J.H. and Puck, T.T. (1958). Genetics of somatic mammalian cells: II. Chromosomal constitution of cells in tissue culture. *The Journal of Experimental Medicine*, 108(2), p.259.
- Todd, P.A. and Brogden, R.N. (1989). Muromonab CD3. *Drugs*, 37(6), pp.871-899.
- Topp, M., Goekbuget, N., Kufer, P., Zugmaier, G., Degenhard, E., Neumann, S., Horst, H.A., Viardot, A., Schmid, M., Ottmann, O.G. and Schmidt, M. (2008). Treatment with Anti-CD19 BiTE Antibody Blinatumomab (MT103/MEDI-538) Is Able to Eliminate Minimal Residual Disease (MRD) in Patients with B-Precursor Acute Lymphoblastic Leukemia (ALL): First Results of An Ongoing Phase II Study. *Blood*, 112(11), p.1926.
- Tordai, A., Brass, L.F. and Gelfand, E.W. (1995). Tunicamycin inhibits the expression of functional thrombin receptors on human T-lymphoblastoid cells. *Biochemical and Biophysical Research Communications*, 206(3), pp.857-862.
- Torkashvand, F. and Vaziri, B. (2017). Main quality attributes of monoclonal antibodies and effect of cell culture components. *Iranian Biomedical Journal*, 21(3), p.131.
- Torres, M. and Dickson, A.J. (2021). Reprogramming of Chinese hamster ovary cells towards enhanced protein secretion. *Metabolic Engineering*, 69, pp.249-261.
- Torres, M., Akhtar, S., McKenzie, E.A. and Dickson, A.J. (2020). Temperature down-shift modifies expression of UPR-/ERAD-related genes and enhances production of a chimeric fusion protein in CHO cells. *Biotechnology journal*, 16(2), p.2000081.
- Torres, M., Hussain, H. and Dickson, A.J. (2022). The secretory pathway—the key for unlocking the potential of Chinese hamster ovary cell factories for manufacturing therapeutic proteins. *Critical Reviews in Biotechnology*, pp.1-18.
- Tousi, F., Jiang, Y., Sivendran, S., Song, Y., Elliott, S., Paiva, A., Lund, A., Albee, K. and Lee, K., (2020). Intact Protein Mass Spectrometry of Cell Culture Harvest Guides Cell Line Development for Trispecific Antibodies. *Analytical Chemistry*, 92(3), pp.2764-2769.
- Travers, K.J., Patil, C.K., Wodicka, L., Lockhart, D.J., Weissman, J.S. and Walter, P. (2000). Functional and genomic analyses reveal an essential coordination between the unfolded protein response and ER-associated degradation. *Cell*, 101(3), pp.249-258.
- Tsujimoto, Y., Nakagawa, T. and Shimizu, S. (2006). Mitochondrial membrane permeability transition and cell death. *Biochimica et Biophysica Acta (BBA)-Bioenergetics*, 1757(9-10), pp.1297-1300.
- Urano, F., Wang, X., Bertolotti, A., Zhang, Y., Chung, P., Harding, H.P. and Ron, D. (2000). Coupling of stress in the ER to activation of JNK protein kinases by transmembrane protein kinase IRE1. *Science*, 287(5453), pp.664-666.

- Urlaub, G. and Chasin, L.A. (1980). Isolation of Chinese hamster cell mutants deficient in dihydrofolate reductase activity. *Proceedings of the National Academy of Sciences*, 77(7), pp.4216-4220.
- Urlaub, G., Käs, E., Carothers, A.M. and Chasin, L.A. (1983). Deletion of the diploid dihydrofolate reductase locus from cultured mammalian cells. *Cell*, 33(2), pp.405-412.
- Urlaub, G., Mitchell, P.J., Kas, E., Chasin, L.A., Funanage, V.L., Myoda, T.T. and Hamlin, J. (1986). Effect of gamma rays at the dihydrofolate reductase locus: deletions and inversions. *Somatic Cell and Molecular Genetics*, 12(6), pp.555-566.
- Urquhart, L. (2019). Top drugs and companies by sales in 2018. *Nature Reviews Drug Discovery*.
- Urra, H., Dufey, E., Lisbona, F., Rojas-Rivera, D. and Hetz, C. (2013). When ER stress reaches a dead end. *Biochimica et Biophysica Acta (BBA)-Molecular Cell Research*, 1833(12), pp.3507-3517.
- Vallone, V.F., Telugu, N.S., Fischer, I., Miller, D., Schommer, S., Diecke, S. and Stachelscheid, H. (2020). Methods for automated single cell isolation and sub-cloning of human pluripotent stem cells. *Current Protocols in Stem Cell Biology*, 55(1), p.e123.
- van Huizen, R., Martindale, J.L., Gorospe, M. and Holbrook, N.J. (2003). P58IPK, a novel endoplasmic reticulum stress-inducible protein and potential negative regulator of eIF2 α signaling. *Journal of biological chemistry*, 278(18), pp.15558-15564.
- Vcelar, S., Jadhav, V., Melcher, M., Auer, N., Hrdina, A., Sagmeister, R., Heffner, K., Puklowski, A., Betenbaugh, M., Wenger, T. and Leisch, F. (2018). Karyotype variation of CHO host cell lines over time in culture characterized by chromosome counting and chromosome painting. *Biotechnology and Bioengineering*, 115(1), pp.165-173.
- Verhoeven, D., Stoppelenburg, A.J., Meyer-Wentrup, F. and Boes, M. (2018). Increased risk of hematologic malignancies in primary immunodeficiency disorders: opportunities for immunotherapy. *Clinical Immunology*, 190, pp.22-31.
- Verma, R., Boleti, E. and George, A.J.T. (1998). Antibody engineering: comparison of bacterial, yeast, insect and mammalian expression systems. *Journal of immunological methods*, 216(1-2), pp.165-181.
- Vidarsson, G., Dekkers, G. and Rispens, T. (2014). IgG subclasses and allotypes: from structure to effector functions. *Frontiers in Immunology*, 5, p.520.
- Vlasak, J. and Ionescu, R. (2011). Fragmentation of monoclonal antibodies. *mAbs*, 3(3), pp. 253-263.
- Vlasak, J., Bussat, M.C., Wang, S., Wagner-Rousset, E., Schaefer, M., Klinguer-Hamour, C., Kirchmeier, M., Corvaia, N., Ionescu, R. and Beck, A. (2009). Identification and characterization of asparagine deamidation in the light chain CDR1 of a humanized IgG1 antibody. *Analytical biochemistry*, 392(2), pp.145-154.
- Wahrheit, J., Nicolae, A. and Heinzle, E. (2014). Dynamics of growth and metabolism controlled by glutamine availability in Chinese hamster ovary cells. *Applied Microbiology and Biotechnology*, 98(4), pp.1771-1783.
- Walsh, G. (2018). Biopharmaceutical benchmarks 2018. *Nature Biotechnology*, 36(12), pp.1136-1145.
- Walsh, G. and Jefferis, R. (2006). Post-translational modifications in the context of therapeutic proteins. *Nature Biotechnology*, 24(10), pp.1241-1252.

- Walter, P. and Ron, D. (2011). The unfolded protein response: from stress pathway to homeostatic regulation. *Science*, 334(6059), pp.1081-1086.
- Wang, C., Du, W., Su, Q.P., Zhu, M., Feng, P., Li, Y., Zhou, Y., Mi, N., Zhu, Y., Jiang, D. and Zhang, S. (2015). Dynamic tubulation of mitochondria drives mitochondrial network formation. *Cell research*, 25(10), pp.1108-1120.
- Wang, J.H. (2013). The sequence signature of an Ig-fold. *Protein & Cell*, 4(8), pp.569-572.
- Wang, S., Liu, A.P., Yan, Y., Daly, T.J. and Li, N. (2018). Characterization of product-related low molecular weight impurities in therapeutic monoclonal antibodies using hydrophilic interaction chromatography coupled with mass spectrometry. *Journal of pharmaceutical and biomedical analysis*, 154, pp.468-475.
- Wang, W., Singh, S., Zeng, D.L., King, K. and Nema, S. (2007). Antibody structure, instability, and formulation. *Journal of Pharmaceutical Sciences*, 96(1), pp.1-26.
- Weissman, J.S. and Kimt, P.S. (1993). Efficient catalysis of disulphide bond rearrangements by protein disulphide isomerase. *Nature*, 365(6442), pp.185-188.
- Wigler, M., Perucho, M., Kurtz, D., Dana, S., Pellicer, A., Axel, R. and Silverstein, S. (1980). Transformation of mammalian cells with an amplifiable dominant-acting gene. *Proceedings of the National Academy of Sciences*, 77(6), pp.3567-3570.
- Williams, A.F. and Barclay, A.N. (1988). The immunoglobulin superfamily—domains for cell surface recognition. *Annual Review of Immunology*, 6(1), pp.381-405.
- Winterfield, L.S. and Menter, A. (2004). Infliximab. *Dermatologic Therapy*, 17(5), pp.409-426.
- World Health Organisation (2013). *WHO Expert Committee on Biological Standardization*. p. 111. Available at: <https://www.who.int/publications/i/item/9789241209786> (Accessed: February 2022).
- Worton, R.G., Ho, C.C. and Duff, C. (1977). Chromosome stability in CHO cells. *Somatic Cell Genetics*, 3(1), pp.27-45.
- Wurm, F.M. (2013). CHO quasispecies—implications for manufacturing processes. *Processes*, 1(3), pp.296-311.
- Xie, L. and Wang, D.I. (1997). Integrated approaches to the design of media and feeding strategies for fed-batch cultures of animal cells. *Trends in Biotechnology*, 15(3), pp.109-113.
- Xing, Z., Bishop, N., Leister, K. and Li, Z.J. (2010). Modeling kinetics of a large-scale fed-batch CHO cell culture by Markov chain Monte Carlo method. *Biotechnology Progress*, 26(1), pp.208-219.
- Xu, C.F., Chen, Y., Yi, L., Brantley, T., Stanley, B., Sobic, Z. and Zang, L. (2017a). Discovery and characterization of histidine oxidation initiated cross-links in an IgG1 monoclonal antibody. *Analytical Chemistry*, 89(15), pp.7915-7923.
- Xu, N., Ma, C., Ou, J., Sun, W.W., Zhou, L., Hu, H. and Liu, X.M. (2017b). Comparative proteomic analysis of three Chinese hamster ovary (CHO) host cells. *Biochemical Engineering Journal*, 124, pp.122-129.
- Yahia, B.B., Malphettes, L. and Heinzle, E. (2021). Predictive macroscopic modeling of cell growth, metabolism and monoclonal antibody production: Case study of a CHO fed-batch production. *Metabolic Engineering*, 66, pp.204-216.

- Yamaji, T., Horie, A., Tachida, Y., Sakuma, C., Suzuki, Y., Kushi, Y. and Hanada, K. (2016). Role of intracellular lipid logistics in the preferential usage of very long chain-ceramides in glucosylceramide. *International Journal of Molecular Sciences*, 17(10), p.1761.
- Yang, G., Hu, Y., Sun, S., Ouyang, C., Yang, W., Wang, Q., Betenbaugh, M. and Zhang, H. (2018). Comprehensive glycoproteomic analysis of Chinese hamster ovary cells. *Analytical Chemistry*, 90(24), pp.14294-14302.
- Yang, Y., Ma, F., Liu, Z., Su, Q., Liu, Y., Liu, Z. and Li, Y. (2019). The ER-localized Ca²⁺-binding protein calreticulin couples ER stress to autophagy by associating with microtubule-associated protein 1A/1B light chain 3. *Journal of Biological Chemistry*, 294(3), pp.772-782.
- Yao, T. and Asayama, Y. (2017). Animal-cell culture media: History, characteristics, and current issues. *Reproductive Medicine and Biology*, 16(2), pp.99-117.
- Ye, J., Rawson, R.B., Komuro, R., Chen, X., Davé, U.P., Prywes, R., Brown, M.S. and Goldstein, J.L. (2000). ER stress induces cleavage of membrane-bound ATF6 by the same proteases that process SREBPs. *Molecular Cell*, 6(6), pp.1355-1364.
- Yoshida, H., Haze, K., Yanagi, H., Yura, T. and Mori, K. (1998). Identification of the cis-acting endoplasmic reticulum stress response element responsible for transcriptional induction of mammalian glucose-regulated proteins: involvement of basic leucine zipper transcription factors. *Journal of Biological Chemistry*, 273(50), pp.33741-33749.
- Yoshida, H., Matsui, T., Yamamoto, A., Okada, T. and Mori, K. (2001). XBP1 mRNA is induced by ATF6 and spliced by IRE1 in response to ER stress to produce a highly active transcription factor. *Cell*, 107(7), pp.881-891.
- Yoshida, H., Oku, M., Suzuki, M. and Mori, K. (2006). pXBP1 (U) encoded in XBP1 pre-mRNA negatively regulates unfolded protein response activator pXBP1 (S) in mammalian ER stress response. *The Journal of Cell Biology*, 172(4), pp.565-575.
- Yoshida, H., Uemura, A. and Mori, K. (2009). pXBP1 (U), a negative regulator of the unfolded protein response activator pXBP1 (S), targets ATF6 but not ATF4 in proteasome-mediated degradation. *Cell Structure and Function*, 34(1), pp.1-10.
- Yu, J., Li, T., Liu, Y., Wang, X., Zhang, J., Wang, X.E., Shi, G., Lou, J., Wang, L., Wang, C.C. and Wang, L. (2020). Phosphorylation switches protein disulfide isomerase activity to maintain proteostasis and attenuate ER stress. *The EMBO journal*, 39(10), p.e103841.
- Zhang, S., Hughes, J.D., Murgolo, N., Levitan, D., Chen, J., Liu, Z. and Shi, S. (2016). Mutation detection in an antibody-producing Chinese hamster ovary cell line by targeted RNA sequencing. *BioMed Research International*, 2016.
- Zhang, T., Bourret, J. and Cano, T. (2011). Isolation and characterization of therapeutic antibody charge variants using cation exchange displacement chromatography. *Journal of Chromatography A*, 1218(31), pp.5079-5086.
- Zhu, M.M., Mollet, M., Hubert, R.S., Kyung, Y.S. and Zhang, G.G. (2017) 'Industrial production of therapeutic proteins: cell lines, cell culture, and purification', in Kent, J., Bommaraju, T. and Barnicki, S. (eds) *Handbook of industrial chemistry and biotechnology*. 13th Edition. Springer Cham, pp. 1639-1669.
- Zhukovsky, E.A., Morse, R.J. and Maus, M.V. (2016). Bispecific antibodies and CARs: generalized immunotherapeutics harnessing T cell redirection. *Current Opinion in Immunology*, 40, pp.24-35.

Zou, L., Lai, H., Zhou, Q. and Xiao, F. (2011). Lasting controversy on ranibizumab and bevacizumab. *Theranostics*, 1, p.395.